Assessment of freezing desalination technologies.

Ahmad, Mansour M. M

Swansea University
Prifysgol Abertawe

Department of Chemical and Biological Process Engineering

Swansea University

ASSESSMENT OF FREEZING DESALINATION TECHNOLOGIES

by

Mansour Ahmad

M.Sc. with Distinction

A Thesis Submitted in Fulfilment of the Requirement for the Degree

DOCTOR OF PHILOSOPHY

Philosophiae Doctor (Ph.D.)

August 2012

Summary

The production of both fresh water and waste streams are progressively increasing over the years due to ongoing population growth coupled with high levels of increase in water consumption. The ongoing growth of human activities, such as industry, recreation, and agriculture, are significantly contributing to the increase in both water demand and severity of degradation of natural water resources. The majority of the industrial wastewaters have a significant impact on the environment; some of which may pose a number of threats to human health and the surrounding environment. Thus, discharge of such waste streams into a surface water and/or groundwater presents a major source of water pollution in many countries. Therefore, these waste streams must be disposed of in an environmentally acceptable manner.

The primary concern of the PhD thesis is to seek the most feasible and applicable freezing desalination technologies that are potentially capable to concentrate the dissolved ionic content of the liquid streams, especially for those causing severe pollution problems. Therefore, various forms of melt crystallisation processes, namely; agitated and static crystallisation processes, ice maker machines, a Sulzer falling film crystallisation process, the Sulzer suspension crystallisation process, and the Sulzer static crystallisation process, were experimentally used and investigated. The experimental investigations were carried out on the laboratory bench scale and/or straightforward pilot plant by using aqueous solutions of sodium chloride and/or process brines as feed samples. The study was focused on a number of important parameters influencing the separation performance of the investigated treatment systems. In general, the resulting experimental data for each innovative process were highly encouraging in minimising the volume of the waste stream, and substantially increasing the amount of product water. The obtained product water was ready for immediate use either as drinking water or as a saline water of near brackish water or seawater qualities. Also, relationships between the influences and the separation performance, in terms of salt rejection and water recovery ratios, were explored and determined for the investigated technologies. Based on the experimental results, the Sulzer melt crystallisation processes were scaled up and were combined into a commercial reverse osmosis membrane desalination plant. As a result, three novel treatment option configurations were proposed for minimising the waste stream, whilst increasing the production rate of drinking water and/or preserving a substantial amount of natural water resource from the RO plant's exploitation.

Declaration

This work has not been previously accepted in substance for any degree and is not being concurrently submitted in candidature for any degree.

Signed: ..... (*Candidate:* Mansour Ahmad)
Date: 07/09/2012

Statement 1

This thesis is the result of my own investigations, except where otherwise stated. Other sources are acknowledged by footnotes giving explicit references. A bibliography is appended.

Signed: ..... (*Candidate:* Mansour Ahmad)
Date: 07/09/2012

Statement 2

I hereby give my consent for my thesis, if accepted, to be available for photocopying and for inter-library loan, and for the title and summary to be made available to outside organisations.

Signed: ..... (*Candidate:* Mansour Ahmad)
Date: 07/09/2012

Acknowledgements

I am ever grateful to God, the Creator and the Guardian, and to whom I owe my very existence.

I would like to thank a number of people and institutions who have contributed in one way or another to this project and extended their valuable assistance in the completion of my thesis:

First and foremost, I would like to express my sincere gratitude to my supervisor **Dr Paul Williams** for his direction, guidance and support throughout my Ph.D research since without his encouragement and motivation I could not have completed this project. Despite his busy schedule at the university, he was always available to me, to discuss my ideas or answer any questions I had on various aspects of my Ph.D study.

I would like to thank **Kuwait Institute for Scientific Research (KISR)** and in particular the scholarship committee for their financial support and providing me with the opportunity to pursue my studies as well as giving me the chance to achieve my ultimate goal in life. Moreover, I owe special thanks to **Dr Yousif Al-Wazzan**, Department Manager of Water Technologies Department at KISR, for all his support and help toward obtaining the scholarship from KISR. I would also like to give sincere and many thanks to **Dr Mahmoud Abdel-Jawad**, Principal Research Scientist at KISR, since without his encouragement and enthusiasm I could have not completed the work (as scheduled in the work plan) on time.

During my Ph.D, I had the privilege to work with **Sulzer Chemtech Ltd** in Switzerland to conduct some of my research. The three months I spent there were exceptionally productive and the staff who were involved showed great interest and enthusiasm in the technical sessions, practical training programs, technical meetings, and oral presentations given by myself. Furthermore, I owe a great deal to **Dr. Severine Dette**, Sales Engineer Fractional Crystallization at Sulzer Chemtech Company, who has been so kind and generous with her time in offering me valuable information about Sulzer's technologies through technical sessions. I really appreciate her help in discussing the experimental data with me, answering and addressing any questions that would assist me to think through my ideas for developing the existing Sulzer's technologies.

Finally, I would like to express gratitude to all my friends, colleagues, family members and especially my loving wife **Mrs. Zainab Ghareeb** for all their faith, patience and moral support during the writing of this thesis.

List of Contents

List of Figures

List of Tables

Nomenclature

Symbol	Representing	Units
AGR	Average growth rate	mm/h, mm/min
APFR	Average product flow rate	kg/h
A_R	Agitation rate	rpm, L/min, amplitude
C, x	Salt concentration of water sample	wt%, mg/L, meq/m^3
C_p	Specific heat capacity of the feed	kJ/(kg.K)
CR	Cooling rate	°C/min, °C/h
E_{min}	Minimum energy requirement	kWh/m^3
FP	Freezing point	°C
m	Mass	kg
m_b	Mass flow-rates of brine	kg/h
m_f	Mass flow-rate of feed water	kg/h
m_i	Mass flow rate of ice slurry	kg/h
m_{LI}	Mass flow rate of the ice slurry out	kg/h
m_{LO}	Mass flow rate of the liquid out	kg/h
m_p	Mass flow-rates of product water	kg/h
m_{salt}	Mass of dissolved salts in the sampled solution	g
m_{SO}	Mass flow rate of liquid in	kg/h
$m_{solution}$	Mass of the sampled solution respectively	g
Q	Circulation pump flow-rate, Volume flow-rate	L/min, m^3/h
$Q_{E,}$	Experimental power consumption	kWh/kg
Q_f	Heat transfer rate for cooling the feed water	kW
Q_p	Heat transfer rate for changing the phase of the liquid	kW
Q_T	Theoretical power consumption	kWh/kg
R	Universal gas constant	J/(mole.K)
R^2	Regression correlation coefficient	Dimensionless
R_i	Weight ratio of crystal slurry	%
R_r	Weight ratio of the residue	%
Rec	Permeate water recovery	%
RT	Running time	h

SR	Salt rejection ratio	%
Sr	Sweating rate	°C/min, °C/h
t	Running time	min
t_C	Running time of crystallisation process	min, h
t_S	Running time of sweating process	min, h
T	Absolute temperature	K
T_1, SPT	Start-point temperature	°C
T_2, EPT	End-point temperature	°C
TDS	Total dissolved solids	mg/L, ppm
U	Energy available	kWh
v	Number of Ions per molecule of solute	Dimensionless
v_w	Molar volume of the water	m^3/mole
V	Volume	m^3
W	Weight	N
WR	Permeate water recovery ratio	%
x_f	Feed concentration	ppm, wt%
x_s	Salt mole-fraction	Dimensionless

Greek Symbols

ΔH_f	Heat of fusion of ice	kJ/kg
Δts	Sweating time	h
π	Osmotic pressure	bar

Subscripts

1	First stage, feed stage, stage number, start-point
2	Second stage, rectification stage, stripping stage, stage number, end-point
b	Brine or residue
C	Crystallisation process
E	Experimental
f	Feed water

i	Ice slurry
Min	Minimum
p	Product water, phase of the liquid
r	Residue
s	Saline solution
S	Sweating process
T	Theoretical
w	Water

Abbreviations

AG	Arabian Gulf
AGMD	Air gap membrane distillation
BP	Bubbling process
CAL	Central analytical laboratories
CAC	Codex Alimentarius Commission standards
DCMD	Direct contact membrane distillation
DRP	Doha research plant
DTB	Draft tube and baffle
DTs	Desalination technologies
DV	Drain valve
ED	Electrodialysis
EDR	Electrodialysis reversal
EU	European Union standards
f	Feed water
FCV	Flow control valve
FDA	Food and Drug Administration standards
FM	Freeze-melting
FO	Forward osmosis
HSB	Highly saline brines
HSIB	High saline industrial brines
HSNB	High saline natural brines
HTM	Heat transfer medium

HTU	Heat transfer unit
IBWA	International Bottled Water Association standards
KBW	Kadhmah bottled water
KISR	Kuwait Institute for Scientific Research
kWh meter	Kilowatt hours meter
LIBNOR	Lebanese standards institution
LPS	Laboratory pilot scale setup
MD	Membrane distillation
MED	Multiple effect distillation
MGD	Millions of gallons per day
Min	Minimum
MSF	Multiple-stage flash distillation
MSS	Mechanically stirred system
MVC	Mechanical vapour compressor
n	Number of sweat fractions
NF	Nanofiltration
PP	Pilot plant
PRO	Pressure retarded osmosis
RED	Reverse electrodialysis
RO	Reverse osmosis
RO brines	Reject brine of the reverse osmosis membrane plant or unit
S	Source of feed
SGMD	Sweeping gas membrane distillation
SCR	Strip chart recorder
TI	Temperature indicator
TR	Temperature ramp
TVP	Theoretical power consumption value for the tap water
TVC	Thermal vapour compressor
t/y	Ton per year
UF	Ultrafiltration
UP	Ultrasonic process
VC	Vapour compression
VMD	Vacuum membrane distillation
WHO	World Health Organization standards

WRD	Water Resources Division
WTD	Water Technologies Department
x	Independent variable of the empirical equation
y	Dependant variable of the empirical equation
ZLD	Zero liquid discharge

CHAPTER I:

INTRODUCTION

Primary environmental impacts from any industry are typically associated with the disposal methods used for the waste streams. Industrial wastewaters are produced in large volumes from various industrial sectors, particularly those that deal with the production of fresh water, oil and gas, food, medical supplies, and chemical processing. Unfortunately, the production of both fresh water and waste streams are progressively increasing over years as ongoing population growth coupled with high levels of increase in water consumption [Fritzmann *et al.*, 2007]. The ongoing growth of human activities, such as industry, recreation, and agriculture, are significantly contributing to the increase in both water demand and severity of degradation of natural water resources. The majority of the industrial wastewaters have a significant impact on environment; some of which may pose a number of threats to human health and the surrounding environment. Thus, discharge of such waste streams into a surface water and/or groundwater presents a major source of water pollution in many countries. Therefore, these waste streams must be disposed of in an environmentally acceptable manner.

Treatment and/or disposal of concentrated brines which have total dissolved solid content in the region of 70,000 ppm up to full saturation, are a common and important problem around the world. The success of any desalination technology for such an application depends on the reliability of the process, product quality, capital cost, energy consumption, complexity of the process and safe disposal. Unfortunately, the treatment of concentrated brines using desalination technologies may be either expensive or technically unfeasible. Existing conventional desalination technologies may also not be capable of concentrating the polluting materials sufficiently for re-use or for their safe disposal. Hence, process development and innovation in this area is of extreme importance for many countries, especially countries such as Kuwait, where desalination and oil industries are considered vital.

The fact that the freeze-melting process can purify and concentrate liquids has been known for many years [Nebbia and Menozzi, 1968]. The simplest natural example is that sea-ice has a much lower salt content than sea-water, a phenomenon used by the inhabitants of the Polar Regions as a source of drinking water. From an industrial-separations viewpoint, freeze-melting process has a number of important advantages:

a) A very high separation factor,
b) High energy efficiency since the latent heat of freezing is low, which leads to lower energy requirement in comparison to other processes (i.e. evaporation-recondensation by multistage flash or vapor compression),
c) Core technology readily available,
d) Insensitive to biological fouling, scaling and corrosion problems because of the low operating temperature, which means less use of chemicals and thus lower operating costs. Also, absence of chemical pretreatment means no discharge of toxic chemicals to the environment.
e) Inexpensive materials of construction can be utilized at low temperature, which results in lower capital cost.

Despite the important advantages of freeze melting processes, this technique has been used only to a very limited extent industrially. This has been largely due to a very conservative approach to the adoption of new technology, the perception that such a process would be mechanically complex, and the lack of appropriate test data. However, these caveats have recently become less important due to the pressing need for more effective solutions to water pollution problems and the development of mechanically simpler freezing technology.

This thesis will look at various forms of melt crystallisation processes, such as; solid layer crystallisation and suspension. The primary concern of this thesis is to seek the most feasible and applicable freezing desalination technologies that are potentially capable to concentrate the dissolved ionic content of the liquid streams, especially for those causing severe pollution problems.

1.1 Project Scope

The primary concern of this PhD study is to explore and to seek methods of improving freeze-desalting technologies to fill some of the existing gaps of know-how in treating and upgrading effluent waters of extreme salinity for reuse at a reasonable cost and reasonable reliability with least harm to the environment.

The scope of this study involves acquisition of relevant test data using demonstration equipment that incorporates the latest developments in process engineering. Several innovative processes were used and examined to treat a range of liquid streams typical of those causing the most severe pollution problems. The resulting experimental data for each innovative process were assessed to provide state-of-the-art technical and economic assessment of the potential of the proposed technology.

1.2 Objectives

In this thesis, attention was focused on two main themes:

a) Assessment of the conventional desalination and freezing desalination technologies for brine applications based on theoretical studies.
b) Performance assessments of various forms of freezing desalination technologies used for desalting/treating a wide range of salt concentrations of feed waters through comprehensive experimental studies.

Therefore the main objectives of this project are as follows:

- To provide a useful thesis for professionals and technologists in all aspects of brine treatment using desalination technologies.
- To present the reasons why conventional desalination technologies have a limited scope in the treatment/disposal of the concentrated brines.
- To review and update the knowledge of recent developments in the various aspects of brine disposal processes using desalination technologies.
- To review and update the knowledge of recent developments in the various aspects of freezing desalination technologies.

- To establish experimental studies based on the most feasible proposed technologies and applied works in the literature.
- To design, prepare, manufacture, operate and examine the adopted approaches.
- To analyse and to evaluate the experimental data of the examined technologies.
- To assess the separation performances of various forms of freezing desalination technologies for saline water applications.
- To establish reference background experimental data on various forms of freezing desalination technologies with a wide range of salt concentrations of feed water using synthetic waters and process brines.
- To investigate the influence of affecting parameters for the adopted technologies.
- To investigate the applicability of melt crystallisation technologies for treating RO brine and concentrated solutions of RO brine.
- To examine and assess the performance of post treatments such as washing and sweating processes.
- To recommend the most feasible technologies, which are potentially capable to treat brine in a sustainable manner with least harm to the environment and at affordable cost.

CHAPTER II:

LITERATURE REVIEW

2.1 Introduction

Saline water refers to an aqueous solution that contains a significant concentration of dissolved salts. This salt concentration is measured in terms of the "Total Dissolved Solids" (TDS) content, and is often known as the "salinity" [Hanbury *et al.*, 1993]. The TDS is commonly reported by researchers in the water desalination field in either, milligrams per litre (mg/L) or in parts per million (ppm) of salt. There are several types of saline water available around the world. The most predominant natural source of saline water is seawater, which has a TDS typically in the range of 35,000 ppm [Hanbury *et al.*, 1993]. Brackish water is another example of saline water, with salinities between 1,000 to 10,000 ppm. Drinking water generally has an average TDS of 500 ppm, which should at least comply with a certified organisation such as the World Health Organisation (WHO) [Hanbury *et al.*, 1993]. Table (2.1) shows the classification of saline water available, and also includes typical examples of each source of saline water [Ahmad and Williams, 2011].

No.	Water Type	TDS Level – (ppm)	Source
1	*Extremely low saline water*	*≈ nil*	*Distilled waters*
2	*Fresh water*	*1,000 <*	*Drinking waters*
3	*Slightly saline water*	*1,000 to 3,000*	*Aquifers, lakes, rivers, and wastewaters*
4	*Moderately saline water*	*3,000 to 10,000*	
5	*Highly saline water*	*10,000 to 50,000*	*Aquifers, lakes, industrial brines and seawater*
6	*Brine*	*50,000 to 70,000*	*Industrial brines, aquifers, and lakes*
7	*Highly saline brine*	*70,000 up to full saturation*	

Table 2.1: *Classification of saline water available [Ahmad and Williams, 2011].*

This study will focus on brine, particularly Highly Saline Brines (HSB), which are defined as saline waters with extremely high concentrations of dissolved constituents of inorganic

elements, ions, and molecules. As shown in Table (2.1), brine and HSB have a TDS in the region of 50,000 ppm up to full saturation. The sources of these brines can be divided into two main categories, which are; High Saline Natural Brines (HSNB) and High Saline Industrial Brines (HSIB). Typical examples of HSNB are high saline aquifers and lakes (such as the Dead Sea in Jordan and the Om-Alaish aquifers in Kuwait), whereas HSIB are those waste streams with extreme salinity, which are generated from seawater desalination plants, chemical processing, food industries and oil refineries [Ahmad and Williams, 2011]. The concentration process for the waste discharges of other industries (such as brackish water desalination plants, utility power plants, medical, and pulp and paper industries) may also end with brines with a high level of TDS [Hoyle and Dasch, 2011].

The application of Desalination Technologies (DTs) for handling HSB is currently one of the major challenges of applied research because these types of waters cannot be desalted using the conventional DTs [Ahmad and Williams, 2009]. Furthermore, this type of brine limits the scope of choice of treatment systems as the desalination process is expensive and has several technological, operational, and regulatory limitations for such applications. Therefore, the primary concern of this chapter is to provide a comprehensive study for justifying why these technologies have limited scope in the treatment of HSB. This chapter will also explore what kinds of methods are being proposed for handling the HSB by using DTs. There are several reasons why the study of the application of DTs for HSB applications are of interest:

(i) Water Supply

Desalting processes for treating HSNB to produce fresh water for water supply purposes is a significant issue for satisfying the needs of human water consumption in regions where there is a lack of fresh water supplies.

This is a growing problem as water shortages affect over 80 developing countries that are home to half of the world's population [Miller, 2003; Clayton, 2006]. Furthermore, over the next 25 years, the number of people affected by severe water shortages is expected to increase fourfold [Miller, 2003]. Currently, water consumption doubles every 20 years, about twice the rate of population growth [Miller, 2003]. Water shortages are also forecast to increase, especially in urban areas where demand for water is growing [Clayton, 2006]. In

many cases HSNB are usually the only available source of water. In addition, environmental aspects must be considered for such applications because all DTs produce two streams; a fresh water (product) stream and a concentrated salt (brine) stream that must be disposed of. Hence, in inland desalination plants, the possibility for disposing the reject brine to a large body of water (such as the sea) is not available.

(ii) Safe Disposal

As mentioned previously, the primary environmental impacts from any industry are typically associated with the disposal method of the concentrated streams that have been produced from the industrial plant [Ahmad and Williams, 2011]. These waste streams are contaminated in some way by man's industrial or commercial activities prior to their release into the environment [Ahmad and Williams, 2011]. Disposal of HSIB is a common and important problem in many industrial plants, such as the oil and gas industries, because of the extreme salinity and chemical composition of these brines and the fact that some of these effluents may contain toxic substances [Brandt *et al.*, 1997]. Furthermore, these brines are generated in large volumes from many industrial plants and pose a threat to the surrounding environment.

Two important examples of where HSIB occur and their problems are:

a) In inland desalination plants. By assuming that the operators decided to minimise and concentrate the reject brine, then getting rid of the reject brine (which has a high level of TDS) is a significant and important problem because, the option of disposing of the brine to a large body of water (i.e. seawater) is not available. Therefore, the use of small plants that use membrane technology, for instance, is restricted in inland areas (in many countries such as Kuwait) because of the concentrate disposal limitations and its consequences, which may lead to contamination of aquifers with more concentrated waste.
b) In oil and gas industries. In drilling for petroleum there is usually a penetration of porous rocks containing salt water with a much more highly concentrated salt content than that of normal ocean seawater, and it may reach the full saturation [Pols and Harmsen, 1994; Spiegler and El-Sayed, 1994; Brandt *et al.*, 1997]. This means that the brines may be produced in large quantities with extreme

salinity, especially in oil fields that have been producing for long periods of time. Wells may produce hundreds of barrels of brine for every barrel of oil [Hoyle and Dasch, 2011]. The chemical composition of a typical brine from these systems makes it unfit for human consumption or for irrigation purposes, which makes it pose a threat to the aqua-life. Therefore the federal effluent limitation guidelines do not permit the discharge of the produced-brine into surface water [Pols and Harmsen, 1994]. As a result, investors of a producing well are usually faced with the problem of having to dispose of significant quantities of brine in an environmentally acceptable manner at reasonable cost and reasonable reliability.

(iii) Harvesting Salts and Other Useful Products

Harvesting valuable minerals from concentrated brines for beneficial uses must be considered as an alternative method of disposal. The brine should really be dealt with as a resource rather than a waste problem. There are many practical examples of salt production from industrial waste concentrate, for instance, salt production plants using thermal processes were established in Kuwait and the United Arab Emirates more than 17 years ago for producing salts from reject brines of desalination plants [Ahmed *et al.*, 2003]. Howe (2009) reviewed the importance of salts in the waste concentrate from desalination utilities. Many marketable mineral salts can be produced from reject brines such as; NaCl, KCl, Na_2SO_4, K_2SO_4, $MgSO_4$, $Mg(OH)_2$, KNO_3, Na_2NO_3 etc. [Howe, 2009]. Table (2.2) shows an overview of the uses for inorganic feedstock's in different applications [Howe, 2009].

Mineral	**Uses**
NaCl	Textile dyeing, aquaculture, soil stabilization, and ice and snow removal
Cl_2	Polymers, plastics, and synthetic fibres
NaOH	Glass, rayon, synthetic fibres, plastics, polyester, soaps, and detergents
$NaSO_4$	Pulp and paper, dyes, and ceramic glazes
Na_2CO_3	Glass, pulp and paper, and rayon

Table 2.2: *An overview of the uses for inorganic feedstock [Howe, 2009].*

Heavy brines at different concentrations are used in several applications such as chemical industries, brine shrimp production, electricity production by salinity gradient power, irrigation of halophytes, and aquaculture [Howe, 2009]. Howe (2009) also reviewed some facts about the consumption of salt (NaCl) in the United States, for instance, 45,000,000 tons of salt are produced annually, and about 70% of these salts are used by chemical industries, where 21,000,000 tons are utilised for the production of chlorine, 4,000,000 tons are used for the production of soda ash, and about 88% of these salts are used in a liquid form (i.e. heavy brine).

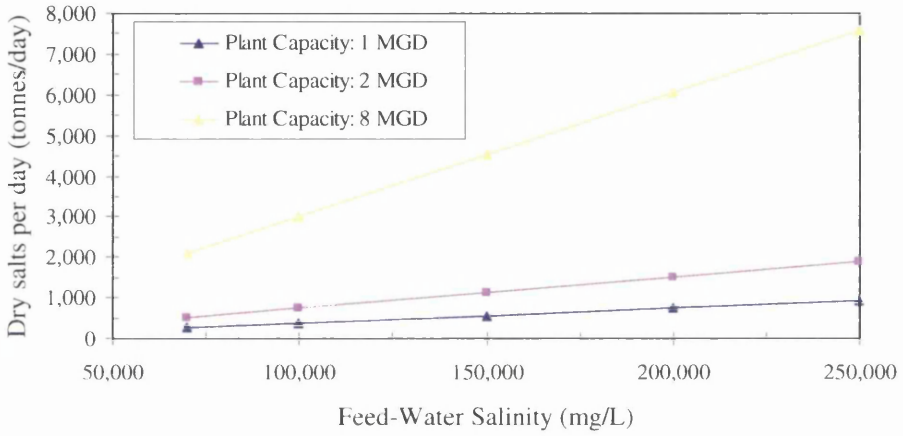

Fig. 2.1: *Dry salts per day versus feed-water salinity [Ahmad and Williams, 2011].*

Simple analytical calculations may also be performed to estimate the amount of dry salts that can be harvested daily from HSB using three different plant capacities of 1, 2, and 8 MGD. For simplification purposes, these calculations assume that the chemical composition of the HSB consists of only pure salt (NaCl salt). Fig (2.1) shows the predicted results of the amount of dry salt that might be produced from HSB feeds of different composition. For instance, by assuming a salt production plant capacity of either 1, 2, or 8 MGD with a feed water which has a TDS of 70,000 ppm, will generate 265, 530, and 2120 tonnes per day, respectively. By increasing the concentration of feed water up to a TDS of 250,000 ppm, then the dry salt production will increase to 946, 1893, and 7571 tonnes per day for the same plant capacities of 1, 2, and 8 MGD, respectively. Although wide varieties of opportunities are available for marketing HSB and their minerals, these streams are often not currently recovered because of a variety of technical challenges, such as osmotic pressure, energy cost, solubility limitations, scaling and fouling problems.

(iv) Harvesting Rare Elements

Rare earth elements are required for a wide range of applications [Kumar *et al.*, 2011]. Seawater represents an infinite source of rare metals since almost all elements in the periodic table including vital trace elements, such as gold, silver, uranium, vanadium, strontium, boron, magnesium, molybdenum, phosphates, silicon, etc. are contained in seawater. These elements are often scarce on land or extraction costs are highly prohibitive [Sugo, 1999; Ohya *et al.*, 2001; Dirach *et al.*, 2005; Jeppesen *et al.*, 2009]. The concentrated brine from desalination plants, on the other hand, represents a concentrate of all elements contained in seawater [Dirach *et al.*, 2005]. Hence, extraction of these elements would be an advantage for desalination plant, leading to them being more environmental friendly and cost effective.

Currently, four compounds are extracted from seawater via the conventional evaporation processes [Jeppesen *et al.*, 2009]. These compounds are principally table salt (i.e. sodium chloride), and the by-products potassium chloride, magnesium and bromide salts [Jeppesen *et al.*, 2009]. Extraction of other compounds from seawater may be feasible, especially for some elements that are highly prohibitive or rare on the land. Therefore, several authors [Ohya *et al.*, 2001; Dirach *et al.*, 2005; Jeppesen *et al.*, 2009] have proposed various extraction schemes for a range of elements.

Element	Seawater (mg/L)	Quantity (t/y)	Major Use	Selling Price ($/kg)	Value (M$/y)
Na	10,500	1.5×10^{6}	Fertilizers	0.13	180
Mg	1,350	1.9×10^{3}	Alloys	2.80	525
K	380	5.3×10^{2}	Fertilizers	0.15	8
Rb	0.12	17	Laser	79,700	1,300
P	0.07	10	Fertilizers	0.02	0
In	0.02	3	Metallic Protection	300	0.9
Cs	5.0×10^{-4}	0.07	Aeronautics	63,000	4
Ge	7.0×10^{-5}	0.01	Electronics	1,700	0.02

Table 2.3: *List of potentially economic extract from the reject brine of membrane desalination plant at la Skhira site in Tunisia [Dirach et al., 2005; Jeppesen et al., 2009].*

Table (2.3) summarises some valuable elements as being potentially economically and technically available [Dirach *et al.*, 2005]. In addition, Table (2.4) shows five valuable rare elements that can be annually extracted from the Pacific Ocean [Sugo, 1999].

Rare Metals	Annual Amount	Annual amount per cross section of
	Plant Capacity (10,000 tons)	Black Current, (t/m^2)
Cobalt, Co	16	0.005
Titanium, Ti	170	0.059
Vanadium, V	340	0.119
Uranium, U	520	0.182
Molybdenum, Mo	1,580	0.553

Table 2.4: *List of potentially economic extracts from the Pacific Ocean (i.e. Black Current Site) in Japan [Sugo, 1999].*

Taking uranium as an example, Gorin (2010) mentioned that the isotopic ratio of uranium in seawater was found to be similar to that as in terrestrial ores. The concentration of uranium in seawater was found to be consistent in various locations around the world, at a concentration level of 3 ppb, which is equivalent to 3 mg U/m^3 [Seko *et al.* 2003; Gorin, 2010]. Although seawater contains extremely low concentrations of uranium, a substantial amount of uranium can be recovered from seawater since there is an enormous amount of seawater, i.e. billions of tons, available in the oceans. Cohen (1983) has calculated the amount of uranium in seawater and the results showed that the 1.4×10^{18} tonnes of seawater contains 4.6×10^{9} tonnes of uranium. Evidence is given in several sources [Heide *et al.*, 1973; Cohen, 1983; Kanno, 1984; Schwochau, 1984; Seko *et al.*, Sugo, 1999; Ohya *et al.*, 2001; 2003; Dirach *et al.*, 2005; Jeppesen *et al.*, 2009; Tamada, 2009; Gorin, 2010; Sather *et al.*, 2010], that there is about 4.5 billion tons of uranium available in the world's oceans, whereas the uranium in terrestrial ores found inland is less than 6 million tons. This means that the available uranium in the world's oceans is much more than that in terrestrial ores. Sugo (1999), on the other hand, has calculated the amount of uranium in the Black Current Site (i.e. Pacific Ocean, in Japan) as approximately 5.2 million tons per year. This amount is almost equivalent to the remaining uranium inventory inland, while Japan consumes about 6,000 tons of uranium per year [Sugo, 1999]. This means that, if only 0.1% of the total

amount of uranium in seawater can be recovered, then the domestic demand for uranium can be supplied in Japan without taking anything from the remaining land based uranium. Consequently, Japanese scientists are devoting their applied research for such applications to take advantage of the appearance of uranium in seawater [Sugo, 1999]. Specific details of various proposed methods for extracting uranium from seawater are available in the literature [Sugo, 1999; Ohya *et al.*, 2001; Dirach *et al.*, 2005; Jeppesen *et al.*, 2009].

Previous studies have stated three important facts on uranium in seawater, which are; (i) the concentration of uranium in one litre of seawater is potentially capable of providing enough energy to power a delivery pump for raising that litre up to 17m uphill [Gorin, 2010], (ii) if 16,000 tonne of uranium per year can be extracted from seawater, then it would supply 25 times the world's electricity usage and twice the world total energy consumption in 1983 [Cohen, 1983], (iii) the estimated amount of uranium in seawater could supply the world's electricity usage, generated from nuclear energy in 1983, for 7 million years [Cohen, 1983].

Currently, the uranium price is $51.98 (September 2011), while it hit $136.22 in June 2007 according to Index Mundi (2011). This means that the available amount of uranium in seawater is worth trillions of dollars of fuel for nuclear power plants [Gorin, 2010].

Due to the fact that uranium metal represents an inevitable resource for nuclear power plants, uranium recovery from seawater becomes one of the most important research areas, especially for those countries, such as Japan, who deal with nuclear power plants. Hence, several uranium extraction methods have been widely developed and tested for recovering uranium metal [Tamada, 2009; Gorin, 2010]. The most promising process deals with absorption of the uranyl ion through binding to a chemical ligand [Schwochau, 1984; Seko *et al.*, 2003; Tamada, 2009; Gorin, 2010; Sather *et al.*, 2010]. Other uranium extraction methods include the use of biological material, such as bacteria and algae, to concentrate the uranium for simplifying the extraction process, and nanomembrane filtering techniques [Heide *et al.*, 1973; Kanno, 1984; Schwochau, 1984; Gorin, 2010;].

In Japan, the supply of electricity, generated from nuclear energy, is threatened by demand of uranium which will exceed the supply in the near future [Sugo, 1999]. Accordingly, a number of research studies on uranium recovery from seawater have been performed for two

decades using various scales from a laboratory scale to an offshore plant scale [Seko *et al.*, 2003]. Extensive development of high performance adsorbents and feasibility studies led to the development of an uranium recovery method which was proposed, used, and tested by Seko *et al.* (2003). Seko *et al.* (2003) have carried out a project using an offshore plant, which utilising a uranium specific non-woven fabric as the adsorbent packed in an adsorption cage with cross-sectional area and height of 16 m^2 and 16 cm, respectively. Three adsorption cages were submerged in the Pacific Ocean at a depth of 20 m, which is located 7 km offshore of Japan [Seko *et al.*, 2003]. Theses adsorption cages consisted of stacks of 52,000 sheets of the uranium-specific non-woven fabric with a total mass of 350 kg [Seko *et al.*, 2003]. The total amount of uranium recovered by the proposed examined system was less than 1 kg in terms of yellow cake over a submersion period of 240 days [Seko *et al.*, 2003].

2.2 Principles of Current Desalination Technologies

Desalination technology can be defined as a treatment system that is capable of producing fresh potable water from a saline water supply at a reasonable cost and reasonable reliability [Hanbury *et al.*, 1993]. The desalting process can be achieved by a number of different techniques (such as thermal and membrane processes) that either removes the salt molecules or the water molecules from the saline water [Spiegler and El-Sayed, 1994]. The conversion of saline water into fresh water requires energy to operate the desalination process [Hanbury *et al.*, 1993; Spiegler and El-Sayed, 1994]. Hence, the energy input into any desalination plant may be in a form of thermal, mechanical or electrical energy, and is often a combination of all three in varying proportions [Hanbury *et al.*, 1993]. However, desalination plants can usually be classed as principally consuming one of the three types of energy [Hanbury *et al.*, 1993; Spiegler and El-Sayed, 1994]. In general, Table (2.5) shows a variety of conventional DTs that have been developed for over 60 years. These technologies are divided into three main categories which include; thermal, membrane, and chemical processes [Buros, 2000].

The capability of any desalination process is dependant on two crucial factors, which are; the salinity and the degree of hardness of the feed water. Therefore, based on the economical and technical feasibility corresponding to the salinity of the feed water, the capability of DTs is identified and summarised in Fig (2.2). However, the degree of hardness of the feed water

(which depends on the chemical composition of the feed water) may contribute to change the capability limit of the DTs that are shown in Fig (2.2).

Processes	Concept	System
Conventional	Thermal	Multi-Stage Flash Distillation
		Multi-Effect Distillation
		Vapour Compression
	Membrane	Electrodialysis
		Reverse Osmosis
	Chemical	Ion Exchange

Table 2.5: *An overview of the conventional desalination technologies.*

The principles of conventional DTs that appear in Table (2.5), are described in more detail in the literature [Hanbury *et al.*, 1993; Spiegler and El-Sayed, 1994; Mulder, 1996; Buros, 2000; United Nations, 2001; Ahmed *et al.*, 2003; Howe, 2009], however, the assessment of conventional DTs for HSB applications can be divided into three sections.

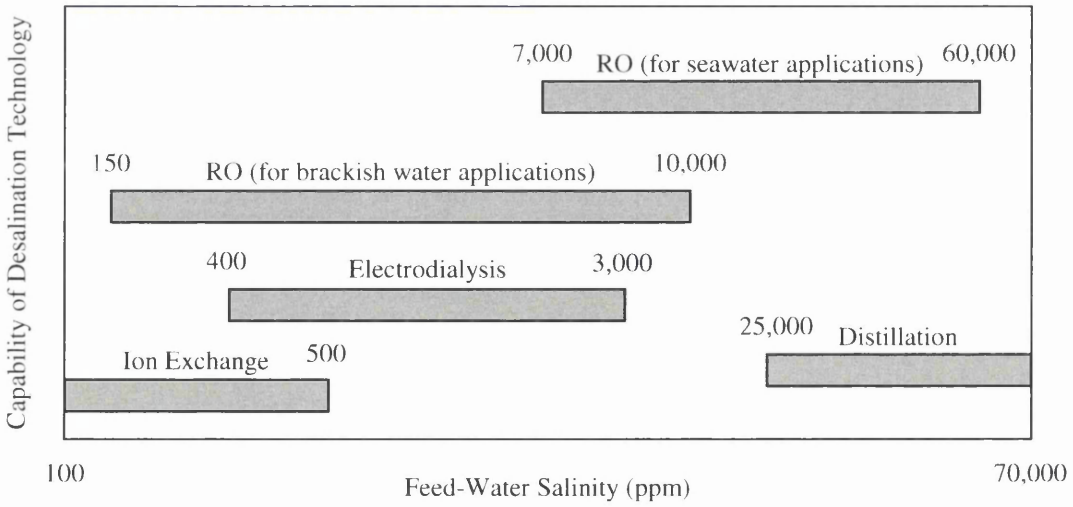

Fig. 2.2: *Feed-water salinity and process applicability.*

2.2.1 Conventional Thermal Desalination

The thermal process reflects the phenomenon of the natural water cycle by heating of saline water and collecting the condensed vapour (distillate) to produce pure water. The

evaporation of water molecules from brine can be accelerated and accomplished by two main mechanisms; boiling and flash evaporation. In the boiling process, the heat transfer and the evaporation take place at the same pressure and location. While in flash evaporation, the liquid to be evaporated is first heated under a pressure in excess of its saturation, which leads the thermal energy being stored in the form of increased liquid temperature. The heated liquid is then introduced into a separate vessel (flash chamber) remote from the heat transfer surface which is maintained at a pressure lower than the saturation pressure corresponding to the temperature of the heated liquid. On entry to the flash chamber, the liquid boils spontaneously (flashes) due to the latent heat being drawn from the thermal capacity of the bulk of the liquid and thus lowering the temperature [Hanbury *et al.*, 1993]. As indicated in Table (2.5), there are several thermal processes which include; Multiple-Stage Flash distillation (MSF), Multiple Effect Distillation (MED), and Vapour Compression (VC) [Spiegler and El-Sayed, 1994].

The MED and MSF processes involve boiling the brine in adjacent chambers at successively lower vapour pressures without adding any source of heat following, the first stage for the MED process [U.S. Congress, 1988], or the brine heater for the MSF process [U.S. Congress, 1988]. However, the main difference between the two concepts is that, in the MED process, the evaporation of brine can be achieved by boiling and flash evaporation, while in the MSF process, the evaporation of brine is accomplished by a flash evaporation [U.S. Congress, 1988]. With regard to the VC process, the heat required for the evaporation of seawater is supplied by the compression of the vapour, either with a Mechanical Vapour Compressor (MVC) or a steam ejector which is known as 'Thermal Vapour Compressor' (TVC) rather than using the direct exchange of heat from steam which is produced from a steam generator i.e. boiler. This process may be used either in combination with other processes such as MED, or by itself [Buros, 2000].

As shown in Fig (2.2), conventional thermal DTs are designed and constructed for saline water with certain limits of total dissolved solids (i.e. 25,000 - 70,000 ppm). These processes are not recommended and unlikely to be used for desalting brackish waters because the capital and operational costs of these plants are prohibitive in comparison to other processes such as membrane technologies [Hanbury *et al.*, 1993]. For HSB applications, conventional distillation processes such as MED and MSF are not suitable for treating these types of water

because of two main reasons. Firstly, technical problems, for such an application, the degree of hardness of the feed water is expected to be proportional to the salinity, which means that there is high risk of scale deposition, fouling, and corrosion, which may occur on the heat transfer surfaces in MSF and MED plants. The formation of a non-alkaline scale in equipment in thermal desalination plants becomes exaggerated at high temperature because calcium sulphate ($CaSO_4$) solubility decreases as the solution temperatures increases [Hanbury *et al.*, 1993] ($CaSO_4$ begins to leave saline water when the top brine temperature approaches 115 °C (203 °F)). In general, scale deposition can form on the tube surfaces of the evaporators and condensers, which leads to a restriction of heat transfer, reducing the performance of the process equipment (i.e. reducing evaporation rates). This has a general detrimental effect on thermal efficiency. Secondly, economical aspects such as the operational and capital costs of the conventional MSF and MED plants are prohibitive and this aspect represents another obstacle for HSB applications. Therefore, conventional distillation processes are technically and economically unfeasible for such HSB applications [Spiegler and Laird, 1980; Hanbury *et al.*, 1993; Buros, 2000]. On the other hand, there are other thermal distillation processes which are available for HSB applications, which do not suffer in their operation from scaling problems and these technologies will be discussed in further detail in section 2.3.

2.2.2 Membranes Processes

A membrane can be described as selective barrier or interface between two phases. Separation by a membrane can be achieved through the membranes porosity. A membrane has the capability to allow selective transport of certain chemical species through, while simultaneously preventing the passage of other substances. In general, membrane processes can be used with various driving mechanisms such as pressure, concentration, electrical potential [Mulder, 1996; Younos and Tulou, 2005].

The most frequently used membrane technology for desalting saline water is pressure-driven Reverse Osmosis (RO). Osmotic pressure is a natural phenomenon by which molecules of water are transported from a compartment having water with a low salt concentration through a semi-permeable membrane into a water compartment with a higher salt concentration. In RO as the name suggests, a pressure is applied to a compartment of higher salt concentration to force the molecules of water to flow in a reverse direction through the

semi-permeable membrane, leaving behind a more concentrated salty water known as 'brine' and a product of pure water. The driving force for salt water separation in this process is applied pressure using a high pressure pump [Mulder, 1996]. Electrodialysis (ED) is a voltage-driven membrane process, which utilises "ion selective membranes" that are preferentially permeable to either positively-charged ions (cations) or negatively-charged ions (anions) [Hanbury *et al.*, 1993]. This process involves an electrical energy to transport chemical constituents of an aqueous solution through the membranes leaving fresh water behind as product water [Hanbury *et al.*, 1993].

As shown in Fig (2.2), RO membranes are used for different salinities of feed water varying from 150 – 60,000 ppm, whereas the ED process is commonly used for feed water which has a TDS in the region of 400 – 3,000 ppm. For HSB applications, a variety of operational problems can be experienced with membrane facilities. The major problems are scaling, fouling, corrosion, high capital cost and intensive energy use [Hanbury *et al.*, 1993]. In a RO process for instance, the separation process utilises energy in the form of pressure to transport water molecules through the semi-permeable membrane. Therefore, this process is energy intensive for HSB because as the TDS concentration rises, the osmotic pressure of the feed solution rises, meaning that more energy is needed to dewater the brine [Hanbury *et al.*, 1993]. This high osmotic pressure leads to an increase in the operational cost. The osmotic pressure can be determined theoretically by the following expression [Hanbury *et al.*, 1993]:

$$\pi = \frac{vRTx_s}{v_w} \qquad (2.1)$$

Moreover, the predicted minimum energy required (i.e. for operation at a given osmotic pressure) can be obtained theoretically [Hanbury *et al.*, 1993]:

$$E_{\min} = \pi \times v_w \qquad (2.2)$$

Fig (2.3) shows the results of calculations for the osmotic pressure and minimum energy required for different feed water concentrations. These analytical calculations assume that the feed water contains only pure salt (NaCl) for simplification.

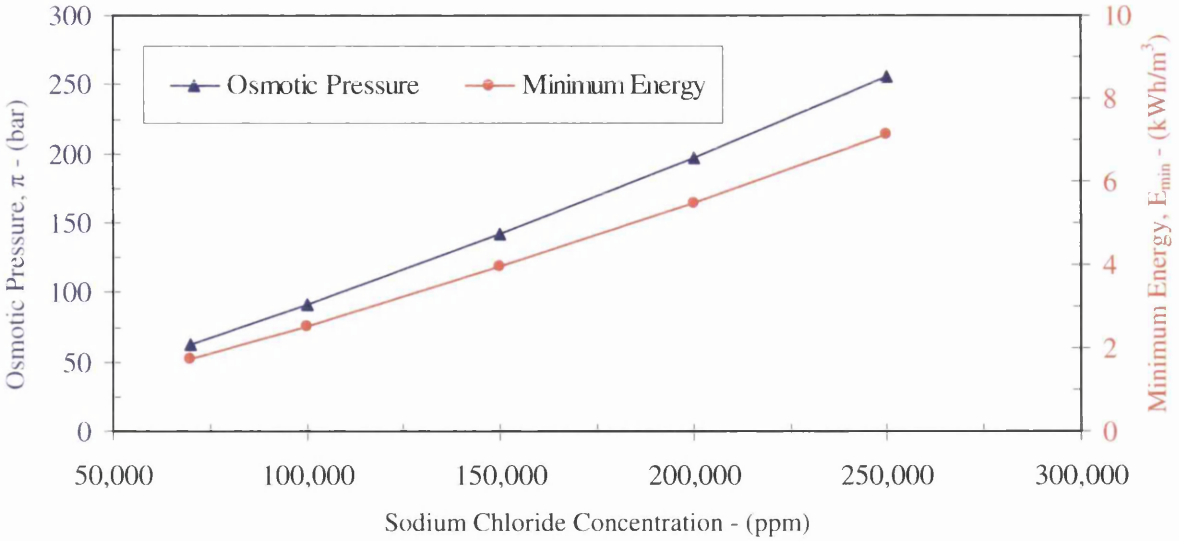

Fig. 2.3: *Osmotic pressure and minimum energy consumption predictions for NaCl at 25°C.*

Fig (2.3) shows that the osmotic pressure varies from 62.3 – 256 bar for the salinities of 70,000 – 250,000 ppm respectively. Furthermore, the osmotic pressure is found to be a strong function of the salinity or more strictly the solute activity. With regard to energy requirements, the energy consumption is proportional to the osmotic pressure of the feed water (see Equation 2.2). As shown in Fig (2.3), the minimum energy consumption varies from 1.73 – 7.11 kW/m^3 for salinities of 70,000 – 250,000 ppm respectively. However, the separation process consumes more energy than the minimum amount obtained through analytical calculations. This is due to the excess of the applied pressure difference across the membrane, ΔP, over the difference in osmotic pressure across the membrane, $\Delta\pi$. Hence, if the RO plant operates at a pressure only just in excess of the osmotic pressure difference which is the condition for the minimum energy consumption, then the water flow (treated water-product) will be very small and salt flow will be finite, resulting in the product water quality being relatively poor [Hanbury *et al.*, 1993]. As the pressure of the operation is increased, the water flow increases, but the salt flow will remain relatively constant and so the quality of the product water will improve. Also, plants operating at pressures only just in excess of the osmotic pressure of the brine will only produce very small fluxes and will therefore require large membrane areas which will increase cost. Therefore, in practice RO plants are operated at pressures which are well in excess of the osmotic pressure of the reject brine [Hanbury *et al.*, 1993]. These results demonstrate that RO is not promising for HSB application because of the high operating pressure required. Current membranes and membrane modules cannot be used under these osmotic pressures. However, by assuming

that there are a new generation of RO membranes that are capable of being used at high operating pressures for HSB applications, then these membranes will be under high risk of scaling deposition and fouling problems because of the degree of hardness accompanied with the salinity of HSB. The scaling problem results in the deterioration of membrane performance, poor efficiency and short membrane life because scale deposits formed at the surfaces of the membranes, act as ionic sieves [Hanbury *et al.*, 1993]. They are usually composed of different minerals such as sulphates, calcium carbonate, and magnesium hydroxide. With regard to the fouling, the build-up of a layer of constituents on the surface of a membrane will interfere drastically with the performance of the membrane in terms of its primary separation function (e.g. removing ions), which means a reduction in product water flux and an increase in salt passage. In the other words, the product water quality will be relatively poor and the flow rate of the product water will decline [Hanbury *et al.*, 1993]. In addition to these technical problems, RO plants will encounter corrosion problems, which lead to an increase in the maintenance costs. This process will also be equipped with expensive pipelines, high pressure pumps and accessories which will eventually increase the capital costs. Nevertheless, for such an application, the outlet reject brine of an RO plant, will be much higher in salt concentration than the feed water, and must be disposed of with the least harm to the environment. Therefore, the RO process is not potentially applicable for HSB applications. On the other hand, in some cases where the brine concentration reaches salinities with a TDS of less than 60,000 ppm, RO plant may play an important role in Zero Liquid Discharge (ZLD) systems (this application is discussed in further detail in section 2.3.2).

In the ED process, the higher the salinity of the raw water, the more the electrical power that is required [Hanbury *et al.*, 1993]. This process is therefore relatively expensive in energy costs for HSB application. This is due to the direct relation between required electrical energy and feed salinity and also trends towards lower current efficiencies in HSB due to increased water transport across the membranes and also to lower membrane selectivity's. Hence a rough estimate of the value of energy consumption of electrodialysis, for HSB applications, can be predicted using [Hanbury *et al.*, 1993]:

$$\text{Total energy} = 0.7\ \frac{kW}{m^3}\ \text{(of product water)} + 0.7\ \frac{kW}{m^3}\ \text{(per 1,000 ppm salt removed)} \qquad (2.3)$$

Fig (2.4) summaries the predicted energy requirement to produce a product water of 500 ppm from feed water salinities of 70,000 – 250,000 ppm. Again, this has been calculated under the assumption that the salt composition of the brine is purely NaCl. For a feed water of 70,000 ppm the energy required is 49.7 kW/m^3 whereas, for a feed of 250,000 ppm, the energy requirement increases to 175.7 kW/m^3. These figures are indicators only for the energy requirement, as this will also depend upon the detailed design, operation and production rates required from the plant. Although the electrodialysis process is, technically, capable of treating HSB, the theoretical results of energy requirement show that this technology is very energy intensive for such an application. On the other hand, with regard to the scaling and fouling problems, the deposition of scales or other fouling agents (including fine particulate matter) on an electrodialysis plant are not as critical as in RO membrane plants [Buros, 2000]. However, such deposition, if allowed to occur in HSB applications, will affect plant performance by causing a reduction in the amount of desalination achieved (poor product water quality) and by decreasing the limiting current density by an order of magnitude leading to eventual membrane failure. Furthermore, the deposition of scaling plugs the membranes, increasing the electrical or hydraulic resistance and power consumption which leads to deterioration in the electrodialysis performance and increases in the operational costs. Therefore, the risk of scaling in ED process should be considered for HSB applications.

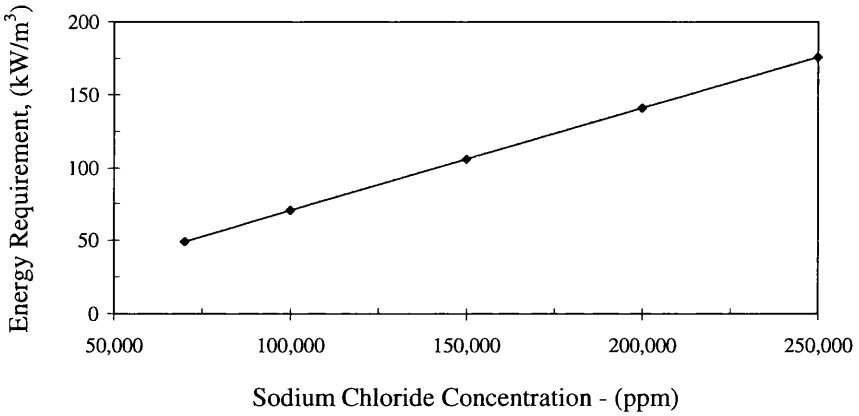

Fig. 2.4: *Energy requirement predictions for electrodialysis versus the salinity.*

One technology that has not been discussed so far is a cross-over technology between thermal and membrane processes called membrane distillation (MD) [Lawson and Lloyd,

1997; Alklaibi and Loar, 2004; El-Bourawi *et al.*, 2006]. MD is a relatively new technology that was first proposed in the late 60's and is a thermally driven process in which only vapour molecules are transported through hydrophobic membranes [Lawson and Lloyd, 1997; Alklaibi and Loar, 2004; El-Bourawi *et al.*, 2006]. MD systems can be classified into four major configurations (i) direct contact MD (DCMD) (ii) air gap MD (AGMD) (iii) sweeping gas MD (SGMD) and (iv) vacuum MD (VMD), for more details on these systems refer to [Lawson and Lloyd, 1997; Alklaibi and Loar, 2004; El-Bourawi *et al.*, 2006]. DCMD and AGMD are best suited for applications involving water whereas SGMD and VMD are best suited for organics [Alklaibi and Loar, 2004]. The benefits of MD compared to other water desalination systems include: 100% (theoretical) rejection of ions, macromolecules, colloids, cells and other non-volatiles, lower operating temperatures than conventional distillation, lower operating pressures than conventional pressure-driven membrane separation processes, reduced chemical interaction between membrane and process solutions, less demanding membrane mechanical property requirements and reduced vapour spaces compared to conventional distillation processes [Lawson and Lloyd, 1997]. However, despite the initial promise, interest in the process faded quickly due in part to the observed lower production rate of water compared to RO [El-Bourawi *et al.*, 2006]. The main barriers to commercial implementation of MD have been due to the relatively low permeate fluxes and low productivity, permeate decay due to flux and temperature polarisation, membrane and module design and high thermal energy consumption [Lawson and Lloyd, 1997; Alklaibi and Loar, 2004; El-Bourawi *et al.*, 2006]. Also the cost of water produced by MD (1.32 $\$/m^3$) is greater than the cost of water produced by RO (1.25 $\$/m^3$) for the same desalination process [Alklaibi and Loar, 2004]. This difference may seem small, however, for a small desalination system producing 1000 m^3/day, this equates to a saving of $25,550 per annum when using RO. Small margins in these reasonably large volume production systems can make a significant difference. In terms of energy efficiency, though, optimized MD plants with internal heat recovery have been shown to be close to MSF plants [Alklaibi and Loar, 2004]. Nonetheless, more recent attempts have been made to revive the use of this technology due to improvements in membranes and module design and the integration of low grade waste and alternative energy sources with MD [El-Bourawi *et al.*, 2006; Al-Obaidani *et al.*, 2008; Curcio *et al.*, 2009; Curcio *et al.*, 2010]. In terms of the treatment of HSB, MD does possess a big advantage. This is due to the fact that MD permeate flux is only slightly affected by the concentration of the feed and thus unlike other membrane processes productivity and

performance remain roughly the same for high concentration feeds [Alklaibi and Loar, 2004].

2.2.3 Chemical Processes

There are several chemical approaches, including processes such as ion exchange and electrum, are widely used for treating/desalting saline waters [Hanbury *et al.*, 1993]. These processes have the potential capability to produce water with extremely low ionic content from a feed water with few tens or perhaps low hundreds of ppm TDS [Hanbury *et al.*, 1993].

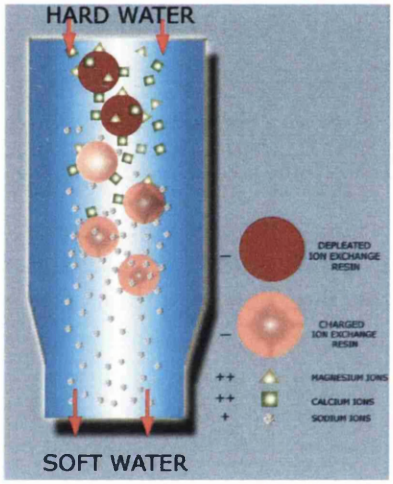

Fig. 2.5: *A schematic illustration of the ion exchange concept for softening process [LeeWebWorks LLC, 2007].*

Ion exchange, as the name of the process implies, involves the interchange of ions between a solution and an insoluble solid which is either a polymeric or mineralic ion exchanger e.g. as ion exchange resins (functionalized porous or gel polymer), natural or synthetic zeolites, montmorillonite, clay [Pintar *et al.*, 2001; Da˛browski *et al.*, 2004; Spiro, 2009; Bochenek *et al.*, 2011]. In the water treatment process, for instance, the undesirable ions in the water supply are replaced with more acceptable ions as the feed water passes through granular chemicals, called ion exchange resins [Bochenek *et al.*, 2011]. This is achieved by removing one type of ion from the feed stream and replacing the ion with an equivalent quantity of another ion of the same charge [U.S. Congress, 1988]. For instance, in softening processes (see Fig (2.5)), hardness ions (such as calcium and magnesium) are replaced with sodium

ions, whereas, in de-alkalization processes, the ions that are contributing to alkalinity, such as; carbonate, bicarbonate, etc..., are removed and replaced with chloride ions [NALCO, 1998]. Other de-alkalization processes utilise weak and strong acid cation resins in a split stream process, where these cations exchange with hydrogen [NALCO, 1998]. This forms carbonic acid which can be removed in a post-treatment system such as a de-carbonator tower. Demineralization, on the other hand, is replacing all cations with hydrogen ions (H^+) and all anions with hydroxide ions (OH^-) [NALCO, 1998].

Ion exchange is used in a wide range of industries such as production of various acids, bases, salts, for industrial drying and treatment gases, in bio-molecular separations as well as food industries [Bochenek *et al.*, 2011]. This technology is commonly used in water and wastewater treatments in commercial and industrial applications such as water softening, demineralisation, and decontamination [Spiro, 2009; Bochenek *et al.*, 2011]. For example, cation exchange resins are typically used for domestic purposes (i.e. homes) and municipal wastewater treatment plants to remove the hardness ions such as; calcium and magnesium from feed stream [Spiro, 2009; Bochenek *et al.*, 2011]. The production of ultra-pure water for industries is also achieved through this technology.

It is impossible to have a uniform scheme of ion exchange systems for different types of applications. A typical example of an ion exchange unit is illustrated in Fig (2.6). The ion exchange reservoir contains a bed of resin which is usually supported by another bed of either graded gravel or anthracite filter media [NALCO, 1998]. Another type of ion exchange system may have a different type of support method that does not include either a gravel or anthracite [NALCO, 1998].

As explained by Bochenek *et al.* (2011), the operation cycle of ion exchange using a fixed-bed column system, which is used for water and wastewater applications, contains two subsequent operational stages: saturation and regeneration [Bochenek *et al.*, 2011]. During the operation process (i.e. saturation), the feed with the undesired ions is distributed over the surface of the bed of ion exchange resin via the upper distribution system. The undesirable ions in the distributed water are replaced with desired ions as the distributed water passes through the bed of exchange resin. The treated water with the desired ions is then withdrawn and collected via a pipe collector, installed below the bed of the ion exchange resin, leading

to a product outlet pipeline [Bochenek *et al.*, 2011]. When the concentration of the undesired ion exceeds the permissible limit, the ion exchange bed must be regenerated periodically to restore its exchange capacity and return it back into the initial conditions [Bochenek *et al.*, 2011]. This step is known as regeneration [NALCO, 1998]. The regeneration method is implemented either by the co-current flow regeneration, which is achieved by flowing the regenerant in an opposite direction to the service flow feed-water, or vice versa i.e. co-current flow regeneration. The former has a lower leakage rate when compared to the latter. The regeneration mode contains two subsequent operational stages: elution and re-equilibrium [Bochenek *et al.*, 2011]. The former is achieved by replacing the retained ions with ions of a regenerant and is then followed by column re-equilibration where the regenerant is washed out in order to bring the fixed-bed column system back to the initial conditions [Bochenek *et al.*, 2011].

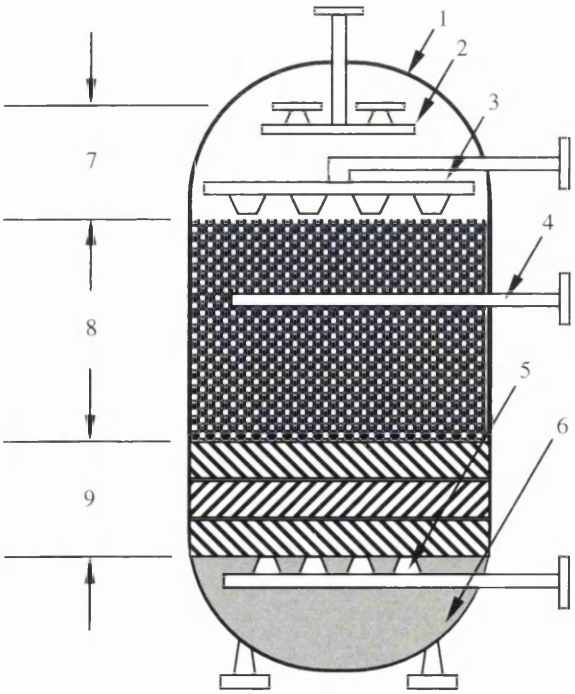

Fig. 2.6: *A schematic view of a typical example of an ion exchange unit, adopted from [NALCO, 1998], where; (1) Ion exchange reservoir, (2) Upper distribution, backwash outlet, and rinse inlet, (3) Chemical inlet and distribution, (4) Sub-surface washer (optional), (5) Lower distributor with strainers, (6) Concrete sub-fill, (7) Free board or rinsing space, (8) Exchange resin, and (9) Support.*

Depending on several factors, such as feed quality, and proper design and running with optimal operating conditions, the ion exchange process is capable of almost entirely eliminating the undesired ion from the treated water, where in some cases the salt concentration of the treated water is reduced to parts per million [NALCO, 1998].

Although other water treatment systems, such as chemical reactions, electro-flotation, reverse osmosis and adsorption, are more effective than ion exchange in terms of ion removal, ion exchange is an attractive process because of the processes relative simplicity [Flores and Cabassud, 1999; Bochenek *et al.*, 2011]. In many cases, the ion exchange process is found to be a more feasible economic option in terms of effective removal of ions from diluted solutions and wastewaters [Pintar *et al.*, 2001; Valverde *et al.*, 2006; Bochenek *et al.*, 2011].

Unfortunately, in the softening processes, the separation performance of ion exchange is seriously impaired and deteriorated when the treatment system deals with high levels of salt concentration of feed [Brown and Sheedy, 2002]. Chen (1984) pointed out that the hardness leakage level is directly proportional to two crucial factors, which are; salt concentration of feed and the hardness concentration in the brine regenerant. This means high purity brine regenerant must be used when the treatment system deals with a high level of salt concentration of feed. Mommaerts (1999) performed analytical solutions to predict the performance of ion exchange for treating saline waters with a TDS higher than 5,000 ppm, the results showed that it is possible to obtain product water with a low hardness level by treating feed with a strong acid cation resin [Brown and Sheedy, 2002]. To date, the ion exchange process is usually used for treating feed streams with a low salt concentration (<3,000 ppm) [U.S. Congress, 1988; Brown and Sheedy, 2002].

In general, it is expected that the higher the salt concentration of feed stream, the more frequent the resins will need to be replaced or regenerated, therefore these processes are considered impractical and not economically feasible for treating waters with high levels of dissolved solids, hence, these technologies are not suitable for HSB applications [U.S. Congress, 1988; Hanbury *et al.*, 1993; Tillberg, 2004].

2.3 Freezing Desalination Technologies

These processes are based on the fact that when saline water freezes, the individual ice crystals consisting of pure water are formed, leaving dissolved organic and inorganic solids behind. However, the ice crystals are usually impure due to inclusion of drops or pockets of the reject brine. Therefore, the ice crystal are usually separated from mother liquor and then washed and melted to obtain potable water.

The fact that freeze-melting can purify and concentrate liquids has been known for many years, with the first recorded examples of the process being in the 1600's [Nebbia and Menozzi, 1968]. According to Nebbia and Menozzi (1968), the Danish physician Thomas Bartholinus (1616-1680) was the first to report that drinking water can be obtained by melting the ice crystals that are formed on the seawater. Robert Bolye (1627-1691) also reported a similar observation at almost the same time, while Jesuit Athanasios Kircher (1602-1680) discussed the reason behind this phenomenon [Nebbia and Menozzi 1968]. Over the past years, Samuel Reyher (1635-1714) described an experiment to analyse the salt content of the sea-ice and found that drinking water can be achieved by melting the ice [Nebbia and Menozzi 1968]. Therefore, the phenomenon was used by travellers and sailors as a source of drinking water [Nebbia and Menozzi 1968]. The British physician Edward Nairne (d. 1806) reported the results of specific gravity of the water obtained by melting the ice, and also measured the freezing point of seawater.

The first apparatus as well as the first publish paper for water desalination by freezing was introduced by Anton Maria Lorgna (1735-1796) in 1786 [Nebbia and Menozzi 1968]. Lorgna carried out the first experiments on desalination by freezing, through producing a block of fresh water ice from seawater. The laboratory apparatus was capable of reducing the TDS of seawater from 36,200 ppm down to traces of salts over a series of successive freezing stages [Nebbia and Menozzi 1968]. Several types of turbid waters were also investigated [Nebbia and Menozzi 1968]. The apparatus was further developed in order to be equipped with a washing process prior to conducting the melting operation. All experimental results showed that the product waters were produced at high standard quality [Nebbia and Menozzi 1968]. Before developing the refrigeration systems, the proposed treatment system was not practical and was limited to the coldest regions and seasons [Nebbia and Menozzi 1968]. According to Nebbia and Menozzi (1968), the first experimental freezing desalination

plant was revived in the late 1930's in Italy by the Institute Superior di Sánita. This desalination plant was operated using the indirect freezing process.

According to Johnson (1976), the first successful pilot plant was demonstrated by the Carrier Corporation. This plant used a vacuum freeze process employing an absorption system. Another company, known as the Structures Wells Corporation, was heavily involved in developing a secondary refrigerant freeze technology. A plant with a capacity of 200,000 gpd was built during the early 1960s [Johnson, 1976]. Colt industries, on the other hand, continued the development of a primary vacuum freeze process, and successfully constructed a pilot plant with a capacity of 100,000 gpd at Wrightville Beach, North Carolina (USA), in the late 1960s. The plant was tested over 2000 h of operation, and the power consumption was less than 47 kWh/1000 g (≈10.34 kWh/m^3), which was encouraging for a non-optimised pilot plant [Johnson, 1976]. The United Kingdom Atomic Energy Authority (UKAEA) in cooperation with Simon Carves, which is commercial organisation, developed a secondary refrigerant process with a plant capacity of 10,000 gpd [Johnson, 1976]. The investigated plant was successfully operated and the results were encouraging enough to scale up the plant capacity up to 1 MGD, and was to be constructed at Ipswich (England), but was then rejected [Johnson, 1976]. In addition to these plants, several freezing desalination plants were built for the purpose of creating drinking water. A pilot plant using vacuum freezing vapour compression technology was constructed in Eilat (Israel); while another plant, utilising secondary refrigerant freezing, was built in Florida (USA); and a pilot plant, using an indirect freezing process, was built in Yanbu (Saudia Arabia) [Rich *et al.*, 2011].

2.3.1 Description of the basic freezing desalination processes

Several approaches using freezing desalination technologies were developed in the period 1950 – 1970 [Spiegler and El-Sayed, 1994]. The classification of the different Freeze-Melting (FM) processes can be divided into three concepts based on contact of refrigerant with the solution; direct contact freezing, indirect contact freezing, and vacuum freezing [Spiegler and Laird, 1980; Spiegler and El-Sayed, 1994; Rahman *et al.*, 2007]. The most commonly known technologies are indirect freezing process with a secondary refrigerant, vacuum-freezing vapour compression process, vacuum-freezing vapour absorption process,

and secondary refrigerant freezing process. In brief, the principle of each technology is described in the following sections.

2.3.1.1 Indirect freezing process with a secondary refrigerant

Figure (2.7) shows the flow process diagram of the main equipment of a simple indirect-refrigeration method. A separate conventional vapour compression refrigeration cycle absorbs heat from the seawater in the freezing chamber, and then delivers heat to the separated ice crystal in the melting unit. The freezer chamber and melting unit simply represent the refrigeration cycle evaporator and condenser, respectively. Hence, the operation of the compressor must be optimised in order to maintain the temperature of the refrigerant below that required in the freezing chamber and higher than that required in the melting unit. The incoming seawater is initially pumped through the heat exchanger to the freezing chamber. Thus, the incoming seawater feed is initially pre-cooled by the heat exchanger before entering the freezing chamber. The heat exchanger is designed to optimise the heat available from the two different cold streams, i.e. rejected brine and melted ice crystal, while reducing the temperature of the incoming seawater feed. The temperature of seawater is further reduced until a critical temperature is reached. As a result, the ice crystals are formed inside the freezing chamber. The ice slurry, including ice crystals and reject brine, is pumped to the separation unit where the ice crystals and reject brine are split into two streams. The separation unit will be discussed later in section 2.3.1.5. The reject brine is removed from the system, while the ice stream is transferred to the melting unit where the ice absorbs heat from the refrigerant through a heat transfer surface, leading to melting of the ice resulting in fresh water, as the refrigerant is condensed. Prior to discharging the melted ice from the system, a small amount of product water is taken to the separation unit as washing liquor. The desired amount of wash liquor does not exceed 5% of the total product water [Johnson, 1976]. The remaining product water is then taken from melting unit to the product discharge passing through the heat exchanger. Thus, the temperature of the incoming feed is reduced.

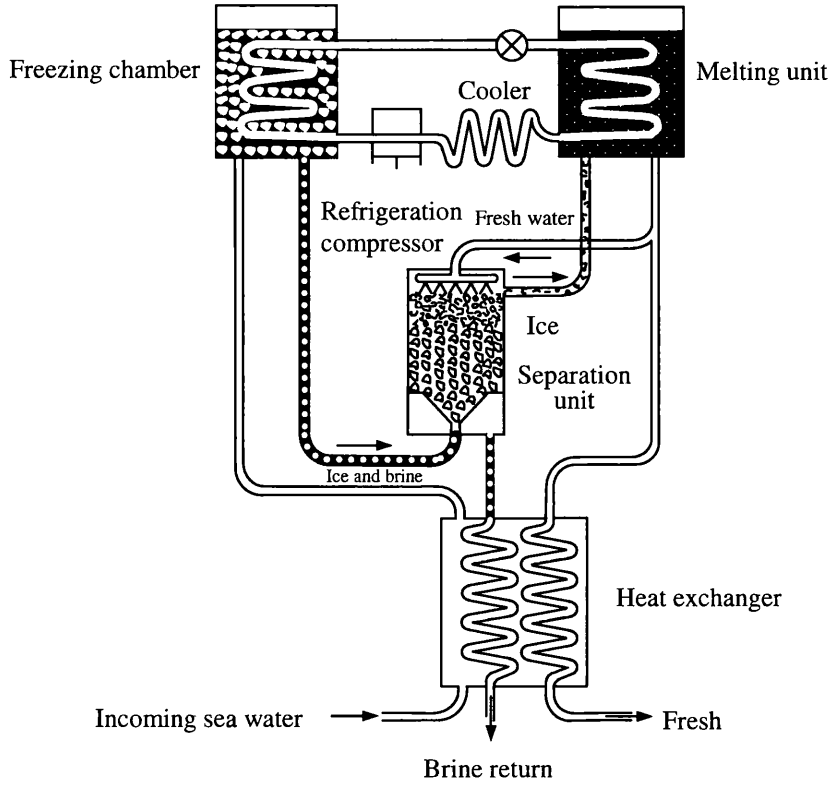

Fig. 2.7: Flow process diagram of the main equipment of an indirect freezing process [Spiegler, 1966].

Although the indirect refrigerant method is a straightforward and simple process, a number of disadvantages can be encountered in applying this technology [Weiss, 1973; Spiegler and El-Sayed, 1994]. For instance, the energy consumption is relatively high, because of the resistance of the heat transfer surface between the refrigerant and saline water [Weiss, 1973]. In order to apply this technology, the freezing chamber and melting unit are required to be built with large metallic heat transfer surfaces. As a result, the equipment becomes more complex and capital cost is prohibitive [Weiss, 1973]. This includes complexity in operating and maintaining the optimal operating conditions. Therefore, this process is not feasible for seawater applications [Weiss, 1973; Spiegler and El-Sayed, 1994].

2.3.1.2 Vacuum-freezing vapour compression process

In the vacuum freeze-vapour compression method, the water itself is used as a refrigerant [Spiegler, 1966]. This is achieved by introducing the seawater into a vacuum chamber. The latter is maintained at an operating pressure equal to the vapour pressure of seawater at/or lower than the freezing point of seawater [Spiegler, 1966]. When the cold seawater is fed to the vacuum chamber, part of the seawater immediately flashes into vapour while the heat

removal causes the formation of ice. Based on Spiegler (1966), the evaporation of the water extracts heat from seawater equivalent to the total latent heat of vaporisation for the mass of evaporated water. This means, in theory, that evaporation of 1 kg of water will produce about 7 kg of ice, as the latent heat of fusion of ice is one-seventh the latent heat of vaporisation of water [Shone, 1987; Spiegler and El-Sayed, 1994; Rahman *et al.*, 2006].

The process flow diagram for the vacuum freeze-vapour compression method is shown in Fig. (2.8). Similar to the indirect-refrigeration method, the incoming feed is cooled by means of a heat exchanger and then sprayed into a freezing chamber [Spiegler, 1966]. The ice and reject brine are taken to the separation unit, where the reject brine and ice are separated. The reject brine is discharged from the system passing through the heat exchanger in order to pre-cool the incoming feed. The remaining ice is taken to the melting unit. The water vapours produced from the freezing chamber are compressed by a compressor and then delivered to the melting unit [Spiegler, 1966]. When the ice crystals and vapours exchange heat, the ice crystals are melted, while the vapours are condensed. Thus, the condensed vapours and melted ice crystals are eventually joined together and become the final product water. The product water is split into two streams where a small amount of final product water is used as washing liquor in the separation unit, while the second stream is taken as product water discharged from the desalination system.

By comparing this technology to the previous process (i.e. indirect freezing process), the production rate is significantly higher. Furthermore, water treatment costs are significantly lower since the water is used as refrigerant. In addition, technical limitations, such as refrigerant supply, water contamination, and refrigerant separation, are avoided when compared to the direct contact freezing process. Therefore, several vacuum freezing desalination units were developed during the past 55 years [Spiegler, 1966]. However, this technology was hindered by the compressor limitations, because it must be maintained at a low temperature while handling a large volume of vapour per unit volume of fresh water being produced [Spiegler and El-Sayed, 1994].

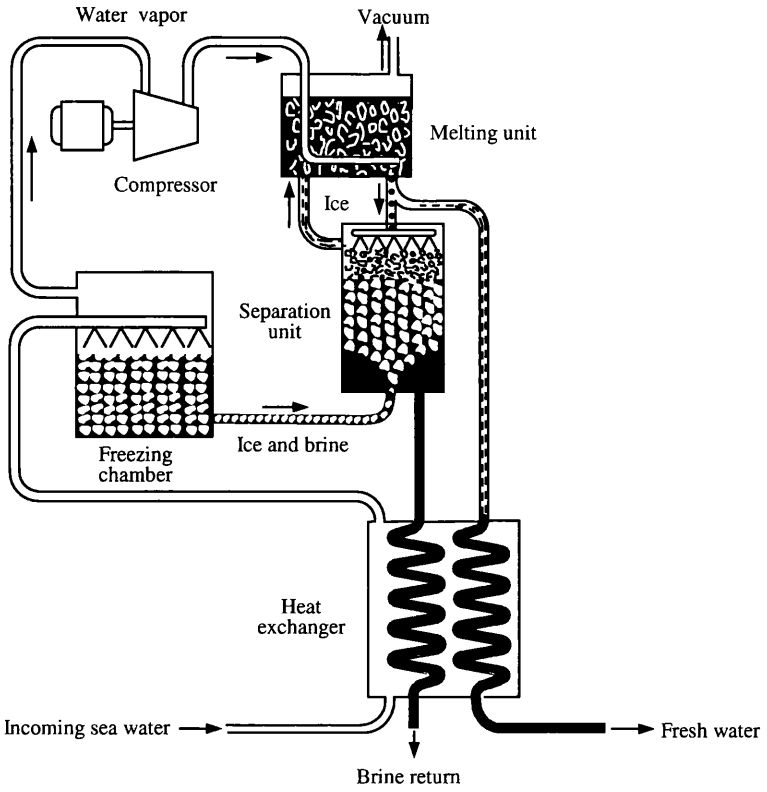

Fig. 2.8: Flow process diagram of the main equipment of a vacuum freezing vapour compression process [Spiegler, 1966].

2.3.1.3 Vacuum-freezing vapour absorption process

In order to avoid the limitations of compressor design, the compression vapour system is replaced by an absorption system [Spiegler and El-Sayed, 1994]. Figure (2.9) shows a schematic flow process diagram of the vacuum-freezing vapour absorption process. The pre-cooled seawater is pumped to the freezing chamber, where vapour and ice are formed as in the previous system. The ice slurry is then delivered to the separation unit, where the ice rises slowly during a washing process (using the counter-current washing method) [Spiegler and El-Sayed, 1994]. The vapour produced from the freezing chamber is absorbed in a concentrated absorbent, usually lithium chloride, which is characterised by having a very low water vapour pressure [Spiegler and El-Sayed, 1994]. During the absorption process, heat is given off while the ice is melted. During the operation, the absorbent must be maintained at a low temperature; otherwise the water vapour pressure of the solution would increase, and it would no longer be able to absorb water vapour from the freezing chamber [Spiegler and El-Sayed, 1994]. The refrigerated and dilute absorbent is pumped to the absorbent generator in order to extract the absorbed water vapour, and then the absorbent is recycled to the absorber

system [Spiegler and El-Sayed, 1994]. The vapour, which was removed from the generator, is delivered to the vapour condenser in order to obtain product water [Spiegler and El-Sayed, 1994].

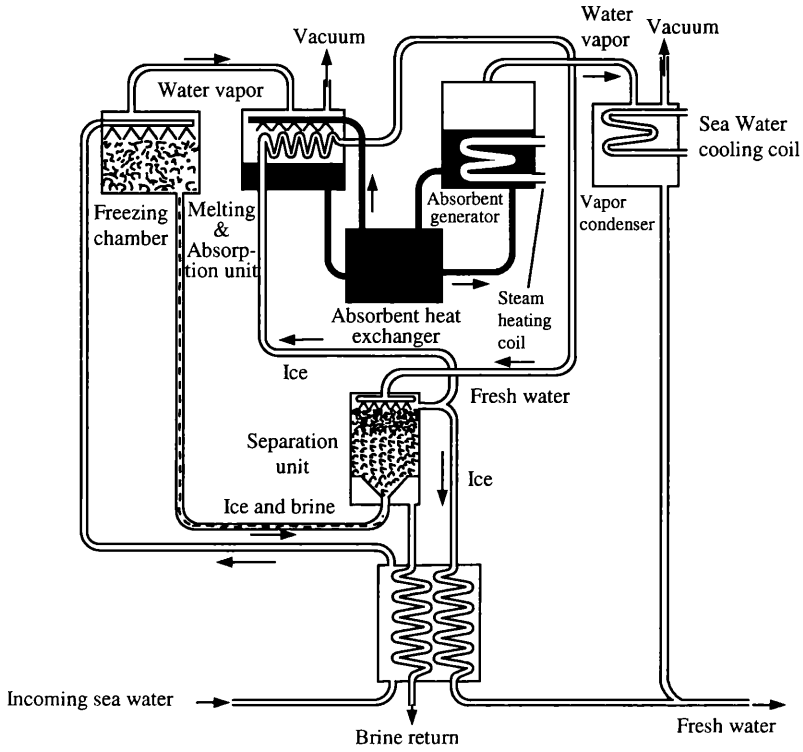

Fig. 2.9: *Flow process diagram of the main equipment of a vacuum-freezing vapour absorption process [Spiegler, 1966].*

2.3.1.4 Secondary refrigerant freezing process

In this process, seawater is directly in contact with an immiscible refrigerant, where the ice crystals are form by the evaporation of the refrigerant. The refrigerant must be insoluble in water. In 1960, butane was first applied as a refrigerant in this technology [Karnofsky and Steinhoff, 1960; Wiegandt, 1960]. According to Spiegler and El-Sayed (1994), the boiling temperature of butane at atmospheric pressure is -0.5°C, which is near to the freezing point of water. Fig (2.10) shows the principle of the secondary refrigerant freezing process. In the freezing chamber, the butane is distributed in the seawater by spraying, where the butane flashes into vapour as the freezing chamber is kept under slightly lower pressure [Spiegler and El-Sayed, 1994]. Thus, heat is removed from seawater, resulting in ice. The ice slurry is pumped to the separation unit, where the ice is separated from the reject brine and then transported to the melting unit. The pressure and temperature of butane vapour from the

freezing chamber is increased by means of the primary compressor. Thus, the hot and pressurised butane vapour enters the melting unit to melt the washed ice. When the butane exchanges heat with the ice, butane is condensed, while the ice is melted. The mixture is then passed to a butane separator (which is also known as decanter), where butane is separated from product water and then compressed once more by means of a secondary compressor. The pressurised butane vapour is condensed to become a liquid prior to entering the freezing chamber, in order to be recycled. As for the product water, the water stream is divided into two sections, where a small amount is taken to the separation unit, while the large amount is discharged to the heat exchanger to pre-cool the incoming feed.

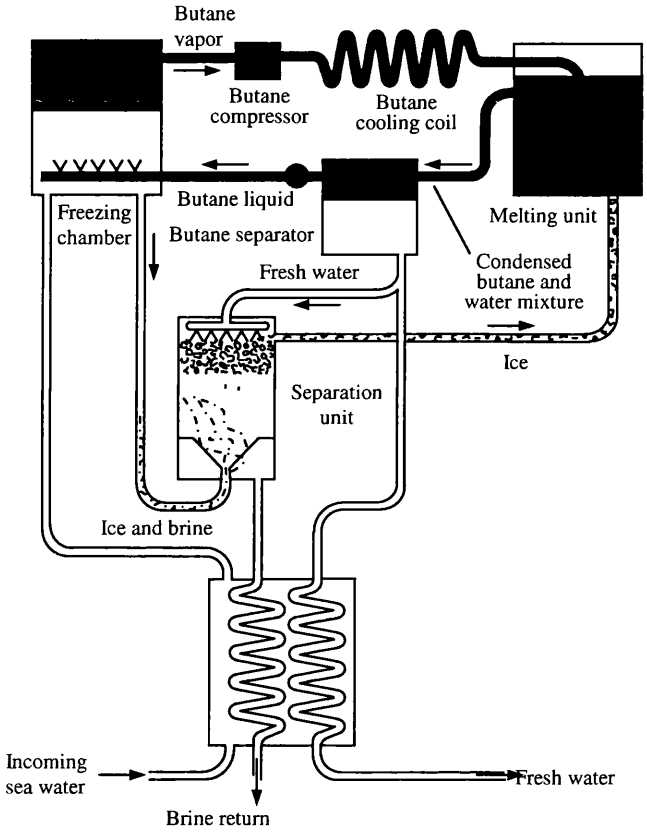

Fig. 2.10: *Flow process diagram of the main equipment of a secondary refrigerant freezing process [Spiegler, 1966].*

2.3.1.5 Separation Unit – Washing System

Different separation units, including; compression, wiping, countercurrent reflux, and centrifuging were previously proposed and investigated either at laboratory or pilot plant scale [Johnson, 1976]. The only washing system found successful and reliable in purifying

ice crystals was the hydraulic piston column, in which a compact bed of ice is produced [Johnson, 1976]. According to Spiegler (1966), almost all freezing desalination technologies used countercurrenet washing with fresh water in a vertical moving bed, known as the wash-separation column, as shown in Fig (2.11). The ice-brine slurry is fed at the bottom of the column. By using hydraulic forces, the bed of ice crystal is moved vertically upward towards the scraper [Spiegler, 1966]. The ice is then washed free of any trapped drops of brine by a continuous countercurrent stream of fresh water, which is fed at the top of the ice pack [Spiegler, 1966]. The washed ice is continuously harvested by means of a scraper, where the harvested ice is then transported to the melting unit to achieve high purity product water [Spiegler, 1966]. According to Johnson (1976), the first commercial wash column system was built in the mid of sixties by Colt Industries.

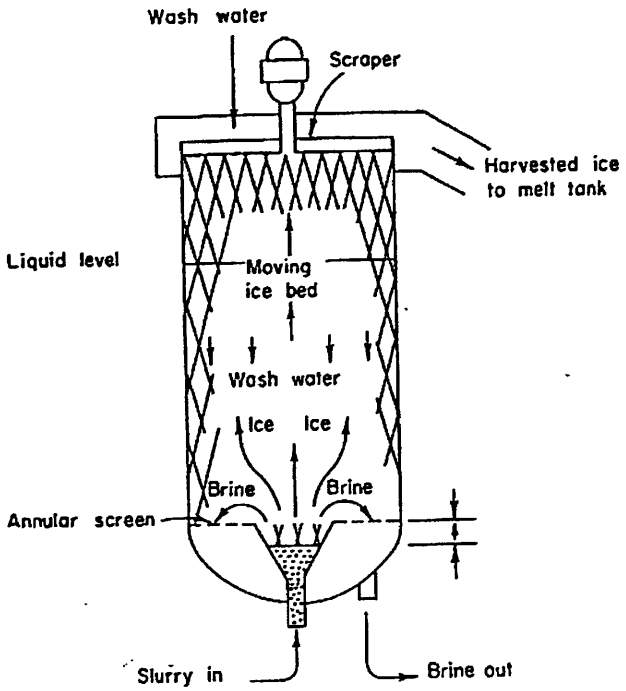

Fig. 2.11: Flow process diagram of the wash-separation column [Spiegler, 1966].

2.3.2 Advantages and disadvantages of freezing desalination technologies

From an industrial separation viewpoint, the greatest potential advantage of freezing desalination technologies are summarised below:

i) Freezing desalination technologies, in theory, require less energy when compared to the evaporation/distillation process, because the latent heat of fusion of ice is only one-seventh the latent heat of vaporisation of water [Shone, 1987; Rahman *et al.*, 2006]. Therefore, theoretically, desalination by freezing could achieve a 75 – 90% reduction in the energy required by a conventional thermal process [Rahman *et al.*, 2006].

ii) The energy cost of a freezing desalination process is theoretically almost similar to that of a RO membrane plants; however, the investment and operational costs for freezing technologies are less than RO membrane plants, because the biological fouling is substantially reduced by low temperature operation [Rahman *et al.*, 2006; Rich *et al.*, 2011].

iii) The advantages of a low operating temperature minimises the major technical problems, such as scaling and corrosion, that are usually encountered in thermal desalination plants [Spiegler and Laird, 1980; Rahman *et al.*, 2006].

iv) The low operating temperature can minimise the capital cost, because many inexpensive plastics or low cost materials can be utilised at low temperature [Spiegler and Laird, 1980; Spiegler and El-Sayed, 1994; Buros, 2000; Rahman *et al.*, 2007].

v) The freezing desalination technologies require very low chemical use due to the absence of pretreatment systems, and therefore this process is environmentally-friendly, because there is no discharge of toxic chemicals to the surrounding environment [Rahman *et al.*, 2006].

vi) By using direct contact freezing desalination technology, a very high surface area and high heat transfer coefficient can be achieved [Rahman *et al.*, 2006].

vii) Freezing desalination process is insensitive to the nature of feed stream in terms of salinity or type of substances in the feed water [Spiegler and Laird, 1980; Rahman *et al.*, 2006].

Despite these advantages, the FM process has been used only to a very limited extent industrially, especially for seawater applications. Commercially, the FM process has not achieved the success of other conventional processes for seawater applications, because of the process complexity and the prohibitive total cost compared to conventional membrane and distillation technologies [Johnson, 1976; Rahman *et al.*, 2007]. In general, the

disadvantages and main reasons behind restricting the application of freezing desalination plants are as follows [Rahman *et al.*, 2007]:

i) Freezing desalination requires complicated equipment to deal with growing, handling, washing, and melting ice crystals.
ii) The final product may be produced with undesirable flavour and aroma.
iii) The freezing technologies require mechanical vapour compressors.
iv) Large scale compressors consume energy intensively when used in desalination.
v) Difficulties in designing large scale plant using freezing desalination technologies and optimising the operating conditions with confidence, because of the process and operation units complexity in the main equipment of the freezing desalination plants, such as freezing chamber, and separation and melting units.
vi) Impure ice crystals are usually produced due to adherence of drops or pockets of the reject brine. As a result, crushing and re-crystallisation of ice may be needed.
vii) Progressive increases in the salinity of reject brine and non-condensable gases.
viii) High quality energy is essential for freezing desalination technologies, while many evaporation processes can be applied with low quality energy.
ix) Mass loss in product water due to certain amount of fresh water taken as wash liquor for washing the ice crystal in the separation unit.
x) Lack of knowledge on ice crystallisation and growth in a slurry system, and limited knowledge in handling ice slurries and separation of ice from brine.

2.3.3 Present and future freezing-melting process

To date, a commercial application of freezing desalination technology processes does not exist. However, a similar concept, in terms of the freeze-melting process, is widely available for use in many different industrial sectors, particularly in food processing [Miyawaki *et al.*, 2005; Hernández *et al.*, 2009; Hernández *et al.*, 2010; Auleda *et al.*, 2011; Sánchez *et al.*, 2011]. Rahman *et al.*, (2007) illustrated various commercial food applications that utilise freeze-melting technologies, which are known as melt crystallisation processes [Rahman *et al.*, 2007]. The solid layer and suspension crystallisation processes are widely used, for such applications. The crystallisers being used in these technologies are classified as indirect contact crystallisers, where the food and refrigerant are fully separated by heat transfer walls

and surfaces [Rahman *et al.*, 2007]. The most commonly used crystallisers are static crystallisation, layer crystalliser growing on rotating drum, dynamic crystallisation, and suspension crystallisation [Rahman *et al.*, 2007]. The food industries have adapted the principles of the freezing desalination technologies, and applied them to take advantage of the technology [Rahman *et al.*, 2007]. In fact, melt crystallisation processes in food industries achieved great success due to the ability of producing high quality products compared to other available technologies around the world [Rahman *et al.*, 2007].

Desalination however, is a massively important process due to the high water usage across the globe, and the constant necessity for clean water [Miller, 2003; OECD, 2004; Rahman *et al.*, 2007]. Therefore, many technologies have been developed for freeze concentration, but some of the most widely used are the falling film principle [Ulrich and Glade, 2003; Hernández *et al.*, 2010; Sánchez *et al.*, 2011] and suspension crystallisation technology [Lemmer *et al.*, 2001; Sulzer, 2004]. In falling-film crystallisation concentration, the fluid to be concentrated flows down over a chilled surface, which causes the crystallization of ice and the further growth of the ice crystals on the surface [Sánchez *et al.*, 2011]. Falling film crystallisation technology will be described later in Chapter 5 in greater detail.

The separation of ice and concentrated solution occurs, because the ice adheres to the surface, while the concentrated liquid flows down along the surface. The suspension crystallisation process consists of a crystallisation section followed by a wash section [Sulzer, 2004; Lemmer *et al.*, 2001]. In the first heat exchanger, tiny needle crystals form, these are then fed into the re-crystaliser holding larger crystals in a slurry. The small crystals then melt and reform on the larger crystals due to lower equilibrium temperatures. These new spherical ice crystals of a larger size are then fed into a wash column and separated from the concentrated solution. One advance in this system in the last decade is the implementation of the batch wash column which uses a piston to compact the crystals into a filter bed. Wash water then flows through the bed and washes out the concentrate before itself freezing on the crystals. The bottom layer of ice is taken off by a scraper at the bottom of the column while the concentrate flows through the top of the piston. The process is finished when all the ice has been scraped away [Sulzer, 2004, Lemmer *et al.*, 2001]. The piston then returns to the start position for the next batch. Several wash columns in series can wash constantly without

stopping so long as they work with corresponding holding times. This technology will be described in detail later in Chapter 6.

Both batch and continuous freeze separation systems exist in industry. Batch separation units are generally kept to the small scale due to higher energy use, while new designs of continuous units are being brought into industries where higher throughput is required. Rodrìguez *et al.* (2000) discuss the key economic factors for the use of freeze separation as an industrial process, and prove through calculation that the capital costs of a large freezing system is much higher than that of a RO unit for a similar level of separation. Due to the RO technology being more available and economically viable the outcome of the paper was that it was the better method for desalination. Hence, it is obvious that freeze concentration technology must be developed to a level, where it is more widely available and economical for all levels of business.

Ice maker machines are extensively used in many commercial and residential areas for the purpose of making ice cubes. They are a good example of the falling film freeze concentration technique. There are a variety of ice maker machines with different production rates of ice cubes (up to 200 tons per day) available nowadays in the market. Heat Transfer Technology AG (2011) recently released a new design for a continuous chip ice machine for use in industry. The BUCO industrial ice maker boasts that by creating chip ice rather than flake ice it can drastically reduce freezing energy costs. Chip ice has an evaporation temperature between -8 and -10 °C while flake ice must be cooled to -35 °C, giving significant energy consumption advantages. The BUCO technology also makes the point that no storage cooling silo is required for very similar separation, and that fragile products are much safer due to no sharp edges like those in flake ice. Similar points are made by Ziegra Ice Machines [Ziegra Ice Machines, 2011]. Heat Transfer Technology AG also discuss the fact that the flexibility of ice thickness, hygienic process and product safety make their process a very strong design for use in the food and pharmaceutical industries. There is good scope for use of ice maker units in industry, where the ice can be collected and either melted in place or taken off to a secondary process.

When the separation performance of thermal distillation becomes infeasible (in terms of product quality and quantity, or energy intensive) in any application and there is no

alternative process, melt crystallisation technologies become the alternative solutions for such applications. Therefore, a number of applications in chemical industries, including: concentration of harmful industrial wastewaters, were reported [Rahman *et al.*, 2007].

2.3.4 Potential technology transfer of melt crystallisation process to desalination

In principle, all melt crystallisation technologies used in either the food or chemical industries could be transferred and applied to the desalination area, including concentrating HSB applications [Rahman *et al.*, 2007]. All methods could lower the food product down to 100 ppm within a multistage process [Rahman *et al.*, 2007]. However, an important point that must be taken into consideration is the economic analysis of the potential melt crystallisation technologies for desalination applications. Suspension crystallisation might be the technology with the most potential as a melt crystallisation process for producing high purity product water from saline water. This is because the technology deals with an ice suspension and washing process as applied in the conventional freezing desalination technologies. However, solid layer crystallisation technologies, namely dynamic and static crystallisation technologies might be feasible for concentrating HSB, since these technologies take advantage of the conventional freezing desalination technologies, in terms of minimising the technical limitations, such as scale and corrosion. In fact, when these technologies are applied to concentrating HSB, then the process will be far simpler compared to freezing desalination technologies. This is due to the elimination of the important limitations, such as complicated ice slurry handling, ice separation and washing processes, since the separation process in solid layer crystallisation depends mainly on the freezing and melting process. Therefore, the melt crystallisation technologies, and more specifically suspension and solid layer crystallisation processes, were adopted in this study and investigated for saline water applications.

In the literature, ZLD systems have combined the FM process with other desalination processes [Rahman *et al.*, 2007]. The most promising ZLD system is the combination of RO and FM processes, while a ZLD system consisting of FM and solar evaporator is proposed as an efficient system to reduce the environmental impact of the HSIB [Rahman *et al.*, 2007]. This method is aimed at producing fresh water and several useful minerals. Based on

economic analysis, it was found that FM might be competitive with solar distillation in many suitable places [Rahman *et al.*, 2007]. In general, all studies show that the hybrid techniques of combining the FM process and other desalination technologies have high potential for future development [Rahman *et al.*, 2007]. In addition, the literature shows that direct contact freezing and eutectic FM processes are suitable for HSB applications [Spiegler and Laird, 1980; Spiegler and El-Sayed, 1994; Rahman *et al.*, 2007]. The disposal of effluents and conversion to by-products can also be achieved by adopting a Freeze-Melting (FM) process [Spiegler and Laird, 1980; Spiegler and El-Sayed, 1994; Rahman *et al.*, 2007].

2.4 Brine Treatment and Zero Liquid Discharge Approaches

Increasing public awareness of the significant impact of industrial effluents on the surrounding environment has contributed to the setting of more restrictive regulations for governing disposal methods, which might restrict many conventional disposal methods (such as, discharging the brines into open waters and inland surface waters, deep well injection and aquifer re-injection) in the future. Moreover, increased demands for water supply coupled with more stringent regulations are forcing desalination utilities to produce fresh water from low quality supplies. These pressing demands are forcing engineers and investors to use a desalination process that is potentially capable of increasing water recovery to the highest level by minimizing the effluents (to the lowest level) with least harm to the environment. These demands can be satisfied by utilising a treatment system known as Zero Liquid Discharge (ZLD) [McKetta, 2002; Sethi *et al.*, 2006; El-Sayed and El-Sayed, 2007].

As its name implies, Zero Liquid Discharge (ZLD) can be defined as a combination of desalination processes, which are aimed at producing high purity of fresh water with the total elimination of waste liquid from the plant [McKetta, 2002]. However, this treatment system does not eliminate the total waste, but reduces the size of waste by converting the effluents into a compact solid waste. Therefore, this technology offers economic advantages and environmental benefits to any industrial plant because more fresh water per unit feed is produced and a compact solid waste is discharged (instead of having large volumes of waste liquid). The produced fresh water from ZLD can be used for different applications such as; drinking water, irrigation, process re-use, boiler feed water, cooling water, environmental discharge, and groundwater recharge [Ahmad and Williams, 2011]. While the compact waste

solid discharge can be either disposed in a way friendly to the environment or transported for additional processing in order to be prepared as useful products. Therefore, the ZLD system is an attractive and powerful concept for disposing of the industrial effluent.

With regard to the description of ZLD systems, since there are many different industrial plants using different types of saline waters, it is impossible to have a uniform scheme of ZLD systems for all industrial plants. The design of this ZLD technology consequently depends on several crucial factors, which include; feed water chemistry, purity demand of fresh water and concentration of the waste liquid that is required for either safe disposal or other beneficial uses. In general, there are numerous design, configurations and operation variations in ZLD facilities, and each system is unique. Moreover, reducing the costs of ZLD becomes one of the major goals of many scientific and commercial sectors around the world in order to make this treatment system a viable option. Therefore, ZLD schemes may include some or all of the processes discussed.

2.4.1 Thermal Technologies

2.4.1.1 Conventional Thermal Technologies

The trend toward ZLD systems requires energy to eliminate the solvent from the effluents. This can be achieved by several thermal processes:

(i) Brine concentrators: These are also known as 'evaporators', and are commercially available in different types based on the following main designs; plate, falling film, rising film, horizontal tube, natural circulation, forced circulation, and flash evaporators [GAE NIRO, 2003]. Hence, the selection of the evaporator type depends on the water chemistry of feed water, the feed temperature related behaviour, viscosity, the encrustation properties of dissolved substances and the production capacity required. The process concepts which might be employed for the brine concentrators are; multi-effect evaporators, thermal vapour compression, mechanical vapour compression, combined processes, and flash evaporation. The vapour compression technique is the most commonly used as a process concept for brine concentrators. However, the selection of process concept depends

mainly on factors which include; water chemistry of the feed water, process availability and economical aspects [GAE NIRO, 2003].

(ii) Crystallizers in ZLD systems are usually followed by an evaporator, which is employed for converting the highly saturated waste liquid to a compact solid waste [GAE NIRO, 2011]. Highly pure fresh water is produced in this process. Crystallizers with longer retention times are operated with less specific energy input, resulting in lower nucleation rates. The impacts between crystals and the blades of the impeller pump are the most effective source for the nuclei production. This is about 100 fold more effective than other impacts (i.e. between the crystal and the wall, or crystal-crystal impacts). Therefore, the types of crystallizers differ mainly in design and the position of the impeller pump. In general, these types are; forced circulation, turbulence (or Draft Tube and Baffle (DTB)) and OSLO (classified-suspension) crystallizers [GAE NIRO, 2011].

(iii) Spray dryers: These are devices used for dewatering concentrated slurries produced from brine concentrators [National Research Council, 2009]. They are capable of separating the solute or suspension as a dry solid by vaporizing the solvent (i.e. water). The advantage of this technology over the crystallizers is that, for continuous production, the form of the dry solids (such as powder, granulate or agglomerate form) can be controlled. This means this technology is an ideal process for harvesting useful salts according to quality standards regarding particle size distribution, residual moisture content, bulk density, and particle shape.

As thermal technologies are well established and devolved, they are the most reliable processes for HSB applications since they do not suffer in their operation from scaling problems. These technologies are therefore, technically the most feasible methods for small scale applications. However, these processes are infeasible for large scale applications because their capital and operational costs are relatively high and may exceed the cost of several industrial plants such as a desalination facility [National Research Council, 2009]. These technologies have only been used to a very limited extend industrially around the world and may also be operated with some DTs to decrease the total cost of ZLD systems [GAE NIRO, 2003].

2.4.1.2 Thermal Solar Technologies

Several technologies using solar energy have been introduced and used in thermal DTs [U.S. Congress, 1988; Hanbury *et al.* 1993; Spiegler and El-Sayed, 1994; Lawson and Lloyd, 1997; Buros, 2000; Younos and Tulou, 2005; Howe, 2009]. The most commonly used are solar humidification and evaporation and solar ponds (more detailed descriptions of these processes are available in the literature [U.S. Congress, 1988; Hanbury *et al.*, 1993; Spiegler and El-Sayed, 1994; Buros, 2000; Younos and Tulou, 2005; Howe, 2009]). There are however differences between these technologies. The solar humidification technique is devoted mainly to desalinating purposes [Hanbury *et al.*, 1993; Lawson and Lloyd, 1997; Buros, 2000]. This process imitates a part of the natural hydrologic cycle in which a transparent cover allows the radiation of the sun to heat directly a layer of saline water so that the production of water vapour (humidification) increases [Hanbury *et al.*, 1993; Spiegler and El-Sayed, 1994; Buros, 2000; Younos and Tulou, 2005]. The water vapour is then condensed on a cool surface, and the condensate collected as fresh water product [Hanbury *et al.*, 1993; Spiegler and El-Sayed, 1994; Buros, 2000; Younos and Tulou, 2005]. The concept of evaporation and solar ponds is similar to solar humidification except in the fact that they are employed to concentrate waste effluents, while the production of water vapour is not utilised. According to the literature, solar or evaporation ponds might be used as an alternative option to using crystallizers or spray dryers in order to reduce the total costs of a ZLD system [Ahmed *et al.*, 2000].

A solar pond technique can be described as an artificial shallow pond, which is used for collecting and storing the solar thermal energy by heating and evaporating the water from the surface layer of the pond through the radiation of sun [Szacsvay *et al.*, 1999; Curcio *et al.*, 2009]. The evaporation process on the surface causes a salinity gradient through the pond depth which establishes three different zones, where salinity at the surface is lower than at the bottom. These three zones consist of an upper convective zone (or surface zone) of uniform relatively low salinity and temperature at the surface, a non-convective gradient zone (or intermediate zone) in the middle of the pond where salinity and temperature are proportional to the depth and a lower convective thermal storage zone (bottom zone) of uniform high salinity and temperature at the bottom of the pond [Ahmed *et al.*, 2000; Pankratz, 2008]. Therefore, the heat energy can be extracted from the bottom zone by using a heat exchanger in order to transfer the thermal energy (at a level of 50 – 90°C) to a wide

range of industrial and agricultural applications such as, heating, agricultural processes, thermal desalination plants, electrical power generation plants and production of marine chemicals [Lawson and Lloyd, 1997; Ahmed *et al.*, 2000; Pankratz, 2008].

With regard to evaporation ponds, this process is similar to the solar pond except that this process has a number of successive ponds connected to each other [Ahmed *et al.*, 2000]. The brine is introduced to the first pond and then flows slowly through a number of ponds towards the final pond where salt precipitation occurs. The ponds become successively more salty moving down the system. Evaporation ponds can be used for different applications such as; concentrating effluents, salt production and mining processes [Ahmed *et al.*, 2000]. The construction of evaporation ponds is relatively easy and they have low maintenance requirements and low operation costs in comparison to the thermal technologies [Ahmed *et al.*, 2000]. Moreover, evaporation ponds do not require mechanical equipment, except for transfer pumps that convey the effluents to the different ponds. Evaporation ponds are the least costly means of disposal, especially in areas where the evaporation rate is high and the costs of flat land are inexpensive [Ahmed *et al.*, 2000].

The advantages of using solar thermal energy in comparison to thermal energy in ZLD systems are that the energy is free, completely renewable, clean and green since no significant effluents (such as CO_2 emission) are emitted to the surrounding environment. Furthermore, dependant on flat land and climate limitations, the total costs of ZLD systems can be reduced by using thermal solar technologies as a final treatment rather than using crystallizers or spray dryers [Ahmed *et al.*, 2000]. However, several factors may restrict the use of these technologies for large scale applications as they require large solar collection areas of low-cost, especially when the evaporation rate is low or the volume of effluent is high. Also, the ponds should be located in warm climate areas, and which are dry, with a high rate of evaporation without any risk of vulnerability to weather-related damage. The pond must also be installed near to the location where the brines are available/generated. In addition, these ponds must be isolated from the water table to protect the surface water/aquifer from the contents of the ponds. In these systems, the water vapour is not collected and condensed for producing fresh water (i.e. waste of fresh water) [Ahmed *et al.*, 2000]. There are some downsides however, as the application of solar ponds requires expensive piping, insulation, armatures, pumps and controls which may have some

maintenance and operational problems [Szacsvay *et al.*, 1999; Ahmed *et al.*, 2000]. In some applications such as in oil-produced brines, the effluents must be well treated prior to being transported to the ponds in order to remove some of the undesired organic substances from the brine because of the negative impact on the environment and human health. One of the main problems with this particular process is the rebirth of harmful gases.

2.4.2 Membrane Technologies

As explained in section 2.2.2 a variety of technical problems can be experienced with membrane technologies, however, according to the water chemistry of feed-water, RO membrane technology may be used as a pre-concentrator system for a ZLD process. This means that the reject brine of RO will be delivered to the ZLD technique for final treatment. The aim of this application is to reduce the total costs of ZLD by reducing the quantity of the waste stream to a minimum. Membrane technologies such as Ultrafiltration (UF) and Nanofiltration (NF) may also be used as a pretreatment system for ZLD technologies or for the industrial plant in order to extract undesired species from feed water and to concentrate the waste discharge (with undesired species) for further treatment through ZLD technologies [Spiegler and Laird, 1980; Pols and Harmsen, 1994].

Forward Osmosis (FO) is another type of membrane based separation process. Unlike RO technology, the FO process utilises osmotic pressure gradients rather than hydraulic pressure. This osmotic pressure gradient can be established by feeding simultaneously a concentrated solution (known as the draw solution) on one side of the membrane and saline water on the other side [Cath and Childress, 2006]. Water molecules will be naturally and spontaneously transported from the feed saline water to the draw solution across membrane, which leads to dilution of the draw solution. Hence, by concentrating the diluted draw solution (by using any desalting system such as distillation or membrane technology), fresh water and draw solute are separated, with the latter being recycled to the FO module. The draw solution plays the main role for establishing osmotic pressure gradients in the FO process, so the process is dependant on the concentration of draw solution [Cath and Childress, 2006; Sethi *et al.*, 2006]. The driving force in FO can be significantly higher than in RO and leads to the FO process having several advantages over the RO process, which include higher water recovery, less operational and capital costs, low fouling potential, and process simplicity and reliability [Spiegler and El-Sayed, 1994; Cath and Childress, 2006; Howe, 2009]. With

regard to HSB applications, the advantages of the FO process show that the FO process might be more feasible than RO for concentrating the industrial wastewater by using a draw solution. In principle, by using a suitable draw solution and reliable process with a new generation of semi-permeable FO membranes, the FO process (as a final treatment system) can achieve the ZLD concept by producing fresh water and precipitating the salt. In general, the literature showed that FO process has been used for industrial wastewaters (in small scale applications), concentrating landfill leachate and seawater applications [Cath and Childress, 2006; Sethi *et al.*, 2006; Howe, 2009].

Membrane contactor processes such as FO and MD can potentially minimize brine volume at lower energy expenditure and with less complexity [Martinetti *et al.*, 2009]. As MD can potentially give 100% rejection of non-volatile solutes, MD's use for ZLD systems has also been investigated [Walton *et al.*, 2004; Martinetti *et al.*, 2009]. However, from the tests conducted so far, the main uses of MD for zero liquid discharge will be on the small scale in connection with other methods such as RO and solar ponds [Walton *et al.*, 2004; Martinetti *et al.*, 2009]. Further research is required in order to develop this technology for large scale operation.

With regard to voltage-driven membrane processes, Electrodialysis Reversal (EDR), which operates on the same principle as an ED unit, except that the polarity of the electrodes is reversed at intervals of several times an hour, causes ions to be attracted in the opposite direction across the membranes [Mulder, 1996]. Hence, scale problems in EDR are not as critical as in RO membranes because ions are removed and fresh water is left behind, while in RO technology the opposite scenario occurs [Mulder, 1996; Tillberg, 2004]. Therefore, technically, EDR technology may be more feasible than RO processes in increasing water recovery from the effluents, resulting in more fresh water being produced, and a cost reduction of the final discharge treatment systems because the reject brine from EDR is reduced to a minimum without having a risk of scale problems. According to Shone (1987), in some instances EDR technology is currently the most viable option for mining applications. EDR technology can also treat water with a free chlorine residual, making this technology more feasible than RO process to reclaim industrial wastewater, where chlorine might be injected in the brine as a disinfectant [Tillberg, 2004]. However, EDR processes consume high amounts of energy for high saline applications, and cannot remove silica and

dissolved organics from the water produced [Tillberg, 2004]. Therefore, RO and EDR technologies might need an intensive pretreatment system in order to achieve reliable operation for such applications.

2.4.3 Comparison of Membrane and Conventional Thermal Technologies for ZLD Systems

Comparison of desalination technologies is a difficult matter due to the different demands required by different feed waters and different processes. The usual metrics which are used to compare processes are the cost and energy required to produce one metre cubed of water. The cost of desalination is very site-specific and is mostly based on the quality of the feed water at the selected site. However, energy is the key to desalination. The fundamental limit for the minimum work needed is equal to the difference in free energy between the incoming feed (i.e. seawater) and outgoing streams (i.e. product water and discharge brine). For normal seawater (3.45 per cent salt) at a temperature of 25 °C, the minimum work has been calculated as equal to 0.86 kWh m^{-3} [DESWARE, 2011]. Table (2.6) shows a comparison of water cost and required energy per cubic metre for a range of desalination technologies.

Parameter	MSF Seawater	MED Seawater	VC Seawater	RO Seawater	RO Brackish Water	ED Brackish water	MD
Cost ($/m^3)	0.7-5.36	0.27-1.49	0.46-1.21	0.45-6.56	0.18-0.70	0.58	1.32
Energy (kWh/m^3)	13.5-81	6.5-77	3.8-33.3	2.3-17	2-3.1	0.1-1.1	1.25

Table 2.6: *Cost and energy requirement for 1 m^3 of desalinated water [Miller, 2003; Alklaibi and Loar, 2004; DESWARE, 2011].*

Table (2.6) illustrates the problem encountered when comparing different technologies. The cost of desalting seawater has reduced in recent years, with the newest reverse osmosis plants producing water for about 0.50 $/$m^3$ [Dreizin, 2006]. The costs have dropped by a factor of about three in the last 10 years. On average for RO systems, the current power consumption

for seawater desalination is less than 3 kWh/m^3, which is a 90% reduction in energy use over the past 40 years. This is because of improvements in membrane technology and energy recovery systems. However, the energy use is still about four times greater than the thermodynamic minimum. For desalination of brackish waters and groundwaters, the energy required is significantly less and the cost is usually less than 50% of that for seawater desalination. This does however raise a problem when considering high saline brines as the energy required, and thus the cost of processing, is going to be more substantial than the values shown in Table (2.6), as the initial brine concentration will be higher than the concentration of seawater. Another problem which also occurs when dealing with high saline brines is that no one technology can accomplish the whole desalination process in one go i.e. RO will become limited at higher brine concentrations as the pressure required to overcome the osmotic pressure of the solution becomes prohibitive. Energy therefore constitutes a large portion of the cost of processing high saline brines and is a prime driver of decisions about which treatment method to use. Generally, the more advanced the treatment the more energy is required.

The energy requirements of ZLD systems may vary according to several factors including system configuration and plant design. Thermal evaporators are known to be a viable and reliable technology for reducing the reject brines of RO plants to a slurry of approximately 20% solids, however, this process requires a large amount of energy, which has been estimated to be more than 18.5 kWh/m^3 of feed-water [Bostjancic and Ludlum, 1994; Bond and Veerapaneni, 2007; Pankratz, 2008; National Research Council, 2009]. Crystallizer and spray drying processes are more capital-cost and energy-intensive than brine concentrators and the energy requirements of a thermal evaporator combined with a crystallizer may exceed 32 kWh/m^3 in order to accomplish the total elimination of waste liquid [Pankratz, 2008; National Research Council, 2009].

El-Sayed and El-Sayed (2007) have conducted mathematical modelling for two different configurations of a thermal vapour compression process and of a ZLD process which incorporates RO membrane technology for ZLD. The vapour compression processes considered were (i) a single stage concentrator combined with a crystallizer and (ii) multistage concentrators preceding a crystallizer [El-Sayed and El-Sayed, 2007]. Both configurations are meant to be retrofits to existing seawater distillation plants [El-Sayed and

El-Sayed, 2007]. The results showed that the single stage concentrator requires an estimated work of 48.7 kWh/m^3 feed and costs about 3.78 \$/m^3 distilled water, while a three-stage configuration requires an estimated work of 46 kWh/m^3 feed and costs about 3.44 \$/m^3 [El-Sayed and El-Sayed, 2007]. Also, the authors stated that the multistage configuration is better for handling large scale applications compared to single stage ones because the large volume rate of vapour can be split into more than one compressor [El-Sayed and El-Sayed, 2007]. There are however unsolved problems and remaining challenges that may restrict the application of this technology (for large scale applications), which include (a) the development of strong light composite materials for the compressor rotor used for handling large volumes at relatively high speeds efficiently and (b) effective methods for containing salt to avoid clogging flow paths [El-Sayed and El-Sayed, 2007].

The RO membrane system considered consisted of 4 stages in series such that the end result is product water and salt (process configuration and estimated operating parameters are in reference [El-Sayed and El-Sayed, 2007]). The specific work of the pumps was computed at 11.1 kWh/ton initial feed or at 11.6 kWh/ton product [El-Sayed and El-Sayed, 2007]. For a capacity of one million gallons per day the power required to drive the pumps was 1822 kW, which is much lower than the ZLD system using a thermal process [El-Sayed and El-Sayed, 2007]. However, the application of RO membranes is restricted by several unsolved problems including (a) concentration polarization which leads to scaling and fouling and (b) the applied pressure for the last two stages may exceed 200 bar. To solve these problems the authors have suggested doping and vibration to solve problem (a) and the use of ceramic membranes for problem (b) [El-Sayed and El-Sayed, 2007].

According to the results of analytical calculations that have been conducted for ideal ZLD process using NaCl aqueous solutions as feed-water theoretical work of ZLD desalting was found to be 2.25 times that of conventional desalination [El-Sayed and El-Sayed, 2007]. This value increased to about 3.6 times the work required for conventional desalination if retrofitting of the existing desalination plants was considered [El-Sayed and El-Sayed, 2007].

2.4.4 Promising Technologies – Opportunities and Challenges

So far existing methods for desalination and processing of high saline brines have been discussed, however, there are also other systems which can be considered for future development. These include freeze-melting processes and salinity gradient power.

(i) Freeze-melting processes

The disposal of effluents and conversion to by-products can also be achieved by adopting a Freeze-Melting (FM) process [Spiegler and Laird, 1980; Spiegler and El-Sayed, 1994; Rahman *et al.*, 2007]. This method depends on the fact that when saline water freezes, the individual ice crystals consist of pure water, leaving dissolved organic and inorganic solids in liquid pockets of high salinity brine. Since salt solution is trapped in the ice during the crystallisation process the ice crystals require washing and then melting to get potable water. In general, the classification of the different FM processes can be divided into three concepts based on contact of refrigerant with the solution; direct contact freezing, indirect contact freezing, and vacuum freezing [Spiegler and Laird, 1980; Spiegler and El-Sayed, 1994, Rahman *et al.*, 2007].

From an industrial separations viewpoint, the greatest potential advantage of FM is that less energy is required when compared to the evaporation/distillation process because the latent heat of fusion of ice is only one-seventh the latent heat of vaporisation of water. Therefore, theoretically, desalination by freezing could achieve a 75 – 90% reduction of the energy required by a conventional thermal process. Furthermore, the advantages of a low operating temperature minimises technical problems such as scaling and corrosion, and also it minimises the capital cost because many inexpensive plastics or low cost materials can be utilised at low temperature [Spiegler and Laird, 1980; Spiegler and El-Sayed, 1994; Buros, 2000; Rahman *et al.*, 2007]. The FM process also requires very low chemical use due to the absence of pretreatment systems, and therefore this process is environmentally friendly because there is no discharge of toxic chemicals to the surrounding environment. Biological fouling is also reduced by low temperature operation. In addition, by using direct contact freezing, a very high surface area and high heat transfer coefficient can be achieved [Rahman *et al.*, 2007]. Despite these advantages, the FM process has been used only to a very limited

extent industrially especially for seawater applications. Commercially, the FM process has not achieved the success of other conventional processes for seawater applications because of the process complexity and the prohibitive total cost compared to the conventional membrane and distillation technologies [Rahman *et al.*, 2007]. However, the literature shows that direct contact freezing and eutectic FM processes are suitable for HSB applications [Spiegler and Laird, 1980; Spiegler and El-Sayed, 1994; Rahman *et al.*, 2007].

In the literature, ZLD systems have combined the FM process with other desalination processes [Rahman *et al.*, 2007]. The most promising ZLD system is the combination of RO and FM processes, while a ZLD system consisting of FM and solar evaporator is proposed as an efficient system to reduce the environmental impact of the HSIB [Rahman *et al.*, 2007]. This method aimed at producing fresh water and several useful minerals. Based on economical analysis, it was found that FM might be competitive with solar distillation in many suitable places [Rahman *et al.*, 2007]. In general, all studies show that the hybrid techniques of combining the FM process and other desalination technologies have high potential for future development [Rahman *et al.*, 2007].

(ii) Salinity gradient power

The principle behind the salinity gradient power is the exploitation of the entropy of mixing two solutions with different salt gradients [Skilhagen *et al.*, 2008; Ahmad and Williams, 2009]. When incorporating a semi-permeable membrane between two compartments containing diluted and concentrated solutions respectively, a net flow of diluted solution towards the concentrated solution side will be observed because of the osmosis phenomenon. If the compartment volume on the concentrated solution side is fixed, then the pressure will increase towards a theoretical maximum of 26 bar for seawater applications [Skilhagen *et al.*, 2008]. This pressure is equivalent to a 270 metre high water column [Skilhagen *et al.*, 2008]. Therefore, a dual purpose plant which would generate power from waste brine before disposal would be an attractive option. Various concepts on the exploitation of salinity gradient power have been proposed [Post *et al.*, 2007; Skilhagen *et al.*, 2008]. Pressure retarded osmosis (PRO) and reverse electrodialysis (RED) are the most frequently studied membrane-based processes for energy conversion of salinity-gradient energy [Post *et al.*, 2007; Skilhagen *et al.*, 2008]. These technologies utilise an alternative energy source which can generate a significant amount of energy which is completely renewable and sustainable,

clean, and green since it does not produce CO_2 or other significant effluents that may interfere with the natural climate [Jones and Finley, 2003]. Technically PRO and RED are not desalination technologies, but they can make use of high saline brines to generate power. Power generation alongside desalination is a common phenomenon in the Middle East.

The main disadvantage of implementing ZLD systems using thermal DTs for treating brines is correlated with the economical feasibility. When an industrial plant (which produces brine effluents) is located in an area where disposal of the brine into a large body water is a possibility (i.e. ecologically permissible), then several novel ideas for the application of PRO plants can be proposed. For instance, the operational cost of ZLD systems can be decreased by incorporating two technologies utilising alternative energy, which are an osmotic power plant and a solar pond [Ahmad and Williams, 2009]. The main role of a solar pond is to reduce the energy consumption (required by the ZLD system) and also to concentrate the brines, while the role of osmotic power plant is to produce electrical power by mixing concentrated brines with a diluted solution such as seawater. This idea may be useful for the oil and gas industries because with the osmotic power plant, the concentrated solution (i.e. high saline brine) can be diluted, and therefore the volume of the diluted brines will be increased, hence, the diluted brine can be split into two streams. One stream can go to the down-hole injection for enhanced oil recovery in the oil production offshore, which means that this method will decrease the salinity of the well, in particular, in oil fields that have been producing for long periods of time. The second stream can be used for the SP to take advantage of the thermal energy available prior to being fed into the ZLD process. It is however, important to point out that the application of salinity gradient power for HSB applications is restricted by several crucial factors, which include; the availability of a large volume of diluted water and the possibility for dumping the brines into the diluted waters (i.e. ecologically, it should be permissible) [Ahmad and Williams, 2009]. Furthermore, because of the concentration polarisation phenomenon in membrane separations, this process is still being researched as the predicted membrane performance and efficiency (i.e. predicted energy) is not achieved [Ahmad and Williams, 2009]. The process also suffers from scaling and fouling problems. In addition, this process can be used only for producing energy prior to disposal of the brine, which means that this technology does not treat the brine and only dilutes it, prior to dumping into a diluted solution or into a solar pond.

2.5 Conclusions

Processing of saline brines is required for several reasons; water supply and water conservation, safe disposal, harvesting the residual salts as by-product and achieving the requirements of the regulatory limitations. HSB must be considered as a resource rather than a waste problem because as well as pure water production, many valuable minerals can be harvested and reused.

There are a wide range of DTs which effectively remove salt from salty water, or extract fresh water from saline water. Most of these technologies rely on either thermal or membranes processes. At the moment there is no "best" method for desalination because every desalination process has its own advantages and disadvantages. This study showed that the success of any desalination system in any application depends on several important factors such as, water chemistry of the feed water and careful study of the site conditions and the application at hand. These factors need to be considered in any theoretical analysis and evaluation of the desalination technologies to seek the most reliable treatment process at reasonable cost with least harm to the environment. The water chemistry of the feed water plays the main role for selecting the appropriate desalination process, for instance, the higher the concentration of dissolved solids in the feed water, the more technical limitations, the more process complicity and higher cost. Therefore, the application of DTs for treating the HSB is currently one of the major challenges of applied research because this type of water cannot be desalted by using the conventional DTs. A variety of technical problems can be experienced with the conventional distillation processes including scaling, fouling, corrosion, capital cost and high energy usage. RO membrane technologies are hindered by high osmotic pressure, scale and fouling problems, while ED is unfeasible because of high operational cost.

HSB also limit the scope of choice of treatment systems due to the fact that the desalination process is either expensive and/or it has several technological, operational, and regulatory limitations for such applications. For example, ZLD systems using thermal distillation processes (such as vapour compression technologies) that do not suffer in their operation from scaling problems are only feasible for small scale applications because these technologies are relatively expensive in capital and operational costs for large scale applications. Therefore, other processes such as membrane and thermal solar technologies

are recommended to be incorporated in ZLD systems to reduce the total costs of whole process. Finally, there are other technologies, such as FO, PRO and FM processes, which need to be considered for future applications as these processes have great advantages that must be appreciated for such applications, especially in energy requirements.

The literature survey was conducted on various forms of freezing desalination technologies, as well as melt crystallisation processes. The developments in freezing desalination technologies were active during the period 1950 – 1970. However, commercial plants using freezing desalination technologies did not achieve success, because of process complexity, difficulty in scaling-up, and the prohibitive total cost, when compared to conventional membrane and distillation technologies. On the other hand, the study showed that the freeze melting process offers a number of important advantages, including (a) a very high separation factor, (b) high energy efficiency (the latent heat of freezing is low), (c) generic applicability, (d) no additives, and (e) ready availability of core technology. Despite these advantages, the freeze melting process has been used only to a very limited extent in concentrating brines. Therefore, this study was devoted to experimentally investigating and evaluating the separation performance of various forms of melt crystallisation technologies for desalting and/or concentrating saline water and brine applications. The adopted and investigated processes are namely dynamic crystallisation, static crystallisation, and suspension crystallisation processes.

CHAPTER III:

EXPERIMENTAL STUDY OF AGITATION SYSTEMS USED FOR THE FREEZE-THAWING PROCESS

3.1 Introduction

The performance of a static crystallization technique with various forms of agitated crystallisation processes was experimentally investigated and assessed for treating a range of liquid streams, using aqueous solutions of sodium chloride. The investigated saline waters ranged from low salinity simulating brackish water up to high concentration typical of those causing the most severe pollution problems such as reject brine of desalination plants. Post-treatment processes, such as washing and sweating, were not considered in this study.

A laboratory bench scale experimental setup was used for investigating and verifying the performance of a static crystallizer with different types of agitation systems for desalting NaCl solutions at different salt concentrations ranging from 5,000 to 70,000 ppm. These laboratory investigations were carried out using a thermo-stated double wall reaction vessel with a capacity of 200 mL. The crystallization process was investigated in batch mode with three agitation systems: a Bubbling Process (BP), a Mechanically Stirred System (MSS), and an Ultrasonic Process (UP). These were examined individually, and the results were analysed and compared to the results of the performance of the crystallizer when no agitation was applied i.e. the static crystallization process.

The specific aims of this experimental investigation was to verify the influence of the initial salt concentration of the feed, crystallisation temperature, crystallisation time, and agitation rate (such as; air pressure for the BP, stir rate for the MSS, and amplitude rate for the UP), upon the salt rejection and water recovery.

3.2 Preparation of Feed Samples

Since aqueous solutions of sodium chloride give results in the desalting process very close to process brines [Barduhn, 1965], different salt concentrations of NaCl solutions were prepared, used, and examined as feed material in this experimental investigation. The initial salt concentration of the feed streams used ranged from 0.5 to 7% by weight of NaCl salt.

Sodium chloride solutions were made by dissolving a weighed amount of sodium chloride (Fisher Scientific – Laboratory Reagent Grade) in a known weight of high purity water (produced via an ultra-pure water purification system, Elix 3, Millipore).

3.3 Physicochemical Analysis and Measuring Instruments

Physical and chemical analysis of all water samples included measurements of Total Dissolved Solids (TDS), electrical conductivity, weight, volume, and temperature. All experimental data including the results of these measurements were recorded and are tabulated in Tables A3-1 – A3-13 in Appendix A3. The accuracy of the results of salt concentration was also ensured through a simple mass balance equation.

The salt concentration of the feed sample was measured using a Russell RL105 conductivity meter with a conductivity probe (CDC139/K) to ensure that the correct concentration had been achieved.

The measurements of TDS were experimentally determined by evaporating a known weight of a water sample to dryness and weighing the solid residue. This is known as the gravimetric method. The equipment involved in obtaining gravimetric measurements are oven, petri dish, and laboratory balance. The volume measurements, on the other hand, were determined by scaled borosilicate glass cylinder. The running time for crystallization process was measured by a stopwatch timer (HS-10W Stopwatch, Casio).

3.4 Experimental Setup

Four experimental setups were prepared, constructed, and tested for investigating and verifying the performance of a static crystallizer with different types of agitation systems for treating aqueous solutions of sodium chloride at different salt concentrations. The principal unit operations that have been considered for the laboratory study are; crystallization, separation, and total melting. The applied crystallisation process is characterized as "the secondary-refrigerant indirect freezing" method, and utilizes a solid layer crystallisation concept.

Fig (3.1) shows the equipment for the crystallisation experiments using a static and agitated crystallisation processes. The experimental setup for the static crystallisation process comprises of a laboratory jacketed beaker (borosilicate glass jacketed reaction vessel with hose connectors) with a capacity of 200 mL, refrigerated immersion cooler (Grant, C2G) attached to the cooling coil (Grant, CW5), refrigerated thermostatic bath (Grant, W6), circulator (Julabo, U3/7), and flexible tubing.

The refrigeration system used for all the laboratory setups was identical, which involves the use of a refrigerated immersion cooler, connected to a cooling coil. The latter is immersed in a Heat Transfer Medium (HTM) that is stored in a thermostatic bath. The circulator is installed above the thermostatic bath, so the cooling coil and suction line of the circulator are immersed in a HTM. The circulator and jacketed beaker are connected by means of flexible tubes. The jacketed beaker was thermodynamically insulated by using foam pipe insulation, while the top surface of the jacketed beaker was entirely open. The thermostatic bath contains 4L of HTM. The HTM represents a mixture of an antifreeze solution (Super Coldmaster antifreeze, Blue) and deionised water. The antifreeze solution was diluted at a weight ratio of 2:1.

The experimental setups for the static and agitated crystallisation processes are identical apart from the agitation system used. The experimental setup for the mechanically stirred crystallisation process was provided with an overhead stirrer assembly, which include; an overhead stirrer (IKA, Model: 2482000), and stirring paddle. The experimental setup for the crystallisation process using a bubbling system, on the other hand, was provided with an air-

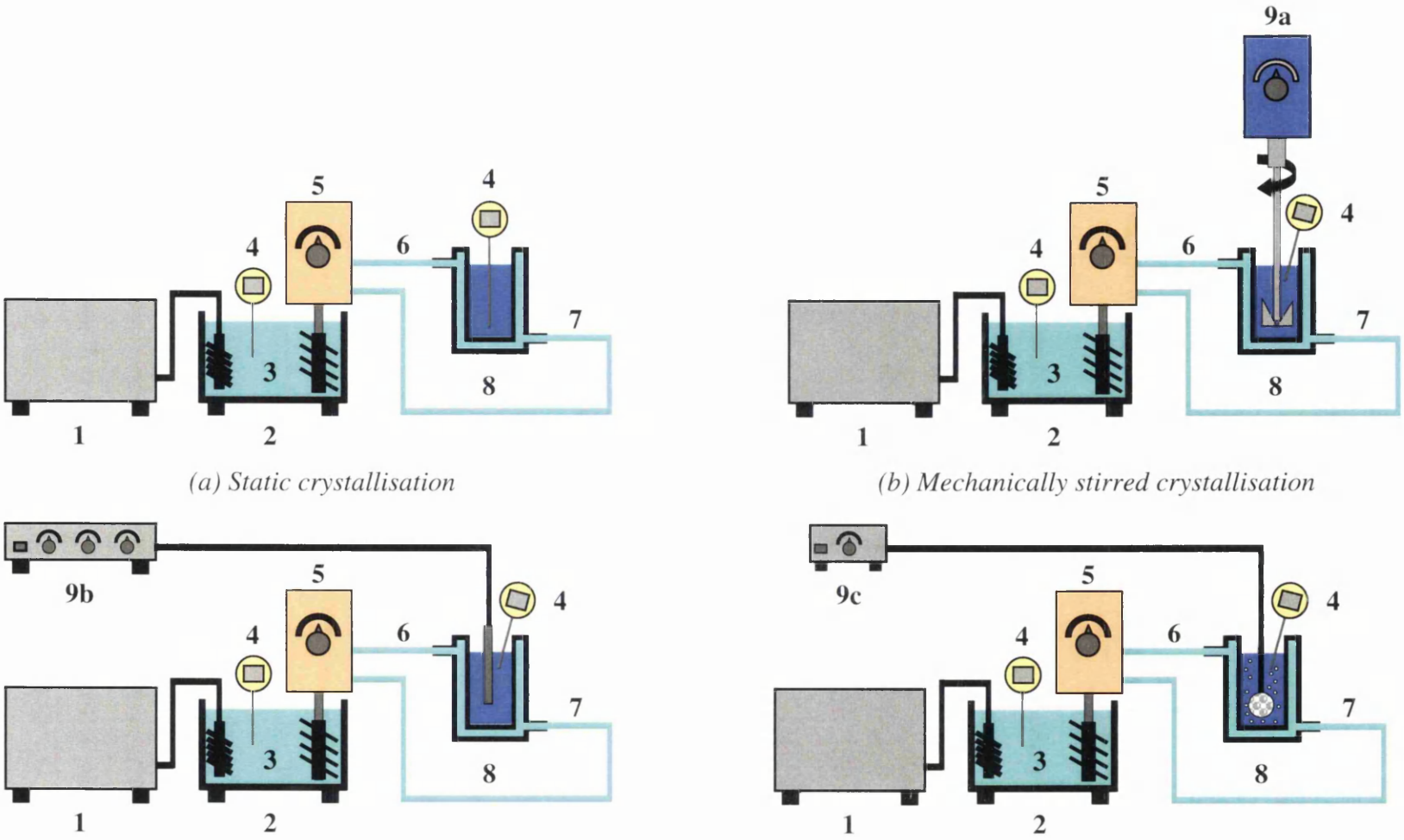

(a) Static crystallisation

(b) Mechanically stirred crystallisation

(c) Crystallisation with ultrasonic device

(d) Crystallisation with air-pump

Fig. 3.1: *Scheme of experimental setups, where; (1) Refrigerated immersion cooler, (2) Refrigerated thermostatic bath, (3) Heat transfer medium (HTM), (4) Digital thermometer, (5) Circulator, (6) and (7) Inlet and outlet HTM flexible tubes, respectively, (8) Jacketed beaker, and Agitation systems; (9a) Mechanical stirring, (9b) Ultrasonic device, (9c) Air-pump.*

pump assembly which includes an air-pump (Resun), flexible airline tubing, and one inch ball type ceramic air-stone diffuser (Won Brothers, Model: AP-WB14514). The experimental setup for the crystallisation process using an ultrasonic radiation system, on the other hand, was provided with the ultrasonic radiation assembly that consisted of an ultrasonic processor device (Ultrasonic Processor, Model: VC 130, Sonics, Vibra-cell), and an ultrasonic probe (CV18, S&M 1101).

All experimental setups utilised two digital thermometers, where the first one (Checktemp, Hanna Instruments) was used for monitoring the operating temperature of HTM, while the second one (Digital Thermometer Instant, Model: 9847N, Taylor) was used to track the temperature of feed/residue during the operational period of the experiment. This was achieved by immersing the semiconductor measuring elements of the digital thermometers into the mentioned solutions by means of supporting equipment.

All experimental setups were also monitored with a Kilowatt Hours Meter (kWh meter) (Efergy smart wireless electricity meter) to measure the energy consumption of the crystallisation operation.

3.5 Experimental Procedure

The operating procedure for the experiments is presented in Fig (3.2). These experiments were carried out in batch mode. Referring to the simplified block diagram in Fig (3.2), prior conducting any experiment, the feed sample was prepared and then the physiochemical analyses were performed on the feed sample. The jacketed beaker was filled with a constant mass of feed material i.e. 200 g. For all experiments, the temperature of the HTM was initially reduced via operation of the refrigerated immersion cooler. When the temperature of HTM reached the desired crystallisation temperature, the circulator was manually turned on, and then simultaneously the operational cycle of pre-cooling takes place to decrease the temperature of the jacketed beaker which includes the feed sample. This is achieved by pumping the HTM from the thermostatic bath to the jacketed beaker at flow rate of 0.8 L/min. The HTM temperature was controlled and set at a desired value through a temperature control knob on the circulator.

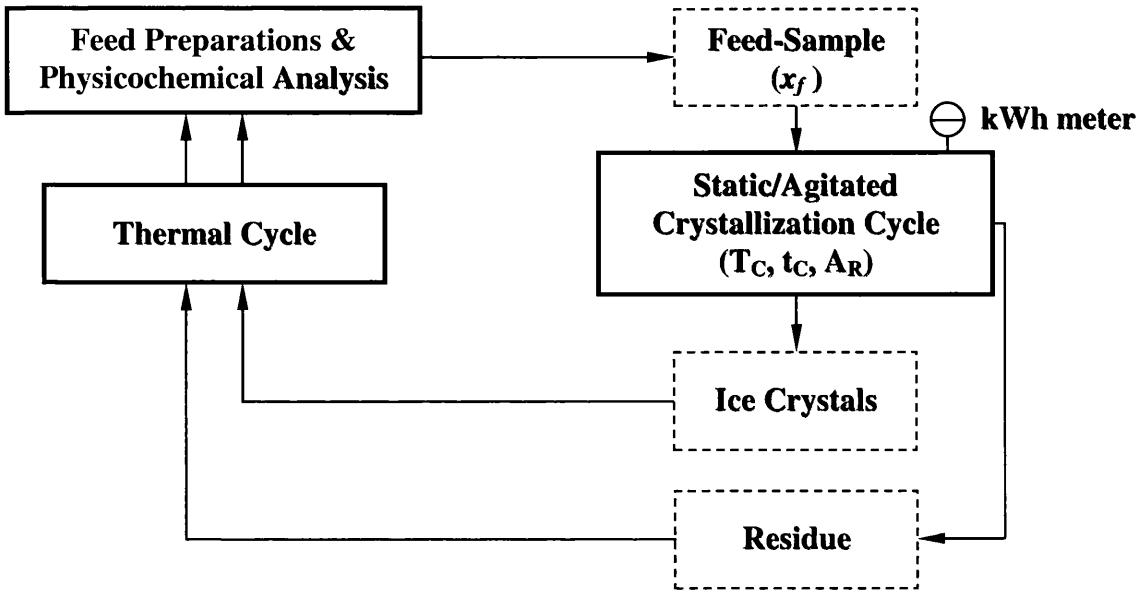

Fig. 3.2: *Simplified block diagram of the operational process for the experiments, where x_f is the feed concentration (ppm), T_C is the temperature of crystallization process (°C), t_C is the running time of crystallization process (minute), and A_R is the agitation rate.*

For all experiments using the agitated crystallisation process, the agitator system used, such as; stirring paddle, air-stone diffuser, or an ultrasonic probe, was dipped into the jacketed beaker and set at distance of 12.5 mm above the lower surface of the jacked beaker in order to avoid ice encasing the agitator. The agitator suspension was supported by means of supporting equipment. The agitation system was turned on prior to starting the pre-cooling operation. The agitation rate (such as air pressure for the bubbling process, stir rate for the mechanically stirred system, and amplitude rate for the ultrasonic process) was set at the predetermined value which remains constant for the duration of the experiment.

For crystallisation experiments using a static approach, the overhead stirrer assembly was devoted only to the pre-cooling process at a rotational speed of 400 rpm, so when the feed temperature reaches the freezing point, the operation of overhead stirrer assembly was terminated and the impeller was rapidly removed from the jacketed beaker. This procedure enhanced and accelerated the pre-cooling process.

When the flowing HTM circulates around the jacketed beaker's surfaces, the HTM absorbs heat from the feed sample through the refrigerated surfaces of the jacketed beaker.

Consequently, the feed temperature was gradually reduced. By continuously circulating HTM around a jacketed beaker, the temperature of the feed sample decreased until the freezing point of the feed was reached. For all experiments, once the temperature of the feed sample reaches the freezing point of the feed, a seed ice crystal was added to achieve nucleation of ice crystals (and to avoid nucleation at high supercooling) which then gradually grow over the duration of the experiment. By continuously circulating HTM around a jacketed beaker, the ice crystals progressively crystallised on the refrigerated surfaces of the jacketed beaker perpendicularly outward to the surfaces leading to the formation on an evenly thin crystal coat on the refrigerated surface. This process simultaneously leads to reduce the mass of residue. After running the experiment for a pre-determined time, the operation of the circulator was terminated and simultaneously the residue (i.e. brine) was drained and retained for further analysis as shown in Fig (3.2). After draining the brine from the system, the ice crystal layer was melted inside the jacketed beaker by flowing hot water through the jacketed vessel. Following sampling, physiochemical analyses were carried out on the residue and product samples as per standard procedure as shown in Fig (3.2).

All tests were performed according to the predetermined values shown in Table (3.1). The crystallisation experiments were conducted under different conditions and operating modes. This was done by changing the mode of crystallisation, and operating conditions, such as initial feed concentration, agitation rate, crystallisation time, and crystallisation temperature.

Run No.	**Crystallisation Mode**	**Feed Salinity**	**Freezing Time**	**HTM Temp.**	**Agitation Rate**
		(wt%)	(min)	(°C)	(rpm), (L/min), or (Amplitude)
1 – 64	Static	0.5 – 7	15 – 60	-11.5	0
65 – 67	Static	0.5	60	-4.8 – -11.5	0
70 – 195	Bubbled	0.5 – 7	30	-11.5	0 – 13.5 L/min
129 – 144	Mechanically Stirred	0.5 – 7	30	-11.5	0 – 900 rpm
169 – 172	Ultrasonic	0.5 – 7	30	-11.5	0 – 100

Table 3.1: *Operating parameters and conditions during crystallisation experiments.*

3.6 Results and Discussion

For the purpose of establishing a phase diagram for the aqueous solutions of sodium chloride (NaCl), the parameter of freezing point depression was determined theoretically over a wide range of salt concentrations, ranging from 0 ppm up to 235,000 ppm. The calculations and the theoretical results are given in Table A3-14 in Appendix A3. Furthermore, the relationship between the electrical conductivity and salt concentration (measured in mg/L) was determined by experimentally measuring the salinity of NaCl solution over a wide range of electrical conductivity values, ranging from 0 to 252 mS/cm. Experimental results are tabulated in Table A3-15 in Appendix A3. The variations of the mentioned theoretical and experimental results of key parameters were plotted on graphs as shown in Figs (3.3) (a) and (b). Based on the experimental results, the empirical polynomial correlations were derived and fitted for the freezing point as a function of TDS value (ppm), and for the TDS value (ppm) as a function of electrical conductivity (mS/cm). These equations were used to instantly calculate the theoretical results of the main key parameters from the conductivity measurement.

Fig (3.3) (a) – (b) shows the theoretical phase diagram, and empirical graphs and equations (including R value) for the NaCl solution. The important observations that can be made from the phase diagram is that the theoretical freezing points of the investigated NaCl solutions (which have TDS values of 0.5, 3.5, and 7.0 wt%) were -0.3, -2.3, -4.8°C, respectively. In contrast, the experimental results were -0.4, -2.2, and -4.7 °C, respectively. According to van der Ham *et al.* (1998), the eutectic temperature for the NaCl solution is -21.2°C, determined at eutectic chemical composition of 23.3 wt% NaCl salt and electrical conductivity of 246 mS/cm.

3.6.1 Static crystallisation process

Two sets of experiments were carried out on the static crystallisation process. The first set was done at a feed concentration of 0.5 wt%, where the crystallisation temperatures ranged from -4.8 to -11.5°C. The actual operational period of the crystallisation process for the experiments was set at 1 h. Results of these experiments are presented in Fig (3.3) (c). The second set of the experiments was performed at various feed concentrations ranging from 0.5 – 7.0 wt%. The crystallisation temperatures were set at -11.5°C, while the actual operational

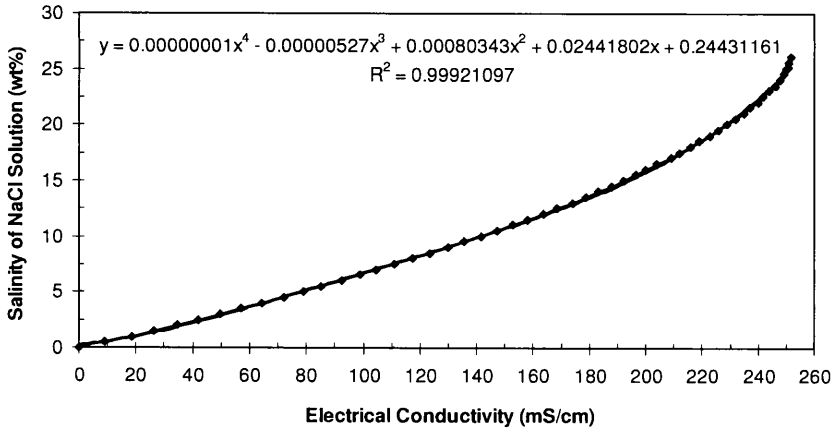

(a) Salinity of NaCl solution vs. electrical conductivity

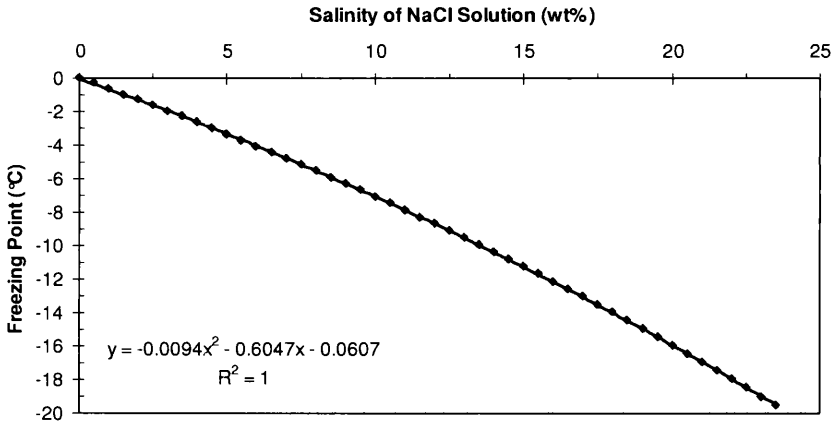

(b) Phase diagram

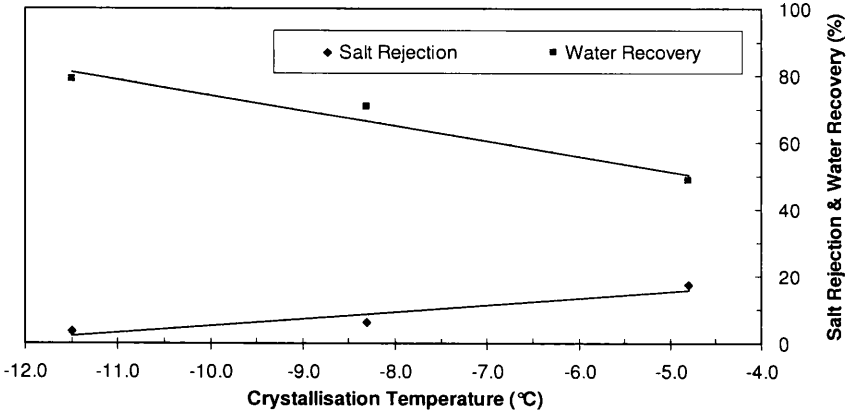

(c) Salt rejection and water recovery vs. crystallisation temperature

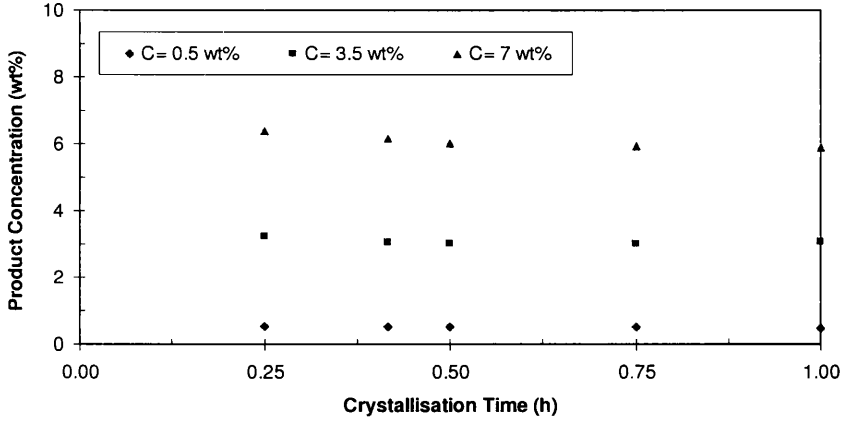

(d) Product concentration vs. crystallisation time

Fig. 3.3: *Summary of the phase diagram and relationships between the main key parameters for the NaCl solution, and experimental data for static crystallisation experiments, where y and x are the dependant and the independent variables of the empirical equation respectively, and R^2 is the polynomial regression correlation coefficient.*

period of crystallisation process for the experiments was varied from 0.25 to 1 hour. Results of these tests are given in Fig (3.3) (d) and Figs (3.4) (a) and (b).

The effect of crystallisation temperature on the salt rejection ratio can be observed in Fig (3.3) (c). The results indicate that the salinity of product water is very sensitive to changes in crystallisation temperature. The results proved that the slow crystal growth rates, dictated by reducing the crystallisation temperature, are of great importance in improving the separation efficiency of the static crystallisation process. The maximum and minimum salt concentrations of product water were 0.41 and 0.48 wt%, respectively, where these values were achieved at a crystallisation temperature of -4.8 and -11.5°C, respectively. However, a dramatic decrease in water recovery ratio was observed when the crystallisation temperature was increased (see Fig (3.3) (c)).

Fig (3.3) (d) shows the influence of the crystallisation time and feed concentration on the quality of product water, in terms of salinity. The salt concentration of product water was found to be proportional to the feed concentration (see Fig (3.3) (d)). As a result, the salinity of product water dramatically decreased (i.e. improved) as the feed concentration decreased. Thus, this clearly indicates that the product quality is sensitive to the variations of the feed concentration. The salinity of product water, on the other hand, was not affected throughout by the variation of crystallisation time, as shown in Fig (3.3) (d). In general, the salinity of product water was on average 0.49, 3.06, and 6.07 wt% for the experiments with NaCl solutions at concentrations of 0.5, 3.5, and 7 wt%, respectively.

Fig (3.4) (a) and (b) shows the influences of feed concentration and crystallisation time on the performance of the static crystallisation process, with respect to salt rejection and water recovery ratios. Fig (3.4) (a) shows that the salt rejection ratio increased slightly as the crystallisation time increased. This was because the thickness of the crystal layer, which is a relatively good heat insulator, increased with increasing crystallisation time. As a result, reduction in the heat transfer rate, accompanied by a reduction in the growth rate, occurred when the crystallisation time increased. By comparing the results of the experiments with feed concentrations of 3.5 and 7 wt%, the salt rejection was slightly reduced as the feed concentration decreased. However, the trend is different for feed water with a salt concentration of 0.5 wt% compared to the results of the experiments with higher feed

concentrations. The salt rejection was noticeably reduced for the case of 0.5 wt% feed concentration. The reason behind this was associated with the investigated crystallisation temperature, which was set at a constant low value, taking into account that the freezing points of the investigated feed samples are not identical. Thus, the temperature difference between the crystallisation temperature and freezing point of feed for the tested feed samples was not same. As a result, the cooling rate becomes higher in the case of 0.5 wt% feed concentration. On the other hand, the water recovery was found to be proportional to the crystallisation time and inversely proportional to the feed concentration as shown in Fig (3.4) (b). For all tests, the ice crystal layers, obtained from all static crystallisation experiments, were found to be rigid.

Within the studied domain, the separation performance of the static crystallisation process was found to not be efficient in purifying the crystal layer and its quality. Relatively poor quality product water was obtained, even for low feed concentrations, which was due to inclusion of drops or pockets of brine within the crystal layer. According to Ulrich and Glade (2003), the main reasons for obtaining high impurity crystal layers are usually associated with the following; (i) nucleation achieved at high super-cooling; (ii) high crystal growth rates; and (iii) adherence of contaminated reject brine at the end of the crystallisation step. Therefore, further optimising the crystallisation temperature can be suggested for each feed concentration case, in order to improve the salt rejection ratio. This is due to the mentioned parameter greatly influencing the salt rejection as previously proven through experimental investigation (see Fig (3.3) (c)). However, the water recovery would be expected to be lower, while optimising the crystallisation rate, leading eventually to a negative effect on the production rate. Therefore, the crystallisation process with various forms of agitation systems was examined at low crystallisation temperature, in order to upgrade the quality of product water without reducing the water recovery ratio by means of crystallisation temperature.

3.6.2 Crystallisation process using mechanically stirred system (MSS)

In the second investigation, the performance of the crystallisation process using MSS for treating different salt concentrations of feed was investigated. The feed concentrations were varied from 0.5 – 7 wt%, while the crystallisation temperature was set at -11.5°C. The actual operational period of the crystallisation process for the experiments was kept constant at 0.5

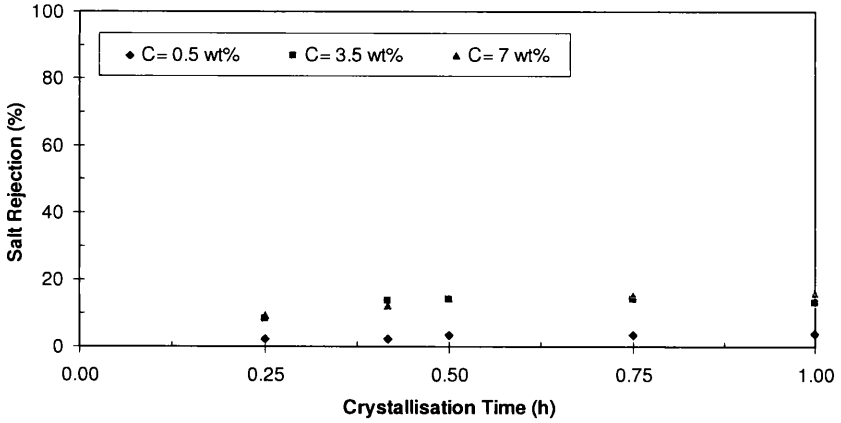

(a) Static crystallisation process: salt rejection vs. crystallisation

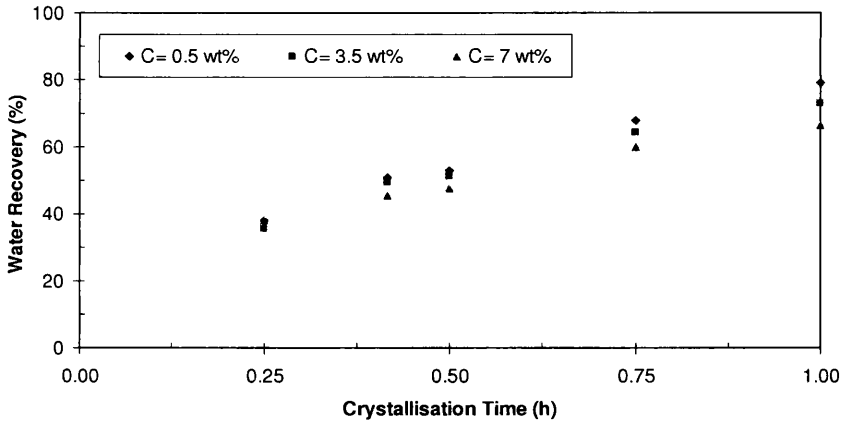

(b) Static crystallisation process: water recovery vs. crystallisation

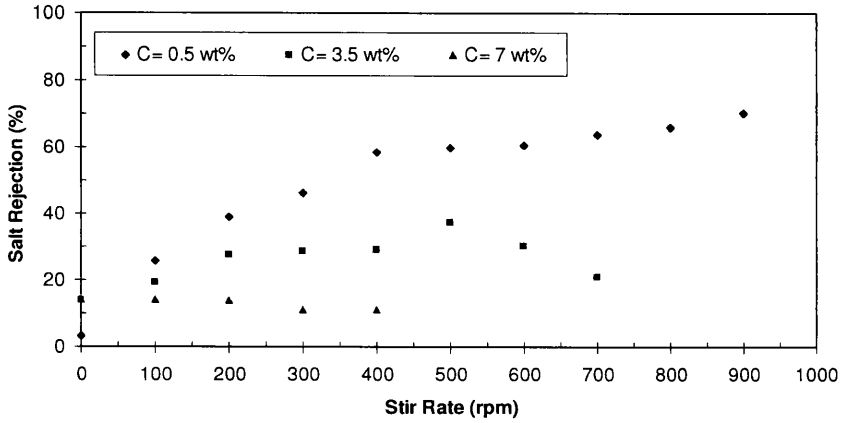

(c) Crystallisation process using MSS: salt rejection vs. stir rate

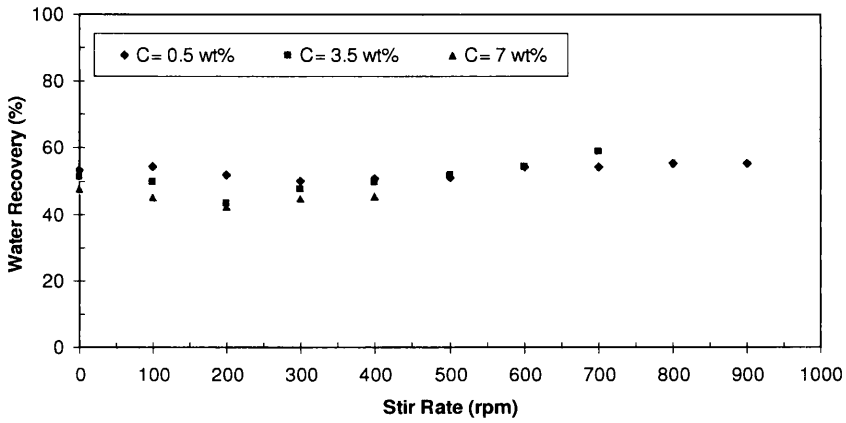

(d) Crystallisation process using MSS: water recovery vs. stir rate

Fig. 3.4: *Experimental data for static and MSS crystallisation experiments. Operating conditions for crystallisation operations are: feed concentration of 0.5 – 7.0 wt%, end-point temperatures are -4.8 – -11.5°C, and crystallisation time ranges from 0.25 to 1 hour.*

h to avoid a high risk of stirrer damage, as the impeller almost reached the crystal layer. The investigated stir rate ranged from 100 up to 900 rpm. Results of salt rejection and water recovery ratios, as a function of the stir rate are shown in Figs (3.4) (c) and (d).

Although the experiments were carried out at a low crystallisation temperature, the results of the salt rejection ratio significantly increased (i.e. improved) as the stir rate increased for the cases of treating feed salinities of 0.5 and 3.5 wt%. For instance, when the stir rate was set at 900 rpm, the salt rejection increased substantially from 2.3 to 70.2% for the case of a feed salinity of 0.5 wt% (see Fig (3.4) (c)). When the stir rate was set at 500 rpm, the salt rejection was significantly increased from 13.6 to 37.3% for the case of treating a feed salinity of 3.5 wt% (see Fig (3.4) (c)). However, a slight reduction in the salt rejection ratio was observed as the stir rate increased for the case of treating a feed with a salinity of 7 wt% (see Fig (3.4) (c)). This clearly indicates that the effectiveness of stir rate is powerful in improving the quality of product water for the cases of treating feeds with low to moderate salt concentration. A significant increase in salt rejection was also observed as the salt concentration of feed decreased (see Fig (3.4) (c)). The water recovery ratio, on the other hand, was not changed by the variation of stir rate as shown in Fig (3.4) (d). However, a slight decrease in the water recovery ratio was noted as the feed salinity increased (see Fig (3.4) (d)).

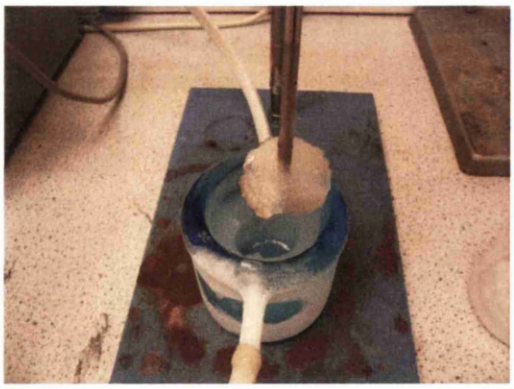

Fig. 3.5: *Undesired ice suspension in a crystalliser*

For the cases of feed salinity of 3.5 and 7 wt%, the maximum investigated stir rates were 400 and 700 rpm, respectively; higher stir rates were not possible, based on visually noting the appearance of an undesired ice suspension (i.e. the ice crystal becomes slushy) inside the

crystalliser as shown in Fig (3.5). The ice suspensions formed in the crystalliser were not considered in this study.

3.6.3 Crystallisation process using ultrasonic process

The third investigation was performed on the crystallisation process using an ultrasonic process. The investigated feed concentrations, crystallisation temperature, and crystallisation time are the same as given previously for the second investigation (see section 3.6.2). The investigated amplitudes ranged from 20 up to 100.

Fig (3.6) (a) and (b) shows the salt rejection and water recovery ratios as a function of the amplitude, measured at different feed concentrations. The results indicate that the ultrasonic process positively enhanced the separation performance of the crystallisation process. In the cases of treating feed salinities of 0.5 and 3.5 wt%, a significant increase in the salt rejection ratio was observed as the amplitude value increased (see Fig (3.6) (a)). Fig (3.6) (a) shows that the maximum salt rejection ratios were 84 and 34 % for feed salinities of 0.5 and 3.5 wt%, respectively. This means that the product water was at 0.08 and 2.32 wt%, respectively. The salt rejection also improved for the case of a feed salinity of 7 wt%. For instance, the salt rejection increased from 14 to 28% (see Fig (3.5) (a)). This clearly indicates that the ultrasonic process is effective in lowering the salt concentration of product water for treating low to high feed concentrations.

Throughout the tests, the crystal layer was not formed on the bottom heat transfer surface of the crystalliser, in comparison to the previous experiments with other experimental setups. The reason behind this was that the probe of the ultrasonic system was positioned above the crystalliser. As a result, the ultrasonic waves prevented the formation of the ice crystal on the bottom heat transfer surface of the crystalliser. Therefore, the water recovery ratio was dramatically decreased as the amplitude increased (see Figs (3.6) (b)). This clearly indicates that the water recovery ratio was inversely proportional to the amplitude. A noticeable decrease in water recovery ratio was also observed as the salt concentration increased (see Fig (3.6) (b)). For the case of a feed salinity of 7 wt%, no product water was obtained from the experiment when the amplitude reached 60 and above (see Figs (3.6) (b)). A similar situation occurred for the case of 3.5 wt% feed salinity, when the amplitude reached 100 (see Fig (3.6) (b)). This was because higher agitation rate results in slushy ice rather than having a

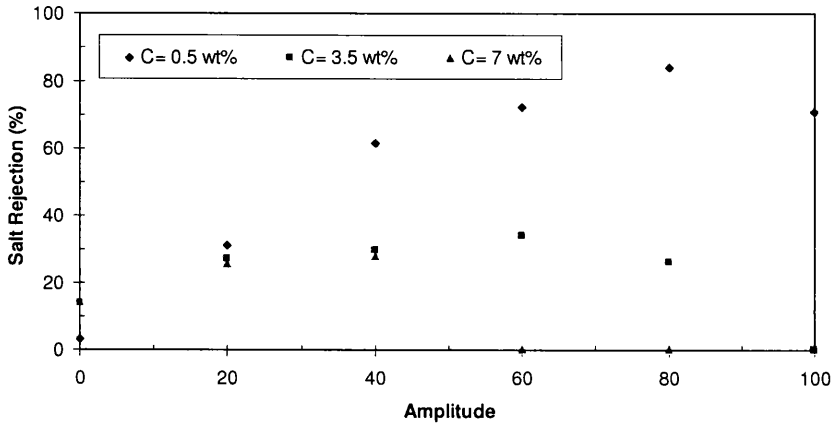

(a) Salt rejection vs. amplitude

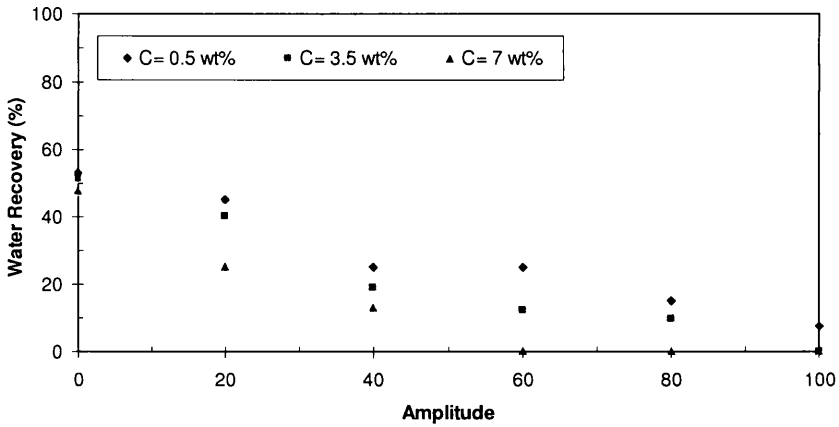

(b) Water recovery vs. amplitude

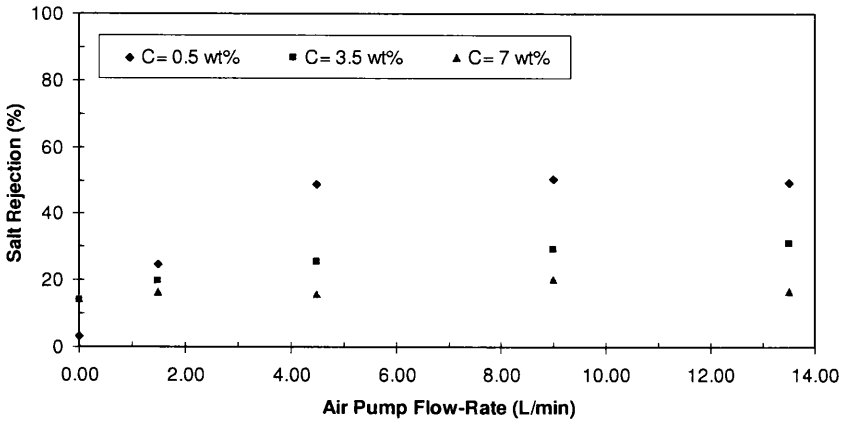

(c) Salt rejection vs. air pump flow-rate

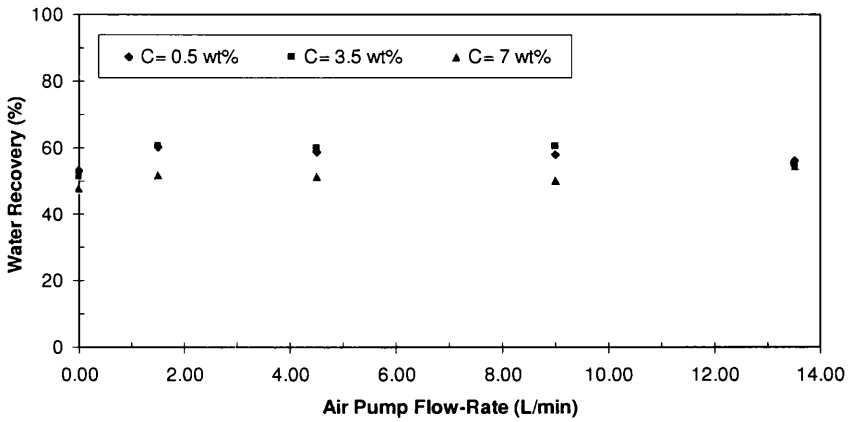

(d) Water recovery vs. air pump flow-rate

Fig. 3.6: *Experimental data for the ultrasonic and bubbled crystallisation experiments. Operating conditions for crystallisation operations are; feed concentration of 0.5 – 7.0 wt%, end-point temperature of – -11.5°C, and crystallisation time of 0.5 hour.*

rigid crystal layer, where these crystals cannot stick to the heat transfer surface as the waves produced by the ultrasonic system break these up.

3.6.4 Crystallisation using bubbling process

In the fourth series of experiments, the potential capability of the crystallisation step agitated by a bubbling process was investigated. The investigated feed concentrations, crystallisation temperature, and crystallisation time are as given previously for the second investigation (see section 3.6.2). The investigated air pump flow-rates ranged from 1.5 up to 13.5 L/min.

Fig (3.6) (c) shows the variation of salt rejection as a function of the air pump flow-rate. The air pump flow-rate also has a strong influence on the quality of product water, where this parameter was found to be effective in removing significant amounts of dissolved salt from the investigated feed concentrations, more specifically feed samples with salt concentrations of 0.5 and 3.5 wt%. Fig (3.6) (c) shows that the salt rejection ratio was significantly increased as the air pump flow-rate increased for the case of feed sample with concentration of 0.5 wt%. However, the salt rejection was reduced with increasing salt concentration of feed samples, which was noticeable for the experiments with feed concentrations of 7 wt% (see Fig (3.6) (c)). In fact, the salt rejection ratio, for such feed concentrations, was not affected by the variation in the air pump flow-rate. In general, the trend of salt rejection results was found to be in agreement with the previous experimental results for the crystallisation processes using mechanically stirred and ultrasonic systems.

As shown in Fig (3.6) (d), the water recovery ratio, on the other hand, increased slightly when the air pump flow-rate reached 1.5 L/min and then the water recovery ratios were stabilised until the air pump flow-rate reached the maximum value. A dramatic decrease in the water recovery ratio was also observed as the feed salinity increased (see Fig (3.6) (d)).

3.7 Conclusions

This chapter presented a series of laboratory investigations, performed on a static crystallizer with different types of agitation systems, for desalting NaCl solutions at concentrations ranging from 0.5 up to 7 wt%. The investigated agitation systems were a bubbling process, a mechanically stirred system, and an ultrasonic process. Several influences, including:

crystallisation temperature, time, and agitation rate, on the degree of desalination, in terms of salt rejection and water recovery ratios, were investigated and assessed.

The results were gathered, analysed, and compared to the results of the performance of the static crystallizer when no agitation was applied. The results of the laboratory experiments showed that, in the case of feed salinities ranging from 0.5 up to 3.5 wt%, the product quality achieved by the crystallizer was significantly improved through agitation, while the lowest salt rejection was achieved when the static crystallisation process was applied. The most effective processes, in terms of salt rejection and recovery, were the bubbling process and mechanically stirred system. Although the ultrasonic process gave the highest salt rejection ratio for the cases of low to high feed concentration, the water recovery ratio was relatively poor when compared to the static crystallisation process, with and without agitation (i.e. bubbling process and mechanically stirred system). Apart from the ultrasonic system, the performance of the agitated and static crystallisation processes declined for high saline applications (i.e. 7 wt%). In general, the results show that the application of agitation systems within the solid layer crystallisation process is encouraging. For commercial applications, the bubbling process might be the most feasible technique, since this method can be easily designed and built for large-scale applications.

CHAPTER IV:

ASSESSMENT OF ICE MAKER USED FOR SALINE WATER APPLICATIONS

4.1 Introduction

The brine treatment process compared to any form of saline water desalination process is by far the most expensive and complicated. This is because brine contains high levels of a wide range of dissolved salts, which result in severe technical problems to the treatment system equipment, and a vast increase in capital and operational treatment costs. For instance, when the TDS value of brine reaches a critical limit, exceeding 70,000 ppm, the majority of desalination technologies, including all conventional membrane and thermal desalination processes, are no longer economical and/or technically feasible to be used as a treatment system [Ahmad and Williams, 2011]. For such applications, however, a unique situation has arisen which paves the way for separation through a freezing process. The proposed technology offers significant advantages over other desalination processes in respect to the technical, economic, and environmental aspects.

Ice maker machines are used extensively in many commercial and residential areas for the purpose of making ice cubes. There are a variety of ice maker machines with different production rates of ice cubes (up to 200 tons per day) available nowadays in the market. In principle, these ice making machines are potentially capable of producing ice cubes from aqueous solutions, as long as the operating temperature of the refrigeration system is considerably lower than the freezing point of the feed streams. When the produced ice cubes are melted to yield product in liquid form, the quality of the product water is expected to be higher than that of the feed water. A certain amount of dissolved salts will be rejected to the remaining residual liquid during the growing crystal layer. However, the degree of separation by freezing, in terms of the salt rejection and water recovery ratios, is dictated by several factors and influences, such as operating conditions and feed quality. With the purpose of verifying and assessing the major factors influencing the performance of the ice maker machine, one commercial ice maker machine was tested for desalting a range of liquid

streams, using aqueous solutions of sodium chloride and process brines, at different salt concentrations.

The primary concern of this study is to provide important new findings on the performance of the ice maker, and more specifically to examine the potential capability of falling film crystallisation for treating brines. The aim of this chapter is to verify the influence of several parameters, namely crystallisation time, feed salt concentration, and circulated feed flow rate, on the purification of ice crystals and yield, in terms of salt rejection and water recovery ratios. Since the degree of purity and concentration can be improved by repeating the freezing stage for the product and residual liquid, respectively [Ulrich and Glade (2003); Sulzer (2004)], the performance of multi-staging crystallisation processes was experimentally assessed for further purification and concentration of the product and residue, respectively. In addition, this laboratory study sheds light on the effectiveness of the falling film crystallisation process upon the rejection of the major components of ionic concentration of various feed materials using process brines, such as Arabian Gulf seawater and RO brines. Post-treatment processes, such as washing and sweating, were not considered in this experimental investigation.

4.1.1 Description of Ice Maker Machine and Basic Operation

An ice maker machine, commercially known as the K40 ice maker (AGH327, Whirlpool), was considered and tested in this study. A typical example of the K40 ice maker machine and the major items of equipment being used in this appliance are presented in Fig (4.1). For the sake of clarification, the proposed ice maker machine will be identified and referred to, in the course of this chapter, as ice maker. The ice maker is classified as a batch type ice maker, so in this ice maker a plurality of individual ice cubes are continuously formed in batches and are harvested and then stored in the storage bin. The technical specifications of the tested ice maker are as follows; (i) The ice maker is capable of producing 40 kg of ice cubes per day. An estimate of 5,600 cubes per day can be produced where approximately 60 – 70 ice cubes per cycle can be achieved. The time cycle averaged about 17 minutes; (ii) The dimensions of the produced ice cube are 29 mm and 29 mm, whereas the thickness of the ice cubes can be adjusted between 10 – 12 mm; (iii) The capacity of the storage bin is 20 kg; (iv) The

dimensions of the ice maker (i.e. width, depth, and height sizes) are 555, 535, and 850 mm; (v) The ice maker consumes 0.19 kWh per kg of ice cubes.

(a) K40 ice maker

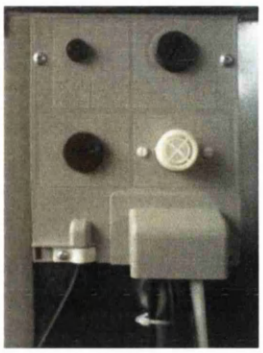

(b) Rear control panel

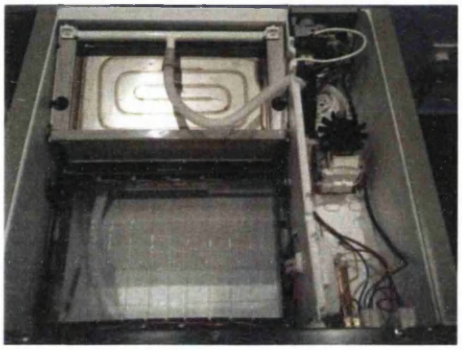

(c) Water recirculation system equipment

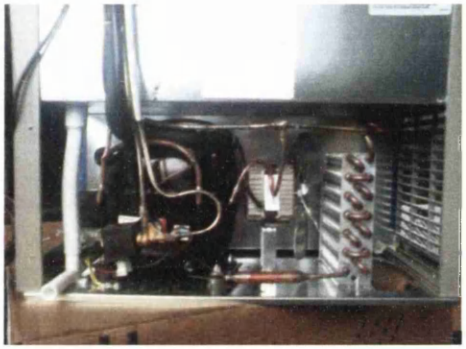

(d) Refrigeration system equipment

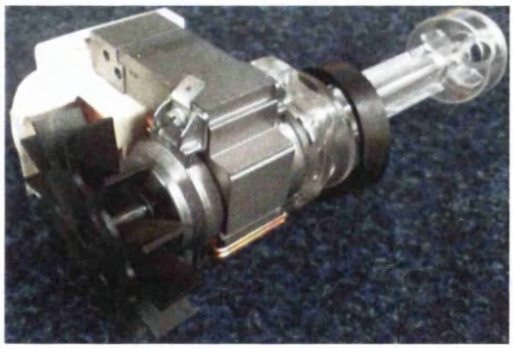

(e) Circulation pump

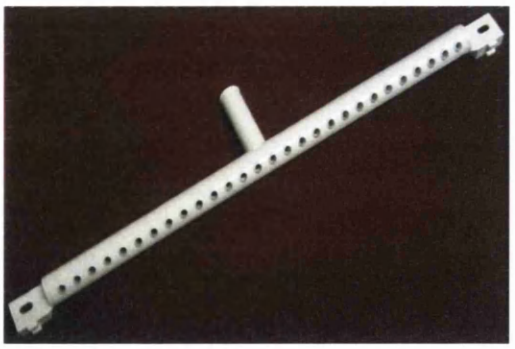

(f) Water distributor

(g) Ice thickness thermostat

(h) Storage bin thermostat

Fig. 4.1: *K40 ice maker and its major items of equipment [Whirlpool, 2011].*

The main operating systems of the ice maker are; (a) electrical and control, (b) filling (c) water recirculation, and (d) refrigeration and heating [Whirlpool, 2009].

(a) Electrical and control system

This system supplies electrical power for the operating systems. Moreover, this system leads and controls the operational cycles of the ice maker by means of an electronic control board. The ice maker is provided with two control panels, namely, front and rear control panels. The front control panel (see Fig (4.1) (a)) contains two switches enable the user to control the operation and cleaning of the ice maker. The rear control panel (see Fig (4.1) (b)) contains two dials that enable the user to adjust the ice thickness and storage bin thermostats. The rear control panel also includes the tubular inlet of the water supply, which is one of the main parts of the filling system.

(b) Filling system

The filling system contains a tubular inlet for the water supply, pipelines, a restricted water inlet valve, and float sensor. The main role of this system is to monitor and control the water level of the collecting tank in order to keep the water level within the allowable limit for the crystallisation process. A low water level within the collecting tank is detected by means of float sensor (known as the float switch or liquid level sensor). The float sensor protects the circulation pump from damage through running dry [Ayres *et al.*, 1954; Whirlpool, 2010]. When the float sensor detects a low level of liquid within the collecting tank or if the tank is empty, then the crystallisation process operation will automatically be terminated. The crystallisation process operation is automatically resumed when the water reaches a predetermined level. This is achieved through the float sensor, which actuates the restricted water inlet valve to be set to a fully open position for filling the collecting tank with feed water. The restricted water inlet valve is an automatic solenoid valve controlled by means of a water level sensor. The ice maker, or more specifically the restricted water inlet valve must be connected to a water supply with a pressure of 2 bar.

(c) Water recirculation system

The water recirculation system is responsible for circulating water and distributing the flowing water evenly as a falling film over the upper surface of the inclined plate during the crystallisation process.

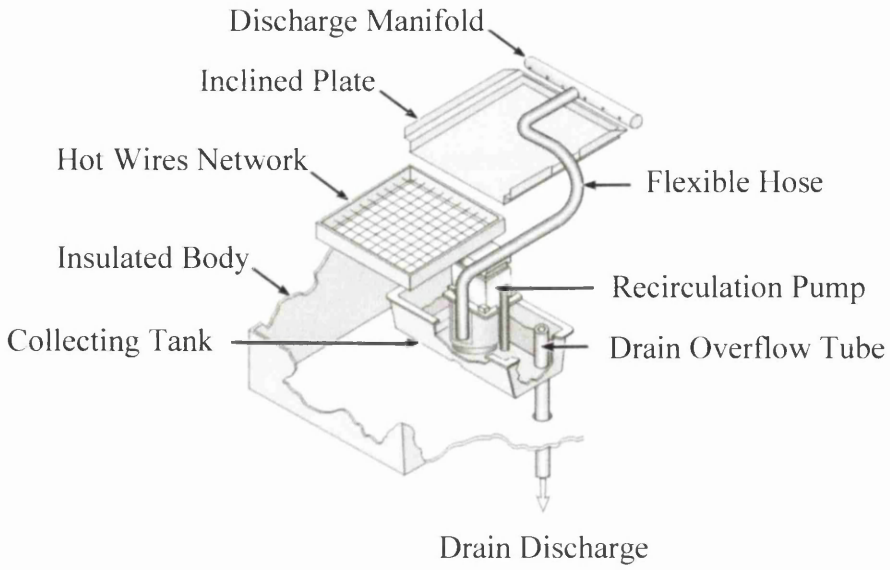

Fig. 4.2: *Simplified schematic diagram of the water recirculation system of the laboratory apparatus (adapted from Whirlpool (2009)).*

As shown schematically in Fig (4.2), the water recirculation system contains a collecting tank, a circulation pump, a flexible hose, a water distributor (i.e. discharge manifold), an inclined plate, and a drain overflow tube. The inclined plate is installed and set downward at angle of 195 degrees above the collecting tank. The dimensions of the inclined plate are 190 mm and 295 mm. The collecting tank with a capacity of 3.5 L is joined with a return manifold, which is positioned above the tank. The return manifold is also joined with the lower end of the inclined plate in order to guide the flowing water coming from the inclined plate to the collecting tank. A hinged deflector, which extends into the path of water flowing in front of the lower extremity of inclined plate, is also used for directing the water flow into a return manifold leading to the collecting tank. A tank rubber bung, which is fixed beneath the collecting tank, is used for draining the remained residual liquid or undesired water from the reservoir. As for the water distributor, this component extends transversely across the upper surface of the inclined plate. The water distributor is provided with 28 longitudinally spaced apertures through which water may flow [Ayres *et al.*, 1954]. The diameter of each aperture is 3.5 mm, while the longitudinal distance between the aperture centres is 10 mm. The length and diameter of the discharge manifold are 287 mm and 16 mm, respectively. The water distributor is provided with a tubular inlet which is located at the centre of the water distributor and this tubular inlet is connected to the circulation pump by means of a flexible hose [Barnard *et al.*, 1971]. The water distributor, return manifolds, and collecting tank are

made of polypropylene, which is capable of resisting reactive chemicals and corrosive environments.

With regard to the circulation pump, this is a pedestal sump type, and is electrically driven by a motor, which is attached to the pump casing by a vertical tube. The motor is positioned above the collecting tank, whereas the casing of the pump is submerged in the collecting tank. The maximum flow rate of the pump was experimentally determined as 6.3 L/min. Details on determining the flow rate are given in Table A4-1 in Appendix 4.

(d) Refrigeration and heating system

The refrigeration system of the ice maker machine is associated with the vapour compression system used to refrigerate and heat the inclined plate during crystallisation and disengaging stages, respectively. The refrigeration system contains a compressor, refrigerant (i.e. Freon R134a), an evaporator, a condenser assembly, a hot gas valve assembly, a capillary tube, a heat exchanger, a condenser accumulator tube and a series of refrigerant pipelines as shown schematically in Fig (4.3). The crystalliser of the ice maker machine is classified as a plate type heat exchanger, which includes an inclined plate that is provided with refrigerant and heating coils secured to the lower and upper surfaces, respectively [Ayres *et al.*, 1954; Ayres and Swanson, 1961; Whirlpool, 2010]. The refrigeration and heating coils are made of stainless steel and copper, respectively, while the inclined plate is made of stainless steel. These materials have excellent heat conduction, as well as excellent wear resistance in corrosive environments [Whitman *et al.*, 2004]. Although copper transfers heat much better than stainless steel, manufacturers usually select stainless steel because it is much more durable and resists corrosion better than copper or brass [Whitman *et al.*, 2004]. In general, the ice making technique may be termed as a solid layer crystallisation process using the falling film concept.

4.1.2 Mechanism of Ice Cubes Production

The operation of ice maker machine depends mainly on a storage bin thermostat (see Fig (4.1) (h)). The storage bin thermostat is installed in the storage bin to ensure that the predetermined amount of ice cubes had been reached. When the storage bin thermostat detects a low level of ice cubes within the storage bin or the bin is empty, then the operation

of ice maker starts automatically, producing the ice cubes. The ice maker produces ice cubes through a number of successive processes, namely (i) filling, (ii) crystallisation, (iii) ice slab separation, and (iv) ice cubes harvesting and storing.

(i) Filling process

Before starting the crystallisation process, the water level of the collecting tank is initially detected by the float sensor to ensure that the allowable water level has been reached.

(ii) Crystallisation process

Referring to the simplified schematic diagram shown in Fig (4.3), the refrigeration system for the crystallisation cycle operates as follows; the compressor receives the low pressure refrigerant gas through a suction valve, and then compresses the gas leading to an increase in the pressure and temperature [Whitman *et al.*, 2004; Whirlpool, 2009]. The hot pressurised refrigerant gas then travels from the compressor to the condenser through the discharge valve. The high pressure gas is cooled by means of a condenser, which leads the refrigerant vapour to condense into a liquid refrigerant, as the temperature of the refrigerant vapour reaches the saturation temperature corresponding to the high pressure in the condenser as reported in the literature [Whitman *et al.*, 2004; Whirlpool, 2009]. As the high pressure liquid refrigerant is transported into the evaporator at low pressure through the drier and capillary tube, reduction in feed pressure of liquid refrigerant to the evaporator is achieved by the capillary tube. When the low pressure liquid refrigerant absorbs heat from the flowing water over the evaporator, the liquid refrigerant evaporates, changing its state from liquid to gas refrigerant. The latter then flows into the accumulator. Following this, the low pressure gas refrigerant flows back to the suction line of the compressor through the heat exchanger.

During the crystallisation cycle, some of the hot gas flows into the condenser accumulating tube and accumulates, because the solenoid hot gas valve is closed [Whirlpool, 2009]. The accumulated gas in the condenser accumulating tube condenses to a liquid and remains in the accumulating tube for a reason which will be explained later in the ice separation cycle.

During the later stages of the crystallisation cycle, where the ice slab forms on the evaporator's surface, part of the low pressure liquid refrigerant passing through the evaporator will not evaporate into a gas, because the heat transfer rate is reduced by the

increasing thickness of the ice slab, which is considered a relatively good heat insulator [Pounder, 1965]. Therefore, the liquid refrigerant will settle in the accumulator while the refrigerant vapour is sucked off through the suction tube located above the accumulator [Whirlpool, 2009]. However, the accumulated liquid refrigerant in the accumulator will eventually be evaporated by flowing a relatively hot gas over the accumulated refrigerant during the ice separation cycle.

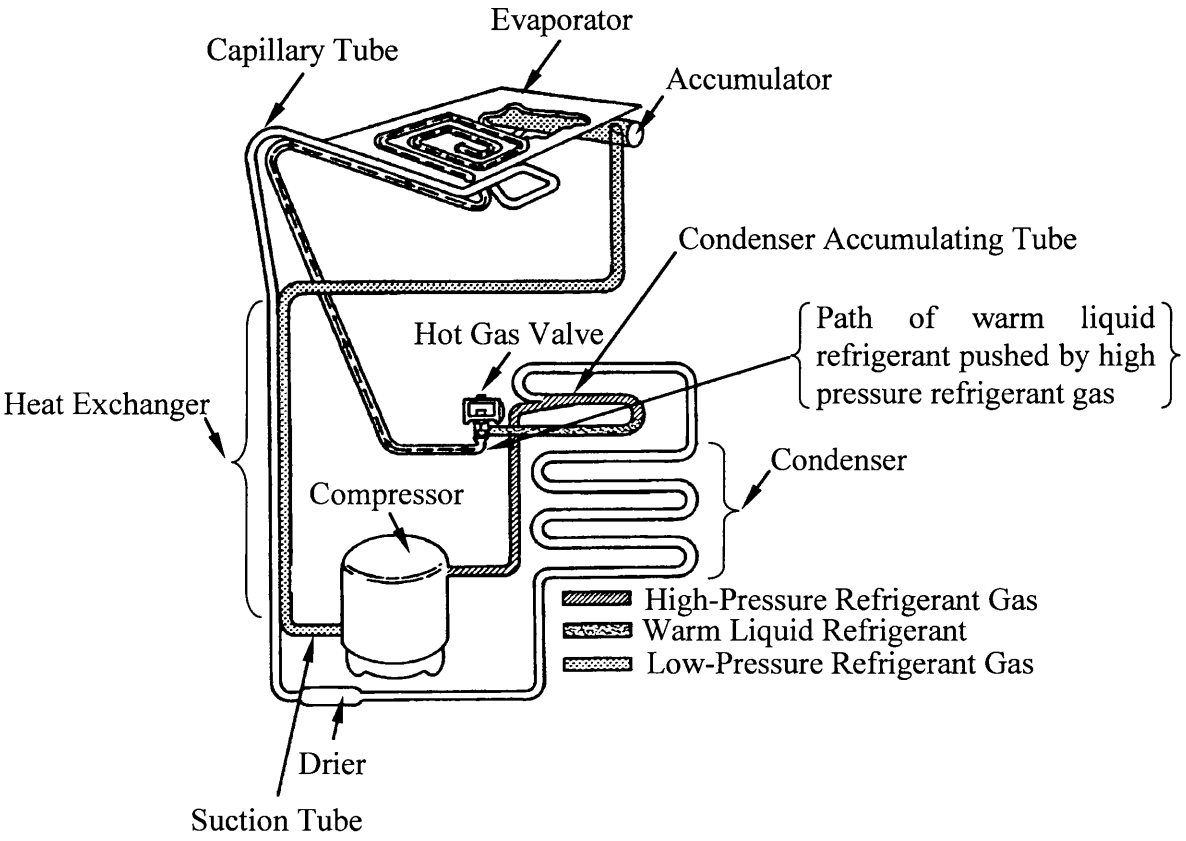

Fig. 4.3: *Simplified schematic flow diagram of refrigeration cycle [Whirlpool, 2009]*

The refrigeration coil, which is thermally connected beneath the inclined plate, will decrease the temperature of the inclined plate from 25°C to about -14°C during the crystallisation cycle.

With regard to the water recirculation cycle, the circulation pump continuously delivers feed upward from the collecting tank to the water distributor through a flexible hose, as shown schematically in Fig (4.4). The water is sprayed and distributed evenly as a falling film over the upper surface of the inclined plate through spaced apertures [Barnard *et al.*, 1971]. When

the water passes over the refrigerated plate as a falling film and reaches the lowest extremity of plate, the water falls back into the collecting tank guided by a return manifold along with a hinged deflector.

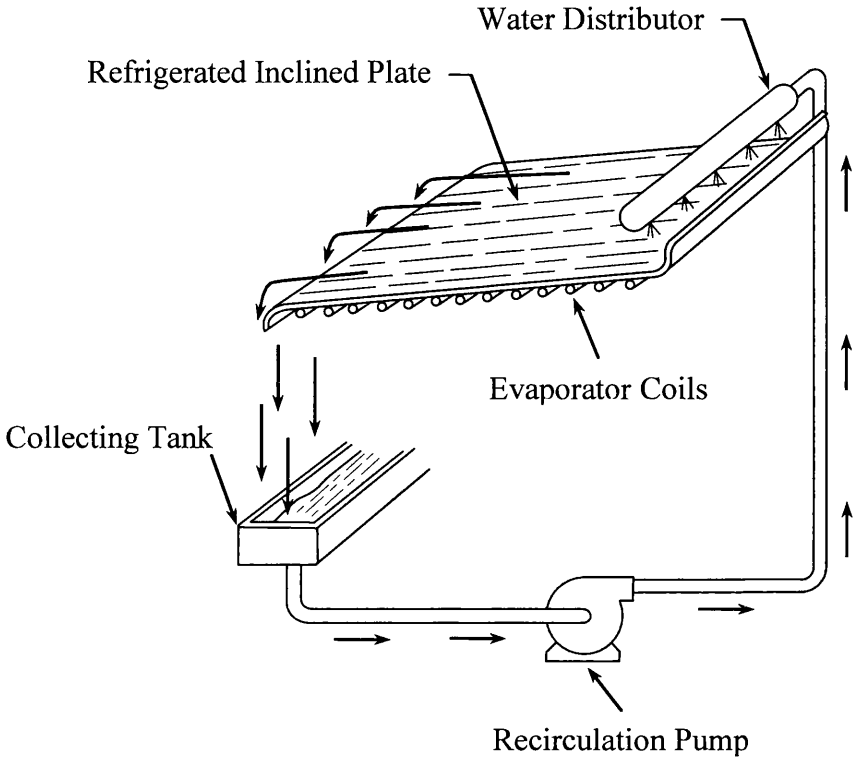

Fig. 4.4: *Schematic flow diagram of water circulation loop existed in the laboratory apparatus. The ice slab is formed by the water circulation and refrigerant loops (adapted from Whitman et al. (2004)).*

When the water passes over the refrigerated plate surface, discharge of heat from the water to the refrigerated plate leads to a gradual reduction of the feed temperature. By allowing water to flow continuously over the refrigerated plate, the temperature of the circulated water within the main equipment of the water circulation system will decrease to a temperature approaching the freezing point of the feed over a period of running time. Once the temperature of the water over the refrigerated plate reaches a certain critical temperature, dependant on the freezing point of feed, nucleation of ice crystals occurs, and then ice crystals form and grow gradually over the upper surface of refrigerated plate perpendicularly outward to the surface leading to the formation of an evenly thin crystal coat on the upper surface of the refrigerated plate [Ayres *et al.*, 1954; Ayres and Swanson, 1961; Whirlpool,

2010]. By continuously re-circulating the cold water above the existing crystal coat, the thickness of crystal coat on the refrigerated plate increases progressively over the operational period, which simultaneously leads to a reduction in the water level within the collecting tank.

The operational cycle of the crystallisation process is controlled by a predetermined thickness of ice slab, which can be adjusted by means of a thermostat knob. This is achieved by installing an ice thickness thermostat element at a certain distance located above the left hand-side of the plate's surface. When the ice thickness thermostat element is contacted by cold water (which is flowing over the surface of the ice slab), the temperature of the element will decrease leading to actuation of the switch in the ice thickness thermostat which terminates the ice making cycle (i.e. crystallisation) [Ayres *et al.*, 1954; Ayres and Swanson, 1961]. However, the evaporator's thermistor terminates the power only to the condenser fan and water circulation pump through an electronic control board, whereas the compressor is still turned "On". Moreover, the electronic control board supplies power to the hot gas valve solenoid to open the valve. This procedure leads to ending the operation of the crystallisation cycle, and simultaneously the ice separation cycle commences.

(iii) Ice slab separation process

The ice separation cycle takes place in order to disengage and release the ice slab from the inclined plate. When the hot gas solenoid valve is open, high pressure refrigerant gas is forced by a compressor to bypass the condenser and flow toward the condenser accumulating tube where the condensed refrigerant gas remaining from the previous operational cycle (i.e. crystallisation) is kept [Whirlpool, 2009]. As shown in Fig (4.3), the high pressure hot gas warms and pushes the liquid refrigerant accumulated in the accumulator tube upward toward the evaporator, which eventually leads to an increase in the temperature of the upper surface of the inclined plate from -14°C up to 11°C during the ice separation cycle [Whirlpool, 2009]. The hot liquid refrigerant evenly heats the plate by means of heating coils, so the thin ice slab is slightly and evenly defrosted and melted; the ice slab is easily and evenly disengaged from the plate, sliding through gravitational force. As the inclined plate is installed in front of the cutting grid, the ice slab then slides down toward the hot wires network by pushing and passing the hinged deflector [Ayres and Swanson, 1961]. The hinged deflector is designed to be swung out of the path of the ice slab by the weight of the

ice slab affected by the gravitational force, which permits the ice slab to slide out of the inclined plate. When ice separation is complete and more specifically the whole ice slab has passed the hinged deflector, then the hinged deflector returns back to its original position via return springs [Ayres and Swanson, 1961].

(iv) Ice cubes harvesting and storing process

The ice maker is provided with a cutting grid (i.e. a network of resistance wires). The operation of the cutting grid depends mainly on the ice harvest paddle lever (which is known as the plastic micro-switch actuating arm or tilt plate mercury switch). This component is installed above the cutting grid, and is designed to be swung out when the ice slab slides by gravity onto a cutting grid. Thus, the ice slab will swing and raise the ice harvest paddle lever in upward position, activating the operation of cutting grid. The latter slowly melts and cuts the ice slab into individual small ice cubes. Consequently the ice cubes fall by gravity into a storage bin for harvesting and storage purposes. When the ice slab is subdivided into ice cubes, the ice harvest paddle lever will return back to its original position, terminating the operation of the cutting grid.

The stated mechanism of ice cube making is automatically and frequently repeated until the storage bin is filled with a predetermined amount of ice cubes (i.e. 20 kg). The maximum allowed limit of ice cubes is detected by means of a storage bin thermostat element. As a result, the temperature of the element will be reduced leading to actuating the switch in the storage bin thermostat, terminating the operation of the ice maker. When the amount of ice cubes in the storage bin is below the predetermined limit (i.e. low level), the element of the storage bin thermostat will not be in physical contact with the ice cubes, resulting in an increase in temperature of the element leading to actuating the switch of the storage bin thermostat for operating the ice maker to produce ice cubes.

4.1.3 Modifications to Ice Maker Machine

In order to use and examine the ice maker for saline water applications, several modifications were carried out on the equipment:

(a) Elimination of the tubular inlet of water supply and restricted water inlet valve

In order to facilitate the filling (i.e. feeding) process, the tubular water supply inlet and the restricted water inlet valve were eliminated from the ice maker by changing the feeding method. This was achieved for each test through three successive steps: (a) the insulated upper wall of the exterior body of the laboratory apparatus was disassembled and manually removed, (b) the feed sample was manually poured into the upper surface of the inclined plate by means a beaker (see Fig (4.5)) where the feed flows directly into a return manifold leading eventually to the collecting tank [Ayres and Swanson, 1961], and (c) before starting the experiment, the insulated upper wall was returned to its original position, to insulate the refrigerated plate during the test.

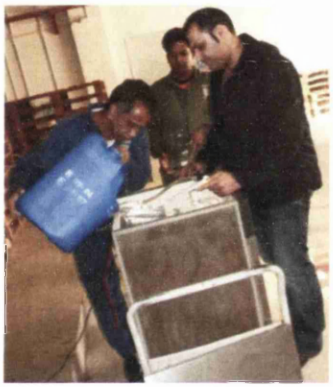

Fig. 4.5: *Feeding process used for each experiment.*

(b) Elimination of the ice thickness element

Termination of the crystallisation process of the existing ice maker machine is controlled by means of an ice thickness thermostat. In order to control the crystallisation process by predetermined running times instead of a determined ice thickness, the ice thickness thermostat was eliminated from the ice maker by placing the element of the ice thickness thermostat away from the inclined plate. After running the experiment for a pre-determined time, the operation of the ice maker was manually switched off, and then the separation process was carried out by manually disconnecting one of the two electrical wires connected to the ice thickness thermostat, and then operating the ice maker to start the separation cycle as described previously in section 4.1.2 (iii). Fig (4.6) shows the two electrical wires of the ice thickness thermostat (in the highlighted circle) where one of them must be disconnected before starting the ice maker to perform the separation process.

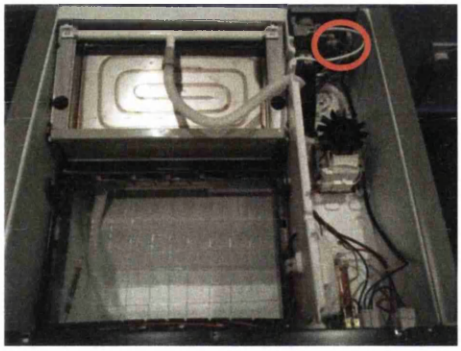

Fig. 4.6: *Top interior view of ice maker.*

(c) Installing a flow control valve

To verify and assess the influence of the flow rate of circulation pump upon the performance of the ice maker, a hand-operated ball valve was used as a flow control valve and this valve was installed in the water circulation loop as shown in Fig (4.7).

(a) Flow control valve

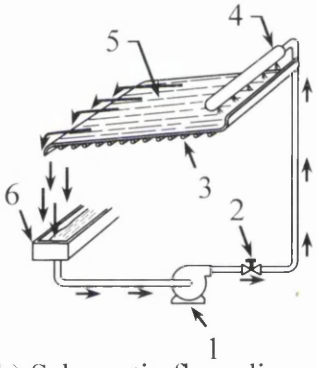

(b) Schematic flow-diagram

Fig. 4.7: *Water circulation loop with a flow control valve in the laboratory apparatus, where; (1) circulation pump, (2) flow control valve, (3) evaporator coils, (4) water distributor, (5) refrigerated inclined plate, (6) collecting tank.*

(d) Elimination of cutting grid, ice cubes storage bin, and bin thermostat

Upon the completion of the separation process, the ice slab was rapidly and manually collected from the inclined plate of the ice maker for chemical analysis. Therefore, equipment such as; the cutting grid, ice cube storage bin, and bin thermostat were not considered in the experiments.

4.2 Preparation of Feed Samples

Two different sources of saline water have been used and tested individually as feed-samples in this experimental study. The feed materials are aqueous solutions of sodium chloride and process brines.

Barduhn (1965) stated that prepared synthetic water using aqueous solutions of sodium chloride (NaCl) gives results very similar to process brines. Therefore, synthetic water using aqueous solutions of NaCl were prepared, used, and examined as feed, in order to validate the potential capability of the falling film crystallisation process for treating a range of liquid streams typical of those causing the most severe pollution problems. The initial salt concentrations of the feed streams, using synthetic waters, ranged from 0.5 to 15 wt% by weight of NaCl salt.

In addition to this, two different sources of process brine were used and tested individually as feed-samples in the laboratory investigations. The examined process brines are: Arabian Gulf (AG) seawater (4.9 wt% by weight of dissolved salt) and reject brine (6 wt% by weight of dissolved salt), produced from a Reverse Osmosis (RO) membrane desalination plant.

As far as the water sample preparation is concerned, according to the mass fraction formula (which was explained previously in Chapter 3), the feed samples, using synthetic water, were prepared by dissolving a predetermined mass of NaCl salt (Sodium Chloride PA-ACS-ISO, Order Number: 131659.1211, Panreac, Made in Spain) into a known mass of deionised water (produced by UV water purification system, Direct-Q3, Trade Name: Direct-Q). With regard to the preparation of process brines, water samples of RO brine were collected from a RO unit, located at the Doha Research Plant (DRP), Kuwait. Arabian Gulf (AG) beach-well seawater was used as feed-water for the mentioned RO plant. Tables (A4-12) and (A4-17) illustrate the major components of ionic composition of these samples.

Process water, such as AG seawater and RO Brine, were collected from the feed stream and reject brine discharge of the Kadhmah Bottled Water (KBW) plant. The KBW plant represents one of the main research projects of the Water Technologies Department's (WTD) of the Water Resources Division (WRD) at the Kuwait Institute for Scientific Research (KISR), located at the Doha Research Plant (DRP) in Kuwait. The KBW plant consists of

two series of RO membrane units (using the series product staging method), as well as a blow moulding machine, a rinsing-filling-capacity machine, a labelling machine, and packaging units including their auxiliary equipment. The feed of the first stage of the RO membrane units is AG seawater. Although the salinity of the reject brine of first stage of RO membrane units are much more than that of the reject brine of the second stage, both reject brines of the two stages are dumped into open AG seawater. The feed samples from the feed stream of the first stage of RO membrane units (i.e. AG seawater) and the dumped RO brines (i.e. the mixed RO brines of two stages) were collected individually from the KBW plant, and tested as feeds in the laboratory investigations. The principles of RO membrane technologies, including the description of reject brines, are described elsewhere [Buros, 1990; Spiegler and El-Sayed, 1994; Lattemann and Höpner, 2003].

4.3 Physiochemical Analysis & Measuring Instruments

Following preparation of feed samples, physicochemical analysis was carried out following the standard procedure for the prepared sample. After completion of the experiments, the physiochemical analysis was then carried out for the product (i.e. melted ice crystals layer) and residue samples. The physiochemical analysis of water samples included measurements of the temperature, Total Dissolved Solids (TDS), electrical conductivity, pH, volume, and weight. Two different types of salinity measurements are considered in the physiochemical analysis, in order to ensure and check the results of the salinity measurements; (i) electrical conductivity and (ii) gravimetric method. The accuracy of salinity measurements (which are obtained by a gravimetric method) was also ensured by using a simple mass balance equation. In addition, when the source of the feed sample was either AG seawater or RO brine, full water chemistry analysis was conducted for all samples of each experiment. The purpose of conducting full water chemistry analysis is to detect the major components of ionic composition found in the feed, product, and residue. A DR 5000 Spectrophotometer (Hach, DR 5000) (see Fig (A4-1) in Appendix A4) along with powders pillows reagent (are tabulated in Table (A4-2) in Appendix A4) were used to detect the major components (ionic composition) of the feed water sample using seawater and RO retentate. The reliability of full chemical analysis of the water samples was ensured by using a charge balance error. Furthermore, the salinity, in term of TDS, was also ensured by comparing the results of TDS obtained through physicochemical analysis and gravimetric method.

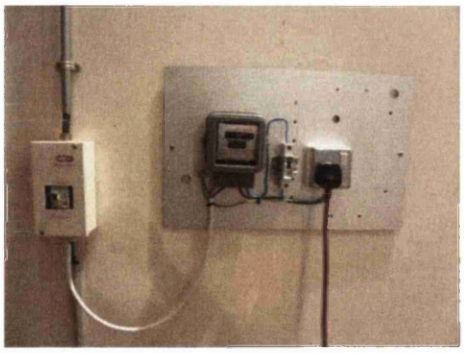

Fig. 4.8: *Kilowatt Hours Meter.*

In addition, a Kilowatt Hours Meter (MF-95, Mitsubishi Electric Corporation) was used to measure and record the energy consumption of the ice maker for each experiment. This was achieved by connecting the electrical fitted plug of the ice maker into the wall socket, which was also electrically connected to the Kilowatt Hours Meter as shown in Fig (4.8).

4.4 Experimental Setup

The experimental setup was prepared and equipped by using and modifying the components of a commercial ice maker machine. The principal unit operations that have been considered for the laboratory study are crystallisation, separation, and total melting. The applied crystallisation process is characterized as "the secondary-refrigerant indirect freezing" method, and utilizes solid layer crystallisation using the falling film principle.

Fig. 4.9: *Stirring hot plate device.*

As shown in Fig (4.9), the experimental setup was provided with a laboratory stirring hot plate device (Cimarec 3, Thermolyne) which was used for melting the ice slab to yield the product in liquid form. Furthermore, this device was used to increase the temperatures of the

product water and residual liquid to room temperature before carrying out the specified physiochemical analyses.

4.5 Experimental Procedure

The operating procedure for the experiments is presented in Fig (4.10). These experiments were carried out in batch mode. Referring to the simplified block diagram in Fig (4.10), prior to conducting any experiment, the feed sample was prepared and then the specified physiochemical analyses were carried out on the feed sample. The collecting tank was then loaded with a constant mass of feed material i.e. 3 kg. The feeding process was previously described in section 4.1.3 (a). Before starting the ice maker (i.e. crystallisation process), the flow rate of the circulation pump was set to a predetermined value using a flow control valve. The ice maker was then operated to start the crystallisation experiment. The crystallisation process is previously described in section 4.1.2 (ii). During the crystallisation cycle, the temperature of the refrigerated plate was rapidly decreased to -14°C, which was experimentally determined by means of digital thermometer (Digital Thermometer Instant, Model: 9847N, Taylor). This crystallisation temperature was maintained constant at this level until the end of the crystallisation cycle.

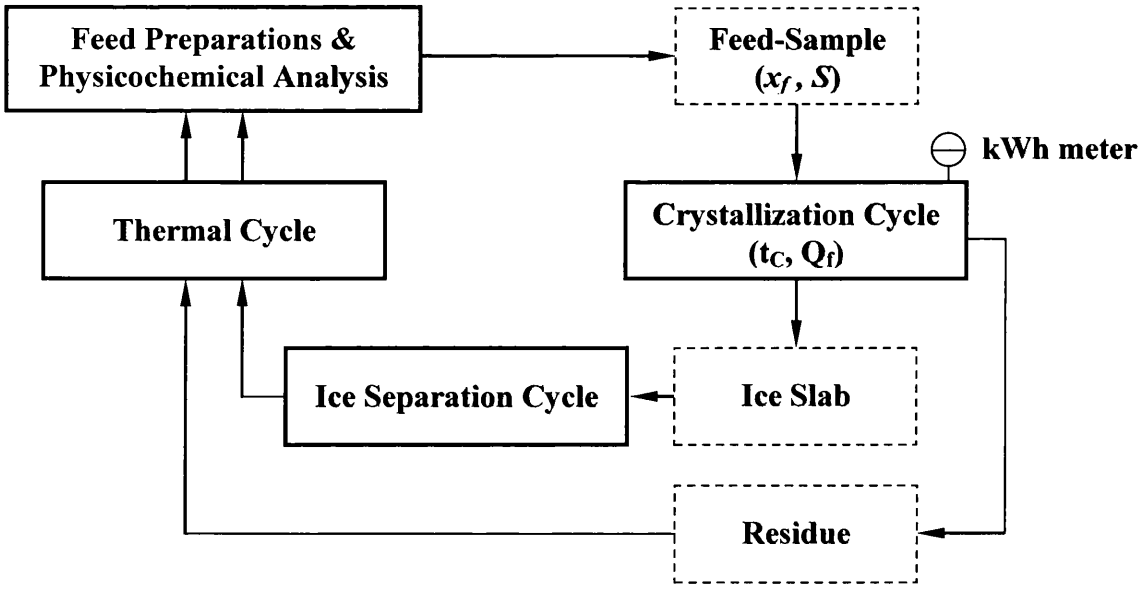

Fig. 4.10: *Simplified block diagram of the operational process for the experimental set-up. Where (x_f) is the feed concentration (%) by weight of salt, (S) is the source of feed, (t_C) is the running time of crystallisation Process (minute), and (Q_f) is the flow rate (L/min).*

After running the crystallisation experiment for a pre-determined time, the operation of the ice maker was terminated and then the separation process of the ice slab was performed. The separation process of the ice slab is previously described in section 4.1.3 (b). When the ice slab was separated from the refrigerated plate, it was rapidly collected and taken for the physiochemical analyses, as illustrated schematically in Fig (4.10). Upon completion of ice slab separation, the operation of the ice maker was switched off, and followed by draining and collecting the residual liquid for the physiochemical analyses, as directed in Fig (4.10). Table (4.1) summarises the operation of the various pieces of equipment involved in each operational cycle. The operating temperatures of the inclined plate throughout the operational cycles are also illustrated in Table (4.1).

Prior to conducting the physiochemical analysis on the ice slab and residual liquid, a thermal cycle was considered for increasing the temperatures of the product water (i.e. melted ice slab) and residual liquid to room temperature as shown in Fig (4.10). This was achieved by using a laboratory stirring hot plate device as mentioned previously. Upon completion of the experiment, the disconnected electrical wire in the ice maker was reconnected to the ice thickness thermostat i.e. returned to its original position. Following this procedure, cleaning and rinsing of the ice maker takes place in preparation for the subsequent experiment.

Main Equipments	Feeding	Crystallisation	Ice separation
Condenser fan	OFF	ON	OFF
Hot gas valve	OFF	OFF	ON
Water circulation pump	OFF	ON	OFF
Compressor	OFF	ON	ON
Operating Temperature (°C)	25	≈ -14	≈ 11
Running Time (min)	≈ 5	Varied	1 - 3

***Table 4.1**: Operating cycles schedule and temperatures [Whirlpool, 2009].*

The crystallisation experiments were carried out according to the predetermined controlling variables and operating conditions that are illustrated in Table (4.2). The crystallisation experiments were conducted at different operating conditions, such as initial feed concentration, source of feed water, flow-rate of circulation pump, crystallisation time, and

number of freezing stages. As illustrated in Table (4.2), three and four successive freezing stages were considered in this study for purifying and concentrating the product and residue, respectively. The single or first stage is commonly known as the feed stage, whereas the rectification and stripping stages represent the repeated stages for purifying the product and concentrating the residual liquid, respectively [Ulrich and Glade (2003); Sulzer (2004)].

Run	No. of Stage	(x_f)	(t_C)	(Q_f)	(S)
		(%)	(min)	(L/min)	(Synthetic Water / Process Brine)
1 – 64	1	0.5 – 7	15 – 120	6.3 – 3.15	NaCl solution
65 – 192	1	4.9	15 – 120	6.3	AGSW
129 – 144	1	7	15 – 120	6.3	RO Brine
145 – 160	3	4.9	90	6.3	AGSW
160 – 163	4	7	60 – 120	6.3	RO Brine

Table 4.2: *Operating parameters and conditions during crystallisation cycle experiments. Where (x_f) is the feed concentration (%) by weight of salt, (S) is the source of feed, (t_C) is the running time of crystallisation process (minute), and (Q_f) is the flow rate (L/min).*

For the crystallisation experiment with multiple freezing stages, the preparation of feed samples differs from the feed stage. This was due to the product and residual liquid of the previous freezing stage becoming the feed for the subsequent rectification and stripping stages, respectively. However, several limitations were encountered during these experiments, which are as follows: (a) the capacity of the collecting tank is limited, (b) the circulation pump is turned off automatically by a float sensor when the water level of the collecting tank reaches 0.5 L, (c) a single crystalliser was available for this experimental investigation, (d) the maximum mass of product water cannot exceed 1.2 kg in any freezing stage, because the apertures of the water distributor were blocked by the ice slab thickness, and (f) the experiments were handled on a batch basis. Therefore, for experiments with rectification stages, the final product of the fourth freezing stage was reprocessed by conducting four successive crystallisation processes where the liquid obtained by melting the ice slab of the previous freezing stage becomes the feed for the following freezing stage, and so on, until achieving the final product of the fourth freezing stage. This means that the first three freezing stages might be individually repeated several times in order to collect the

desired amount of feed (i.e. final product from third freezing stage) to be used as feed for the fourth freezing stage. On the other hand, the experiments with stripping stages were achieved by conducting four successive crystallisation processes, where the residual liquid drained from the previous freezing stage becomes feed for the subsequent freezing stage and so on until the final residue from the fourth freezing stage is obtained. This means that the first three freezing stages might be repeated several times in order to collect sufficient amounts of feed (i.e. final residue from third freezing stage) to be used as feed for the fourth freezing stage.

For all tests, the ice maker was placed away from any source of heat, such as heat producing appliances, heating ducts, and direct sunlight to avoid thermal losses in the ice maker that might be enhanced through the mentioned sources of heat, which may eventually contribute to degrading the performance of the crystallisation process [Whirlpool, 2010], and may also negatively affect the empirical data. Nevertheless, the mentioned ice maker machine was also insulated from the surrounding environment, and heat sources through insulated walls installed in the body, and was also insulated through interior shelves and partitions.

4.6 Results and Discussion

Before performing the first experiment of each day, the ice maker is initially operated with tap water, both to cool down the refrigeration system, and clean and rinse the water recirculation system. This was considered essential for obtaining good experimental results, exercising fair engineering judgement seeking accuracy. Experimental results were gathered and analysed to obtain quantitative information on the degree of desalination and concentration by an ice maker using the falling film crystallisation process. A complete record of the experimental data, full physiochemical analysis, and performance parameters versus crystallisation time are given in Table A4-3 – A4-20 in Appendix 4, found on the CD attached to the thesis (see file name: Appendix, Microsoft Excel spreadsheet, Sheet: Appendix 4, Tables: A4-3 – A4-20).

For clarity, the salt concentration of the water sample (C) is measured in (wt%) and ((mg/kg) $\approx$ (mg/L)). These measurements were both obtained by the gravimetric method, and computed using the equations below:

$$C = \frac{m_{Salt}}{m_{Solution}} \times 100 \quad (4.1)$$

$$C = \frac{m_{Salt}}{m_{Solution}} \times 10^6 \quad (4.2)$$

where m_{Salt} and $m_{Solution}$ represent the mass of dissolved salts in the sampled solution and mass of the sampled solution respectively; both are measured in (g).

4.6.1 Influence of feed salinity

In the first series of experiments, the influence of feed salinity on the degree of desalination achieved by the unit, in terms of salt concentration of product water and water recovery ratio, was investigated. This was done by individually testing three different feeds; in this respect, NaCl solutions and two different types of process brines were used as feed samples. The tested feed concentrations and types are presented in Table (4.2). The actual operating time of the crystallisation process in the experiments, were varied from 15 to 90 minutes, for feed salinities of 3.5 wt% and less, and were varied from 15 to 120 minutes for feed concentration higher than 3.5 wt%. These experiments were performed at an average circulation pump flow-rate of 6.15 L/min. A summary of the experimental results is given in Fig (4.11), which shows the influence of feed concentration on the quality of product water. Agreement in the experimental results for NaCl solutions and process brines is clearly observed. As expected, the quality of product water, in terms of salinity, is proportional to the feed salt concentration as shown in Figs (4.11) (a) and (b). The lower feed concentration using NaCl solutions leads to a decrease in the salinity of product water, i.e. improving the salt rejection ratio. For instance, Fig (4.11) (a) shows that the salt concentration values of feed samples fed individually to the ice maker are 0.5 wt%, 3.5 wt%, and 7 wt%. The results showed that the ice maker was capable of reducing the salinity values of product water down to an average of 0.22 wt%, 1.85 wt%, and 3.55 wt%, for the same feed samples, respectively. When the ice maker was fed with seawater (having salt concentration of 4.91 wt%) and then RO brine (feed concentration of 6.11 wt%), it was able to reduce the salinity values of product water down to an average of 2.60 wt% and 3.71 wt%, for these feed samples respectively. Although, the experimental results were quite encouraging, at this point of research, the ice

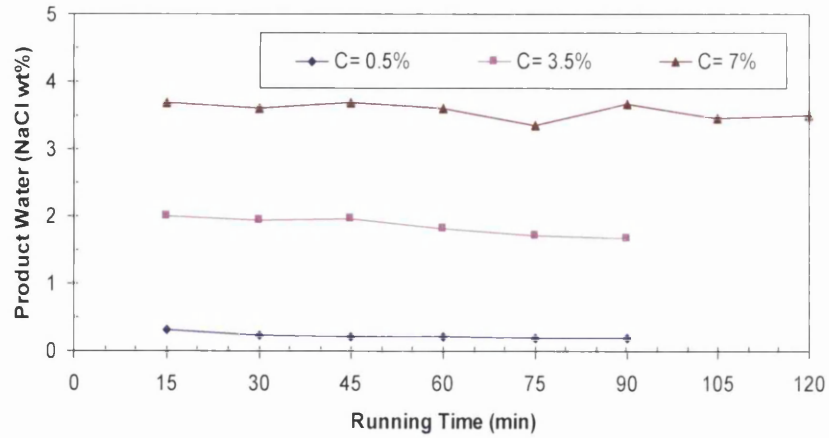

(a) Feed samples using NaCl solutions

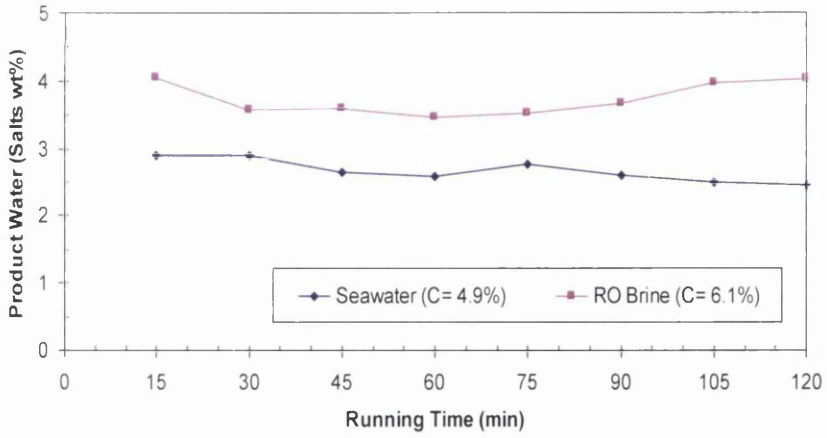

(b) Feed samples using process brines

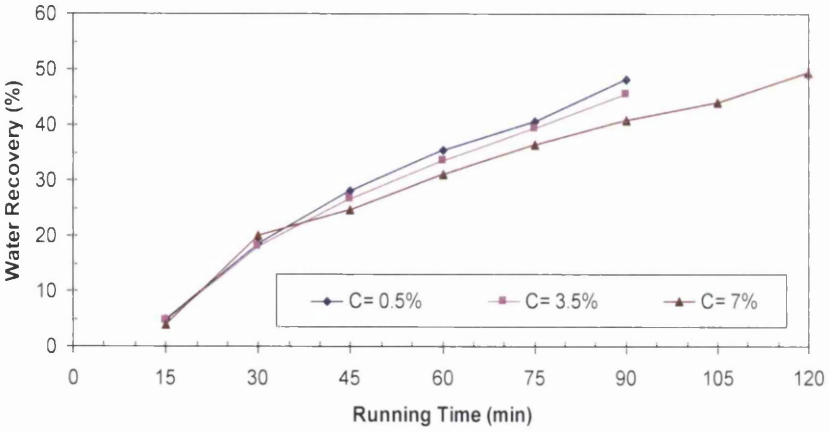

(c) Feed samples using NaCl solutions

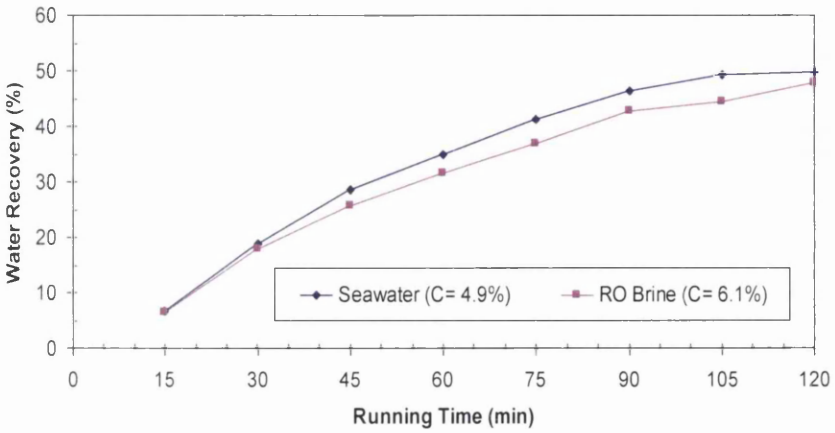

(d) Feed samples using process brines

Fig. 4.11: *Product concentration and water recovery ratios versus running time, where; C= salt concentration of feed, measured in wt%.*

maker did not produce a final, near potable quality product. However, for the case of seawater treatment, the ice maker produced final water close to the brackish water quality that can be further desalted by brackish RO membranes to produce potable water. In the case of RO brine treatment, the ice maker produced final water of near seawater quality that could be recycled and easily treated by seawater RO membranes to reach a final product water of near drinking water quality. For example, Figs (4.11) (b) and (d) shows that the maximum salt concentration of product water and water recovery ratio were about 4 wt% and 48%, respectively. This gives a clear indication that the ice maker using falling film crystallisation process might be a feasible process for concentrating RO brines in order to minimise the volume of the waste streams of RO desalination plants, and more specifically, inland desalination plants.

The water recovery ratios, on the other hand, were found to be inversely proportional to the feed salt concentration as shown in Figs (4.11) (c) and (d). However, the water recovery ratios were found proportional to the running time, as shown in Figs (4.11) (c) and (d). Consequently, the experiments using feed samples with high salinities (such as NaCl solutions with a salt concentration of 7 wt% and process brines) required longer crystallisation time (i.e. 120 minutes) to reach the water recovery ratio of 50%, as shown in Figs (4.11) (c) and (d). For each freezing stage, the maximum water recovery ratio could not exceed 50%, because the thick ice slab started to block the apertures of the water distributor.

4.6.2 Influence of ice thickness

The second group of experiments were carried out with feed samples using NaCl solutions with salt concentration of 0.5, 3.5, and 7 wt%. The actual operational period of crystallisation process for the experiments was varied from 15 to 90 minutes. These experiments were carried out with an average flow-rate of 6.15 L/min. The ice thickness was analytically determined by assuming the dimensions and shape of solid layer ice slab is a rectangular block. Fig (4.12) shows the influence of ice thickness on the quality of product water and residue, in terms of salinity, as well as the salt rejection and water recovery ratios.

For the experiments using feed samples with a salt concentration of 0.5 wt%, the quality of product water, in terms of salinity, was found to be inversely proportional to the ice thickness

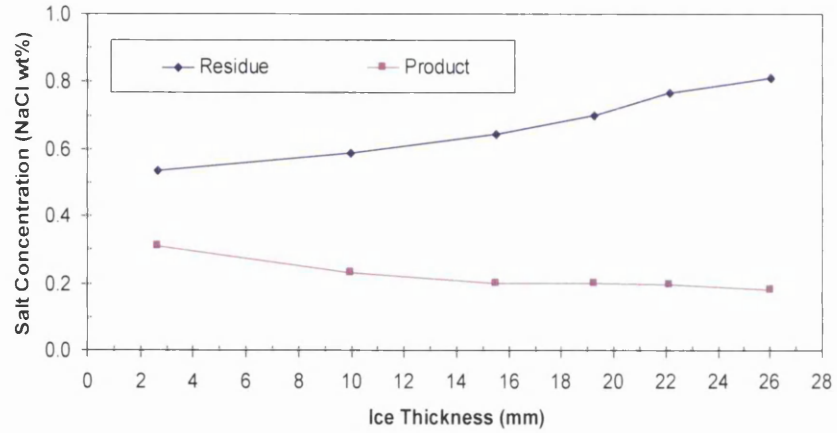

(a) Results using feed samples of 0.5 wt% NaCl salt

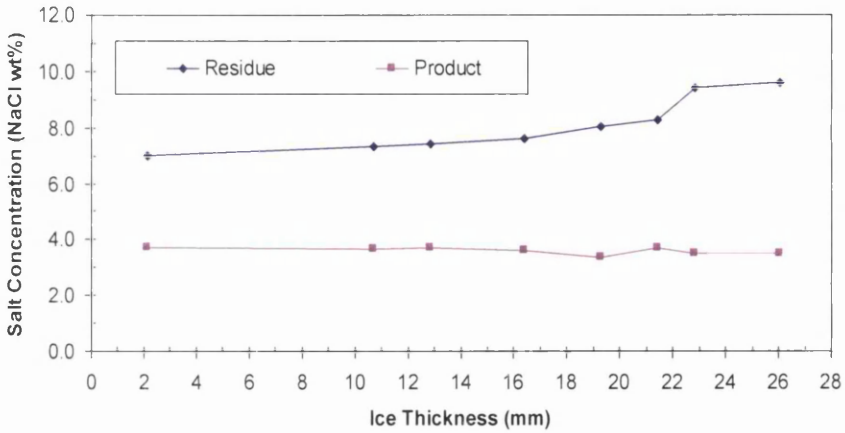

(b) Results using feed samples of 7 wt% NaCl salt

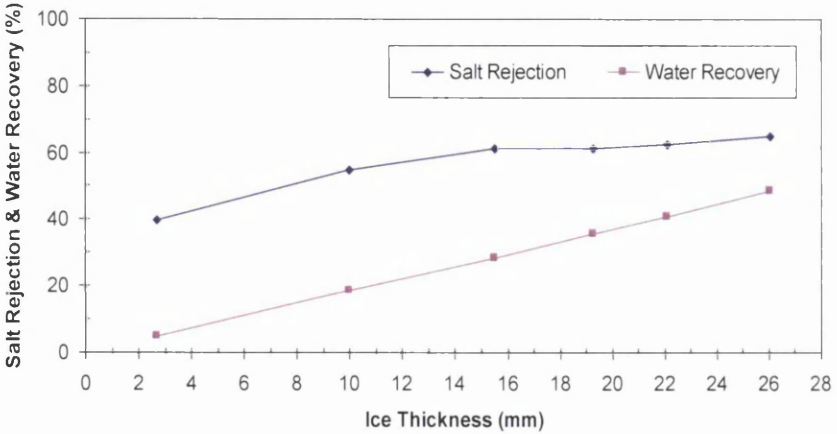

(c) Results using feed samples of 0.5 wt % NaCl salt

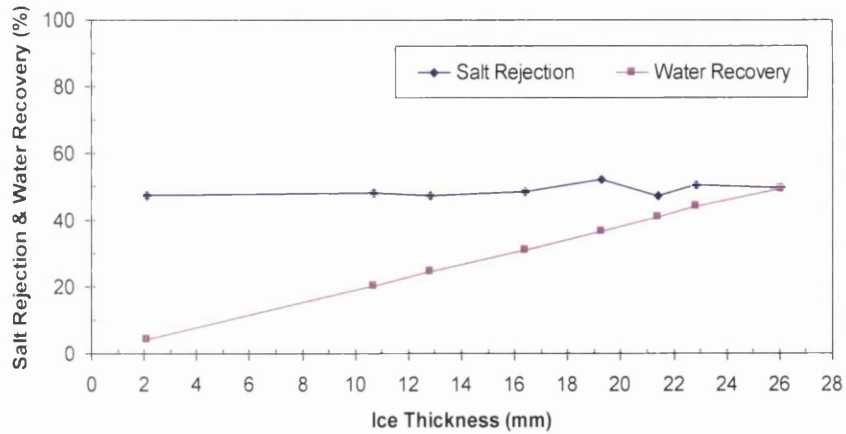

(d) Results using feed samples of 7 wt% NaCl salt

Fig. 4.12: *Influence of ice thickness on the salt concentration of water samples, salt rejection ratio and water recovery ratio.*

as shown in Fig (4.12) (a). The salt rejection and water recovery ratios were found to be proportional to the ice thickness, as shown in Fig (4.12) (c). Similar behaviour was again noted in the experiments using feed samples with a salt concentration of 3.5 wt%, as illustrated in Table A4-4 in Appendix 4. The reason behind the improving product quality as the ice thickness increased is associated with a decrease in crystallisation temperature, i.e. an increase in the cooling rate. The cooling rate is usually dictated by two crucial factors, which are crystallisation temperature and time. However, the thickness of the ice slab, which is a relatively good heat insulator, played a main role in reducing the heat transfer rate by increasing the crystallisation temperature on the surface of the existing ice slab, resulting in an improvement in product water quality as the ice thickness increased. For the experiments using feed samples with a salt concentration of 7 wt%, there was no significant change in the quality of product water observed during the variation of ice thickness as shown in Fig (4.12) (b). The reason behind this can be explained when the treatment of highly saline water was taken into account. As the production of ice crystal increases, the remaining residual liquid becomes more concentrated, which negatively affects the separation performance, as discussed previously in section 4.6.1. The water recovery ratio was found to be proportional to the ice thickness, as shown in Fig (4.12) (d). For all tests, the salinity of residue was found to be proportional to the ice thickness, as shown in Figs (4.12) (a) and (b).

4.6.3 Energy consumption

For the first series of experiments, the energy consumed by the ice maker in each test was experimentally and theoretically determined.

The experimental power consumption (Q_E), measured in kWh/kg, was determined using:

$$Q_E = \frac{Q_e}{m_p} \tag{4.3}$$

where Q_e is the power consumption, measured in kW, and m_p is the production rate, measured in kg/h. In each experiment, Q_e was measured by a kilowatt hours meter and compared to the electrical loading of 450 W, which is given in the ice maker data sheet and specification, provided by the ice maker's manufacturer. The average power consumption

results were found to be approximately the same as the electrical loading given in the manufacturer's specification.

The theoretical power consumption (Q_T), measured in kWh/kg, was determined via:

$$Q_T = \frac{Q_f + Q_p}{m_p} \tag{4.4}$$

where Q_f is the heat transfer rate for cooling the feed water, (kW), and Q_p is the heat transfer rate for changing the phase of the liquid, (kW).

Thus, Q_f is given by:

$$Q_f = m_f C_p (T_2 - T_1) \tag{4.5}$$

where m_f is the mass of feed, C_p is the specific heat capacity of the feed water, and T_1 and T_2 are start-point and end-point temperatures of the feed.

Q_p is calculated from:

$$Q_p = m_p \Delta H_f \tag{4.6}$$

where ΔH_f represents the heat of fusion of ice, measured in kJ/kg.

Fig (4.13) shows plots of the experimental and theoretical results of the power consumption versus the water recovery ratios. For the experiments with NaCl solutions as feed samples, the experimental power consumption was found to be inversely proportional to the production rate as shown in Fig (4.13) (a). Similar behaviour was also observed for the experiments using process brines as feed samples, as shown in Fig (4.13) (b). This clearly indicates that designing the ice maker for large scale application would result in a significant reduction of power consumption. Also, Figs (4.13) (a) and (b) shows that the experimental

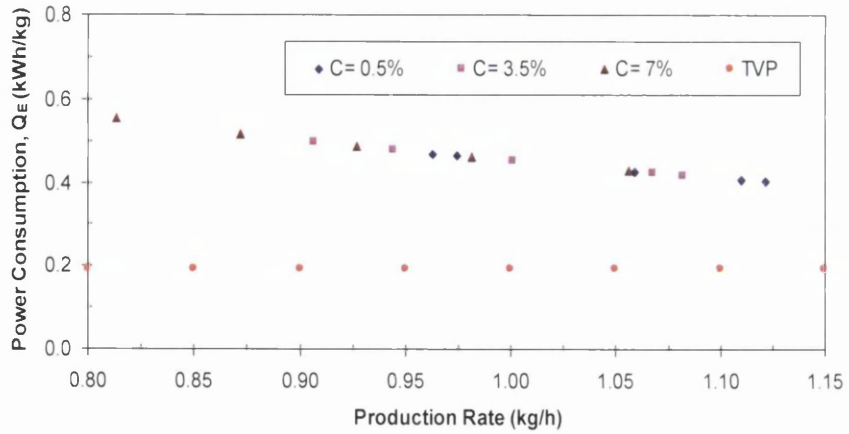

(a) Experimental power consumption for treating NaCl solutions

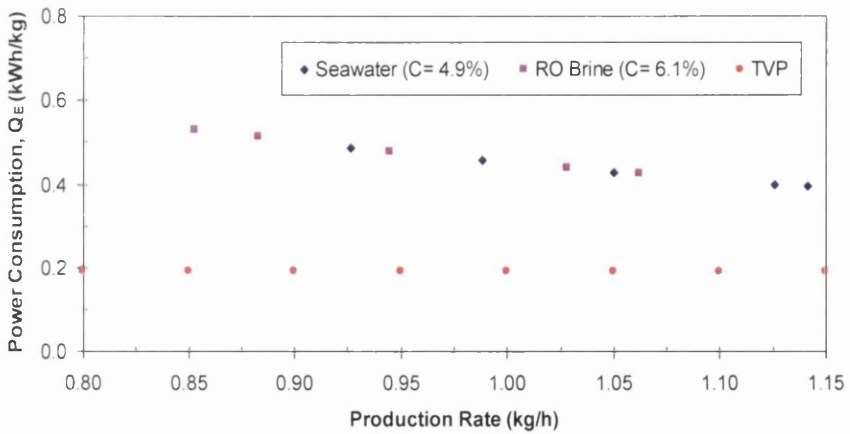

(b) Experimental power consumption for treating process brines

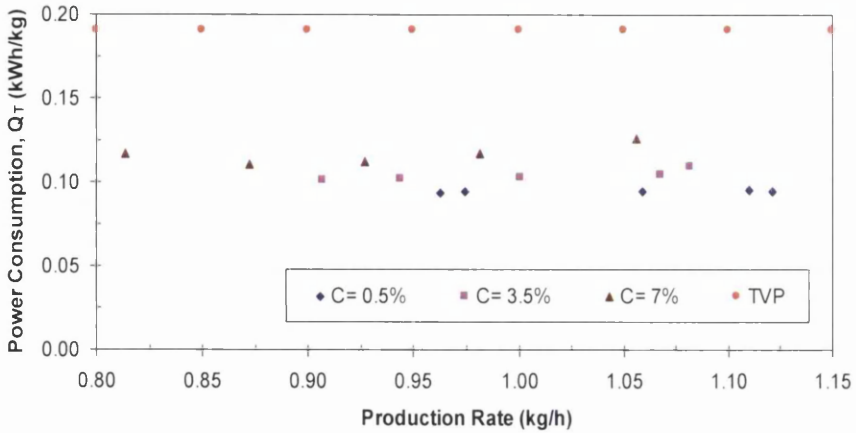

(c) Theoretical power consumption for treating NaCl solutions

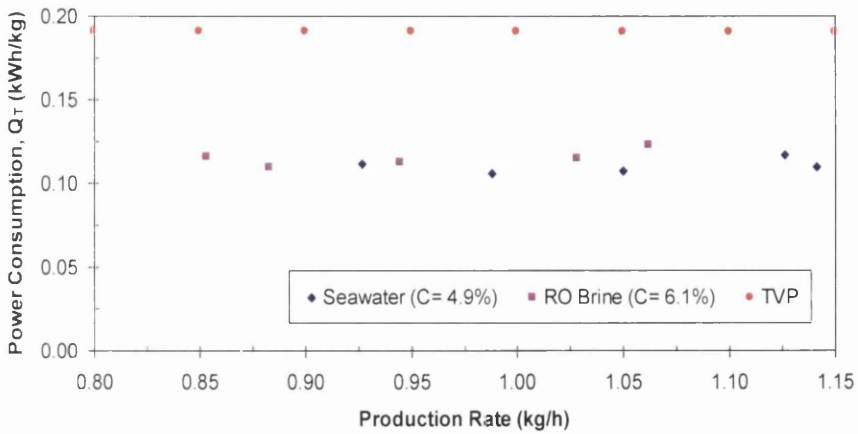

(d) Theoretical power consumption for treating process brines

Fig. 4.13: *Summary of the experimental and theoretical results of the energy consumption of the ice maker, where; C is the salt concentration of the feed, measured in wt%, and TVP is the theoretical value for tap water (0.19 kW/kg).*

power consumption was slightly increased as the salt concentration of feed sample increased. For example, the averaged values of experimental power consumption were 0.43, 0.45, and 0.51 kWh/kg in treating feed samples comprising NaCl solutions at salt concentrations of 0.5, 3.5, and 7 wt%, respectively, whereas the treatment of seawater and RO brine consumed 0.47 and 0.51 kWh/kg, respectively, taking into account that the ice maker consumes 0.19 kWh/kg for the cases of producing ice cubes from tap water as specified by the supplier. This behaviour was found to agree with the results of the theoretical power consumption, as shown in Figs (4.13) (c) and (d). This clearly confirms that the power consumption is the proportional to the salt concentration of feed sample. In general, the values of the experimental power consumption do not reflect the actual power consumption of the treatment system. The reasons behind this are (i) the tested ice maker contains several items of equipment not needed for desalination; (ii) the demonstrated results of the experimental power consumption reflected the power consumption of the ice maker used for small scale applications; (iii) the absence of pre-cooling unit (i.e. heat exchanger) to recover most of the cold from the residual liquid and the melted ice by cooling the incoming feed water; and (iv) depending on the operating conditions, the examined operating temperature and cooling rate limits might be too low for the tested water samples. Hence, a full scale demonstration with suitable items of equipment and optimal operating conditions must be examined to estimate the actual power consumption.

4.6.4 Influence of the feed flow-rate

In the third series of experiments, the influence of the feed flow-rate on the separation performance of the ice maker was investigated. These experiments were performed with NaCl solutions having salt concentrations of 0.5 wt% and 7 wt%. The actual operational period of the crystallisation process for the experiments was varied from 15 to 90 minutes. The laboratory investigation was carried out with an average feed flow-rate of 6.30 and 3.15 L/min. The flow-rate of 6.30 L/min represents the maximum flow-rate that can be obtained, whereas the flow rate of 3.15 L/min was achieved by manual adjustment through the installed flow control valve. The predetermined flow-rates of feed were experimentally measured before starting the experiment. Fig (4.14) shows the influence of flow rate on the product concentration, water recovery, and salt rejection ratios.

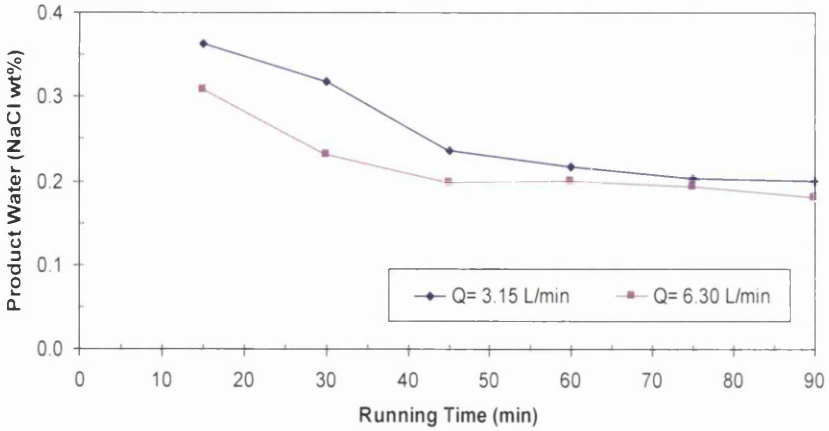

(a) Results using feed samples of 0.5 wt% NaCl salt

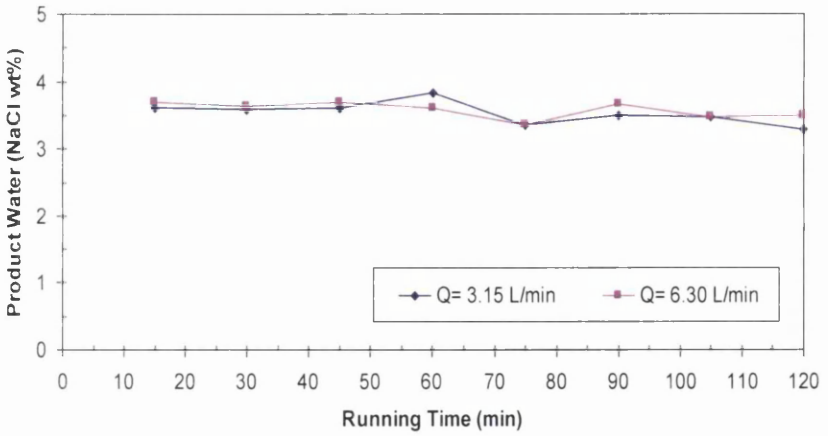

(b) Results using feed samples of 7 wt% NaCl salt

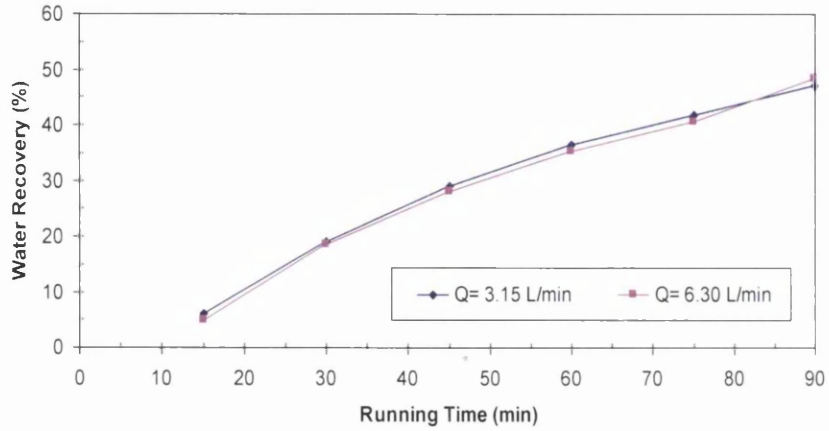

(c) Results using feed samples of 0.5 wt% NaCl salt

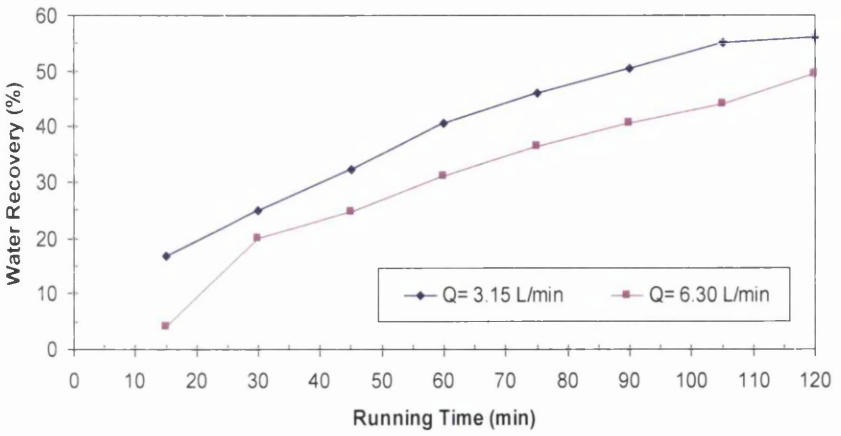

(d) Results using feed samples of 7 wt% NaCl salt

Fig. 4.14: *Influence of circulation pump flow-rate on product concentration and water recovery, where Q is the circulation pump flow-rate.*

The experiments with a feed concentration of 0.5 wt% demonstrated that salinity was inversely proportional to the feed flow-rate, as shown in Fig (4.14) (a). The amount of impurity in the ice slab was significantly reduced by increasing the feed flow rate. This indicates that the effectiveness of such a dynamic effect is helpful in improving the quality of product water in cases of treating feeds with low salt concentration, as confirmed by Ulrich and Glade (2003). As the solid ice layer is growing, the rejected liquid film adhering to the surface of ice slab becomes more concentrated. This liquid film must be rapidly washed and replaced with a lower concentration of incoming liquid film; otherwise the boundary layers of ice slab will be formed with poor separation. Therefore, separation performance of the ice maker was improved by increasing the feed flow-rate. This clearly indicates that the feed flow-rate can improve the quality of product water for the case of feed solutions with low salt concentrations. However, the water recovery ratio was not affected by the feed flow-rate as shown in Fig (4.14) (c). This clearly indicates that the feed flow-rate cannot change the water recovery ratio in the case of feed solutions with low salt concentrations, especially when the experiments were carried out at low a crystallisation temperature, i.e. low cooling rate.

For the cases of treating a feed with a salt concentration of 7 wt%, the product quality was not affected by changing the feed flow-rate, as shown in Fig (4.14) (b). The water recovery ratio is considerably increased by decreasing the flow-rate of the feed, as shown in Fig (4.14) (d). The reason behind this was that the ice crystal layers were found to be quite slushy and not rigid when compared to the experiments using feed samples with a low salt concentration. Therefore, the flow rate of the feed must be reduced to obtain a rigid crystal layer. Consequently, the rejected liquid film is allowed more residence time above the surface of the ice slab, which helps the ice crystals to grow much faster, leading to an increased production rate. Therefore, the water recovery ratio was found to be inversely proportional to the feed flow-rate using higher salinity feeds.

4.6.5 Multi-stage process (rectification stage)

In the fourth series of experiments, the influence of a multi-stage ice maker (falling film process) on the degree of desalination, in terms of product quality, water recovery, and ionic rejection, was studied. This was achieved by treating Arabian Gulf beach-well seawater as the initial feed sample. Continuous rectification stages were performed in three successive

freezing stages, namely a feed stage, and then first and second rectification stages, to determine the degree of seawater desalination through the ice maker. The actual operational period of the crystallisation process for these experiments was constant at 90 minutes. These experiments were carried out with an average circulation pump flow-rate of 6.15 L/min. The experiments for the feed and first rectification stages were individually repeated 9 and 3 times, respectively, to collect the water samples for physiochemical analysis and also to collect final feed water for the second rectification stage (i.e. final stage), which was performed only one time to produce the final product water. A summary of the experimental data and physiochemical analysis for the water samples of each freezing stage is given in Tables (4.3) – (4.5).

Table (4.3) shows that the average TDS value of seawater fed to the feed stage was 49,074 ppm, whereas the feed stage, and first and second rectification stages were able to output product water with average TDS values of 26,047, 17,996, and 9,529 ppm, respectively. Table (4.3) shows that the salt rejection ratios were 46.95, 30.91, and 47.05%, for the same freezing stages, respectively. The overall salt rejection ratio was 80.59% (see Table (4.4)). The overall results proved that the ice maker tested was capable of reducing the TDS value of seawater from 49,074 ppm down to 9,529 ppm over three successive freezing stages (see Table (4.3)). Table (4.3) shows that the water recovery ratios were 46.33, 65.83, and 65.23%, for the same freezing stages, respectively. The water recovery ratios for the first and second rectification stages are higher than that in the feed stage, because water recovery ratio is inversely proportional to the salt concentration of feed water. Table (4.4) shows that the overall product water recovery ratio was 19.89%. This investigation clearly indicates that the number of rectification stages is proportional to the salt rejection ratio and inversely proportional to the water recovery ratio. Although the results are quite encouraging in terms of the salt rejection ratio, however the ice maker, over three successive freezing stages, did not produce a final product reaching drinking water standards that is ready for immediate use (see Table (4.5)). Table (4.5) compares the major ion composition of final product water to drinking water standards. In this case, the ice maker produced a saline water of near brackish water standards that can be further easily desalted either by increasing the number of rectification stages or by using brackish water RO membranes to obtain a final product of potable water. Table (4.5) shows that the TDS values of the residual liquid of the feed, and

Stage	Water Sample	Parameters	Unit	Value
Stage 1	Feed Water	Mass	(kg)	3.000
		TDS	(ppm)	49,074
	Product Water	Mass	(kg)	1.390
		TDS	(ppm)	26,047
	Residual Water	Mass	(kg)	1.610
		TDS	(ppm)	70,976
Stage 2	Feed Water	Mass	(kg)	3.000
		TDS	(ppm)	26,047
	Product Water	Mass	(kg)	1.975
		TDS	(ppm)	17,996
	Residual Water	Mass	(kg)	1.025
		TDS	(ppm)	41,517
Stage 3	Feed Water	Mass	(kg)	3.000
		TDS	(ppm)	17,996
	Product Water	Mass	(kg)	1.957
		TDS	(ppm)	9,529
	Residual Water	Mass	(kg)	1.043
		TDS	(ppm)	33,935

Table 4.3: *Summary of the performance data for the feed and two rectification stages.*

Stage	Sample	Parameters	Unit	Value
Overall	Feed Water	Mass	(kg)	9.837
		TDS	(ppm)	49,074
	Product Water	Mass	(kg)	1.957
		TDS	(ppm)	9,529
	Residual Water	Mass	(kg)	7.880
		TDS	(ppm)	58,895

Table 4.4: *Overall data for the performance data for the feed and two rectification stages.*

Parameter	Unit	Feed stage			Rectification stage 1		
		Feed	Product	Residue	Feed	Product	Residue
pH	-	7.13	6.94	7.29	6.94	6.80	7.10
TDS	(mg/L)	49,074	26,047	70,976	26,047	17,996	41,517
Conductivity	(mS/cm)	63.6	31.4	89.0	31.4	21.5	51.2
Ca^{2+}	(mg/L)	1,080	554	1,444	554	488	914
Mg^{2+}	(mg/L)	1,387	550	1,490	550	475	968
Na^{+}	(mg/L)	16,523	5,642	15,304	5,642	4,993	13,683
Cl^{-}	(mg/L)	25,480	8,700	23,600	8,700	7,700	21,100
$(HCO_3)^{-}$	(mg/L) as Ca CO_3	175.6	95.6	228.0	95.6	79.1	211.1
$(SO_4)^{2-}$	(mg/L)	3,900	1.200	3,800	1.200	1,050	3,200
NO_3^{-}	(mg/L)	2.7	2.40	5.50	2.40	2.00	4.30

Table 4.5: *Major physiochemical analysis of water samples for the feed and two rectification stages in comparison with European standards of drinking water (adopted from Sumerjian (2011)).*

Parameter	Unit	Rectification stage 2			European standards of drinking water
		Feed	Product	Residue	
pH	-	6.80	6.78	7.07	6.5-9.5
TDS	(mg/L)	17,996	9,529	33,935	-
Conductivity	(mS/cm)	21.5	11.5	41.4	< 2.5
Ca^{2+}	(mg/L)	488	271	837	< 100
Mg^{2+}	(mg/L)	475	224	894	< 80
Na^{+}	(mg/L)	4,993	3,320	12,840	< 200
Cl^{-}	(mg/L)	7,700	5,120	19,800	< 250
$(HCO_3)^{-}$	(mg/L) as $Ca\ CO_3$	79.1	59.1	169.2	-
$(SO_4)^{2-}$	(mg/L)	1,050	790	2,300	< 240
NO_3^{-}	(mg/L)	2.00	1.40	2.90	< 50

Table 4.5: *(Cont'd.)*

first and second rectification stages were 70,976, 41,517 and 33,935 ppm, respectively. The residual liquids of the first and second rectification stages can be further easily treated and concentrated by recycling these waste streams back into the feed stage, whereas the residual liquids of feed stage can be further treated and concentrated through stripping stages. The latter will be addressed for the case of concentrating RO brines in section 4.6.6.

With regard to ionic rejection, Table (4.5) shows that the average hardness ion values of Ca^{2+}, Mg^{2+}, and $(SO_4)^{2-}$ for the investigated seawater fed to the ice maker were 1,080, 1,387, and 3,900 mg/L, respectively. The ice maker, over three successive freezing stages, was able to reduce these ions down to 271, 224, and 790 mg/L, respectively. Table (4.5) also shows that the investigated seawater contains monovalent ions, such as Na^{+} and Cl^{-}, with ionic concentrations of 16,523 and 25,480 ppm, respectively, whereas these ionic concentrations were reduced to 3,320 and 5,120 ppm, for the same ions respectively, over the three successive freezing stages.

In general, the ionic rejection ratios were found to be proportional to the number of rectification stages. The ionic concentrations of the residual liquids, on the other hand, are reduced as the number of rectification stages increased. This was due to the feed of the subsequent stage being the product of the previous stage.

The calculations of the theoretical power consumption consumed by the feed stage, and first and second rectification stages give about 0.105, 0.097, and 0.096 kWh/kg, respectively, whereas the values of the experimental power consumption were 0.49, 0.34, and 0.34 kWh/kg, for the same freezing stages, respectively, as given in the Table A4-11 in Appendix A4.

4.6.6 Multi-stage process (stripping stage)

In the fifth series of experiments, the influence of a multi-stage ice maker (falling film) process on the degree of concentrating a RO brine, in terms of product quality, water recovery, concentration ratio, and ionic rejections, was investigated. This was accomplished by using RO brine as initial feed sample for the feed stage. A continuous multi-stage freezing process was performed in four successive stages, namely a feed stage, and first, second, and third stripping stages, to determine the potential capability of using the ice maker as a

treatment system for concentrating RO brine. The actual operational period of the crystallisation process for the feed, and first, second, and third stripping stages were 60, 90, 90 and 120 minutes respectively. The experimental investigation was carried out with an average feed flow-rate of 6.15 L/min. The experiments for the feed, and first and second stripping stages were individually repeated 4, 4, and 1 time(s), respectively, to collect the water samples for physiochemical analysis and also to collect the final feed water for the third stripping stage (i.e. final stage); this stage was carried out once to concentrate the residual liquid as much as possible. A summary of the experimental data and physiochemical analysis for the water samples of each freezing stage is given in Tables (4.6) – (4.7).

Table (4.6) shows that the average TDS value of the RO brine fed to the process was 61,104 ppm, whereas the residual liquid from the feed, and first, second, and third stripping stages were concentrated with average TDS values of 73,178, 88,172, 97,786, and 114,102 ppm, respectively. Table (4.6) shows that the TDS values of the product water were 34,247, 59,385, 59,541, and 70,490 ppm, for the same freezing stages respectively, while the salt rejection ratios were 43.95, 18.85, 32.47 and 27.91 respectively. According to mass balance calculations, the ice maker was able to produce final product water with an overall TDS value of 51,393 ppm, which is close to the quality of Arabian Gulf beach-well seawater, with respect to the salt concentration (see Table (4.6)). The overall water recovery and salt rejection ratios were about 84.51 and 15.89%, respectively, where Table (4.6) shows that the total concentration ratio was 15.49%. Table (4.6) shows that the overall results proved that the ice maker tested was able to increase the TDS value of RO brine from 61,104 ppm up to 114,102 ppm over four successive freezing stages with concentration ratios of about 69, 48, 75, and 63% respectively. The concentration ratios for the first and third stripping stages are less than in the feed and second stripping stages, respectively, which was mainly due to the residual liquid remaining in the collecting tank from the previous freezing stages (i.e. feed and second stripping stages) being used directly as feed water for the subsequent freezing stages (i.e. first and third stripping stages).

This investigation clearly indicates that the overall concentration ratio was significantly decreased as the number of the stripping stages increased. The results are highly encouraging, in terms of the concentration ratio and treated water (i.e. product quality). The

Stage	Water Sample	Parameters	Unit	Value
Stage 1	Feed Water	Mass	(kg)	3.000
		TDS	(ppm)	61,104
	Product Water	Mass	(kg)	3.000
		TDS	(ppm)	34,247
	Residual Water	Mass	(kg)	2.070
		TDS	(ppm)	73,178
Stage 2	Feed Water	Mass	(kg)	3.000
		TDS	(ppm)	73,178
	Product Water	Mass	(kg)	1.563
		TDS	(ppm)	59,385
	Residual Water	Mass	(kg)	1.437
		TDS	(ppm)	88,172
Stage 3	Feed Water	Mass	(kg)	3.000
		TDS	(ppm)	88,172
	Product Water	Mass	(kg)	0.754
		TDS	(ppm)	59,541
	Residual Water	Mass	(kg)	2.246
		TDS	(ppm)	97,786
Stage 4	Feed Water	Mass	(kg)	3.000
		TDS	(ppm)	97,786
	Product Water	Mass	(kg)	1.123
		TDS	(ppm)	70,490
	Residual Water	Mass	(kg)	1.877
		TDS	(ppm)	114,102
Overall	Feed Water	Mass	(kg)	9.073
		TDS	(ppm)	61,104
	Product Water	Mass	(kg)	7.668
		TDS	(ppm)	51,393
	Residual Water	Mass	(kg)	1.405
		TDS	(ppm)	114,102

Table 4.6: *Summary of the performance data for the feed and three stripping stages.*

Parameter	Unit	Feed stage			Stripping stage 1		
		Feed	Product	Residue	Feed	Product	Residue
pH	-	7.41	7.18	7.81	7.81	7.42	7.96
TDS	(mg/L)	61,104	34,247	73,178	73,178	59,385	88,172
Conductivity	(mS/cm)	76.6	41.8	91.7	91.7	74.4	109.3
Ca^{2+}	(mg/L)	1,476	780	2,098	2,098	1,632	2,160
Mg^{2+}	(mg/L)	1,463	892	1,980	1,980	1,200	1,300
Na^{+}	(mg/L)	20,881	10,116	29,570	29,570	19,454	30,413
Cl^{-}	(mg/L)	32,200	15,600	45,600	45,600	30,100	46,900
$(HCO_3)^{-}$	(mg/L) as $Ca\ CO_3$	241.2	110.0	330.0	330.0	210.0	343.0
$(SO_4)^{2-}$	(mg/L)	4,800	2,900	6,900	6,900	5,100	7,000
NO_3^{-}	(mg/L)	2.0	0.60	3.40	3.40	1.70	3.50

Table 4.7: *Major physiochemical analysis of water samples for conducting the feed and three stripping stages.*

Parameter	Unit	Stripping stage 2			Stripping stage 3		
		Feed	Product	Residue	Feed	Product	Residue
pH	-	7.96	7.62	8.07	8.07	7.98	8.12
TDS	(mg/L)	88,172	59,541	97,786	97,786	70,490	114,102
Conductivity	(mS/cm)	109.3	74.6	119.8	119.8	88.4	136.2
Ca^{2+}	(mg/L)	2,160	1,848	2,400	2,400	2,092	2,724
Mg^{2+}	(mg/L)	1,300	1,232	1,116	1,116	309	1,813
Na^{+}	(mg/L)	30,413	20,362	33,785	33,785	24,706	38,973
Cl^{-}	(mg/L)	46,900	31,400	52,100	52,100	38,100	60,100
$(HCO_3)^{-}$	(mg/L) as Ca CO_3	343.0	246.0	368.0	368.0	336.0	382.0
$(SO_4)^{2-}$	(mg/L)	7,000	5,400	7,500	7,500	7,000	7,800
NO_3^{-}	(mg/L)	3.50	1.80	5.30	5.30	3.50	4.30

Table 4.7: *(Cont'd.)*

results proved that the ice maker was able to concentrate the RO brine by a considerable amount whilst simultaneously producing a final product of near seawater quality. This product water can easily be further desalted by feeding it to seawater RO membranes to obtain a final product water to drinking water standards.

As for the ionic composition, the average hardness ion values of Ca^{2+}, Mg^{2+}, and $(SO_4)^{2-}$ for the RO brine fed to the feed stage, were 1,476, 1,463, and 4,800 mg/L, respectively, as illustrated in Table (4.7). The ice maker, over four successive freezing stages, was able to significantly increase the hardness ions up to 2,724, 1,813, and 7,800 mg/L, for Ca^{2+}, Mg^{2+}, and $(SO_4)^{2-}$, respectively. Table (4.7) also shows that the RO brine contains monovalent ions, i.e. Na^{+} and Cl^{-}, with ionic concentration of 20,881 and 32,200 ppm, respectively, which were dramatically increased to 38,973 and 60,100 ppm, for the same ions, respectively, over four successive freezing stages. In general, the ionic concentrations of the feed and residual liquid were found to be proportional to the number of stripping stages. This was due to the residual liquid of the previous freezing stage becoming the feed for the subsequent freezing stage.

The calculations of the theoretical power consumption for the feed stage, and first, second, and third stripping stages gave about 0.112, 0.107, 0.125, and 0.119 kWh/kg respectively. The values of power consumption from experiments were 0.48, 0.66, 0.90 and 1.10 kWh/kg, for the same freezing stages respectively, as given in the Table A4-16 in Appendix A4. In comparison to the case of seawater desalination (see section 4.6.6), the power consumption from experiments for concentrating RO brines is much higher than that in desalting seawater. This is affected by the reduction in production rate since the value of the electrical loading was constant for all experiments. This clearly indicates and confirms that the salt concentration has a strong influence on the power consumption.

4.7 Conclusions

The primary concern of this study was to assess the viability of desalting saline water by means of an ice maker. The proposed treatment system was tested using NaCl solutions over a wide range of salt concentrations. Alongside the NaCl solutions, process brines, including Arabian Gulf seawater and RO brine, were considered in this laboratory investigation. In addition, different parameters influencing the separation performance of the ice maker were

studied. The process brines were also investigated over a number of freezing stages for the purpose of water desalination and brine concentration.

The overall experimental results showed that the tested treatment system was not capable of providing drinking water even from the low salt concentration feeds. In contrast, the investigation showed that the ice maker was effective in concentrating high salinity feeds, while producing saline water that could subsequently be easily desalted using any type of conventional desalination technology. As a result, the volumes of waste streams, such as RO brine, could be substantially reduced. For such an application, the experimental results were highly encouraging, and proved that the investigated ice maker was technically feasible and might be competitive with other available commercial brine concentration systems. In order to further assess the actual separation efficiency of the falling film crystallisation technology (which utilises similar technology as the ice maker) in the concentration of high salinity feeds under a wider range of operating conditions (with and without use of sweating operation), a full scale industrial pilot plant for the Sulzer falling film crystallisation process was considered, used and investigated in the subsequent chapter.

CHAPTER V:

INVESTIGATING THE FEASIBILITY OF THE FALLING FILM CRYSTALLISATION PROCESS FOR TREATING REVERSE OSMOSIS BRINES

5.1 Introduction

The majority of articles on the falling film crystallisation process focused on process design and operation to improve the purity and yield of crystalline layers [Ulrich and Glade, 2003]. These articles have shed light on a wide range of application areas, including pharmaceuticals, and chemical and food processing [Ulrich and Glade, 2003]. However, there is a marked absence of research in the area of RO brine concentration, which has been overlooked entirely.

The preliminary investigation of the ice maker, for which results were given in Chapter 4, proved that the falling film crystallisation process was capable of producing a substantial amount of final product water, which was comparable in salt concentration to RO feed. As a result, a small amount of highly concentrated solution of RO brine remained. Consequently, as presented in Chapter 4, great benefits can be realised for RO membrane desalination plants, particularly those located inland. Accordingly, to investigate the actual performance of the falling film crystallisation process for concentrating RO brine, an industrial pilot scale plant was adapted, tested and assessed in this study. The pilot plant used Sulzer falling film crystallisation technology, as well as a post-treatment crystallisation system, known as the sweating process. According to Sulzer's experts, the adopted technology has not previously been tested for saline water applications. As a result, there was no reference data available on the proposed treatment system for such applications. Hence, this study presents the first investigation to explore and provide quantitative and valuable information concerning the separation efficiency of the adopted process. Indeed, performance cannot be predicted

without carrying out experiments, since the actual performance of the process depends not only on the physicochemical properties of RO brine (such as equilibrium diagrams), but also on other factors concerning the process operation. Thus, this investigation provides useful and important information on designing a complete commercial plant used as a pre-concentrator system for future application to RO brine concentration. In particular, the tested pilot plant represents a straightforward scale up pilot plant.

The overall objective of this chapter is to assess and validate the actual technical feasibility of using Sulzer's falling film crystallisation technology as a pre-concentration system for concentrating RO retentate and producing final product water, which is comparable to seawater in quality, and hence ready for immediate use as feed water for a RO membrane plant. The specific aims of this study are:

i) To operate and test the pilot plant with use of the sweating process, and collecting experimental data at different operating conditions.

ii) To validate and assess the influence of feed salt concentration, crystallisation time, sweating time and operating temperatures, on the performance of the Sulzer falling film crystallization technology and sweating process.

iii) To identify the optimal operating limits for key operating parameters in the crystallisation and sweating operations.

iv) To investigate the performance of the rectification and stripping stages using the adopted technology for achieving further purification and concentration of the product and residue, respectively. Alongside the RO brine, Arabian Gulf seawater was also used and tested as feed in this investigation.

v) To validate and assess the process's technical merits for future application on a commercial scale.

vi) To establish reference data on the performance of the Sulzer falling film crystallisation processes for concentrating RO retentate. This includes a reference physiochemical profile for water samples.

vii) To assess the separation effectiveness, under the influence of the falling film crystallisation and sweating processes, in the rejection of the major components of ionic concentration (e.g. Ca^{2+}, Mg^{2+}, $(SO_4)^{2-}$, $(HCO_3)^-$, Cl^- , Na^+, etc) for the process brine samples.

5.1.1 Description of the Falling Film Crystallisation Process and Basic Operation

Melt crystallisation technologies are applied extensively in the purification of a wide range of chemical substances in various application areas, such as chemical processing, pharmaceuticals, and food processing. There are two main melt crystallisation process types, namely suspension, and solid layer crystallisation [Ulrich and Glade, 2003; Sulzer, 2004]. Suspension crystallisation will be described later in Chapter 6. Solid layer crystallisation technologies are classified, according to operating mode, into two main categories: batch and continuous modes. The solid layer crystallisation in batch mode uses either a static (e.g. stagnant melt with use of natural convection or forced convection principles) or dynamic process (e.g. flowing melt with use of tube flow or falling film principles) [Ulrich and Glade, 2003; Sulzer, 2004]. The solid layer crystallisation with a continuous method is either a static (e.g. stagnant melt with use of zone melting or drum crystalliser) or dynamic (e.g. flowing melt with use of belt crystalliser) process [Ulrich and Glade, 2003; Sulzer, 2004].

The Sulzer falling film crystallisation process is characterised as a dynamic process, i.e. flowing melt with use of the falling film principle, in batch operating mode. The Sulzer falling film crystalliser differs from conventional falling film crystallisers and the ice maker machine (which was tested and assessed in Chapter 4) in that it distributes the flowing melt and Heat Transfer Medium (HTM) evenly as a falling film (via distribution systems) over the inside and outside surfaces of the tubes, respectively, as illustrated in Figs (5.1) and (5.2). This means that neither the shell side nor the inside of the tubes is filled with HTM or melt, but in return, falling film principles are applied instead [Ulrich and Glade, 2003; Sulzer, 2004]. Ulrich and Glade (2003) mentioned that the refrigerant vapour condenses into a liquid refrigerant, which is distributed on the outside tubes to wet them for refrigerating and warming purposes. This technique enhances the refrigeration method by maintaining a constant temperature distribution along the length of the inside and outside surfaces of crystallizers, leading eventually to obtaining a more homogeneous thicknesses of ice [Ulrich and Glade, 2003]. Furthermore, this method improves the efficiency of post-purification processes, including the sweating step [Ulrich and Glade, 2003; Sulzer, 2004].

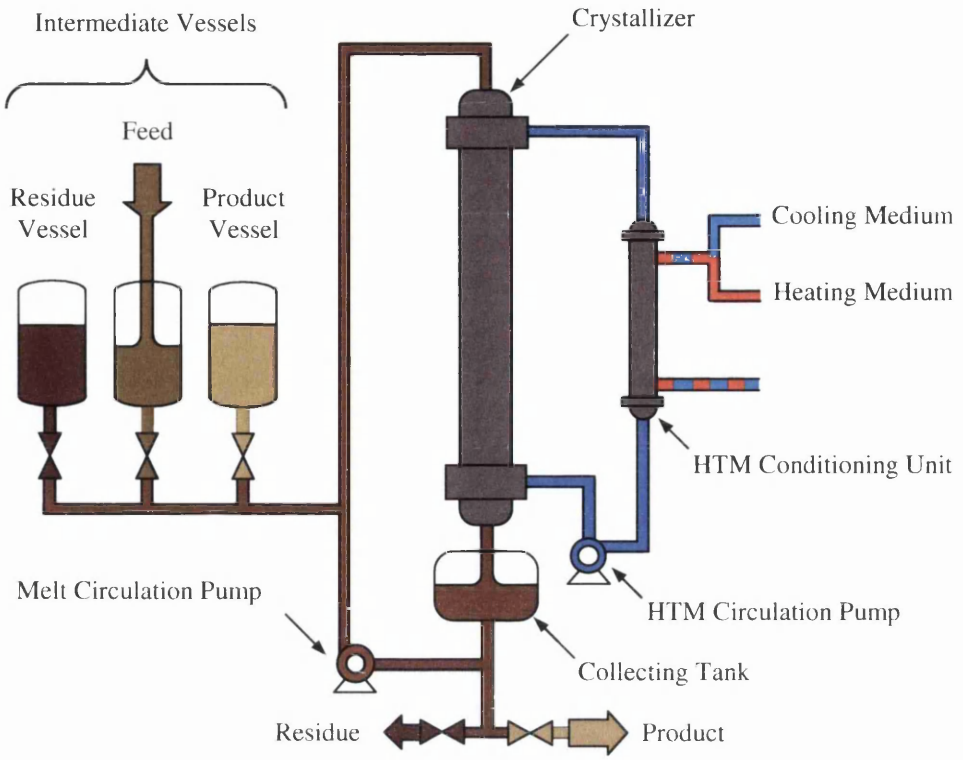

Fig. 5.1: *Typical Sulzer falling film crystallisation plant, adapted from Ulrich and Glade (2003), and Sulzer (2004).*

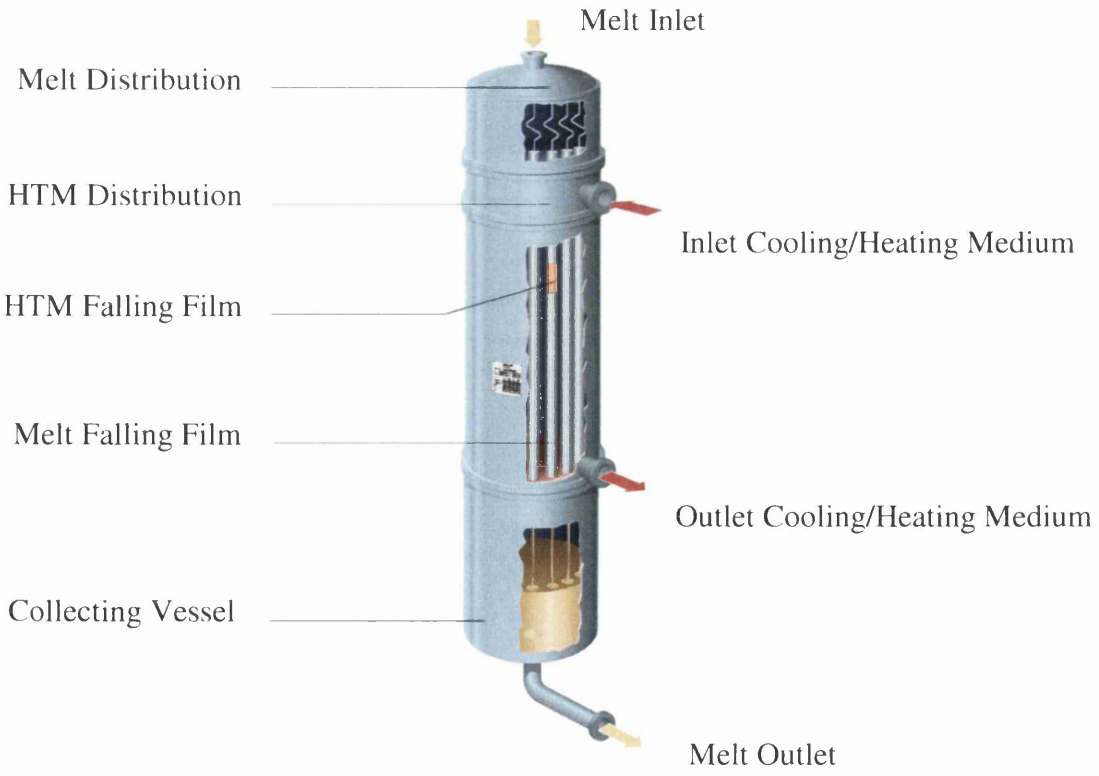

Fig. 5.2: *Typical Sulzer falling film crystalliser, adapted from Sulzer (2004).*

A typical example of the Sulzer falling film plant is illustrated in Fig (5.1), and consists of a crystalliser, collecting tank, HTM conditioning unit, HTM circulation pump, melt circulation pump, and intermediate storage vessels (which are used for storing feedstock, product, and residue samples). The principles of the Sulzer falling film crystallisation process, shown schematically in Fig (5.1), are described in more detail in the references [Ulrich and Glade, 2003; Sulzer, 2004]. As shown schematically in Fig (5.2), the melt and HTM distribution systems are installed above the tubes, whereas the tubes are placed above the collecting tank. The commercial Sulzer crystalliser consists of several hundred vertical tubes (up to 1,100 tubes) surrounded by a shell [Ulrich and Glade, 2003]. According to Ulrich and Glade (2003), a commercial Sulzer plant containing two crystallisers with 1,100 tubes each, means that the diameter of each crystalliser is 4 m, and is capable of producing 100,000 tons annually of a product with purity in the parts per million range.

According to Sulzer (2004), falling film crystallisation is most commonly used in the separation of organic materials ranging from isomer separation to tar chemical mixtures, and from organics acid to monomers. Some typical applications are separation of Bisphenol A, acrylic acid, benzoic acid, fatty acids, pharmaceutical intermediate, nitrated aromatics, caprolactam, naphthalene, monochloroacetic acid, palm oil, dichlorobenzene, tetrachlorobenzene, chloro-nitrobenzene, hexachlorobenzene, mono-, di-, and trinitrotoluene, isocyanates, alpha-/beta-naphthol, diphenylphenol, xylenole, p-xylene, aqueous solutions, chlorinated aromatics, p-cresole, p-phenylene-diamine, phenol, and anthracene [Myerson, 2002; Ulrich and Glade, 2003; Sulzer, 2011].

The principles of operation of the Sulzer falling film crystallisation plant include six successive processes, namely (i) filling, (ii) pre-cooling, (iii) nucleation, (iv) crystallisation, (v) partial melting (sweating), and (vi) melting. These processes are applied in a non-adiabatic environment and operated under atmospheric pressure [Sulzer, 2005].

(i) Filling process

Initially, the collecting tank is filled with a predetermined amount of feed by opening the feed valve, whereas the product and residue vales are in the fully closed position as shown in Fig (5.1). When the collecting tank is filled with the desired amount of feed, then the feed vessel valve is closed.

(ii) Pre-cooling

Pre-cooling is activated by means of the HTM conditioning unit (using cooling medium) and the melt circulation pump. The melt circulation pump frequently delivers feed from the collecting tank to the melt distribution as shown schematically in Figs (5.1) and (5.2). The melt distribution distributes the melt evenly as a falling film over the interior surface of the tube as shown schematically in Fig (5.2). When the flowing water passes the interior surface of the tube, the melt is then cooled by means of a concurrent falling film of HTM on the outside surface of a tube [Sulzer, 2005].

(iii) Nucleation

When the temperature of feed reaches a predetermined value (i.e. 10°C) above the freezing point of feed, nucleation is achieved by stopping the melt circulation pump and simultaneously reducing the temperature of cooling medium. Due to the fact that the inside surface of the tube was washed during the pre-cooling process, ice crystals are nucleated and form from the remaining parts of the melt adhered in the tube's surface.

(iv) Crystallization

The crystallisation process is achieved by pumping the pre-cooled fluid over the surface of the tube, which includes nucleated ice crystals, to form a thin layer of ice as a cylindrical shell inside the crystalliser. By continuously circulating the cold melt, a thin crystalline layer is allowed to grow inwardly from the refrigerated surface. Consequently, the water level in the collecting tank will decrease as the thickness of the ice layer increases. When the thickness of the ice layer reaches a certain limit (which is dictated by; crystallisation time, crystallisation temperature, salt concentration of the residue, or water level in a collecting tank), then the crystallisation process is deactivated and the residue is removed from the collecting tank through the residue line. The residue is then either transported to the drain discharge or to an intermediate storage vessel for carrying out multistage operation. This means that the residue can be further treated and concentrated using the intermediate residue vessel as feedstock and repeating the previous steps.

(v) Partial melting (Sweating)

According to Ulrich and Glade (2003), the sweating process is defined as a temperature-induced purification step based on a partial melting process performed by gradually

increasing the temperature of the tube up to a certain level close to the freezing point of the required product. Thus, substantial amounts of impurities adhering to the crystal surface of the crystalline and those brine buckets, contained in pores of the crystalline structure, can be rejected and drained under the influence of gravity [Ulrich and Glade, 2003]. When the temperature of the tube increases, the viscosity of the impurities will be decreased, leading to easy and enhanced draining off [Ulrich and Glade, 2003]. Therefore, the purity of ice crystals can be significantly improved by the sweating process.

On completion of removing the residue from the collecting tank, the partial melting process (i.e. sweating phase) is accomplished by flowing the heating medium into the crystalliser through a HTM conditioning unit. Consequently, the tube wall of the crystalliser is heated gradually to induce partial melting. The melted ice (i.e. sweat fraction) is drained off or transported either to the respective storage vessel or used in multistage operation, for a subsequent purification step. This means that the residue can be further treated by recycling the sweat fraction into the intermediate feed or residue vessel in order to be used as a feedstock and repeating the previous steps.

(vi) Melting

The melting process is operated by increasing the temperature of the heating medium through a HTM conditioning unit. Consequently, the remaining crystal layer is melted and collected as either product or transported into the intermediate storage vessel for a subsequent purification step in multistage operation.

5.1.2 Multi-Stage Design and Basic Operation

Any degree of purity and/or concentration can be obtained by using the intermediate vessel as feedstock and repeating the freezing stage [Ulrich and Glade, 2003; Sulzer, 2004]. For Sulzer commercial plants, the number of freezing stages can be varied between one to seven stages [Ulrich and Glade, 2003; Sulzer, 2004]. These stages can be performed in sequence through a single crystalliser using a batch method, to reduce the capital and operational costs, however, this option may be limited by several factors, including plant capacity [Ulrich and Glade, 2003].

Fig (5.3) illustrates the mass flow in a three-stage process as an example of multi-stage design. As mentioned previously, the three stages in the process are commonly known as feed, rectification, and stripping stages [Ulrich and Glade, 2003; Sulzer, 2004]. The feed stage represents the first freezing stage, which is mainly used for both purifying and concentrating the product and residual liquid, respectively [Ulrich and Glade, 2003; Sulzer, 2004]. The rectification and stripping stages represent the repeated stages for purifying the product and concentrating the residual liquid, respectively [Ulrich and Glade, 2003; Sulzer, 2004]. Fig (5.4) shows the HTM temperature profile for the feed, rectification, and stripping stages. Fig (5.4) also shows the temperature profile of the main processes, i.e. crystallisation, partial melting, and total melting for each freezing stage. The operating conditions of each stage may differ from the other, as dictated by several factors, including the characteristics of feed material, and achieving the desired quality and quantity of the product and/or residual liquid. Therefore, the operating HTM temperatures of the main processes of the feed stage are higher and lower than those in stripping and rectification stages respectively, as shown in Fig (5.4). This is due to the salt concentration of the feed material fed to the rectification and stripping stages being lower and higher, respectively, in comparison to that in the feed stage. Fig (5.5) demonstrates the scheme of falling films of melt and HTM throughout the freezing stage.

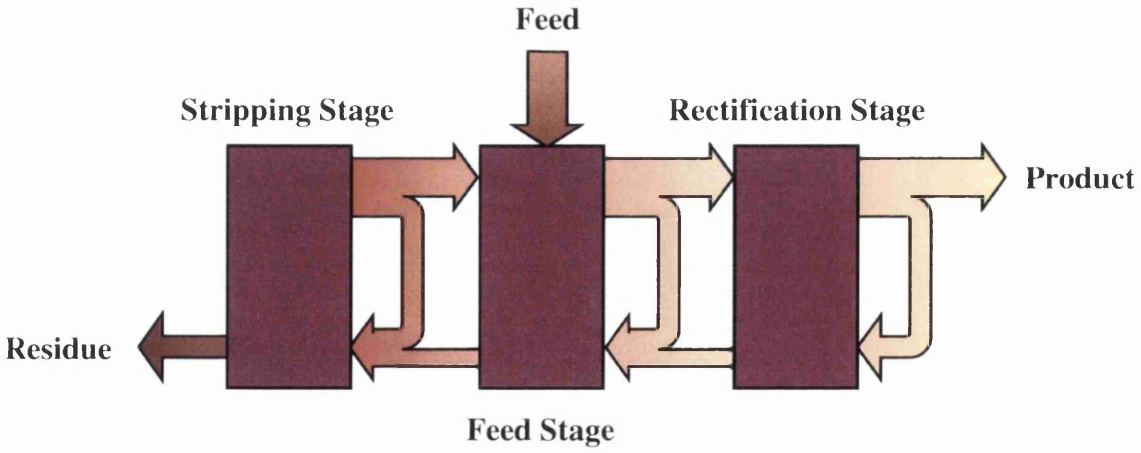

Fig. 5.3: *Mass flows in a three-stage process [Ulrich and Glade, 2003; Sulzer, 2004].*

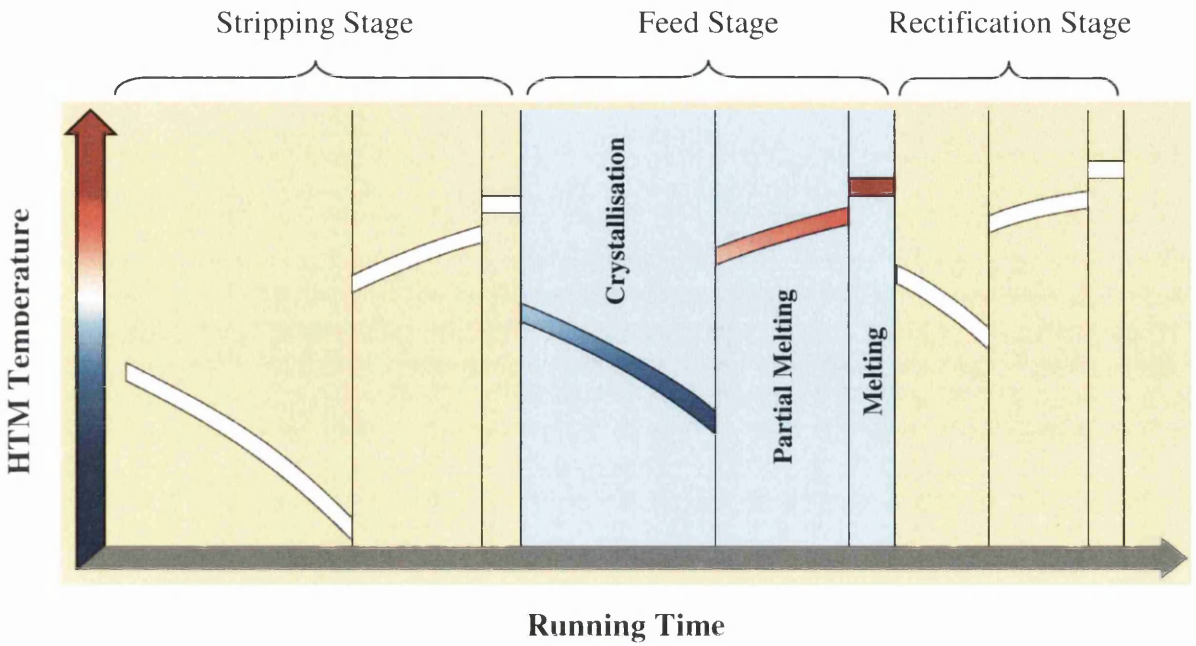

Fig. 5.4: *Temperature-time profile of the falling film crystallisation, adapted from Ulrich and Glade (2003), and Sulzer (2004).*

(a) Crystallization (b) Partial melting (sweating) (c) Melting

Fig. 5.5: *Process phases [Ulrich and Glade, 2003; Sulzer, 2004].*

As illustrated in Fig (5.1), on completion of the feed stage, the residue (including the sweat fractions) and product are collected in the residue and product vessels, respectively. Fig (5.4) shows the temperature-time profiles of the feed stage. By repeating the feed stage several times, the residue and product vessels are then filled with enough amounts to fully load the crystalliser as shown in Fig (5.3). Consequently, the rectification stage is then activated and the final product is obtained, whereas the residue (including the sweat fractions) from the rectification stage is collected into the feed vessel. Fig (5.4) shows the temperature-time profiles of the rectification stage, which utilises higher HTM temperatures compared to that in the feed stage and this is due to the freezing point of the feed. On completion of the rectification stage, the stripping stage is activated leading to concentration of the residue. The product from the stripping stage will be collected into the feed vessel, whereas the residue

(including the sweat fractions) is drained off. Fig (5.4) shows the temperature-time profiles of the stripping stage, which utilises lower HTM temperatures compared to that in the feed stage.

5.2 Preparation of Feed Samples

Two different sources of process brines were used and tested individually as a feed-sample in this study. The examined process brines are: Arabian Gulf (AG) seawater (4.9% by weight of dissolved salt) and reject brine (6% by weight of dissolved salt), produced from a Reverse Osmosis (RO) membrane desalination plant. The majority of the experimental work was carried out with RO brines as feed material. The feed water samples were collected from the RO unit at the Doha Research Plant (DRP), Kuwait Institute for Scientific Research (KISR), in Kuwait. These feed water samples were transported from KISR (Kuwait) to Buch SG (Switzerland), where the laboratories of Sulzer Chemtech Ltd are located. The preparation of feed materials was carried out as described in Chapter 4.

5.3 Physicochemical Analysis & Measuring Instruments

The physicochemical analysis of water samples was carried out as described in Chapter 4 (section 4.3). In addition, the measurements of freezing point were covered in this investigation. Furthermore, the temperature profiles and running times of the pre-cooling, crystallisation, partial melting, total melting, and freezing stage of each test were monitored and recorded. However, the pH measurements were not considered in this study. The physicochemical analysis of water samples was performed experimentally using the measuring instruments, auxiliary equipment, tools, and laboratory facilities of Sulzer Chemtech Ltd (Buchs SG, Switzerland). For further investigation, several sets of water samples were sent to both the Doha Desalination Research Plant (DRP) laboratory and the Central Analytical Laboratories (CAL) at KISR (Kuwait) for performing similar chemical analysis and also carrying out full chemical analyses on water samples to detect the major ionic composition. Results of these measurements are tabulated in Tables A5-4 – A5-9 in Appendix A5.

The salt concentration of the feed sample was measured via a conductivity meter (Cond 3110, Tetra Cond 325) and a conductivity probe (Conductivity probe model: TetraCon 325,

Wissenschaftlich-Technische Werkstätten GmbH) to ensure that the correct concentration was achieved. The measurements of TDS were experimentally determined, using the gravimetric method, by evaporating a known weight of the water sample to dryness, and weighing the solid residue. The equipment involved in obtaining gravimetric measurements are an oven (Heraeus instruments, Type: UT 12P, D-63450 Hanau, Kendro Laboratory Products), Petri dish, and laboratory balance (Mettler PM 460, Delta Range, CH-8606). The accuracy of salt concentration results was assured through a simple mass balance equation. The volume and weight measurements, on the other hand, were determined by a laboratory beaker, scaled borosilicate glass cylinder (Barcode: CYL-350-020J, Fisher Scientific) and a laboratory balance (Mettler Toledo, Model: PM30-K). The running time for the crystallization process was measured by a stopwatch timer (HS-10W Stopwatch, Casio).

The freezing points were experimentally measured with an instant digital thermometer (P650 series, Serial No.: 65006040472) and a temperature sensor (Pt100, IEC A 240119-1), while the refrigeration system consisted of the following equipment; (a) thermostatic bath (Haake C, Type: 001-0505, Nr: 840096), (b) PID temperature controller (Haake PG 40, Type: 000-9030, Nr: 830264), (c) bath circulator (Haake F3, Type: 000-9601, Nr: 840117), and Heat Transfer Medium (HTM), which is a mixture of ethylene glycol and deionised water.

The measuring instruments involved in the full water chemistry analysis, including their measuring procedures, are described in Chapter 4.

5.4 Experimental Setup

Figs (5.6) and (5.7) show the Sulzer falling film crystallisation pilot unit used by Sulzer for investigating new fields of application. This pilot plant was used and tested in this study. The description of the pilot plant and basic operation is available in section 5.1.1. Although Sulzer Chemtech Ltd commercialises complete test units that are completely equipped with all necessary equipment, including the cooling compressors [Ulrich and Glade, 2003; Sulzer, 2011], the examined pilot plant does not include a complete built-in refrigeration unit. The pilot plant is connected to a Heat Transfer Medium (HTM) conditioning unit, which represents the main refrigeration system (Elektroschema NR 1.054.692, Dowtherm-Kühlanlage-65°C, Für Kristallisations-Labor, R 404a, Dowtherm, using organic heat transfer

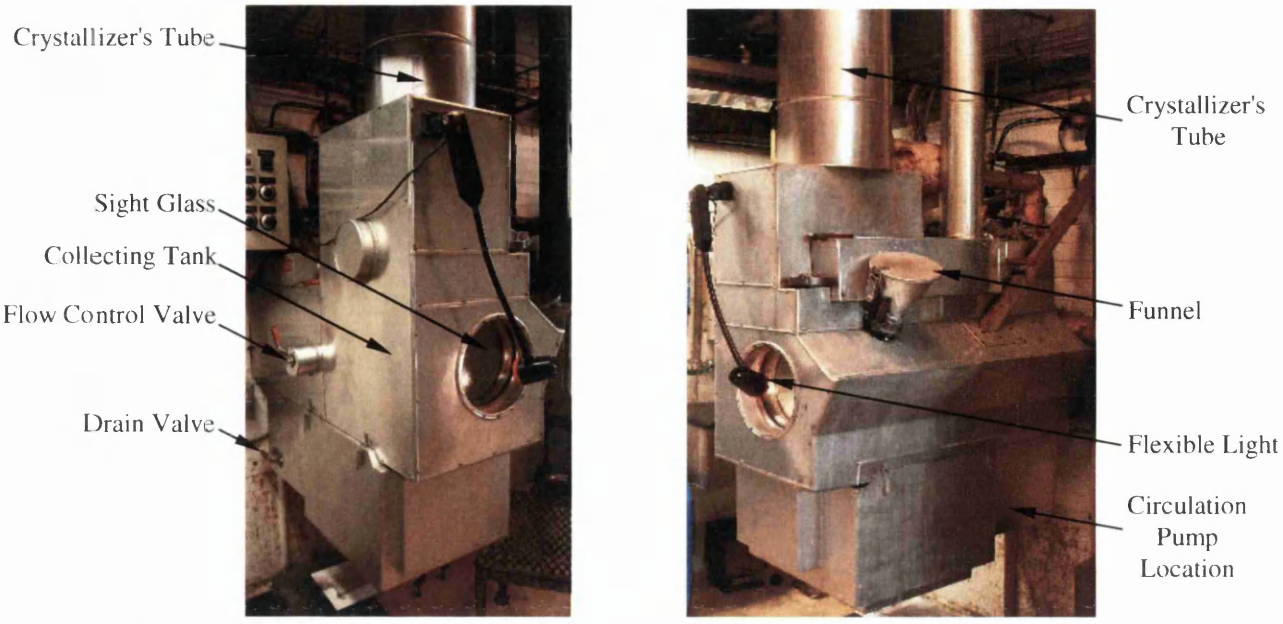

(a) Left-hand side view of pilot plant (b) Right-hand side view of pilot plant

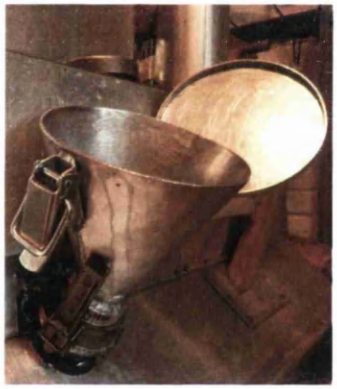

(c) Funnel

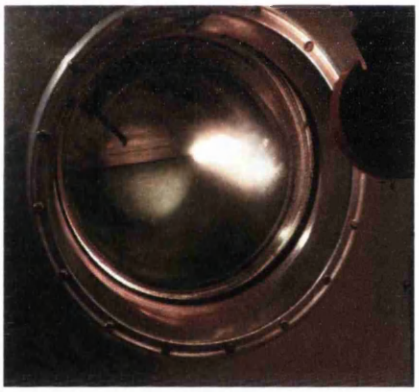

(d) Sight glass & water level Indicator

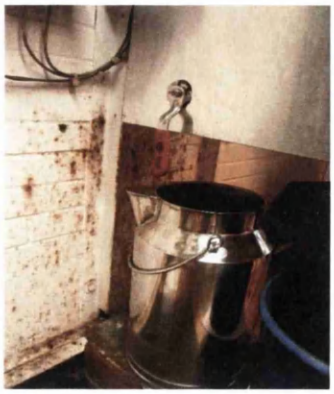

(e) Drain valve (i.e. sampling point)

(f) Monitoring ice suspension

Fig. 5.6: *Tested Sulzer falling film crystallisation pilot plant.*

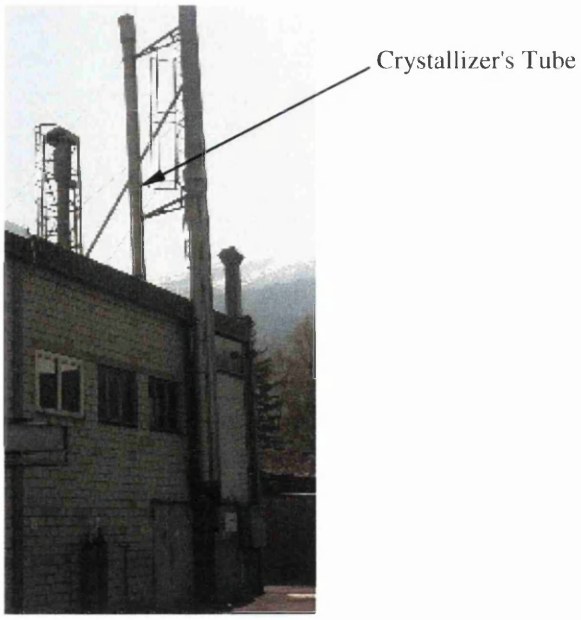

Fig. 5.7: *Outside-view of the tested pilot plant.*

fluids and R404a, ANr./Bj 67 1130/1996, Pressure 17 bar, Compressor S6J-16,2Y) used for all the pilot plants situated at Sulzer's plant. Apart from the refrigeration system, the pilot plant is completely equipped with all necessary measuring instruments and control devices. In addition, the pilot plant is provided with an emergency shutdown switch, which is a manually-operated push button used to shutdown the operation system of the pilot plant in an emergency situation. The crystalliser and collecting tank are made of stainless steel, which is thermodynamically insulated from the surrounding environment (see Figs (5.6) (a) and (5.7)).

The tested pilot plant is a straightforward scale up pilot plant. In comparison to the ice maker (tested and evaluated in Chapter 4), the feed capacity of the tested pilot plant was about tenfold more. Furthermore, the tested pilot plant provides a higher specific production rate, in terms of water recovery ratio, within a single-stage process. In addition, the examined pilot plant provides a greater operating depth in different key operating parameters for both crystallisation and sweating operations.

The pilot plant is provided with a desktop computer and Strip Chart Recorder (SCR) (Eurotherm Chessell, Model No.: 4180M) as illustrated in Figs (5.8) (a) and (b), respectively. The desktop computer is provided with a software package for leading and controlling the

operation of the pilot plant. The installed software package is known as "MovieconX Evolution Ten" and was published by Sulzer Chemtech Ltd. The package monitors the operational status and records the experimental data, such as the measurements of running time, melt temperature, HTM operating temperature, and flow rate of melt circulation pump throughout the freezing stage, which includes pre-cooling, crystallisation, partial melting, and total melting processes. At the same time, some of the majority of the key operating parameters were controlled through a software package installed in a computer-controlled system connected to the pilot plant. The strip chart recorder data acquisition system, on the other hand, is used for continuous tracking of the process, printing the trends of temperature profiles of melt and HTM throughout the freezing stage. These temperatures are measured by means of thermocouples placed at the inlet and outlet pipelines of the tube. Fig (5.9) shows that the temperature indicators (TI-101) and (TI-102) are used for monitoring the inlet and outlet temperatures of the melt respectively, while the temperature indicators (TI-204) and (TI-205) are used for monitoring the inlet and outlet temperatures of the HTM, respectively, as shown in Fig (5.9).

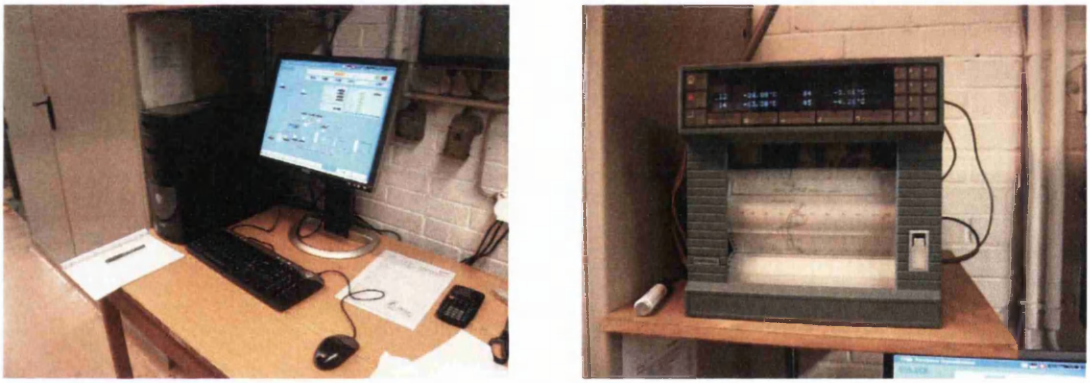

(a) Desktop computer (b) Strip chart recorder (SCR)

Fig. 5.8: *Apparatus for controlling and maintaining the pilot plant.*

Fig (5.9) also shows that the tested pilot plant consists of the following equipment; collecting tank (T-1), crystalliser's tube (S-1), melt circulation pump (P-1), flow control valve (FCV), drain valve (DV), funnel (F), temperature indicators (i.e. (TI-101), (TI-102), (TI-204), and (TI-205)), HTM circulation pump (P-3), and HTM conditioning units (which are used for supplying cooling medium (C-1) and heating medium (H-1)). All valves involved in the HTM conditioning units are classified as automatic valves, while the valves dealing with the

melt are classified as manual valves; these are the flow control valve (FCV) and the drain valve (DV).

The pilot unit is provided with a single-tube falling film crystalliser as shown in Figs (5.6) (a), (5.7), and (5.9). This crystalliser is installed above the collecting tank, and consists of a single vertical tube, and two distribution systems for the melt and HTM. The length and inner diameter of the tube are 12 m and 70 mm, respectively. As mentioned previously, the pilot plant is a straightforward scale-up pilot tested, where a commercial scale crystallizer may be built by adding a number of tubes of the same size of the length and inner diameter of the tested crystallizer's tube. The used melt circulation pump, on the other hand, is classified as a centrifugal pump. This pump is installed behind the collecting tank and is hidden by insulated panels (see Figs (5.6) (b)). The operation of this pump is controlled and driven by the computer. The flow rate of the melt circulation pump can be controlled by the computer's software and a flow control valve.

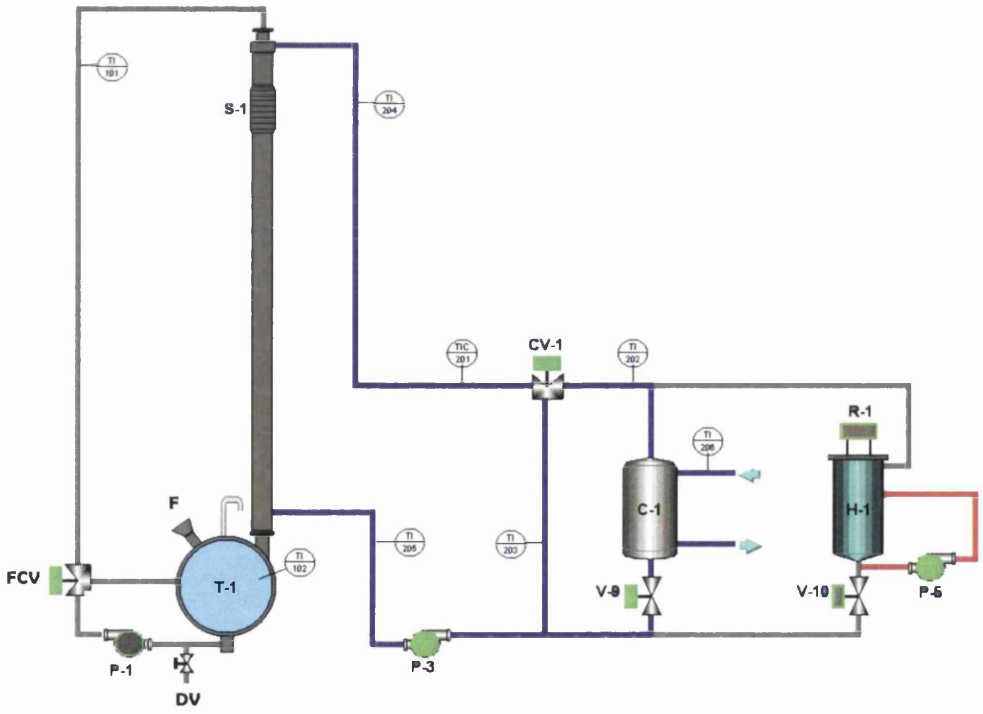

Fig. 5.9: *Process flow diagram of the pilot-plant, adapted from screenshot of the pilot plant software package.*

As illustrated in Figs (5.6) (a) and (b), the collecting tank is provided with the following: (i) A reservoir with a capacity of 35 L (see Fig (5.6) (a)), which is joined with a crystalliser

tube, where the reservoir is positioned below the tube; (ii) A funnel is attached with a lid (see Fig (5.6) (c)), which is used for facilitating the filling process. The funnel is installed on the right-hand side above the collecting tank. The lid is used to cover the funnel and seal the collecting tank throughout the freezing stage. (iii) A sight glass with a water level scale which enables the user to visually monitor the return flow behaviour inside the collecting tank, since the pilot plant is considered a closed system. Throughout the freezing stage, the sight glass helps detect the water level (see Fig (5.6) (d)), and visually observe the appearance of the undesired ice suspension inside the collecting tank (see Fig (5.6) (f)). The sight glass is installed in front of a collecting tank as shown in Fig (5.6) (a). (iv) A flexible light (see Fig (5.6) (b)) is installed on the front side of collecting vessel (above the sight glass) to illuminate the inside of the collecting tank to visually monitor the water level, and the appearance of the ice suspension as stated previously. (v) A resistance wire (i.e. heat source element), which is wrapped around the collecting reservoir in order to control the feed temperature inside the tank throughout the operation of the freezing stage. The thermal energy provided by the resistance wire is controlled by a computer.

The flow control valve is a hand-operated three-way ball valve, which is installed on the left-hand side behind the collecting tank as shown in Fig (5.6) (a). This valve is used for controlling; (i) the flow rate of the falling film of the melt inside the tube, and (ii) the flow rate of the circulated feed into the collecting tank through a bypass pipeline. The pilot plant also has a drain valve, which is a hand-operated ball valve installed on the left-hand side, beneath the collecting tank, as illustrated in Figs (5.6) (a) and (e). The purpose of this valve is to remove (or collect) the residual feed, sweat fractions, and product sample from the collecting tank under the influence of the gravity. This valve is used as the sampling point.

5.5 Experimental Procedure

The operating procedures for crystallisation and sweating experiments using the mentioned pilot plant are shown schematically in Fig (5.10). These experiments were carried out in batch mode. Before performing the first experiment of each day, the main refrigeration system was initially operated to cool down the refrigeration unit.

The physiochemical analyses were initially performed on the feed sample. Before starting the experiment, a predetermined weight of feedstock was experimentally measured by means of a laboratory balance via a stainless steel barrel. The drain valve of the pilot plant was set to fully closed position, and then the collecting tank was manually filled with the predetermined amount of feed through a funnel. On completion of the filling process, the funnel was manually covered with a lid and then the SCR was operated, before activating the pilot plant.

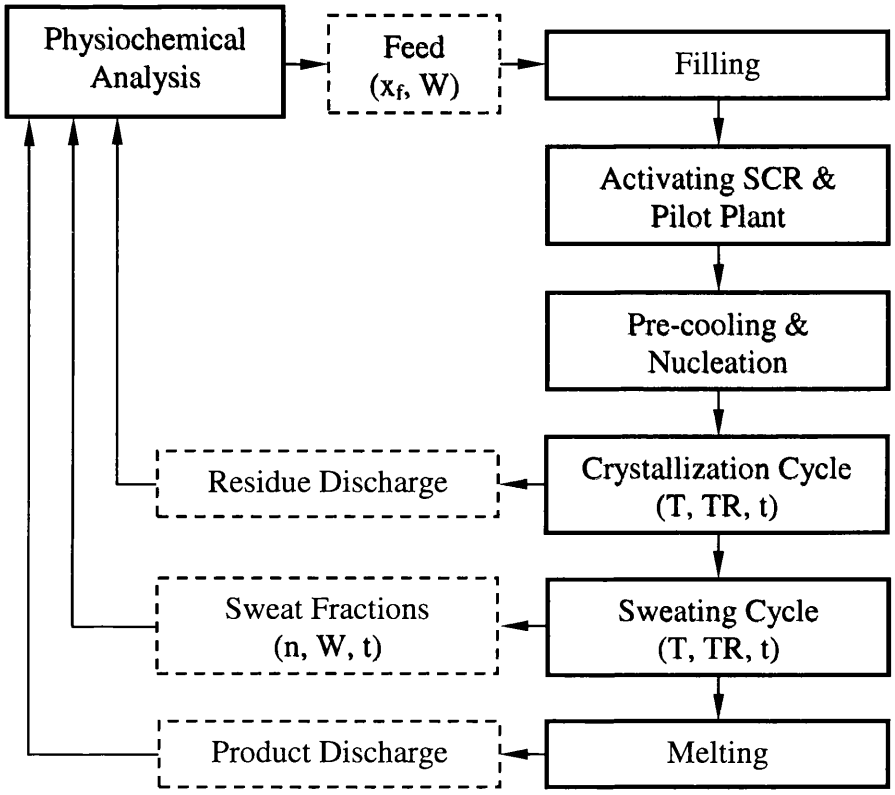

Fig. 5.10: *Simplified block diagram of the operational process for the experimental set-up. Where (x_f) is the feed concentration (ppm), (W) is the sample weight (kg), (t) is the running time (minute), (T) is the temperature (°C), (n) is the number of sweat fractions, and (TR) is the temperature ramp.*

5.5.1 Preparation and Activation of the SCR

The SCR has a keyboard, including a numeric keypad, as well as eight keys (such as "Home", "Enter", "Cancel", etc...) located in the front of the recorder, whose functions depend on the particular operation being performed. For instance, the recorder can be operated by clicking on the following keys; "Home", "Chart", "On/Off", and then "On". In

order to shutdown the unit, the same procedure applies, except the final option is switched to "Off". Once the unit is operational, tracking of temperature profiles is performed simultaneously, irrespective of whether the pilot plant is activated or not. These temperature profiles were continuously printed along the actual running hours. A complete record of these temperature profiles is shown in Appendix 5 (see file name: Appendix_5_A5-1).

5.5.2 Preparation and Activation of the Pilot Plant

On completion of the filling procedures and activation of the refrigeration system and the SCR, the computer control system was prepared ahead of operation of the pilot plant. As illustrated schematically in Fig (5.11), the software package presents a schematic process flow diagram on the display screen for executing the operating control strategy. The package offers eight operational buttons (i.e. icons), which are "Precooling", "Crystallization", "Partial Melting", "Total Melting", "Standby", "On", "Off", and "Reset", as shown at the top of the display screen. The software displays and records the running times of the precooling, crystallisation, partial melting, and total melting processes as shown in Fig (5.11). Furthermore, the running time of the freezing stage, which is identified as the "Stage Time", is also displayed and recorded. Alongside the SCR, the operating temperature profiles of melt and HTM were continuously tracked and recorded by means of a software package. These graphs can be shown on the display screen by selecting the graph icon (see Fig (5.11)).

In order to prepare and manage the operation of the pilot plant during the course of the experiment, the computer control system was initially activated by selecting the "ON" button, which is located at the top right corner of the window (see Fig (5.11)). The HTM temperature and ramp are driven and controlled through the "HTM Settings" box (see Fig (5.11)). The desired operating settings of the HTM temperature and ramp can be specified before starting the experiment; furthermore, these settings can also be changed at any time while carrying out the test, depending on experimental conditions. In order to specify the desired operating settings of the HTM temperature and ramp, the boxes in front of "Temperature" and "Ramp", which are available under a "HTM Settings" box (see Fig (5.11)), must be individually selected, and then the desired value can be inserted according to the operating conditions of the experiments. For all experiments, the "Min Limit" and "Max Limit" settings, which are also available under a "HTM Settings" box (see Fig (5.11)), were set to constant values, which are -50°C and 50°C, respectively. The "Switch Temperature"

value, within the "Cooling" box (see Fig (5.11)), was also set to a constant value of 30°C for all tests. The "Tracing" box contains seven buttons (see Fig (5.11)), whose functions depend on the particular operation being carried out. Throughout the experiments, the settings of the seven buttons were adjusted to the "On" mode, whereas their main buttons were set to an automatic mode (see Fig (5.11)). The operating temperature of the collecting tank, known as heating power tank (which is measured in percentage (%)), is driven and controlled through the box positioned in front of the "Tank", which is available under a "Tracing" box (see Fig (5.11)). In order to specify the predetermined heating power of the collecting tank, the box in front of "Tank" (see Fig (5.11)) must be initially selected, and then the desired heating power ratio can be changed according to the operating conditions of the experiments. This procedure was also applied for the melt circulation pump, where the flow rate of the feed is identified as pumping power ratio, which is also measured in percentage (%). In order to specify the desired pumping power ratio, the box positioned above the melt circulation pump (P-1) logo (see Fig (5.11)) must be initially selected, and then the value of the pumping power ratio can be changed according to the operating conditions of the experiments.

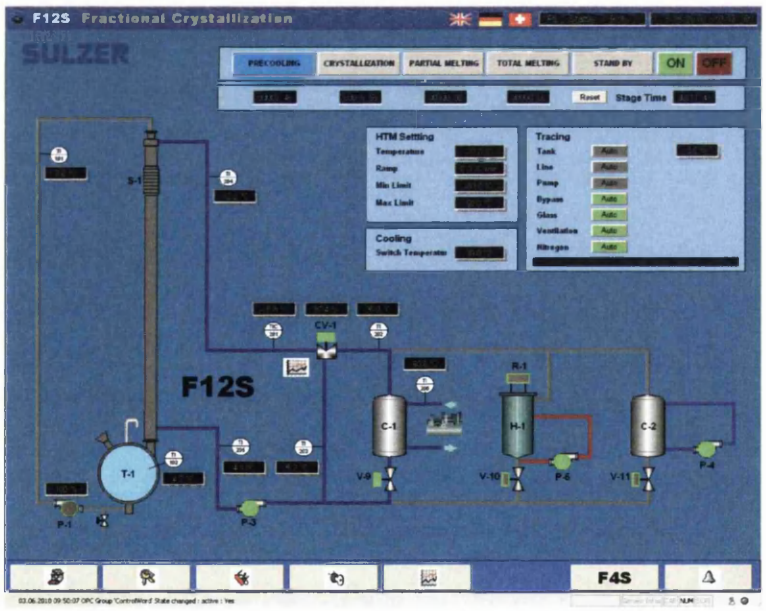

Fig. 5.11: *Screenshot of the pilot plant software.*

Following this, the pre-cooling, crystallisation, partial melting, and total melting processes were operated in sequence order for all tests.

(i) Pre-Cooling Process

In practice, the pre-cooling process was operated by conducting three successive steps: (i) the HTM conditioning units were operated by selecting the "PRECOOLING" button. This procedure will simultaneously activate the internal circulation of the HTM distributed as a falling film on the outside surface of the crystalliser tube by means of the HTM circulation pump. (ii) The temperature and the ramp of the HTM were then reduced to 0°C and 0°C/min, respectively. (iii) Prior to operating the melt circulation pump, the flow control valve was manually adjusted to a position, where the no bypass option is available. The melt circulation pump is then operated by selecting the "CRYSTALLIZATION" button, and the settings of the pumping power ratio and heating power tank were rapidly set to 100% and 0%, respectively.

(ii) Nucleation Process

According to Sulzer, the nucleation process must be started when the temperature difference between the freezing point of the melt and temperature of the inlet feed reached 10°C. When the temperature of the inlet feed, which is detected by means of a temperature indicator (TI-101) (see Fig (5.11)), had decreased to 7°C, the nucleation process takes place by deactivating the melt circulation pump through selecting the "PRECOOLING" button, and then rapidly changing the HTM temperature from 0°C to the predetermined crystallisation temperature (e.g. -12°C), whereas the ramp of HTM remained at a constant value of 0°C/min.

(iii) Crystallisation Process

When the temperature of the outlet HTM (which is detected by a temperature indicator (TI-205) (see Fig (5.11)) reached the freezing point of the feed (i.e. -3°C), then the crystallisation process was activated by selecting the "Crystallization" button, which simultaneously activates the melt circulation pump. The pumping power ratio and heating power tank were rapidly set to 85% and 20%, respectively, for the majority of the tests. The flow control valve was then rapidly adjusted whereby the bypass mode is operational to reduce the flow of the falling film, and so avoid the collapse of the nucleated ice from the crystalliser's tube; otherwise, an undesired ice suspension will form inside the collecting tank (see Fig (5.6) (f)).

For the crystallisation experiments, where ramping was not considered, the ramp for the HTM was kept at 0°C/min until the end of the crystallisation experiment. For the crystallisation experiments where ramping was considered, the ramp for the HTM was not adjusted to a predetermined value (e.g. -0.5 °C/min) until the nucleation phenomenon begins. Otherwise, the feed would be supercooled, leading eventually to carrying out the experiment with a very low HTM temperature and ramp. Therefore, the ramp for the HTM was adjusted to the desired value as soon as a slight rise in the outlet HTM temperature (detected by a temperature indicator (TI-205) see Fig (5.11)) was observed after the nucleation phenomenon, which was monitored through a SCR. A slight rise in the outlet HTM temperature after the nucleation phenomenon is caused by the liberation of the heat of crystallisation at the rapidly moving freezing front [Turnbull, 1965]. Following this procedure, the temperature and ramp of the HTM remained unchanged until the end of the crystallisation experiment. For all tests, the operation of the crystallisation process was deactivated based on the experimental conditions, which were dictated by either crystallisation time or when the water level in the collecting tank reaches the minimum allowed limit (i.e. achieving maximum water recovery ratio).

(*iv*) Partial Melting Process

Following completion of the crystallisation process, the partial melting process takes place by selecting the "partial melting" button (which terminates the operation of the melt circulation pump). At this point, the residual liquid was collected into a stainless steel barrel through a drain valve (see Fig (5.6) (e)). The residual liquid was then taken for physiochemical analysis. A sampling time of two minutes was set for collecting the residue sample before activating the HTM temperature and ramp for carrying out the partial melting process. On completion of the sampling procedures, the HTM temperature and ramp were changed to the desired values corresponding to the operating conditions of the crystallisation or sweating experiments, whereas the heating power tank were set to 100% for all tests.

For the crystallisation experiments, the values of the HTM temperature and ramp were increased to 15°C and 0°C/min, respectively. The sweat fractions were not collected and therefore the drain valve was then set to the fully closed position. The total melting process cannot be operated directly, because the melt circulation pump will be simultaneously activated, which will expose the pump to a high risk of damage due to running the pump dry,

since the collecting tank is still empty. Therefore, the remaining ice crystals were initially melted through the partial melting process to recover enough product water to be able to run the pump during the final process, namely total melting, to yield the final product water.

For the sweating experiments, the values of the HTM temperature and ramp were adjusted to the predetermined values dictated by the operating conditions of the sweating experiments (e.g. -7°C and 0.5°C/min, respectively). Based on the mass and the sampling time, the sweat fractions were collected into a number of vessels through a drain valve (see Fig (5.6) (e)). The sweat fractions were then taken for physiochemical analysis. On collection of the sweating fractions, the drain valve was set to the fully closed position, and then the HTM temperature and ramp were increased to 15°C and 0°C/min, respectively, for performing the partial melting process prior to conducting the final step, i.e. total melting.

(v) Total Melting Process

The total melting process takes place as soon as the water level in a collecting tank reached a predetermined limit (i.e. 10L). At this water level, the melt circulation pump can be operated without risk of pump damage, which might occur in running the pump dry. In practice, this was achieved by selecting the "Total Melting" button, and rapidly adjusting the pumping power ratio to 100%. However, the flow control valve was adjusted to reduce the flowing film inside a tube for a period of three minutes. This was done to gently disengage the large layers of ice crystals from the crystalliser's tube. This procedure prevents water leaking through the gap between funnel and lid, which might occurred from big splashes of water created by large chunks of ice falling from the tube into the collecting tank, when the pumping power ratio is set to 100% with the no bypass option applied. Following this, the flow control valve was adjusted to a position where the no bypass option is available, until the end of the total melting. When the temperature of the inlet feed, which is detected by means of a temperature indicator (TI-101) (see Fig (5.11))) had decreased to 15°C, the total melting process was then terminated by selecting the "Stand By" button followed by the "Off" button. The product, i.e. the melted ice crystals, was collected and taken for physiochemical analysis.

5.6 Results and Discussion

Due to the absence of design data in the literature, and the difficulty in predicting the performance of the Sulzer falling film crystallisation process for desalting and/or concentrating process brines, laboratory investigations were carried out. Experimental data were gathered and analysed to provide quantitative information on the separation performance of this technology for saline water applications, and more specifically for concentrating RO brines. Throughout the experimental investigations, no pre-treatment system or chemical additives were considered for use, either before or during the tests. For clarity, the HTM temperature of the crystallisation process is identified, and referred to, in the course of this chapter, as the crystallisation temperature.

A complete record of the phase diagram and the relationships between the key parameters, process data, temperature profiles, full physiochemical analysis, and performance parameters versus crystallisation and sweating times are given in Appendix 5, found on the CD attached to the thesis (see file name: Appendix, Microsoft Excel spreadsheet, Sheet: Appendix 5, Tables: A5-1 – A5-12).

The nucleation process for the experiments was explained previously in section 5.5.2. However, the operating procedures for the crystallisation experiments were varied from one experiment to another depending mainly on the crystallisation temperature. For instance, the crystallisation process takes place when the temperature of the outlet HTM (see Fig (5.11)) reached the freezing point of the feed, i.e. -3°C. However, this procedure was applied to the group of experiments where the crystallisation temperatures were above -10°C. For the group of experiments with crystallisation temperature below -10°C, the crystallisation process was rapidly started when the temperature of the outlet HTM reached -4°C. The reason was to ensure enough residence time to allow adequate heat removal for nucleating and forming ice on the surface of the crystalliser tube. This procedure also avoids damaging the ice formed at the beginning of the crystallisation process, leading to formation of an undesired ice suspension inside the collecting tank. For all tests, the duration of the nucleation process was about three minutes on average, which was found to be enough to accomplish nucleation and formation of ice crystals, before the crystallisation process was started. At the beginning of the crystallisation process, the settings of the pumping power ratio and tank heating power were adjusted to 85% and 20% respectively, for those experiments with a crystallisation

temperature above -10°C, whereas these settings were adjusted to 75% and 30% respectively, for those experiments with a crystallisation temperature below -10°C.

Variations in pumping power ratio settings were considered, so as to reduce the feed flow rate, and avoid dislodging the ice crystals formation on the crystalliser tube during the crystallisation process. Variations in the tank heating power were also considered, with the practical aim of eliminating ice suspension formation in the collecting tank during the crystallisation process. According to the experimental operating conditions, the settings of the melt circulation pump and flow control valve must be adjusted and optimised, in order to reduce the flowing film inside the tube, and increase turbulence inside the collecting tank (through a bypass pipeline), which helps eliminate the formation of ice suspension inside the collecting tank. However, high turbulences may reduce the performance of the melt circulation pump due to air bubbles, and makes monitoring the water level inside the collecting tank more difficult. The pumping power ratio and tank heating power were rapidly set to 85% and 20% respectively, for the majority of the tests. The flow control valve was then rapidly adjusted, whereby the bypass mode is operational to reduce the flow of the falling film, and so avoid dislodgment of the nucleated ice from the crystalliser tube; otherwise, an undesired ice suspension will form inside the collecting tank (see Fig (5.6) (f)).

Throughout the experiments, the formation of an ice suspension inside the collecting tank was eliminated by applying one of the following methods; (i) reducing the flow rate of the flowing film inside the crystalliser tube via the pumping power ratio setting. (ii) Reducing the flow rate of the flowing film inside the crystalliser tube by adjusting the flow control valve. (iii) Increasing the setting of the tank heating power through a "Tracing" box. This action helps warm the collecting tank in order to eliminate the formation of an ice suspension by melting. (iv) Increasing turbulence inside the collecting tank through use of a bypass valve (i.e. flow control valve). This can be accomplished by increasing the flow rate through the pumping power ratio setting, and simultaneously adjusting the bypass valve. (v) Decreasing the "Temperature" of "HTM Setting" box at low level; however, this procedure may be limited by the operating conditions of the experiment.

For the purpose of establishing a phase diagram for the tested feed materials, and instantly estimating the results of TDS and freezing point by means of electrical conductivity, the

parameters of salt concentration (measured in wt% and TDS), and freezing point, were measured experimentally over a wide range of electrical conductivity, ranging from 424 μS/cm up to 220 mS/cm. The variations of the experimental results of key parameters were plotted on graphs as shown in Fig (5.12). Based on the experimental results, the empirical polynomial correlations were derived and fitted for the freezing point as a function of TDS value (ppm), salt concentration (wt%), and electrical conductivity (mS/cm). Furthermore, the empirical polynomial correlations were also derived and fitted for the electrical conductivity (mS/cm) as a function of salt concentration (wt%). These equations were also used to instantly determine the results of the main key parameters through the conductivity measurement.

Fig (5.12) (a) – (b) show the experimental phase diagram, and empirical graphs and equations (including R value) for the Arabian Gulf seawater and RO brine. The important observations that can be revealed from the phase diagram are as follows: (i) the freezing points of Arabian Gulf seawater and RO brine were -2.4°C and -3.1°C respectively. (ii) the eutectic temperature for the Arabian Gulf seawater and RO brine was -20.45°C, which was obtained at weight ratio, TDS value and electrical conductivity of 23.85 wt%, 238,560 ppm and 220 mS/cm respectively.

Table (5.1) summarises the results of the major physiochemical characteristics of the tested feed samples i.e. Arabian Gulf seawater and RO brine. When the salt concentration and major ionic composition of Arabian Gulf seawater is compared to that in the RO brine (see Table (5.1)), a number of important observations can be revealed:

a) There was a clear difference in the salt concentration and the major ionic composition of the Arabian Gulf seawater when compared to RO brine.
b) RO brine was 1.25 times more highly concentrated than seawater. Thus, RO brine was more complicated than seawater, in terms of the challenge and difficulty for desalting this type of saline water.
c) The ions in RO brine were more highly concentrated than in the seawater. However, the seawater and RO brine both contained NaCl salts, which is by far the most dominant dissolved salt when compared to other salts. For instance, the

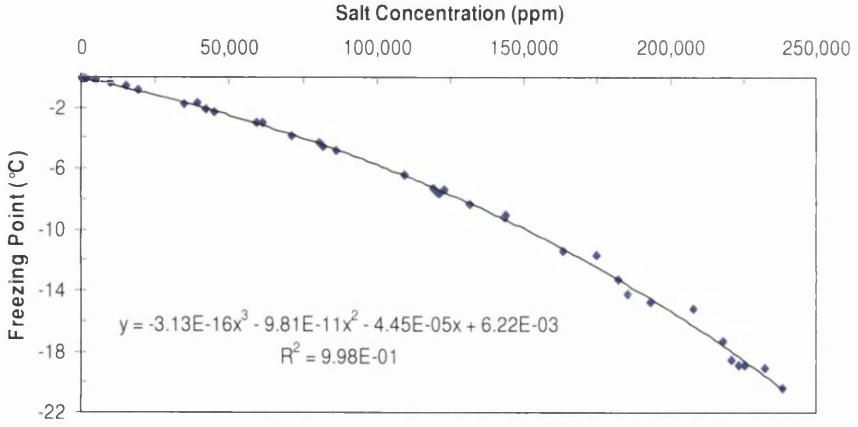

(a) Phase diagram

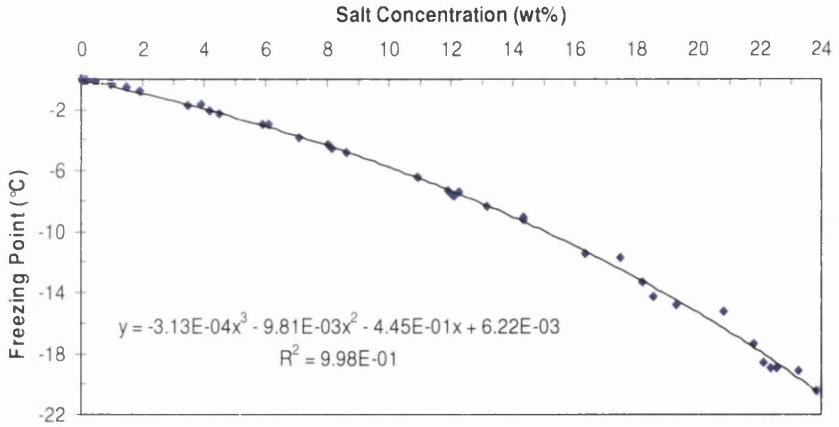

(b) Salt concentration vs. freezing point

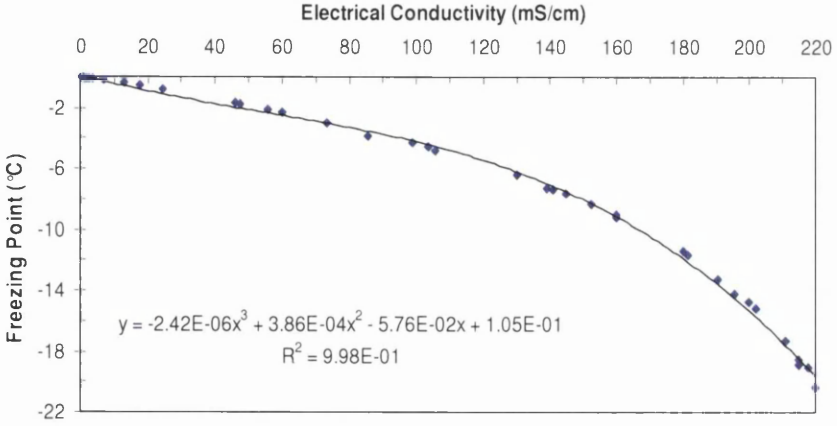

(c) Conductivity vs. freezing point

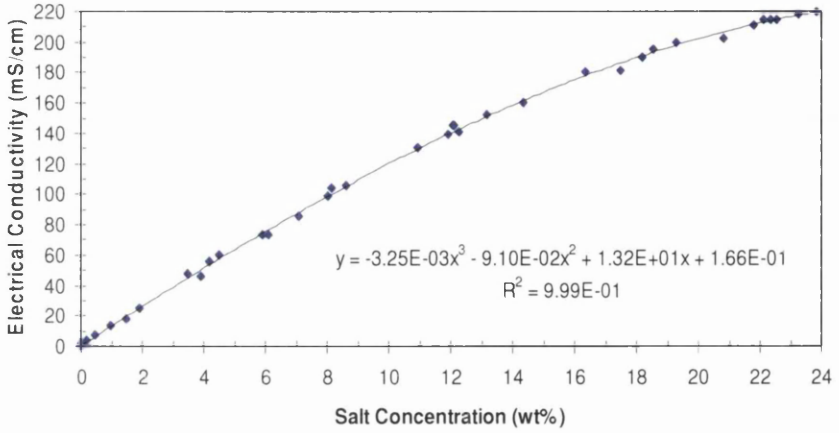

(d) Salt concentration vs. conductivity

Fig. 5.12: *Summary of the phase diagram and relationships between the main key parameters for the Arabian Gulf seawater and RO brine, where; y and x are the dependant and the independent variables of the empirical equation respectively, and R^2 is the polynomial regression correlation coefficient.*

seawater and RO brine contain about 85.6% and 86.7% of monovalent (Cl^-, Na^+) ions respectively, whereas the percentage of hardness ions (i.e. Ca^{2+}, Mg^{2+}, $(SO_4)^{2-}$, and $(HCO_3)^-$) were about 13.3% and 13.1% respectively.

d) For monovalent (Na^+, Cl^-) ions, the concentration of the Na^+ ion of seawater and RO brine reached 33.67% and 34.17% of the TDS respectively, whereas the concentration of the Cl^- ion of seawater and RO brine were 51.92% and 52.7% of the TDS respectively.

e) For the concentration of hardness ions, i.e. Ca^{2+}, Mg^{2+}, $(SO_4)^{2-}$, and $(HCO_3)^-$, in seawater and RO brine respectively: Ca^{2+} ion reached 2.2% and 2.4% of the TDS; Mg^{2+} ions were 2.2% and 2.4% of the TDS; $(SO_4)^{2-}$ ions were 7.95% and 7.86% of the TDS; and $(HCO_3)^-$ ions reached 0.36% and 0.39% of the TDS.

Parameters	Units	Water Samples	
		Arabian Gulf seawater	RO brine
Salt Concentration	(wt%)	4.91	6.11
Salt Concentration	(mg/L)	49,074	61,104
Electrical Conductivity	(mS/cm)	63.6	76.6
Freezing Point	(°C)	-2.52	-3.1
Ca^{2+}	(mg/L)	1,080	1,476
Mg^{2+}	(mg/L)	1,387	1,463
Na^+	(mg/L)	16,523	20,880
Cl^-	(mg/L)	25,480	32,200
$(HCO_3)^-$	(mg/l as $CaCO_3$)	175.6	241.2
$(SO_4)^{2-}$	(mg/L)	3,900	4,800

Table 5.1: *Summary of major physiochemical analysis of the tested water samples.*

5.6.1 Crystallisation experiments using feed stage (without the sweating process)

In the first series of experiments, the potential of the Sulzer falling film crystallisation process (without use of the sweating process) was investigated for concentrating and treating RO brine. These experiments were carried out in a feed stage process, i.e. single freezing stage. The influence of several parameters, namely crystallisation temperature and time, cooling rate, feed concentration, and average growth rate on the salt rejection and water recovery ratios was examined. The actual operating period of the crystallisation process in

the experiments was varied from 23.3 to 120 minutes. The crystallisation experiments were carried out at different operating HTM temperatures, ranging from -6°C down to – 28.4°C, at various HTM cooling rates varied from 0 to -0.75°C/min. These experiments were carried out at maximum water recovery ratio, which was dictated when the water level in the collecting tank reached the minimum allowed limit, i.e. 5L. A complete record of the temperature profiles for these experiments is given in Appendix 5 (see file name: Appendix_5_A5-1).

Results of salt concentration of product, salt rejection, water recovery, and crystallisation time as a function of the end-point cooling HTM temperature and rate are shown in Figs (5.13) (a) – (e).

Fig (5.13) (a) shows the variation of the salt concentration of product water, as a function of the end-point cooling HTM temperature at different cooling rates. A clear tendency of decreasing salt concentration in the product water with rising end-point crystallisation temperature and cooling rate can be observed. The results indicate that the adopted process is sensitive to the variations of end-point cooling HTM temperature from -6 to -18°C as shown in Fig (5.13) (a). However, no significant change in the salt concentration of product water was observed when the end-point cooling HTM temperature was reduced from -18°C down to -28.4°C, where the product concentration stabilised at an average value of 4.5 wt% as shown in Fig (5.13) (a). This indicates that the tested pilot plant, at lower operating temperature and cooling rate limits, was capable of providing product water at lower salt concentration than that of seawater, as shown in Fig (5.13) (a). This means that the tested process becomes insensitive to the end-point cooling HTM temperature and cooling rate as long as the desired product concentration is closer to the RO feed. Also, Fig (5.13) (a) shows that the maximum and minimum salt concentration of product water sample was 4.61 and 2.65 wt% respectively. This means that the salt concentration of product water measured is lower than the salt concentration of RO feed (see Fig (5.13) (a)) at all times, as indicated in Fig (5.13) (a). The behaviour of the treatment system for the given conditions was insensitive to a wider range of crystallisation temperatures when the desired quality of product water is equal to that of RO feed. The results suggested that the commercial plant using the adopted crystalliser can be technically designed and built with a wider range of crystallisation

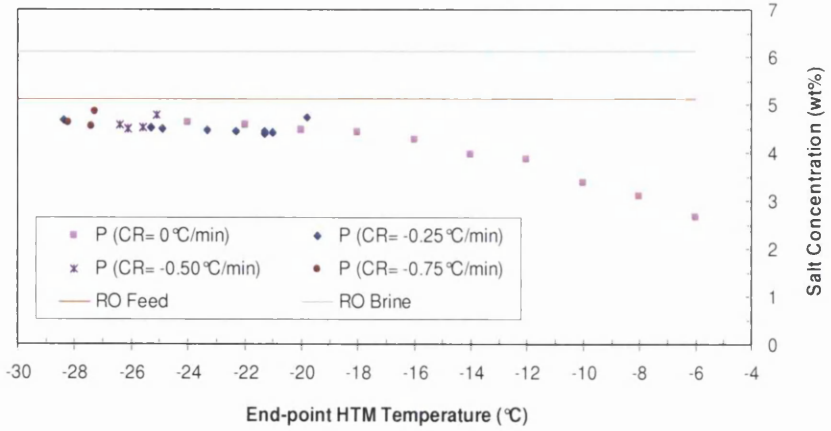

(a) Product concentration vs. operating HTM temperature

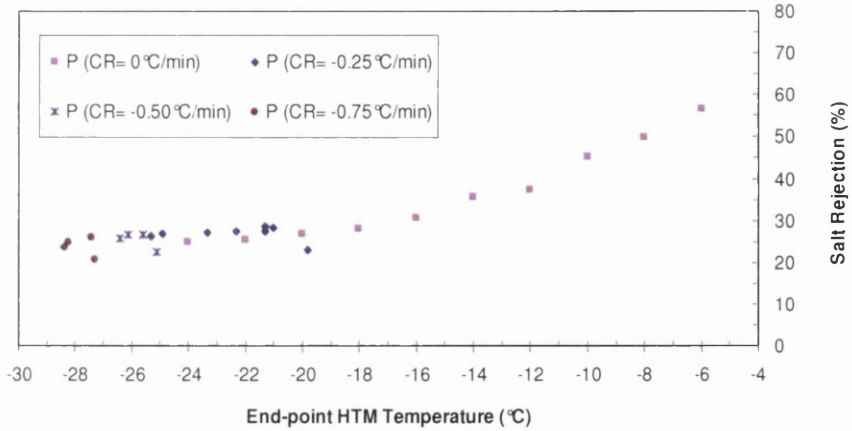

(b) Salt rejection vs. operating HTM temperature

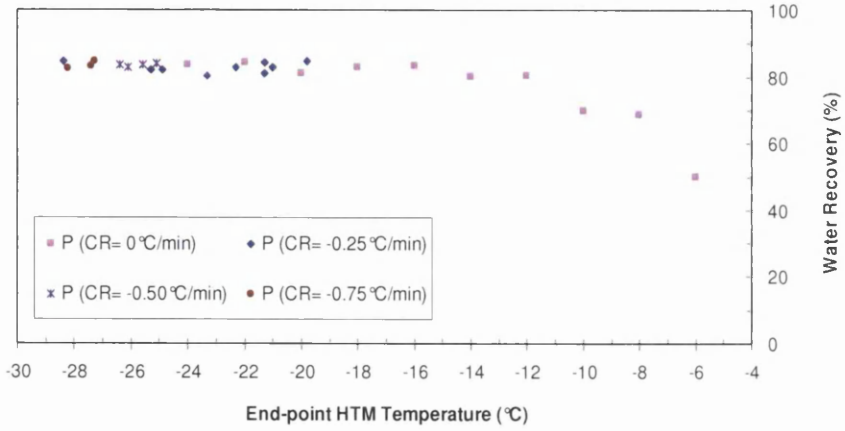

(c) Water recovery vs. operating HTM temperature

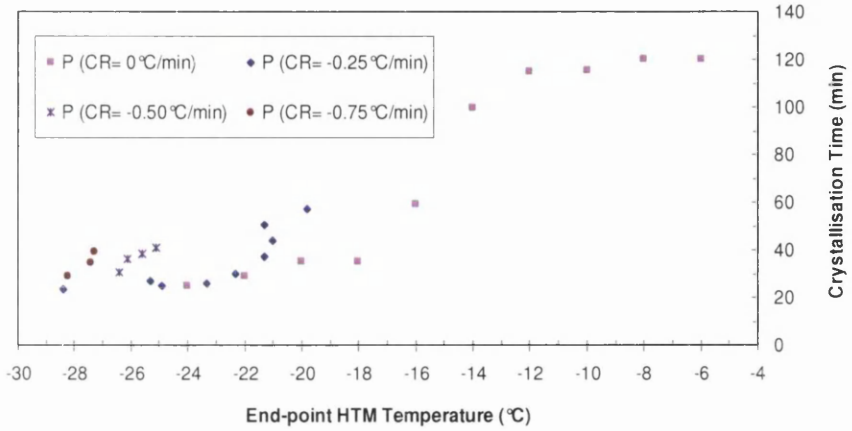

(d) Crystallisation time vs. operating HTM temperature

Fig. 5.13: *Performance of feed stage using Sulzer falling film crystallisation (without the sweating process) for treating RO brine, where; P is the product water, CR is the cooling rate, and HTM is the heat transfer medium.*

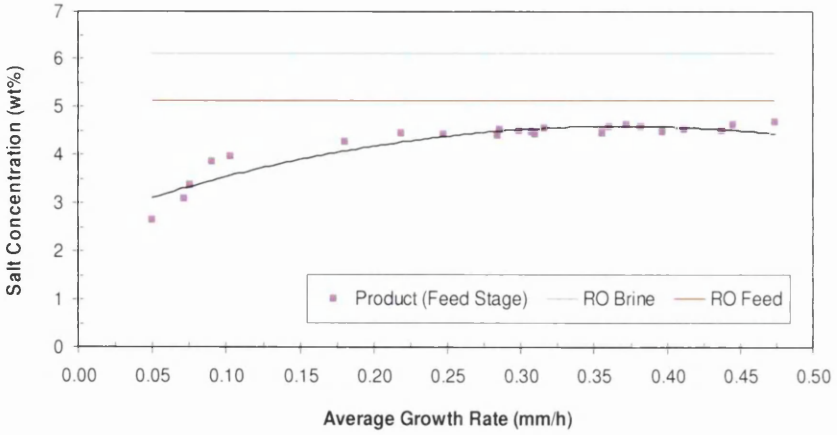

(e) Growth rate vs. product concentration

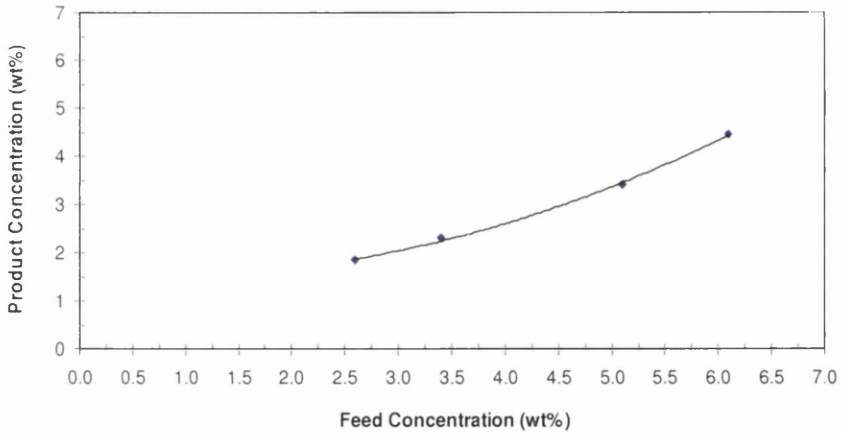

(f) Influence of feed concentration on separation performance

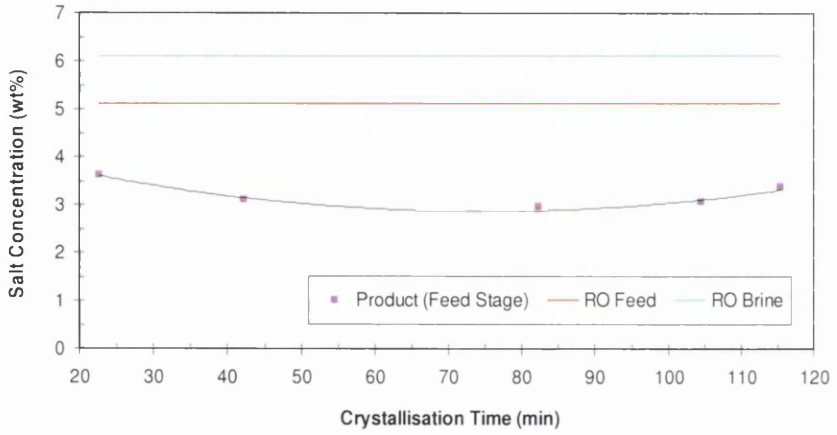

(g) Crystallisation time vs. product concentration (tested at HTM temperature of -10°C)

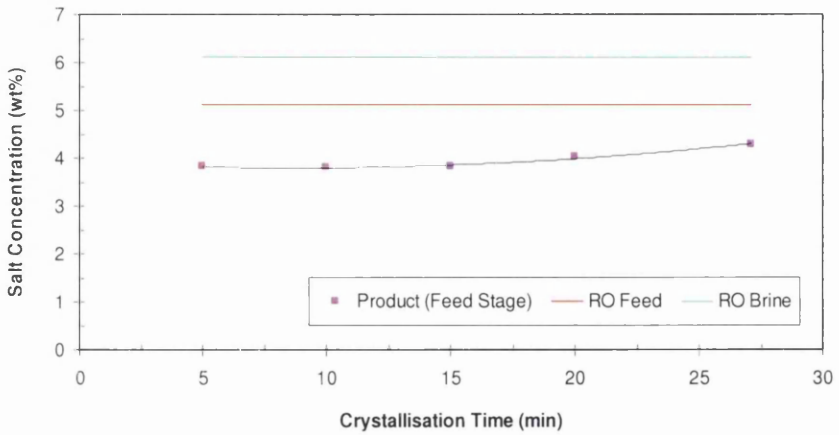

(h) Crystallisation time vs. product concentration (tested at HTM temperature of -20°C)

Fig. 5.13: *(Cont'd.)*

temperatures and cooling rates for RO brine concentrations. This includes lower operating limits to produce a substantial amount of the desired quality of product water (i.e. RO feed quality), leading eventually to a significant decrease in the capital costs. However, designing commercial plants with lower crystallisation temperatures might be limited by a significant increase in the power consumption. Thus, the capital and operational costs must be optimised prior to that, in terms of the final decision on plant capacities and conditions, including crystallisation temperature and cooling rate. In general, the crystallisation experiments, which were carried out under different ranges of crystallisation temperature and cooling rate, suggested that the adopted technology is feasible for concentrating RO brines and simultaneously producing saline water of near seawater salt levels that can be recycled to a conventional desalination plant.

Fig (5.13) (b) shows the effect of the end-point cooling HTM temperature with different cooling rates on salt rejection ratio. The influence of end-point cooling HTM temperature on the salt rejection is similar to that observed for product concentration, since the results depend mainly on the feed and product concentrations. The salt rejection ratio is proportional to the end-point cooling HTM temperature and cooling rate of HTM, as shown in Figs (5.13) (b). The maximum and minimum salt rejection ratios were 56.6% and 24.5% respectively, achieved at operating end-point HTM temperatures of -6 and -24°C respectively. These results were obtained at a cooling rate of 0°C/min. For experiments with lower cooling rates, there was no significant change in the salt concentration of product water observed, and the averaged value of the salt rejection was 25%, as shown in Fig (5.13) (b).

Fig (5.13) (c) shows the influence of end-point cooling HTM temperature with different cooling rates on the water recovery ratio. The water recovery ratios were found to be inversely proportional to the end-point cooling HTM temperature and cooling rate. The minimum and maximum water recovery ratios were 49.8% and 84.6% respectively, achieved at operating end-point HTM temperatures of -6 and -24°C respectively. The calculations of the maximum water recovery ratio for RO feed quality product water gave about 92%, which, in practice, can be obtained easily through the tested pilot plant. This is because the tested crystalliser is capable of producing a crystal layer with a maximum volume of 46L (exceeding the total volume of collecting tank), when the crystalliser is completely filled with cylindrical ice. Nevertheless, the specified theoretical value of maximum water recovery

ratio was not reached throughout the experiments, because the melt circulation pump would be exposed to a high risk of damage as the collecting tank would be almost empty for such operating conditions. In general, the water recovery results give a clear indication that the pilot plant, involving a single freezing stage, was capable of concentrating the RO brine and simultaneously producing a substantial amount of final product water of near seawater concentration, which can be recycled to join the feed stream and then easily desalted through a RO membranes desalination plant.

Fig (5.13) (d) shows plots of the end-point cooling HTM temperature versus the actual operating time of the crystallisation process. As expected, the running time of the crystallisation process can be substantially reduced by decreasing the end-point cooling HTM temperature and cooling rate. This means that the production rate can be substantially increased by the end-point cooling HTM temperature and/or cooling rate.

Within the studied domain, the results of average growth rates were also considered and analytically computed, by assuming the dimensions and shape of solid layer ice to be cylindrical. The average growth rate is controlled by the crystallisation temperature and cooling rate. Fig (5.13) (e) shows the variation of product water salt concentration, as a function of the average growth rate. The average growth rate also has a strong influence on the quality of product water, in terms of salinity, where this parameter was found to be effective in removing significant amounts of dissolved salt from RO brine over a single stage of layer growth. For instance, the salt concentrations of product water were reduced from 4.44 wt% to 2.65 wt% when the average growth rate decreased from 0.22 mm/h to 0.05 mm/h. These results showed that the adopted process is sensitive to variations in growth rate. However, there was no significant change in the salt concentration of product water observed, as the average growth rate varied from 0.22 to 0.47 mm/h, as shown in Fig (5.13) (e).

In the second series of experiments, the influence of feed concentration on the performance of the adopted technology was investigated. These experiments were carried out in a feed stage process with four different salt concentrations of RO brine ranging from 2.6 wt% to 6.1 wt%. The crystallisation experiments were carried out at maximum water recovery ratio, HTM temperature of – 16°C and cooling rate of 0°C/min respectively. The actual operating

period of the crystallisation process in the experiments varied from 0.53 to 1.33 h. A complete record of the temperature profiles for these experiments is given in Appendix 5. A summary of the experimental results is given in Fig (5.13) (f), which shows the influence of feed concentration on the quality of product water, in terms of salt concentration. Agreement with the experimental results, which were given in Chapter 4, is clearly observed. The quality of product water, in terms of salinity, is proportional to the feed salt concentration as shown in Figs (5.13) (f). The lower feed concentration can significantly decrease the salt concentration of product water, resulting in improvement in the separation performance of the pilot plant. For instance, Fig (5.13) (f) shows that the salt concentrations of feed samples fed individually to the tested pilot plant are 2.6%, 3.4%, 5.1% and 6.1%. The results showed that the falling film crystallisation process was capable of reducing the salt concentrations of product water down to an average of 1.84%, 2.3%, 3.4% and 4.45%, for the same feed samples respectively.

The third series of the crystallisation experiments were carried out at end-point crystallisation temperatures of -10 and -20°C, whereas the cooling rates for these tests were set at a constant value of 0 °C/min. These tests were performed to detect and monitor the behaviour of the salt concentration of the product water for different crystallisation times. For the tests with an end-point crystallisation temperature of -10°C, five tests were conducted at various crystallisation times, which varied from 22.58 to 115.53 minutes. For the tests with an end-point crystallisation temperature of -20°C, five experiments were carried out at various crystallisation times ranging from 5 to 27.10 minutes. A complete record of the temperature profiles for these experiments is given in Appendix 5. Figs (5.13) (g) and (h) show a comparison between the salt rejection results, versus crystallisation time. For the tests with HTM temperatures of -10°C, the salt concentration of product water varied according to the crystallisation time. The maximum and minimum salt concentration values of product water were 3.63 wt% and 2.95 wt% respectively. These results were achieved at crystallisation times of 22.6 and 82.4 min respectively, as shown in Fig (5.13) (g). For the tests with HTM temperatures of -20°C, the salt concentration of product water varied slightly according to the crystallisation time, where the maximum and minimum salt concentration values of product water were 4.29 wt% and 3.83 wt% respectively. These results were obtained at crystallisation times of 5.0 and 4.3 min respectively, as shown in Fig (5.13) (h). By comparing Fig (5.13) (g) to Fig (5.13) (h), a clear tendency of decreasing product water salt

concentration with lower end-point crystallisation temperature can be observed, which confirmed the previous observations on the influence of crystallisation temperature on the product quality presented in Fig (5.13) (a). Furthermore, the trend in the results for salt concentration of the product water versus the average growth rate, as given in Appendix 5 (A5-10), is in agreement with the experimental data presented in Fig (5.13) (e).

For the design of commercial plants, the recommended crystallisation temperatures range from -12°C to -16°C when the cooling rate is set to 0°C/min, whereas the recommended crystallisation temperature should not be higher than -12°C when the cooling rate is set to below 0°C/min. Commercial plants with higher crystallisation temperatures (i.e. > -12°C) would require careful operation, and close monitoring to nucleate and form ice crystals that can be adhered to the crystalliser at the beginning of the crystallisation operation. Otherwise, several limitations might be encountered leading to an ice suspension forming inside the collecting vessel, while plants with lower operating temperatures (i.e. < -16°C) would be expected to be limited by operational cost.

5.6.2 Multi-stage process (feed and rectification stages) without the sweating process

In the fourth series of experiments, the influence of a multi-stage process, using the Sulzer falling film crystallisation process, on the degree of water desalination, in terms of salt rejection, water recovery, and ionic rejection, was investigated. A feed sample of RO brine was treated using two successive freezing stages, namely feed and rectification stages. The experiments were carried out at the maximum water recovery ratio. The crystallisation temperature and ramp of the feed and rectification stages were set to -16°C and 0 °C/min respectively. The actual operational periods of the feed and rectification stages were 0.83 h and 0.37 h respectively. A summary of the experimental and water chemistry data for the water samples of each freezing stage is given in Tables (5.2) – (5.4). A complete record of the temperature profiles for these experiments is given in Appendix A5.

Table (5.2) shows that the feed and rectification stages were able to lower the TDS value of the RO brine from 61,104 ppm to 32,451 ppm. Table (5.2) shows that the TDS value of the product water from each stage was 44,512 and 32,451 ppm respectively. Thus the residual liquids, which were rejected from the feed and rectification stages, were concentrated with average TDS values of 147,840 and 95,258 ppm, respectively. The salt rejection ratios for

Stage	Water Sample	Parameters	Unit	Value
Feed Stage	Feed Water	Mass	(kg)	29.174
		TDS	(ppm)	61,104
	Product Water	Mass	(kg)	24.555
		TDS	(ppm)	44,512
	Residual Liquid	Mass	(kg)	4.619
		TDS	(ppm)	147,840
Rectification Stage	Feed Water	Mass	(kg)	24.555
		TDS	(ppm)	44,512
	Product Water	Mass	(kg)	18.740
		TDS	(ppm)	32,451
	Residual Liquid	Mass	(kg)	4.152
		TDS	(ppm)	95,258

Table 5.2: *Summary of the performance data for the feed and rectification stages.*

Stage	Water Sample	Parameters	Unit	Value
Overall	Feed Water	Mass	(kg)	29.174
		TDS	(ppm)	61,104
	Product Water	Mass	(kg)	18.740
		TDS	(ppm)	32,451
	Residual Liquid	Mass	(kg)	10.434
		TDS	(ppm)	112,566

Table 5.3: *Overall data for the performance data for the feed and rectification stages.*

Parameter	Unit	Feed Stage			Rectification Stage			Total Residue*
		Feed	Product	Residue	Feed	Product	Residue	
pH	-	7.41	7.18	7.24	7.18	7.16	7.19	7.19 – 7.24
TDS	(mg/L)	61,104	44,512	147,840	44,512	32,451	95,258	112,566
Conductivity	(mS/cm)	76.6	55.1	165.1	55.1	39.5	117.1	134.8
Ca^{2+}	(mg/L)	1,476	920	4,760	920	656	2,112	2,948
Mg^{2+}	(mg/L)	1,463	877	3,717	877	419	3,051	2,860
Na^{+}	(mg/L)	20,881	15,628	56,481	15,628	12,126	34,174	38,602
Cl^{-}	(mg/L)	32,200	24,100	87,100	24,100	18,700	52,700	59,529
$(HCO_3)^{-}$	(mg/L) as Ca CO_3	241.2	170.3	450.2	170.3	168.2	300.9	319.0
$(SO_4)^{2-}$	(mg/L)	4,800	3,200	12,000	3,200	2,360	8,900	8,854
NO_3^{-}	(mg/L)	2.0	1.7	3.3	1.7	1.1	4.6	3.29

Table 5.4: *Major physiochemical analysis of water samples for the feed and rectification stages without use of a sweating process for treating RO brine.*

the feed and rectification stages were 27.2 and 27.1%, respectively, whilst the water recovery ratios were 84.17 and 81.86 %, for the same freezing stages respectively. Table (5.3) shows that the overall salt rejection and product water recovery ratios were 46.89% and 64.24%, respectively.

Table (5.4) shows the ionic composition of water samples of all the streams in the process. The results showed that the multi-stage process using the crystallisation process did not produce a final product reaching brackish water standards. Therefore, a post-treatment crystallisation process must be considered, when a high purity product water is required.

5.6.3 Crystallisation and sweating experiments using feed stage

In the fifth group of experiments, the potential of the adopted technology, using crystallisation and sweating processes, was investigated for desalting and concentrating RO brine. These experiments were carried out in a feed stage process, and were performed at the maximum water recovery ratio. The tested salt concentrations of feed ranged from 2.6 to 6.1 wt%. The crystallisation temperature and ramp for the experiments were -16°C and 0 °C/min respectively, whereas the sweating experiments were carried out using a start-point HTM temperature of -16°C and sweating ramp of 0.5°C/min. A complete record of the temperature profiles for these experiments is given in Appendix A5. For clarity, the sweating time is identified and referred to, in the course of this chapter, as time elapsed from increasing the temperature of the crystalliser until the end of collecting the last sample of sweating fractions. The crystal mass ratio is analytically computed by dividing the extracted mass of sweating fraction to the original mass of the product water, i.e. the mass of product before performing the sweating process.

In Figs (5.14) (a) and (b) the influence of salt concentration of feed water on the quality of product water is shown. The crystalline impurities were found to increase with increasing feed concentration, and to decrease with increasing crystal mass ratio and sweating times. For instance, for desalting the RO brine, the concentration of crystals was reduced from 4.31 wt% to 3.32 wt% after carrying out the sweating process at a mass crystal ratio of 17.19% and sweating time of 26.40 min. In the case of desalting Arabian Gulf seawater, Figs (5.14) (a) and (b) show that the salt concentration of crystals was reduced from 3.33 wt% to 2.64

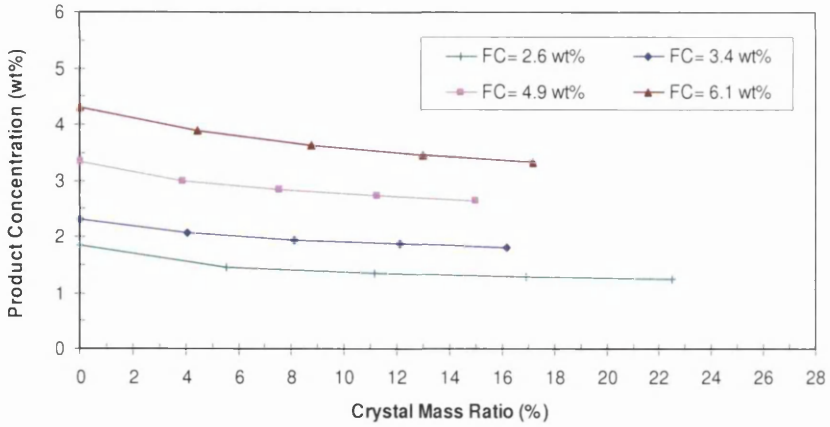

(a) Crystal mass ratio vs. product concentration (at different FC)

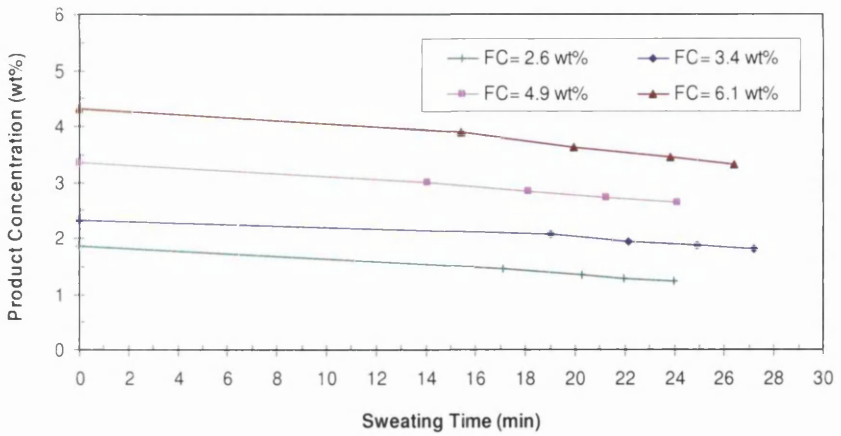

(b) Sweating time vs. product concentration (at different FC)

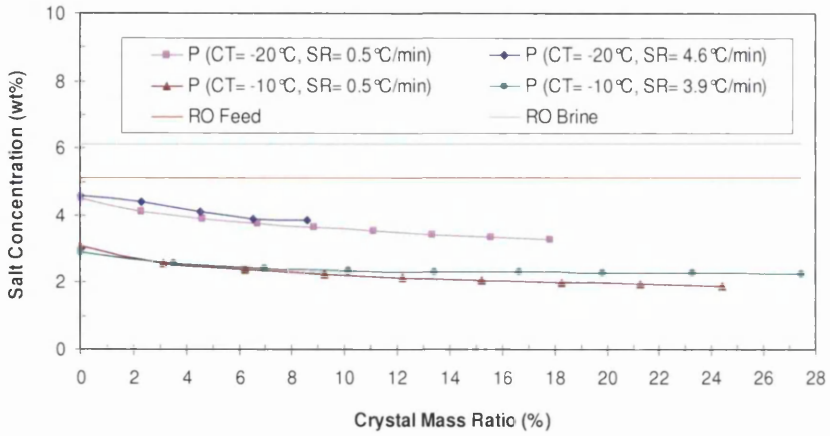

(c) Crystal mass ratio vs. product concentration (at different CT & SR)

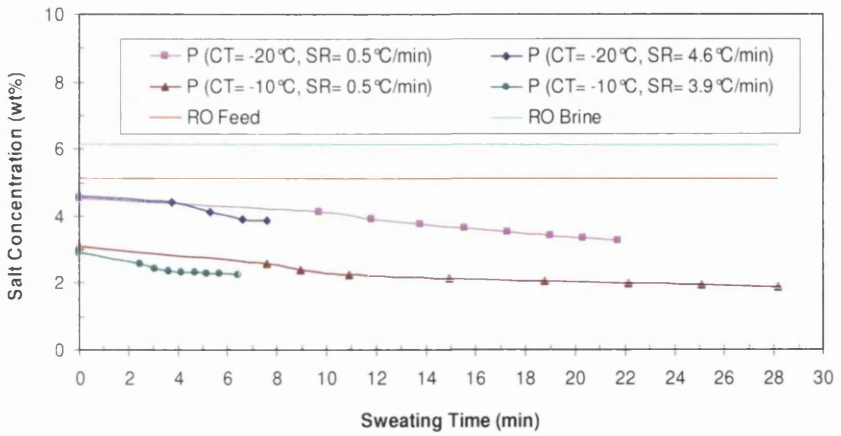

(d) Sweating time vs. product concentration (at different CT & SR)

Fig. 5.14: *Performance of feed stage using Sulzer falling film crystallisation (with sweating) process for treating RO brine, where; FC is the feed concentration, P is the product water, CR is the cooling rate, and CT is the HTM temperature of the crystallisation process.*

wt% after carrying out the sweating process at a mass crystal ratio and sweating time of 15% and 24.13 min respectively.

In general, the variation in the behaviour of the product concentration versus the mass crystal ratio represents a reflection of the sweating efficiency. At the beginning of sweating operation where the first sweat fraction was taken, a dramatic fall in the product concentration can be observed as shown in Figs (5.14) (a) and (b). This was due to the remaining impure melt, adhered to the surface of the crystal layer, being removed efficiently by the initial sweating step. As the sweating continued, a slight decrease in the product concentration was observed, because the impurities were further inside the crystalline slab, and effectively trapped and occluded. Therefore, further sweating would be a progressive melting process for the remaining crystalline mass, which corresponds to a poor sweating efficiency. This procedure must also take into account that the product lost (i.e. mass crystal ratio) should be within an average of 10% [Ulrich and Glade, 2003]. Although the sweating time can be varied from 10 min to 30 h, the sweating operation should be performed at the shortest retention time possible (about one-third of a crystallisation process); otherwise, the production rate will dramatically decline [Ulrich and Glade, 2003]. The production rate is a crucial factor for desalination applications. The production rate will be negatively affected by the sweating process because of the product loss, and an increase in the time retention of the freezing stage. From an economic point of view, the reduced amount of product water due to the sweating step for the rise in purity was not worthwhile for the purpose of desalination, as the pilot plant with sweating process did not produce a final product water suitable for human consumption.

For the cases of operating the pilot plant without sweating, the HTM temperature and cooling rate of the partial melting process were usually set to 15 °C and 0 °C/min. This procedure was applied to accelerate the process of partially melting the crystalline mass in order to recover enough product water, which enables the user to run the pump during the total melting process, to yield the final product water. These operating conditions were also considered in the subsequent sweating experiments, in order to carry out the sweating process in the fastest possible way, and also determine the trend for crystalline impurity, as a function of the crystal mass ratio and sweating times under these operating conditions.

Therefore, the sixth group of experiments was carried out with feed samples using RO brine to investigate the affect of the sweating rate on the salt concentration of product water. The experiments were carried out at maximum water recovery ratio. These experiments were also performed in a feed stage process, which was examined at crystallisation temperatures of -10 and -20°C. The crystalline impurity content was measured at different sweating rates ranging from 0.5 to 4.6 °C/min.

Figs (5.14) (c) and (d) show the variation of product water salt concentration, as a function of the crystal mass ratio and sweating time at different crystallisation temperatures and sweating rates. The salt concentration of product water increases with decreasing crystallisation temperature, as observed previously in different experiments. For the experiments with a crystallisation temperature of -20 °C and sweating rate of 0.5 °C/min, the salt concentration of product water was reduced from 4.6 to 3.27 wt% when the crystal mass ratio increased from 0 % to 17.85 % (see Figs (5.14) (c)). For the experiments with a crystallisation temperature of -20 °C and sweating rate of 4.6 °C/min, the salt concentration of product water was reduced from 4.6 to 3.83 wt%, when the crystal mass ratio increased from 0 % to 8.60% (see Figs (5.14) (c)). When the crystal mass ratio reached 8.60%, the sweating process could not be continued, because the remaining crystal mass inside the crystalliser tube was dislodged, and fell into the collecting vessel. This experiment was repeated several times and the same behaviour was observed, indicating that the maximum crystal mass ratio could not exceed 8.60%. For the experiments with a crystallisation temperature of -10 °C and sweating rate of 0.5 °C/min, the salt concentration of product water was reduced from 2.89 to 1.86 wt%, when the crystal mass ratio increased from 0% to 24.41% (see Figs (5.14) (c)). For the experiments with a crystallisation temperature of -10 °C and sweating rate of 3.9 °C/min, the salt concentration of product water was deceased from 2.89 wt% to 2.38 wt%, when the crystal mass ratio varied from 0 % to 27.50% (see Figs (5.14) (c)). The remaining crystal mass was not dislodged from the crystalliser tube as seen in the previous experiments at -20 °C. The experimental results proved that lowering sweating rate can slightly reduce the product concentration. This gives clear evidence that the performance of the adopted technology cannot produce a final product of near drinking water at a reasonable production rate. Figs (5.14) (d) shows that the sweating time was significantly reduced by increasing the sweating rate. For instance, the sweating time was reduced from 21.73 min to 7.62 min when the sweating rate was changed from 0.5 to 4.6 °C/min. From an economic point of view, the

product concentration was not significantly changed by changing the sweating rate, indicating that the user can carry out the sweating process in the fastest possible way to reduce the time retention of the freezing stage, if the sweating process is essential for such an application.

5.6.4 *Multi-stage processing (feed, rectification, and stripping stages) with a sweating procedure for treating RO brine*

The purpose of the seventh series of experiments was to evaluate the performance of a multi-stage process, using falling film crystallisation and sweating processes, for desalting and concentrating RO brine. The multi-stage process consisted of three successive freezing stages, i.e. feed, rectification, and stripping stages, and was operated at the maximum water recovery ratio. The experiments determined the performance of each freezing stage, with respect to the salt concentration of product water and ionic rejection. The crystallisation temperature and ramp for the feed and rectification stages were -16°C and 0 °C/min respectively, whereas the sweating steps were carried out at a start-point HTM temperature and sweating ramp of -16°C and 0.5°C/min respectively. A complete record of the temperature profiles for these experiments is given in Appendix A5. The stripping stage was initially tested with a crystallisation temperature of -22°C (see run 80 in Table A5-3 in Appendix 5); however, the test was terminated at the beginning of the crystallisation operation, because of the collapse of the nucleated ice from the crystalliser tube, which led to a substantial amount of undesired ice suspension inside the collecting tank. This is because the initial crystal layer adhering like an encrustation on the cooled surfaces of the crystalliser tends to be porous, with a sponge-like structure, since the crystal layer was contained substantial amounts of impurities. This type of crystal layer tends to be weak in structure and does not stick well to the cooled surface of crystalliser, and cannot resist the incoming flow of circulated melt, which flows as a falling film. To prevent this problem, the stripping stage requires a well-controlled driving force and flow rate. Therefore, the experiment for the stripping stage was carried out with the crystallisation temperature and ramp at -26°C and 0 °C/min respectively; furthermore, the flow rate of melt circulation pump was reduced at the beginning of the crystallisation operation for 5 min, and then increased to the optimum flow rate. In general, the crystallisation operation of the stripping stage needs intensive monitoring to avoid the appearance of an ice suspension inside the collecting vessel. The sweating steps were carried out at a start-point HTM temperature of -26°C and sweating ramp of 0.5°C/min. The actual operational period of the crystallisation process for the feed, rectification, and

stripping stages were 0.87, 0.75, and 0.56 h respectively, whereas the actual operational periods of the sweating process were 0.6, 0.45, and 0.47 h, for the same freezing stages respectively. The amount of feed used each time was approximately 30 kg, so the experiments for the feed stage were individually repeated 6 times to collect the water samples for physiochemical analysis, and also to collect enough feed water for the rectification and stripping stages, which were performed only one time to produce the final product water.

A summary of the performance data for the multi-stage process and physiochemical analysis for the water samples of each freezing stage is given in Tables (5.5) and (5.6). Furthermore, the salt concentration of product water, water recovery ratio, and salt rejection ratio for each freezing stage is shown in Fig (5.15).

Table (5.5) shows that the average TDS value of the brine fed to the feed stage, rectification, and stripping stages were 61,104, 33,701, and 141,974 ppm, whereas these freezing stages were capable of lowering the feed waters down to 33,701, 17,913, and 113,787 ppm respectively. The calculations of the salt rejection ratios give 44.84, 46.85, and 19.85%, for the same freezing stages respectively. The overall results proved that the tested technology was capable of reducing the TDS value of RO brine from 61,104 ppm down to 17,913 ppm over two successive freezing stages (see Table (5.5)). The calculation of the overall salt rejection ratio for these stages was 70.68%. The results clearly indicate that the salt rejection ratio was improved by adding one more freezing stage (i.e. rectification stage); as a result, the salt rejection ratio is proportional to the number of freezing stages. The calculations of the water recovery ratios were 69.85, 71.79, and 69.72%, for the same freezing stages respectively. The water recovery ratios for the freezing stages were approximately the same, because the crystallisation processes for these freezing stages were performed at the same and maximum ratios. The calculation of the overall water recovery ratio gives 50.15%. The experimental results clearly indicate that the water recovery ratio declined from 69.85% down to 50.15% by adding a rectification stage. This indicates that the water recovery ratio is inversely proportional to the number of freezing stages.

Table (5.5) shows that the TDS values of the residual liquid of the feed, rectification and stripping stages were 124,576, 73,886 and 218,033 ppm respectively. The residual liquid of

Stage	Water Sample	Parameters	Unit	Value
Feed Stage	Feed Water	Mass	(kg)	30.931
		TDS	(ppm)	61,104
	Product Water	Mass	(kg)	21.604
		TDS	(ppm)	33,701
	Residual Water*	Mass	(kg)	9.327
		TDS	(ppm)	124,576
Rectification Stage	Feed Water	Mass	(kg)	30.827
		TDS	(ppm)	33,701
	Product Water	Mass	(kg)	22.132
		TDS	(ppm)	17,913
	Residual Water*	Mass	(kg)	8.695
		TDS	(ppm)	73,886
Stripping Stage	Feed Water	Mass	(kg)	27.648
		TDS	(ppm)	141,974
	Product Water	Mass	(kg)	19.276
		TDS	(ppm)	113,787
	Residual Water*	Mass	(kg)	8.372
		TDS	(ppm)	218,033

Table 5.5: *Summary of the performance data for the feed, rectification, and stripping stages.* * *Residual liquid includes the overall results of the actual residual liquid and sweat fractions.*

Parameter	Unit	Feed Stage							Total Residue
		Feed	Product	Residue	Fraction (1)	Fraction (2)	Fraction (3)	Fraction (4)	
pH	-	7.41	7.17	7.39	7.35	7.50	7.49	7.48	7.35 - 7.50
TDS	(mg/L)	61,104	33,701	145,393	130,368	93,503	77,988	64,409	124,576
Conductivity	(mS/cm)	76.6	41.1	163.2	150.9	115.2	97.5	80.8	145.8
Ca^{2+}	(mg/L)	1,476	1,008	4,288	3,308	2,080	1,632	1,296	3,244
Mg^{2+}	(mg/L)	1,463	909	3,076	2,304	2,075	2,044	1,657	2,576
Na^{+}	(mg/L)	20,881	13,164	47,403	41,567	27,819	23,410	16,082	37,877
Cl^{-}	(mg/L)	32,200	20,300	73,100	64,100	42,900	36,100	24,800	58,410
$(HCO_3)^{-}$	(mg/L) as Ca CO_3	241.2	153.4	498.6	452.4	312.8	256.4	201.2	407.6
$(SO_4)^{2-}$	(mg/L)	4,800	3,200	12,150	9,640	7,270	6,560	6,710	9,970
NO_3^{-}	(mg/L)	2.0	2.0	3.1	3.1	2.8	2.6	2.2	2.9

Table 5.6: *Major physiochemical analysis of water samples for the feed, rectification, and stripping stages with use of sweating process for treating RO brine.*

Parameter	Unit	Rectification Stage							Total Residue
		Feed	Product	Residue	Fraction (1)	Fraction (2)	Fraction (3)	Fraction (4)	
pH	-	7.17	7.00	7.20	7.25	7.28	7.20	7.19	7.00 - 7.28
TDS	(mg/L)	33,701	17,913	97,880	73,917	46,814	38,202	31,746	73,886
Conductivity	(mS/cm)	41.1	21.4	119.9	92.6	58.1	46.9	38.6	92.4
Ca^{2+}	(mg/L)	1,008	498	2,160	1,640	1,040	800	636	1,605
Mg^{2+}	(mg/L)	909	521	2,109	2,070	928	753	682	1,618
Na^{+}	(mg/L)	13,164	8,041	32,423	30,543	16,795	14,007	13,034	25,638
Cl^{-}	(mg/L)	20,300	12,400	50,000	47,100	25,900	21,600	20,100	39,536
$(HCO_3)^{-}$	(mg/L) as Ca CO_3	153.4	120.2	320.0	259.3	180.3	160.2	150.2	255
$(SO_4)^{2-}$	(mg/L)	3,200	1,260	7,000	6,000	3,200	3,000	1,580	5,254
NO_3^{-}	(mg/L)	2.0	1.1	2.8	2.3	2.1	1.9	1.6	2.4

Table 5.6: *(Cont'd.)*

Parameter	Unit	Stripping Stage						Total Residue
		Feed	Product	Residue	Fraction (1)	Fraction (2)	Fraction (3)	
pH	-	7.39	7.60	7.15	7.20	7.28	7.40	7.15 - 7.40
TDS	(mg/L)	145,393	113,787	217,482	212,038	198,966	177,876	218,033
Conductivity	(mS/cm)	163.2	135.9	210.0	207.0	199.5	186.4	210.3
Ca^{2+}	(mg/L)	4,288	3,230	4,716	4,660	4,456	4,436	4,632
Mg^{2+}	(mg/L)	3,076	1021	1,419	1,389	1,300	1,264	1,376
Na^{+}	(mg/L)	47,403	38,908	78,464	72,628	64,846	56,416	72,648
Cl^{-}	(mg/L)	73,100	60,000	121,000	112,000	100,000	87,000	112,032
$(HCO_3)^{-}$	(mg/L) as Ca CO_3	498.6	350.3	520.2	500.3	497.5	460.6	505.9
$(SO_4)^{2-}$	(mg/L)	12,150	9,360	15,900	16,120	14,780	13,800	15,484
NO_3^{-}	(mg/L)	3.1	2.2	5.1	4.8	4.5	3.3	4.7

Table 5.6: *(Cont'd.)*

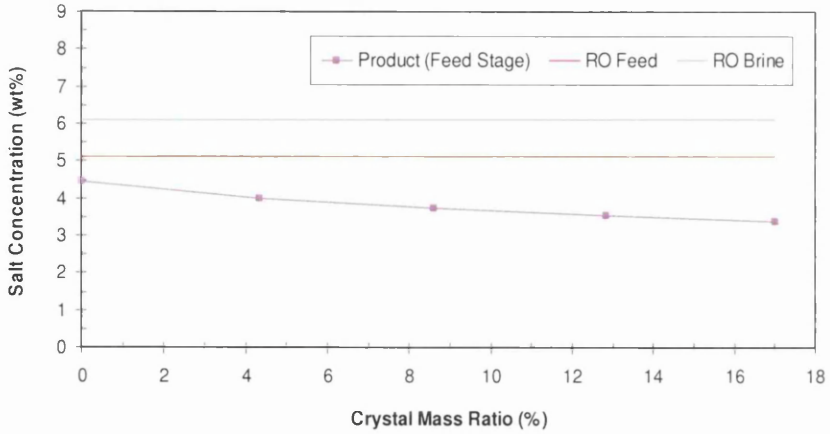

(a) Crystal mass ratio vs. salt concentration for the feed stage

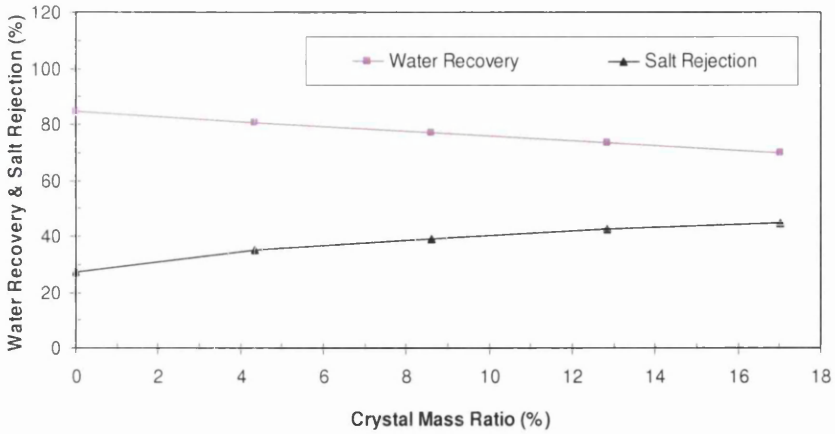

(b) Crystal mass ratio vs. WR and SR for the feed stage

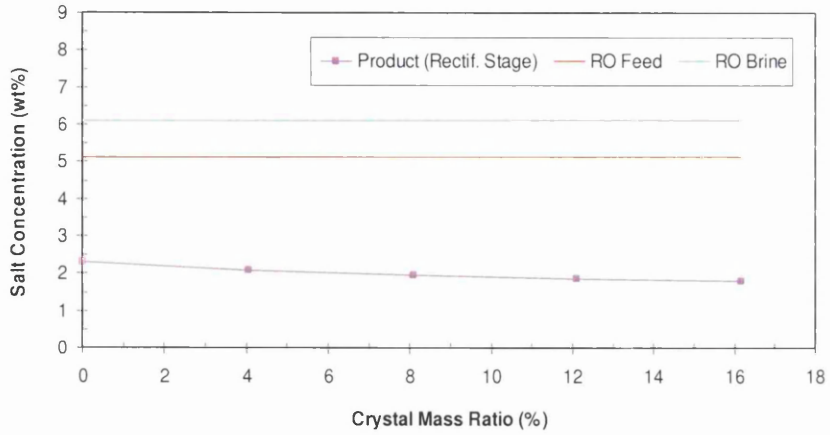

(c) Crystal mass ratio vs. salt concentration for rectification stage

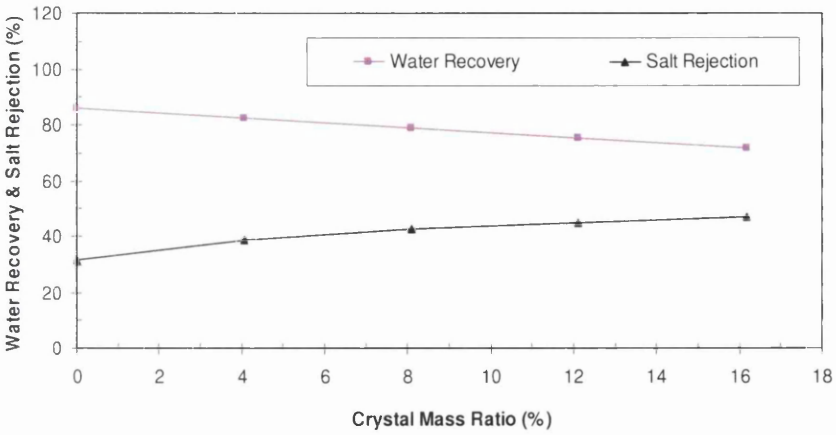

(d) Crystal mass ratio vs. WR and SR for rectification stage

Fig. 5.15: *Performance of feed, rectification, and stripping stages, using falling film crystallisation and sweating processes, for treating RO brine, where WR is the product water recovery ratio and SR is the salt rejection ratio.*

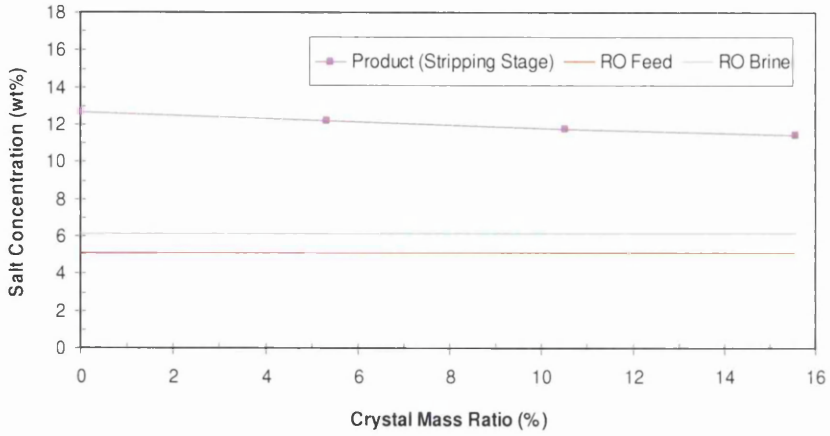

(e) Crystal mass ratio vs. salt concentration for the stripping stage

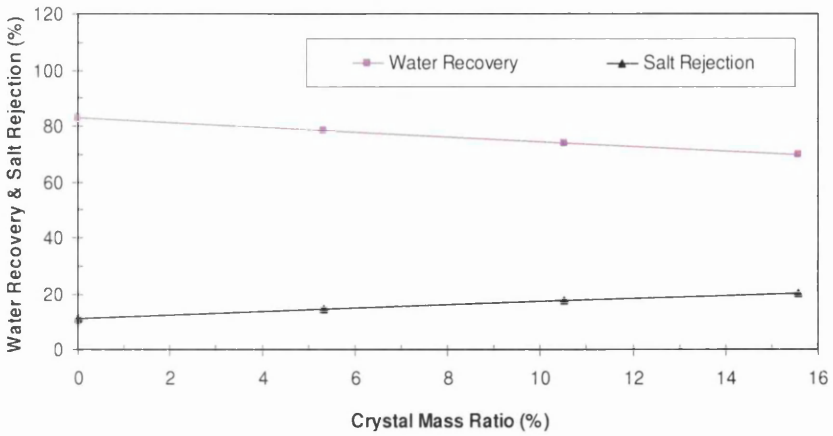

(f) Crystal mass ratio vs. WR and SR for the stripping stage

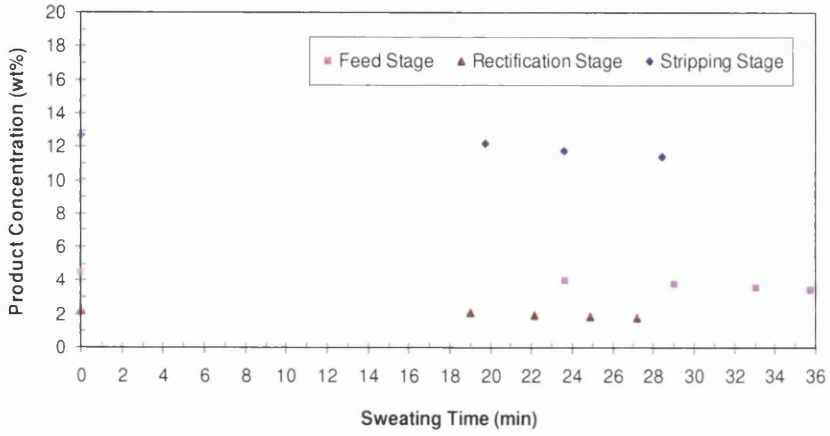

(g) Sweating time vs. salt concentration for the multi-stage process

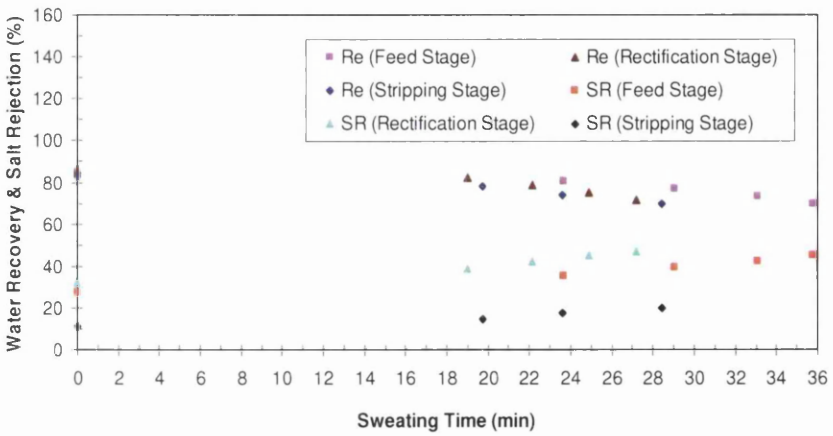

(h) Sweating time vs. WR and SR for the multi-stage process

Fig. 5.15: *(Cont'd.)*

the rectification stage can be further treated and concentrated by recycling this waste stream back to join the main feed stream of the feed stage, whereas the residual liquids of the feed and stripping stage cannot be treated and concentrated through the stripping stage. Although the sweating process was conducted with considerable loss of final product, poor separation performance was observed in the stripping stage. This was due to the high salinity feed fed to the stripping stage, which led to a crystal layer tending to be porous, in a sponge-like structure, where the impurities were kept further inside the structure of the crystal layer and occluded. The performance of the stripping might be improved by using a higher crystallisation temperature and higher sweating rate with considerable mass loss in the final product water through the sweating operation. However, a moderately effective sweating process with a significant decrease in the production rate (due to considerable loss of final product water) is expected for such operating conditions.

As for the chemistry data of the water samples obtained from each freezing stage, Table (5.6) shows that the ionic composition of the major ions in each process stream.

With regard to the purification efficiency of the sweating process, the salt concentrations of the product water were found to be proportional to the mass of sweat fraction as shown in Fig (5.15). Fig (5.15) also shows the influence of crystal mass ratio on the salt rejection ratio, and water recovery ratio. The salt rejection ratio was found to be proportional to the crystal mass ratio, whereas the water recovery ratio was found to be inversely proportional to the crystal mass ratio. By comparing the results of the fraction in each freezing stage (see Table (5.6)), the salt and ionic concentrations of the fraction were deceased when compared to that in the previous fraction. For the feed and rectification stages, the impurity concentration in the last sweat fraction (i.e. fraction 4) is almost the same as the impurity concentration in the remainder of the crystal mass i.e. product water (see Table (5.6)). This means that, a further sweating process will be a waste of product and sweating time, since there is no significant difference between the salt concentration of product and last sweat fraction. In fact, a further sweating operation will only be a total melting process for the remaining crystal mass. The remaining impurities can be considered to be locked-in inside the crystal mass, which can be further purified by one of the following methods: (a) optimising the operating conditions of crystallisation and sweating operations; or (b) applying a multistage process. In contrast with the stripping stage (see Table (5.6)), the sweating operation can proceed further since the

impurity concentration of last sweat fraction (i.e. fraction 3) was still higher than that in the impurity concentration in the remainder of the crystal mass. This means that the sweating time needed to be extended further, in order to purify the remainder of the crystal mass, i.e. product water. However, the suggested application will significantly increase the overall time of the freezing stage, and decrease the overall water recovery ratio, which will eventually lead to a significant reduction in the production rate of the stripping stage. Thus, the stripping stage using the adopted technology was found not to be technically feasible for further concentrating the already concentrated solutions of RO brine. A static crystallisation process might be an alternative solution in such applications.

Based on visual observation, there was clear signs of solid salts precipitation in the remaining residual liquid, and in the pilot plant equipment while carrying out the experiment for the stripping stage. Table (5.5) demonstrates and confirms the signs of precipitation of salts composed of Ca^{2+}, Mg^{2+}, and $(SO_4)^{2-}$ ions, since the calculations of the percentage losses in their ionic concentration are about 26, 9, and 14 % respectively. The reason for the solid salts precipitation may be explained by one of the following; (i) the stripping stage was examined at very low crystallisation temperature, which was lower than the eutectic temperature of some salts in the residual liquid. Following van der Ham *et al.* (1998), a summary of several eutectic points and eutectics of chemical composition for different binary salt-water systems are shown in Fig (5.16). For example, sodium sulphate precipitated as $Na_2SO_4.10H_2O$ at a eutectic composition of 12.7 wt% and eutectic temperature of -3.6°C; (ii) the solubility limit of some salts in the residue might have been reached. Table (5.7) shows the solubility limits of major salts available in seawater; and (iii) precipitation of solid sodium sulphate (i.e. $Na_2SO_4.10H_2O$) in the residue, when the temperature of residue is reduced below -8.2°C [Pounder, 1965]. The solid salt phase begins to appear in the residue, although the eutectic temperature for the sodium sulphate salt is -11°C [Pounder, 1965].

The results proved that the sweating processes was able to lower the salt concentration of product water and ionic concentrations, and more specifically was found effective in feed and rectification stages (see Table (5.6) and Fig (5.15)). However, the main disadvantages of the sweating process are; reduction in water recovery ratio (see Fig (5.15)) and an increase in the running time of the freezing stage. On the other hand, the study proved that the purification efficiency of the sweating process was strongly dependant on the salt

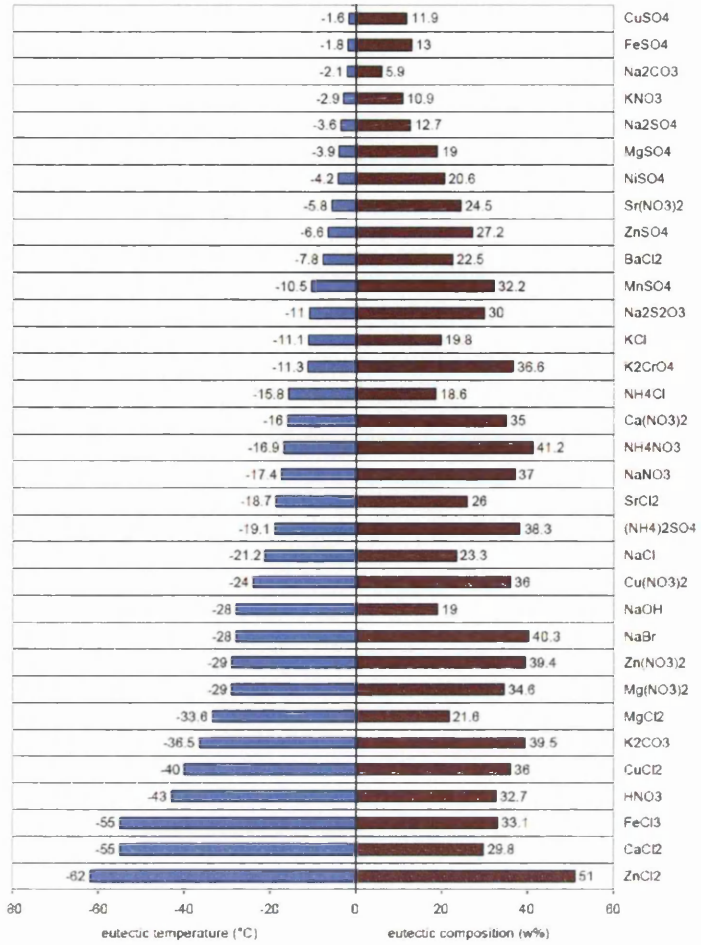

Fig. 5.16: *Summary of several eutectic temperatures and chemical composition of binary salt – water systems [van der Ham et al., 1998].*

Salt	Seawater Concentration*	Salt Concentration
	($kg_{(f)}/kg_{(s)}$)	($mg/kg_{(s)}$)
$CaCO_3$	1.9	370
$Mg(OH)_2$	1.9	440
$CaSO_4$	3.33	5,130
NaCl	8.9	278,000
KCl	10.5	9,030
$MgCl_2$	13.4	63,700

Table 5.7: *Results of measurements of solubility limits of major salts available in seawater, where subscript notations such as (f) and (s) mean feed and solution respectively. * Seawater concentration is determined as a geometric progression of the mass ratios i.e.* $(M_{(initial)})/((M_{(initial)})-(M_{(deionised\ water)}))$ *[El-Sayed and El-Sayed, 2007].*

concentration of the original mass of crystal layer, as shown in Fig (5.15). Figs (5.15) (g) and (h) showed that the purification efficiency of sweating processes declined considerably on increasing the salt concentration of the original mass of the crystal layer.

Although the results are quite encouraging in terms of the separation performance, the adopted technology, over two successive freezing stages, did not produce a final product close to potable water standards, with respect to salt concentration and ionic compositions, as illustrated in Table (5.6). However, the adopted technology produced a saline water of near brackish water standards that can be further easily desalted by: (a) optimising the crystallisation and sweating operations by compromising the purification efficiency and product loss; (b) increasing the number of rectification stages; and (c) using one of the conventional desalination technologies, such as brackish water RO membranes, to obtain a final product of drinking water.

5.6.5 *Multi-stage processing (feed and rectification stages) with a sweating step for desalting Arabian Gulf seawater*

In the eighth series of experiments, the purification efficiency of a multi-stage Sulzer falling film process was examined and evaluated for seawater desalination application. The experiments were carried out in a multi-stage process, using two successive freezing stages, which are the feed and rectification stages. Arabian Gulf beach-well seawater was used as the feed sample for the feed stage. The multistage process was examined at maximum water recovery ratio. The experiments determine the purification efficiency of the crystallisation and sweating processes in each freezing stage, in terms of the salt concentration of product water and ionic rejection. The crystallisation temperature and ramp for the feed and rectification stages were -16°C and 0 °C/min respectively, whereas the sweating steps were carried out at a start-point HTM temperature of -16°C and sweating ramp of 0.5°C/min respectively. The actual operational period of the crystallisation process for the feed and rectification stages were 1.33, and 0.53 h respectively, whereas the actual operational period of the sweating process were 0.4, and 0.47 h, for the same freezing stages respectively. A complete record of the temperature profiles for these experiments is given in Appendix A5. The amount of feed used each time was approximately 30 kg, so the experiments for the feed stage were individually repeated twice to collect the water samples for physiochemical

analysis, and also to collect enough feed water for the rectification stage, which was performed only once to produce the final product water.

A summary of the experimental data and physiochemical analysis for the water samples of each freezing stage is given in Tables (5.8) and (5.9). Table (5.8) shows that the average TDS value of Arabian Gulf seawater fed to the feed stage was 49,074 ppm, whereas the feed and rectification stages were able to produce a final product water with average TDS values of 26,446, and 12,289 ppm respectively. Table (5.9) shows that the TDS values of the residual liquid of the feed and rectification stages were 103,955 and 51,052 ppm respectively. The residual liquids of the rectification stages can be further easily desalted by recycling this residue back to join the main stream of the feed stage, whereas the residue of the feed stage must be treated and concentrated through the stripping stage.

The calculation of the salt rejection ratios give 46.11 and 53.53%, for the feed and rectification stages respectively, while calculation of the water recovery ratios give 70.81 and 63.48%, for the same freezing stages respectively. The overall salt rejection and water recovery ratios, of the examined multi-stage process, were 74.96% and 44.95% respectively. The performance results obtained provided clear evidence that the investigated multistage process was capable of providing product water with a TDS value of 12,289 ppm from Arabian Gulf seawater. Although the examined treatment system did not produce high quality product water closer to drinking water standards, it produced saline water with almost the same quality as brackish water, in terms of salinity and ionic composition, as indicated in Table (5.9). In order to obtain potable water, this near brackish water can be further easily desalted by one of the following methods; (i) optimising the crystallisation and sweating process for the multistage process; (ii) adding one rectification stage or more; or (iii) using a conventional brackish water desalination technology, such as membranes.

With regard to ionic rejection, Table (5.9) shows that the average hardness ion values of Ca^{2+}, Mg^{2+}, and $(SO_4)^{2-}$ for the tested seawater fed to the feed stage were 1,080, 1,387, and 3,900 mg/L respectively. The examined multistage process was able to reduce these ions down to 392, 402, and 980 mg/L respectively. Table (5.9) also shows that the tested seawater contains monovalent ions, such as Na^{+} and Cl^{-}, with ionic concentrations of 16,523 and

Stage	Water Sample	Parameters	Unit	Value
Feed Stage	Feed Water	Mass	(kg)	35.028
		TDS	(ppm)	49,074
	Product Water	Mass	(kg)	24.802
		TDS	(ppm)	26,446
	Residual Water*	Mass	(kg)	10.226
		TDS	(ppm)	103,955
Rectification Stage	Feed Water	Mass	(kg)	24.602
		TDS	(ppm)	26,446
	Product Water	Mass	(kg)	15.617
		TDS	(ppm)	12,289
	Residual Water*	Mass	(kg)	8.985
		TDS	(ppm)	51,052

Table 5.8: *Summary of the performance data for the feed and rectification stages. * Residual liquid includes the overall results of the actual residual liquid and sweat fractions.*

Parameter	Unit	Feed Stage							Total Residue
		Feed	Product	Residue	Fraction (1)	Fraction (2)	Fraction (3)	Fraction (4)	
pH	-	7.13	6.80	6.74	6.78	6.85	6.80	6.81	6.74 – 6.85
TDS	(mg/L)	49,074	26,446	136,188	118,145	70,145	55,118	43,975	103,955
Conductivity	(mS/cm)	63.6	31.9	155.8	140.0	88.6	68.9	54.4	126.1
Ca^{2+}	(mg/L)	1,080	861	3,156	2,928	1,560	1,078	1,000	2,513
Mg^{2+}	(mg/L)	1,387	715	2,837	1,970	1,407	1,057	919	2,198
Na^{+}	(mg/L)	16,523	8,567	43,188	39,945	24,836	18,870	16,082	35,429
Cl^{-}	(mg/L)	25,480	13,212	66,600	61,600	38,300	29,100	24,800	54,636
$(HCO_3)^{-}$	(mg/L) as Ca CO_3	175.6	153.4	456.3	360.8	240.9	190.3	172.6	364.7
$(SO_4)^{2-}$	(mg/L)	3,900	2,645	8,200	7,900	5,300	4,100	3,100	6,882
NO_3^{-}	(mg/L)	2.7	2.2	8.1	7.2	5.3	3.4	3.0	6.6

Table 5.9: *Major physiochemical analysis of water samples for the feed and rectification stages with use of a sweating process for desalting Arabian Gulf seawater.*

Parameter	Unit	Rectification Stage							Total Residue
		Feed	Product	Residue	Fraction (1)	Fraction (2)	Fraction (3)	Fraction (4)	
pH	-	6.80	7.23	7.18	7.23	7.26	7.24	7.24	7.18 - 7.26
TDS	(mg/L)	26,446	12,289	62,831	51,496	29,937	23,717	19,070	51,052
Conductivity	(mS/cm)	31.9	14.7	78.8	64.2	36.3	28.5	22.8	63.6
Ca^{2+}	(mg/L)	861	392	1,248	1,040	544	492	480	939
Mg^{2+}	(mg/L)	715	402	763	1,657	829	778	574	860
Na^{+}	(mg/L)	8,567	6,031	21,075	17,962	12,386	10,311	8,625	16,637
Cl^{-}	(mg/L)	13,212	9,300	32,500	27,700	19,100	15,900	13,300	25,657
$(HCO_3)^{-}$	(mg/L) as Ca CO_3	153.4	110.0	190.6	182.3	140.6	136.2	130.0	168.6
$(SO_4)^{2-}$	(mg/L)	2,645	980	5,480	4,600	3,480	2,410	1,260	4,192
NO_3^{-}	(mg/L)	2.2	0.7	2.4	2.0	1.3	1.2	1.0	1.9

Table 5.9: *(Cont'd.)*

25,480 ppm respectively. These ionic concentrations were lowered to 6,031 and 9,300 ppm, for the same ions respectively, through the examined multistage process.

A summary of the important experimental data from field testing is shown in Fig (5.17). In these plots the purity of the final product water, water recovery ratio and salt rejection ratio are plotted against the crystal mass ratio. The purity of the final product waters (for the feed and rectification stages respectively) was slightly reduced on increasing the crystal mass ratio (see Fig (5.17) (a) and (c)). Similar behaviour was also observed with the water recovery ratio, which decreased as the crystal mass ratio increased; this was due to the mass loss during the sweating process, as shown in Fig (5.17) (b) and (d). The salt rejection was found to be proportional to the crystal mass ratio, as shown in Fig (5.17) (b) and (d).

5.6.6 Scaling-up of the Sulzer falling film crystallisation technology

The performance results obtained, provided evidence that the Sulzer falling film crystallisation technology, using a single freezing stage without the need for a sweating process, would be an ideal treatment system for concentrating RO brine. This technology was capable of producing a substantial amount of final product water to near Arabian Gulf seawater quality, whilst simultaneously reducing the waste stream as far as possible. The scale-up for such an application is straightforward, since the commercial scale crystallizer can be easily built by adding a number of crystallizer tubes similar in size to those tested.

The Kadhmah RO desalination plant was used as an example for scaling-up the integration of the RO desalination plant with the Sulzer falling film crystallisation process under continuous operation. The laboratory investigations were actually carried out with RO brine, discharged from the mentioned RO desalination plant. The example for scaling-up will present an estimation of the mass and salt concentration of the three liquid streams for each treatment system, which are essential for the assessment of the water treatment costs.

The proposed treatment system was scaled-up according to the experimental results obtained from run 72 (see Table A5-2 in Appendix A5). However, the salt concentration of product water of the Sulzer falling film crystallisation plant was changed and balanced to the feed concentration of Kadhmah (RO membrane) desalination plant. This means that the TDS value of the product water of the Sulzer plant was equivalent to the feed salinity of the water

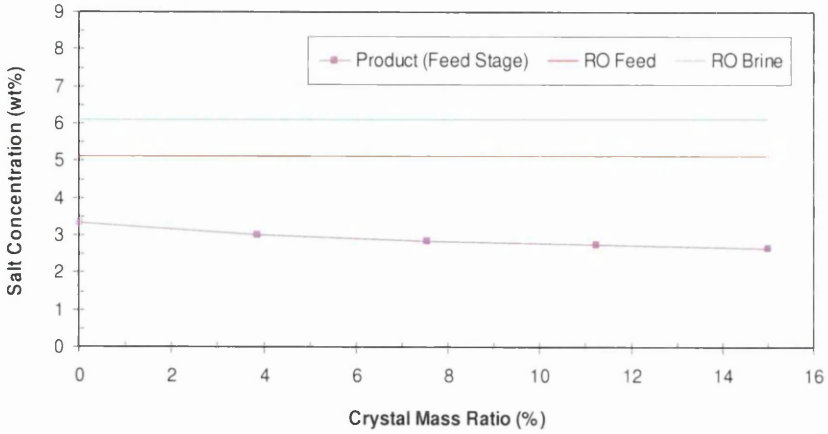

(a) Crystal mass ratio vs. salt concentration for the feed stage

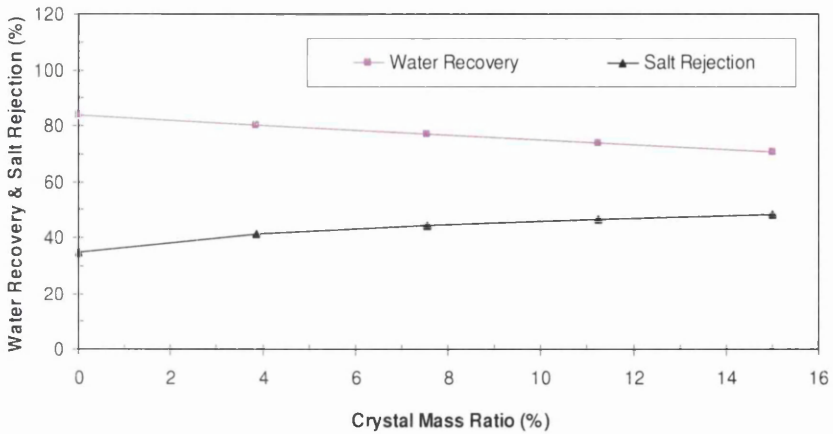

(b) Crystal mass ratio vs. WR and SR for the feed stage

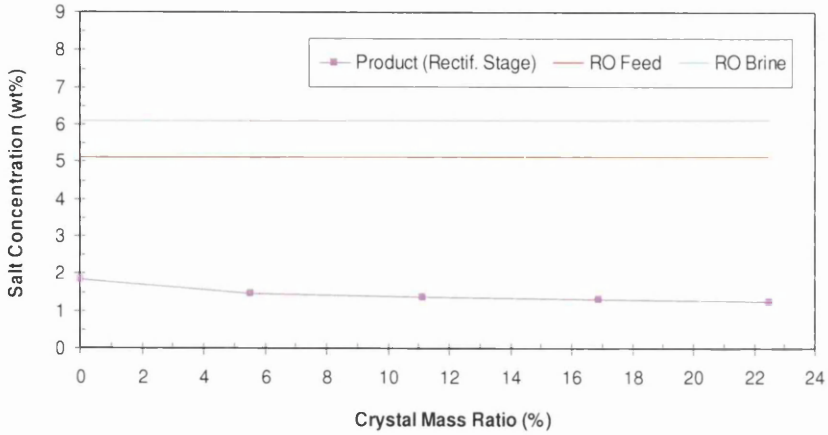

(c) Crystal mass ratio vs. salt concentration for rectification stage

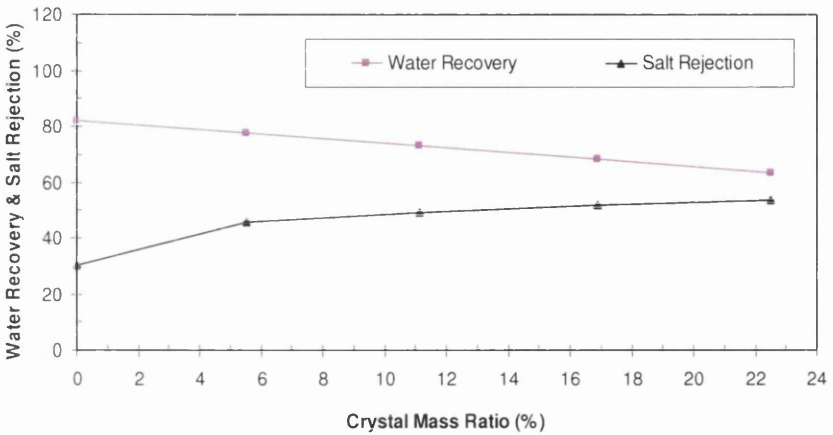

(d) Crystal mass ratio vs. WR and SR for rectification stage

Fig. 5.17: *Performance of feed and rectification stages, using falling film crystallisation and sweating processes, for treating Arabian Gulf seawater, where WR is the product water recovery ratio and SR is the salt rejection ratio.*

desalination plant. This was achieved simply by adding a predetermined mass of the residue (according to the calculation of mass and salt balance) to the product water of the pilot plant. Consequently, the total water recovery ratio of the freezing stage was changed, and slightly increased from 84.2 to 87.8%. The TDS values of feed and residue streams of the Sulzer plant were determined from the experiment (i.e. run 72). The volume flow-rate of the feed stream of Sulzer plant was equivalent to that in the discharged RO retentate from the water desalination plant. The volume flow-rate of the product of the Sulzer plant was theoretically determined according to the adjusted water recovery ratio (i.e. 87.8%), whereas the volume flow-rate of the residue was simply computed from the mass balance formula.

A novel treatment option configuration, involving integration of a RO plant and the Sulzer falling film crystallisation plant, is shown schematically in Fig (5.18). According to Sulzer, the proposed commercial plant can be built without any technical problem; however, such an application might be limited by capital and/or operational costs. Fig (5.18) shows that the volume flow-rate of RO retentate is significantly decreased from 21.9 to 2.67m^3/h by means of a Sulzer plant. Besides, the product water of Sulzer plant, which is recycled to join the main feed stream of RO plant, has significantly reduced the volume flow-rate of the intake feed from 27.3 to 8.07m^3/h as shown in Fig (5.18).

Table (5.10) shows the estimated annual rates of all liquid streams of the Kadhmah RO plant, Sulzer commercial plant, and combined water desalination plant. The estimated annual rate of feed water for the RO plant is 239.15 ton/year, whereas the RO plant produces drinking water with an estimated annual production rate of 34.17 ton/year. As a result, a substantial annual rate of highly concentrated process brine (i.e. 191.84 ton/year) will be discharged to the receiving environment, i.e. into the Arabian Gulf, for the case of Kadhmah RO plant. According to Lattemann and Höpner (2003), physiochemical characteristics and volume of the waste stream of RO membrane desalination plants can cause severe impacts on the marine environment. Thus, the question now arises; what is the available disposal option and environmental impact of such a large volume of waste stream for the case of inland desalination plants. The Sulzer falling film crystallisation plant can be considered as a great solution for concentrating the waste streams of desalination technologies.

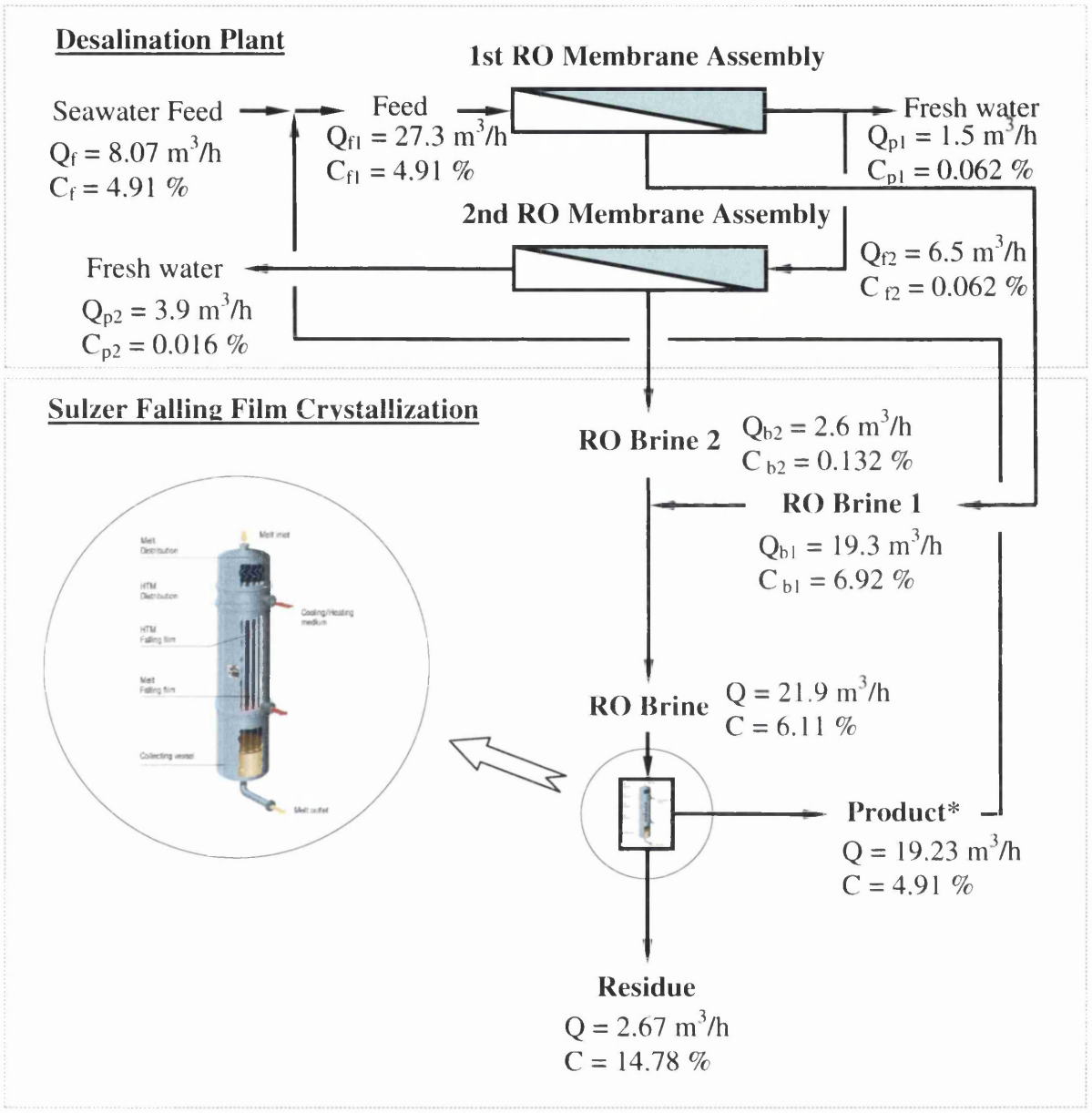

Fig. 5.18: *Combination of a commercial seawater Reverse Osmosis (RO) membrane desalination plant coupled with the Sulzer falling film crystallization plant, where; Q is the volume flow-rate (m^3/h), and C is the salt concentration (wt%), (subscript f= feed-water, p= product water, b= brine, and 1 and 2 refer to the stage number).*

Kadhmah RO Plant			Sulzer Falling Film Plant			Combined Plant		
Feed[1]	Product[2]	Brine	Feed	Product	Residue	Feed[1]	Product[2]	Residue
(t/y)	(t/y)	(t/y)	(t/y)	(t/y)	(t/y)	(t/y)	(t/y)	(t/y)
239.15	34.17	191.84	191.84	168.45	23.39	70.7	34.17	23.39

Table 5.10: *Estimation of the annual rates of all water streams of the Kadhmah RO desalination, the Sulzer falling film crystallisation plant, and the combined plants, where (t/y) represents ton per year.*

[1] The annual rate of the feed intake.

[2] The first stage of the RO membrane assembly produces product water at 8 m^3/h, and 6.5 m^3/h of this is fed to the second stage RO membrane assembly, while the remaining product water from the first stage (i.e. 1.5 m^3/h which is equivalent to 13.14 t/y) is not used and drained (see Fig (5.18)).

When a commercial scale Sulzer plant is incorporated into the Kadhmah RO plant (see Fig (5.18)), then the estimated annual rate of RO retentate from the RO plant can be significantly reduced from 191.84 to 23.39 ton/year as illustrated in Table (5.10). Such a combination can also preserve a large volume of natural water resource from exploitation by recycling the treated water (i.e. product of Sulzer plant) into a RO membrane plant, in order to be used as feed (see Fig (5.18)). The calculations showed that the estimated annual rate of the main feed intake of the RO plant can be substantially reduced from 239.154 to 70.7 ton/year. The actual annual feed rate of the feed of the RO plant is still the same (i.e. 239.154 ton/year) since there is an internal recirculation of the treated water in the combined plant (see Fig (5.18)). This means that the estimated annual rate of the preserved natural water resources is 168.45 ton/year, where the actual feed water of the RO plant is compensated by producing seawater from the RO brine by means of a Sulzer falling film crystallisation plant.

5.6.7 Energy consumption and production rate

The theoretical power consumption for the commercial scale of Sulzer falling film crystallisation plant was determined based on the results of the scaling-up example (see Fig (5.18)). The theoretical power consumption was computed by the heat transfer rates for cooling the feed water and for changing the phase of the liquid, which were explained in Chapter 4. The calculations of the theoretical power consumption for the mentioned plant give 92.55 kWh/m^3. In addition to this, the theoretical power consumption was computed for

all experiments. For instance, Fig (5.19) shows plots of the theoretical results of the power consumption versus the end-point HTM temperature at different cooling rates for the first series of experiments. The theoretical result of the power consumption averaged about 108 kWh/m^3. This clearly indicates that the theoretical result of the power consumption was slightly reduced when comparing the results computed from the experimental investigations to that in the case of the commercial scale of Sulzer plant. This is due to the significantly increased production rate in the case of the commercial scale Sulzer plant.

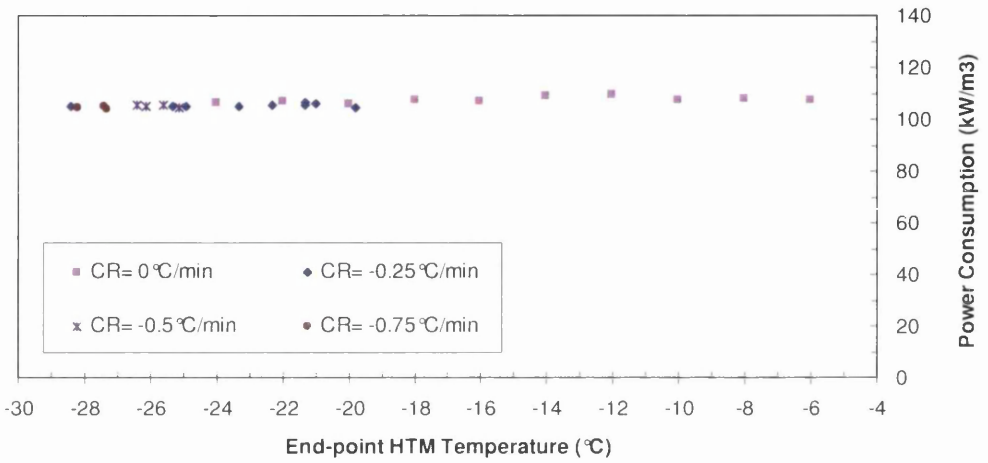

Fig. 5.19: *Production rate and power consumption versus end-point HTM temperature for the first series of the experiments.*

In addition, Fig (5.20) shows plots of the theoretical power consumption and the production rate versus the end-point HTM temperature at cooling rate of 0 °C/min for the first series of experiments. As expected, a clear tendency of reduced production rate as the end-point crystallisation temperature increased can be observed. This confirmed the previous observations on the influence of crystallisation temperature on the crystallisation time and water recovery ratio. As a result, the production rate was found to be inversely proportional to the end-point HTM temperature, as shown in Fig (5.20). The theoretical power consumption was unaffected by slightly increasing the production rate as shown in Fig (5.20). This is because the experimental investigations were carried out at a very low production rate.

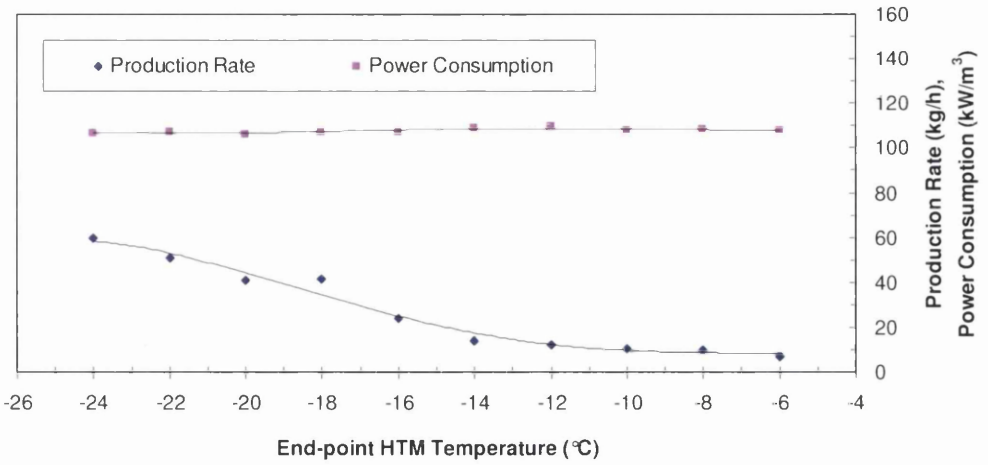

Fig. 5.20: *Production rate and power consumption versus End-point HTM temperature.*

Fig (5.21) shows that the influence of the feed concentration on the power consumption. The power consumption increased slightly as the salt concentration of feed water increased. This behaviour was found to agree with the results obtained in Chapter 4.

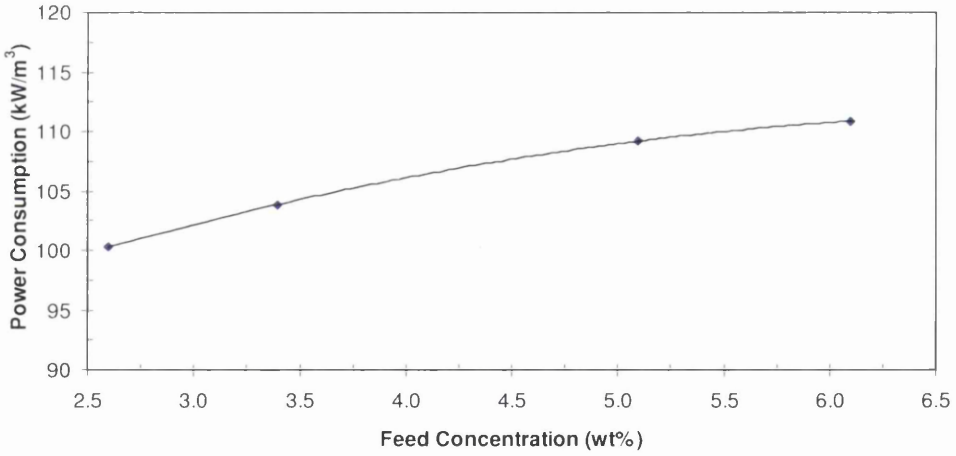

Fig. 5.21: *Feed concentration versus power consumption.*

5.7 Conclusions

In this study, the performance of falling film crystallisation and sweating processes, using Sulzer's falling film crystallisation pilot plant, was assessed and validated for concentrating RO retentate as well as desalting Arabian Gulf seawater. Several parameters influencing the separation performance of crystallisation and sweating processes were investigated in a pilot plant operating in batch mode. Furthermore, a multistage process, with and without use of sweating process, was tested for the mentioned process brines.

In general, the experimental results showed that feed concentration, crystallisation temperature, cooling and sweating rate, and average growth rate, had a significant influence on the separation performance of the treatment system. The performance results of the pilot plant were clearly similar to those of the ice maker, as given in Chapter 4. The Sulzer falling film crystallisation pilot plant, within a single freezing stage, and without use of a sweating process, was able to concentrate a significant amount of RO brine, while producing saline water to near seawater quality. In fact, the major physiochemical analysis of the product water showed that the product water was higher, in terms of quality, than typical RO plant feed water. This means that the product water was ready for immediate re-use as feed water to a RO desalination plant. The experimental results showed that the maximum water recovery ratio was 86%. Therefore, the results for the RO brine experiments were highly encouraging for RO brine concentration. Based on these results, the investigated treatment system was scaled up for such an application. As a result, a substantial annual rate of waste stream could be recycled and reused as RO feed, while preserving a large volume of natural water resource from exploitation, as well as minimising the waste stream as far as possible.

On the other hand, the results for the stripping stage using the falling film crystallisation process were not encouraging. Although a sweating process was used, the stripping stage provided final product water with a salt concentration much higher than in RO brine. Thus, the falling film crystallisation process is not technically feasible for treating the highly concentrated RO brine. As for the Arabian Gulf seawater experiments, the results were quite encouraging, because the proposed treatment system did not produce a final product water of near drinking water standards, but within brackish water standards, which can easily be desalted by any brackish water desalination system.

CHAPTER VI:

INVESTIGATING THE FEASIBILITY OF THE SUSPENSION CRYSTALLISATION PROCESS FOR TREATING REVERSE OSMOSIS BRINES

6.1 Introduction

This chapter tackles an optimisation approach used to boost the production of drinking water in inland desalination plants from brackish and surface water using RO membrane technologies. This optimisation approach can be achieved by desalting and concentrating the waste streams (RO retentate) through a suspension crystallisation technology. A hybrid process which comprises of the existing melt crystallisation technologies in Sulzer's portfolio (falling film or suspension crystallisation process, integrated with a static crystallisation process), can be introduced as a pre-concentrator system for the water desalination plant and ZLD process. Such a combination can increase the total permeate water recovery (by using a suspension crystallisation system) or preserve natural water resources from exploitation by recycling treated water into a RO plant as feed (using falling film crystallisation system). The residual liquid of the suspension or falling film crystallisation plants can be further concentrated and processed via a subsequent treatment system involving a static crystallisation process (see Chapter (7)). As a result, a small volume of highly concentrated solution of RO retentate will remain. This final residual liquid can be further treated and processed via a ZLD process for producing more fresh water and/or a discharging a compact solid waste in a way friendly to the environment.

Intensive studies on the suspension crystallisation process have investigated the influence of operating parameters on the performance of the crystallisation and washing processes for the separation of organic chemicals and metals [Ulrich and Glade, 2003]. According to Sulzer's experts, the suspension-based melt crystallisation technology has not previously been tested for saline water applications. As a result, there is no reference data available on the application of suspension crystallisation technologies for RO retentate treatment. This chapter presents the first experimental study to explore the potential capability of using

Sulzer's suspension-based melt crystallisation process to treat a range of liquid streams causing the most severe pollution problems.

In an effort to help developing arid countries, such as Kuwait, to satisfy the water supply and safe disposal demands, a combination of a commercial seawater desalination plant using RO membrane and a suspension crystallisation pilot plant was investigated. This hybrid system is aimed at increasing the overall permeate water recovery, and simultaneously concentrating the RO retentate as much as possible. Such a combination of treatment systems will preserve natural water resources from exploitation, especially in the case of brackish and inland desalination plants.

The main objective of this chapter is to determine the viability and technical feasibility of using suspension crystallisation technology as a pre-concentration system for concentrating RO retentate and producing final product water of near potable quality, ready for immediate use. The specific aims of this study are;

i) To operate the pilot plant and collect and maintain experimental data for different process configurations in order to validate and assess the technical viability of the suspension crystallisation process for treating different salt concentrations of RO retentate, through initial trial tests and technology refinement using pilot industrial scale plant.

ii) To validate and assess the proposed system's technical merits for future application on a commercial scale.

iii) To establish reference data for estimating the performance of the suspension crystallisation technology for treating RO retentate. This includes a reference physiochemical profile for water samples.

iv) To assess the separation effectiveness of the suspension crystallisation process with use of a piston type wash-column unit upon the rejection of the major components of ionic concentration (e.g. Ca^{2+}, Mg^{2+}, $(SO_4)^{2-}$, $(HCO_3)^-$, Cl^-, Na^+, etc) for the water samples.

v) To develop and identify the operating ranges for the main elements of the suspension crystallisation pilot plant, e.g. crystallisation temperature, stroke,

residue temperature, wash temperature, time cycle action, and tracing feed temperature.

6.2 Description of Suspension Crystallisation and Basic Operation

Suspension-based melt crystallisation is a highly selective, low energy consuming and solvent-free separation process used for the purification of organic chemicals [Ulrich and Glade, 2003; Tähti, 2004; Sulzer, 2011]. This technology is capable ideally of achieving high purity products and ecological production methods [Ulrich and Glade, 2003; Sulzer, 2011]. Suspension-based melt crystallisation has previously been used for purifying various chemicals and concentrating waster water. Some typical applications are; acetic acid, acetonitrile, adipic acid, benzene, caprolactam, durene, ethyl lactate, hexamethylendiamine (HMD), ionic liquids, lactic acid, methylene diphenyl isocyanate (MDI), methacrylic acid, o-phenylphenol, p-Diisopropylbenzene, p-Dichlorobenzene, p-Chlorotoluene, p-Nitrochlorobenzene, p-Xylene, phenol, trioxane, and waster water [Ulrich and Glade, 2003; Sulzer, 2011]. According to Ulrich and Glade [2003], the important advantages of the suspension-based melt crystallisation approach are: (i) superior purification can be produced from a single crystallisation stage, (ii) higher crystal production rate per unit volume of equipment, (iii) suspension crystallisation process uses less energy to attain the same separation as solid layer crystallisation, (iv) the suspension crystallisation process is often carried out in a continuous mode, whereas solid layer crystallisation is usually carried out in batch mode.

Fig (6.1) (a) shows a typical skid mounted pilot plant unit used for small commercial scale applications or investigating new fields of application. Suspension crystallisation plants for medium and large scale commercial applications with various capacity ranges are also available at Sulzer Chemtech Ltd. Fig (6.1) (b) shows a commercial skid mounted unit, using Sulzer's suspension-based melt crystallisation technology. This commercial unit, for instance, was installed and used for Methylene diphenyl isocyanate (MDI) applications at Huntsman in the Netherlands [Sulzer, 2011].

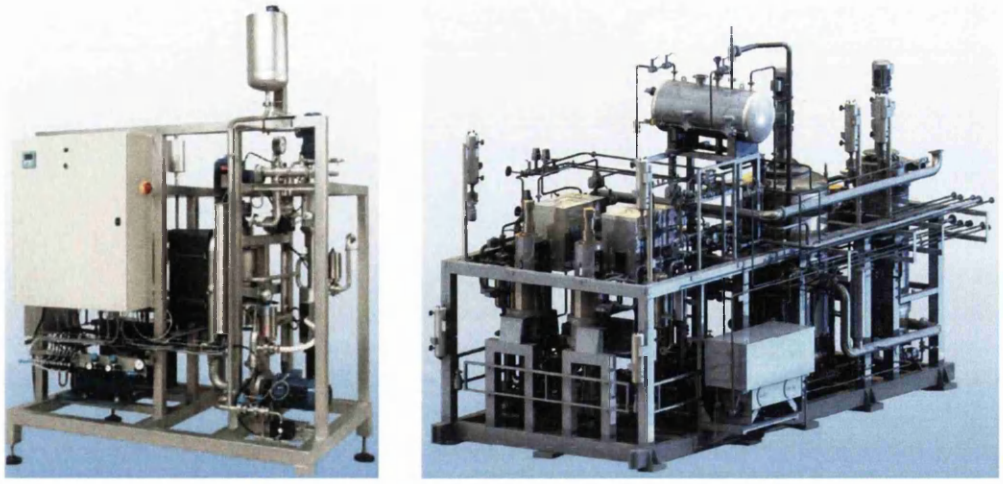

(a) Skid mounted test pilot unit (b) Commercial skid mounted unit

Fig. 6.1: *A typical plant using suspension-based melt crystallisation [Sulzer, 2011].*

According to Sulzer (2011), suspension crystallisation plants consist of two loops, i.e. crystallisation and separation loops, as shown in Fig (6.2). The main equipment in the crystallisation loop include a crystalliser, a stirred growth vessel, and a circulation pump. The separation loop, on the other hand, contains a piston type wash column, circulation pump, scraper, tube heat exchanger, and product and residue valves, as illustrated in Fig (6.2). The crystalliser is classified as a type of tubular and scraped surface heat exchanger, and is shown in more detail in Fig (6.3). This means that the crystalliser includes scraper blades, which are installed on a rotating shaft driven by a motor. This crystalliser is a single insulated thermo-stated double wall reaction vessel, made of stainless steel, which consists of a vertical tube in which the crystal layer is supposed to grow as a cylindrical shell (during the crystallisation operation). However, these crystals are removed from the crystalliser's surface to the bulk liquid by means of scraper blades.

By continuously circulating the cooling medium around the crystalliser, the ice crystals are nucleated and progressively crystallised on the refrigerated surfaces of the crystalliser. These ice crystals are then rapidly removed from the crystalliser's surface by the scraper, and then transported to the stirred growth vessel as a suspension, by the circulation pump. The crystals gradually grow in size within the bulk liquid inside the stirred growth vessel. The stirred growth vessel is made of an insulated vessel and an overhead stirrer assembly as shown in Fig (6.2). When the crystals reach the desired size and mass ratio (between the crystals and the bulk) in the crystallisation loop, the crystal slurry then proceeds to the separation loop, where the crystals are washed in a wash column and then recovered as product via a heater.

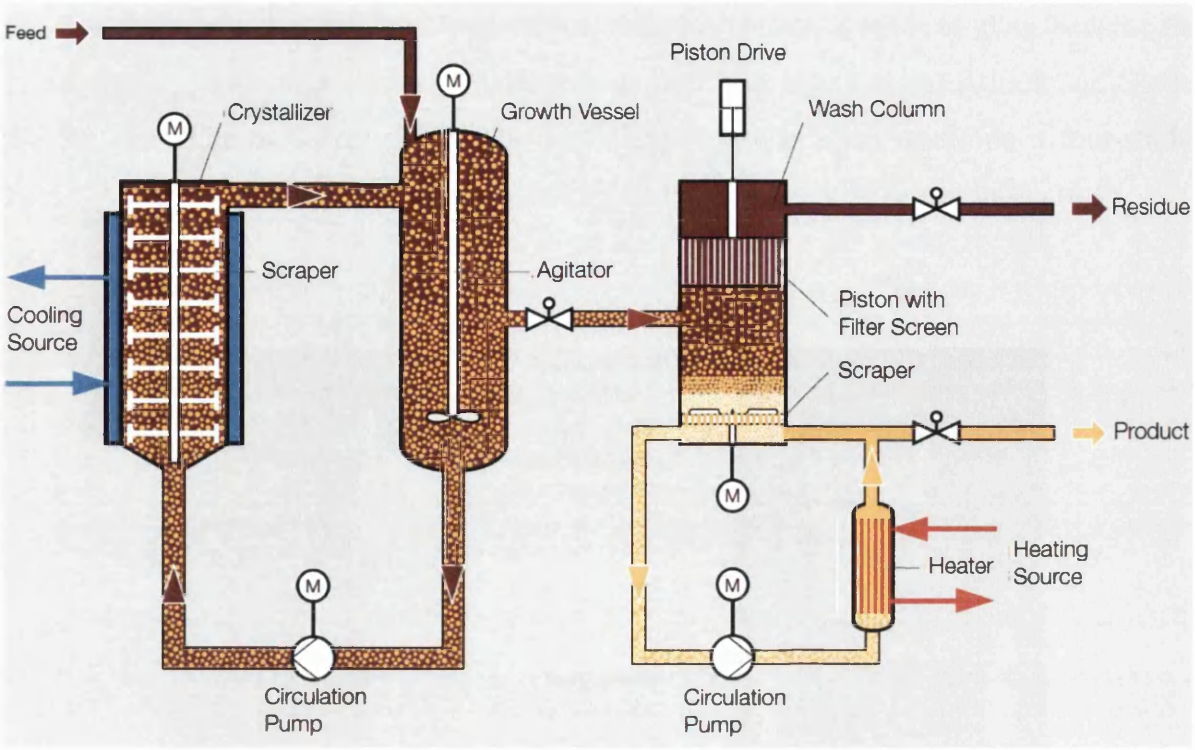

Fig. 6.2: *Flow process diagram of main equipment [Sulzer, 2011].*

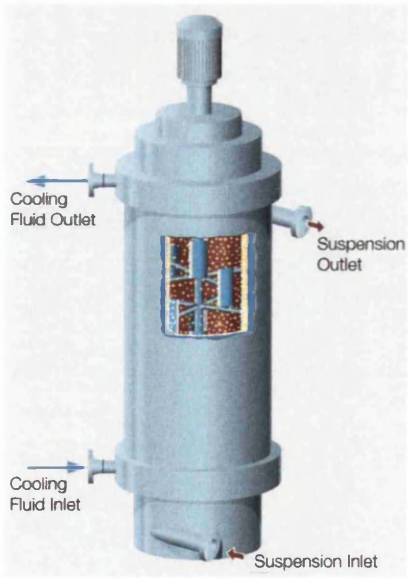

(a) A typical crystalliser

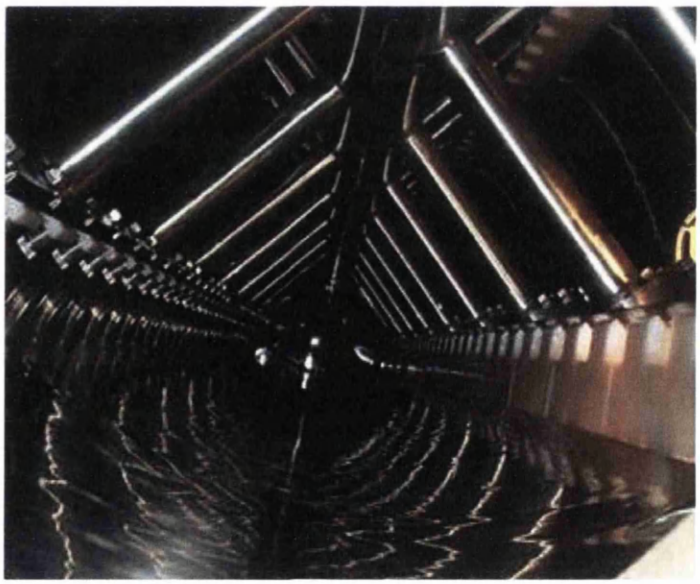

(b) Internal view of crystalliser vessel

Fig. 6.3: *A typical tubular and scraped surface heat exchanger [Sulzer, 2011; GEA, 2011].*

The wash column is classified as a piston type wash column. The wash column consists of a piston, cylinder, and scraper as shown in Fig (6.4) (a). The piston head is covered with a filter screen, which is attached to the reciprocating shaft driven via a pneumatic piston drive or a hydraulic cylinder to achieve a reciprocating motion. The scraper is attached to a rotating

shaft driven by a motor. For food applications, the wash column is made of glass, because the washing process is controlled with light cells as shown in Fig (6.4) (b) [Ulrich and Glade, 2003]. According to Sulzer (2011), the piston type wash column works on a four-stroke cycle; (i) filling, (ii) compressing, (iii) washing, and (iv) scraping as shown in Fig (6.5).

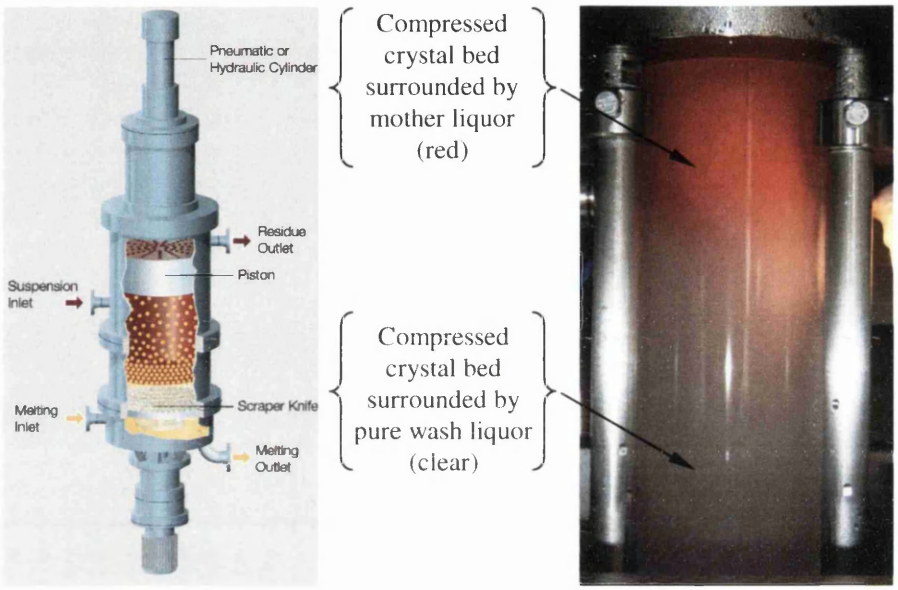

(a) Piston type wash column (b) Glass cylinder and light cell of wash column

Fig. 6.4: *A typical Sulzer wash column [Sulzer, 2011].*

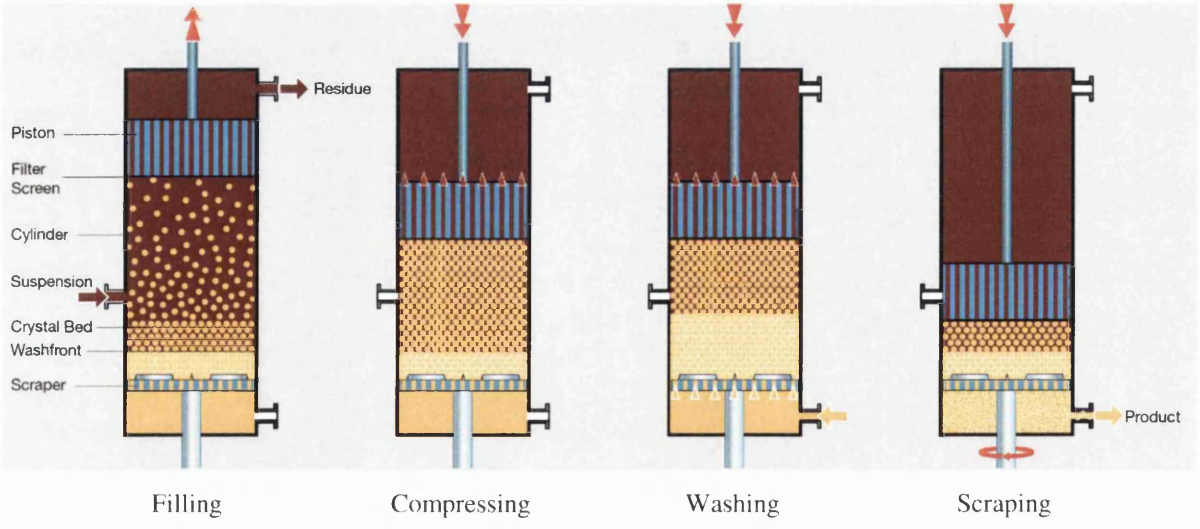

Fig. 6.5: *Four stroke cycles of the piston type wash column, adapted from Sulzer (2011).*

(i) Filling stroke

When the piston moves upwards, the cylinder is filled with slurry (i.e. suspension) from the crystallisation loop, through a slurry valve. This method enables the cylinder to be filled with the pressurised suspension [Ulrich and Glade, 2003; Sulzer, 2011]. At the same time, the residual liquid above the piston is either pressurised back to the crystallisation loop or removed from the process as final reside through a residue valve. The filling stroke ends when the piston reaches the top dead centre position.

(ii) Compression stroke

At this stage, the piston starts to move downwards forcing the liquid residual to pass through the filter screen as shown in Fig (6.5). The porosity of the filter screen prevents the passage of ice crystals from the space between the piston and the crystal bed. As the piston continues moving downwards, the residual liquid is squeezed out as much as possible from the crystals, leading to a packed bed of ice crystals above the existing crystal bed [Ulrich and Glade, 2003; Sulzer, 2011]. The compression operation continues until the ice crystals prevent further downward movement of the piston [Ulrich and Glade, 2003].

(iii) Washing stroke

As the piston continues moving downwards, the crystal bed is pushed to the zone of pure wash liquid, leading to an increase in the pressure of the melting loop [Ulrich and Glade, 2003]. A pressure difference will be created across the crystal bed, which forces the purified liquid in the melting loop to move upwards through the scraper openings and the crystal bed, thereby washing the crystals as shown in Fig (6.5) [Ulrich and Glade, 2003; Sulzer, 2011]. The wash front gets displaced and moves upwards against the piston movement [Sulzer, 2011].

(iv) Scraping

The fourth stroke starts with activation of the rotating disk, which includes scraping knives. As the piston continues moving downwards, the ice crystals are removed from the crystal bed. The scraper knives cut off pieces from the crystal bed, which are then simultaneously removed into the melting loop [Sulzer, 2011]. The scraping operation is deactivated when the piston reaches its bottom dead centre [Sulzer, 2011].

6.3 Preparation of Feed Samples

Different process brines, such as RO retentate and residue samples of the antecedent freezing stages using the suspension crystallisation system, have been used and examined individually as feed-water for the pilot plant. The preparation of feed material (RO retentate) was carried out as described in Chapter 5.

6.4 Physicochemical Analysis & Measuring Instruments

The physicochemical analysis of the water samples and the measuring instruments are described in Chapter 5. However, neither the DRP laboratory nor CAL could perform full chemical analyses for the product and residue water samples because of the presence of the colour indicator (Chromotrope FB, Sigma-Aldrich), which was mixed with the feed before starting the experiments. Therefore, the product and residue water samples were sent to Anchem Laboratories Ltd. (United Kingdom) for carrying out full chemical analyses to detect the major ionic composition.

In addition, the measurements of running time, residue temperature, HTM operating temperature (i.e. crystallisation temperature), washing temperature, stroke, time adjustment, running time of cycle action and adjustment, etc, were monitored and recorded. At the same time, some of these variables were controlled through a software package installed in a computer-controlled system connected to the pilot scale. Results of these measurements are tabulated in Tables A6-1 – A6-2 in Appendix 6.

6.5 Experimental Setup

Fig (6.6) shows the skid mounted pilot plant unit (Freeze Tec, Rig No.: 0-02-503-000, Type: FTC-1C Chem., Sulzer Chemtech Ltd.) used by Sulzer for investigating new fields of application. This pilot plant was used in this experimental study. The description of the pilot plant and basic operation is available in Section 6.2. This pilot plant, however, does not include a stirred growth vessel, so during the crystallisation operation, the crystals gradually grow and mature in size within the bulk liquid inside the crystalliser, instead of using a stirred growth vessel.

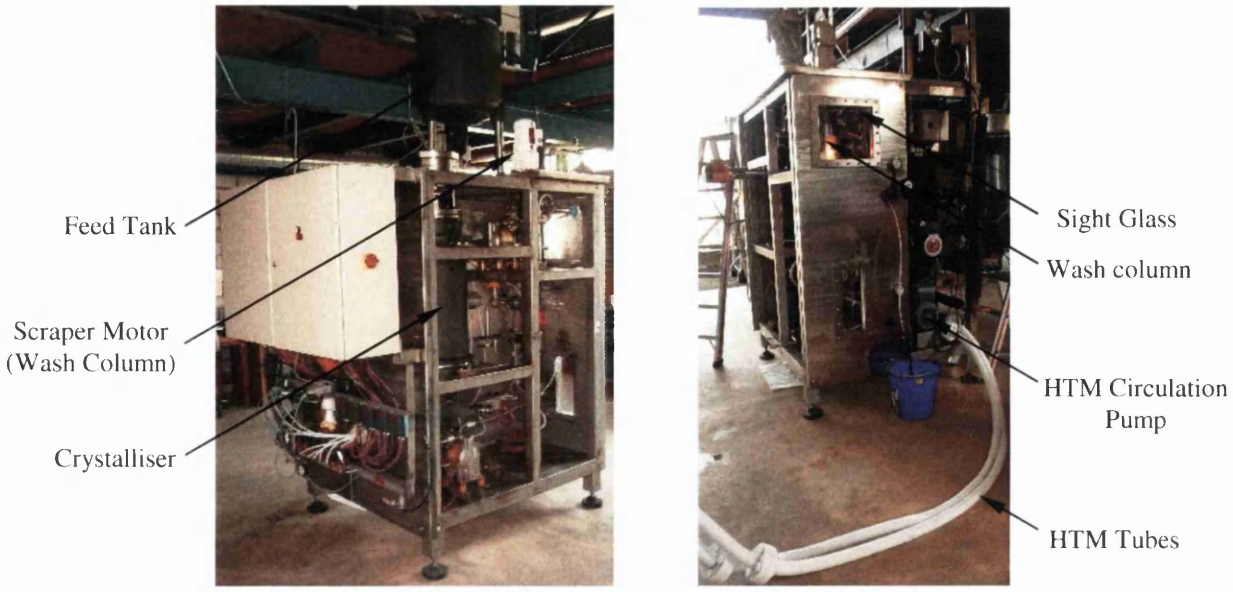

(a) Pilot plant left-hand view (b) Pilot plant right-hand view

Fig. 6.6: *Skid mounted pilot plant.*

Although Sulzer Chemtech Ltd commercialises complete test units that are completely equipped with all necessary equipment, including the cooling compressors [Ulrich and Glade, 2003; Sulzer, 2011], the examined skid mounted pilot plant does not include a complete built-in refrigeration unit. The pilot plant is provided with a heat exchanger, which is connected to a heat transfer unit (LAUDA, ITH Series, Type: W350/25kW) via tubes for low temperature applications, as shown in Fig (6.7) (a). The heat transfer unit utilises synthetic thermal oil as the HTM. Apart from the heat transfer unit, the skid is completely equipped with all necessary measuring instruments and control devices. The crystalliser and feed tank are made of stainless steel, which is thermodynamically insulated from the surrounding environment (see Fig (6.7)). The pilot plant also contains a wash column with a visible wash front, as shown in Fig (6.7) (c).

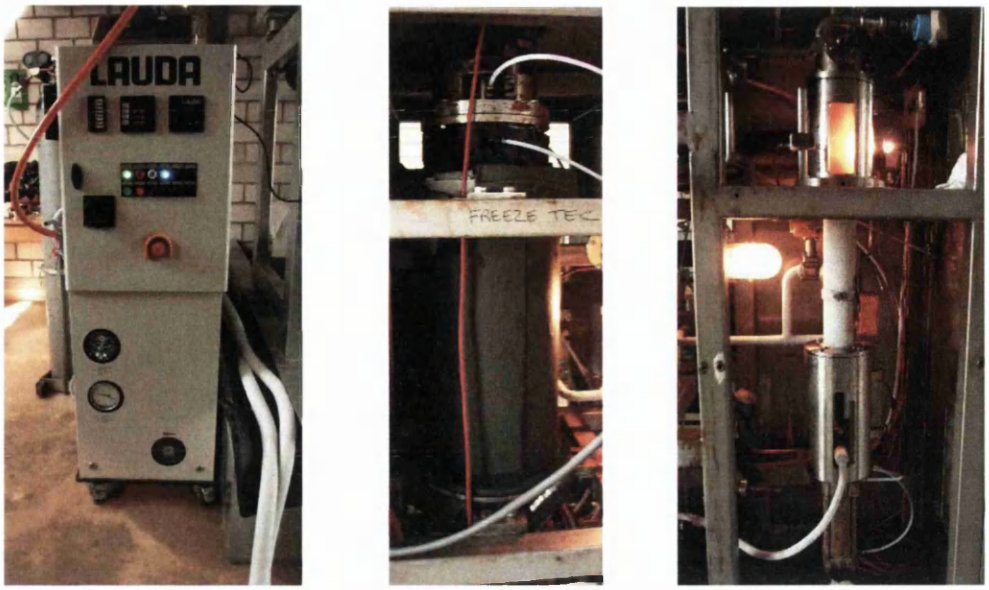

(a) Heat transfer unit (b) Crystalliser (c) Wash column

Fig. 6.7: *Pilot plant apparatus.*

Fig (6.8) shows the crystallisation loop (1), and the separation loop (2) within the pilot plant. The crystallisation loop consists of a feed tank (3), a melt circulation pump (M-102) (4), a crystalliser (5), an ice scraper motor (M-101) (6), a refrigerant circulation pump (M-104) (7), a refrigerant heat exchanger (8), a heat transfer unit (9), and a slurry supply valve (YV-201) (10). The separation loop consists of a piston type wash column (11), an ice scraper motor (M-200) (12), a melting loop (13), a filtrate discharge valve (YV-202) (14), a filtrate recycle valve (YSV-205) (15), a filtrate reject valve (YV-203) (16), and a product output valve (YV-204) (17). The melting loop (13) contains a product circulation pump (known by Sulzer as a Meltloop pump) (M-220) (18), meltloop pressure valve (YSV-206) (19), product heat exchanger (20), and heating system (known by Sulzer as a Melter) (H-200) (21). The pilot plant is also provided with a cabinet light (22), and air heating system (23). The purpose of the cabinet light is mainly for illumination purposes. The air heating system comprises a heater and fan. The air heating system is used to avoid ice encasing the main components and pipelines of the pilot plant. The pilot plant also contains other equipment, such as a feed pump (YSV-400) and an external wash pressure system (P-225); however, these items of equipment were not used in the experiments. For identification purposes, codes were given to equipment items in order to identify them in the software package (e.g. the code for the melt circulation pump is M-102).

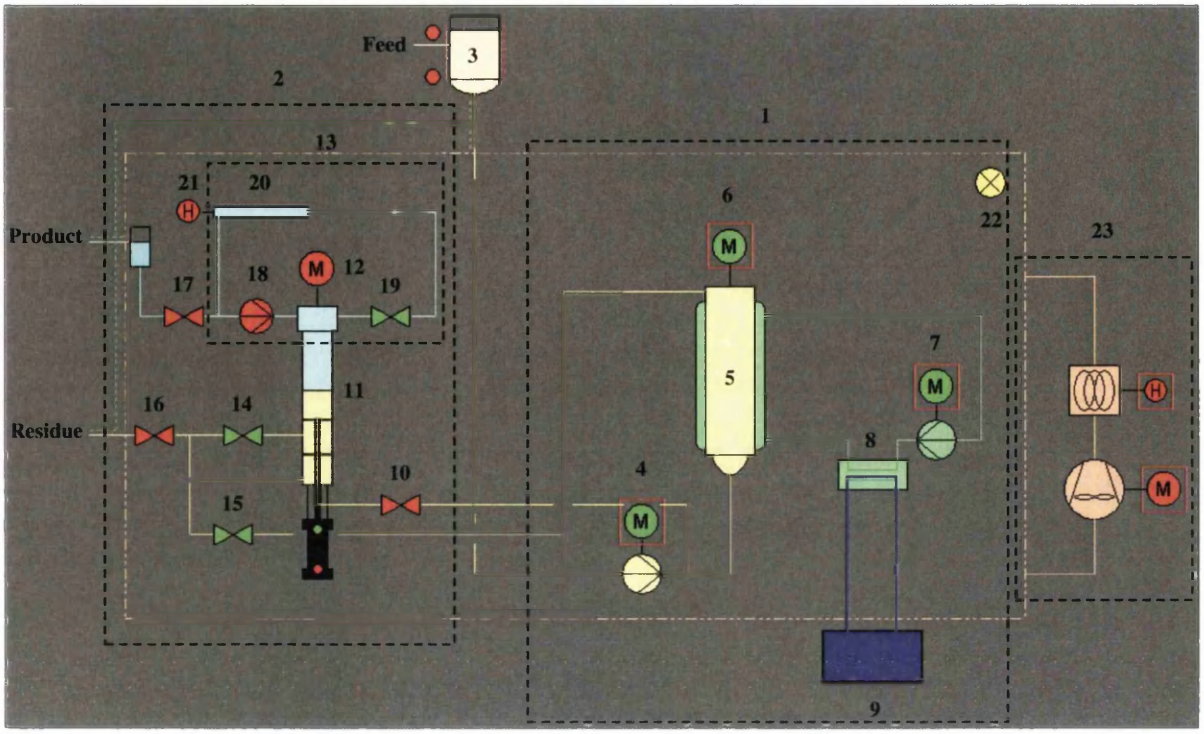

Fig. 6.8: *Flow process diagram of the pilot plant (adapted from a screen shot of the computer package).*

All valves involved in the pilot plant are classified as automatic valves, except for the five valves that deal with the melt, which are hand-operated ball valves. The feed valve is used to allow feed fluid to flow from the feed tank to the crystallisation loop by gravity. The product and residue valves are used for the purpose of sampling. Two bleed valves have been used to remove air pockets present in the crystallisation and separation loops, before starting the experiment.

The pilot plant is connected to a notebook computer as illustrated in Fig (6.9). The notebook computer holds a software package for leading and controlling the operation of the pilot plant. Moreover, the software package records and compiles the operational data of the pilot plant. The installed software package is known as "Plot-Chem", and was published by Sulzer Chemtech Company. Fig (6.9) (b) shows a screen shot of the pilot plant software used in the experimental investigation.

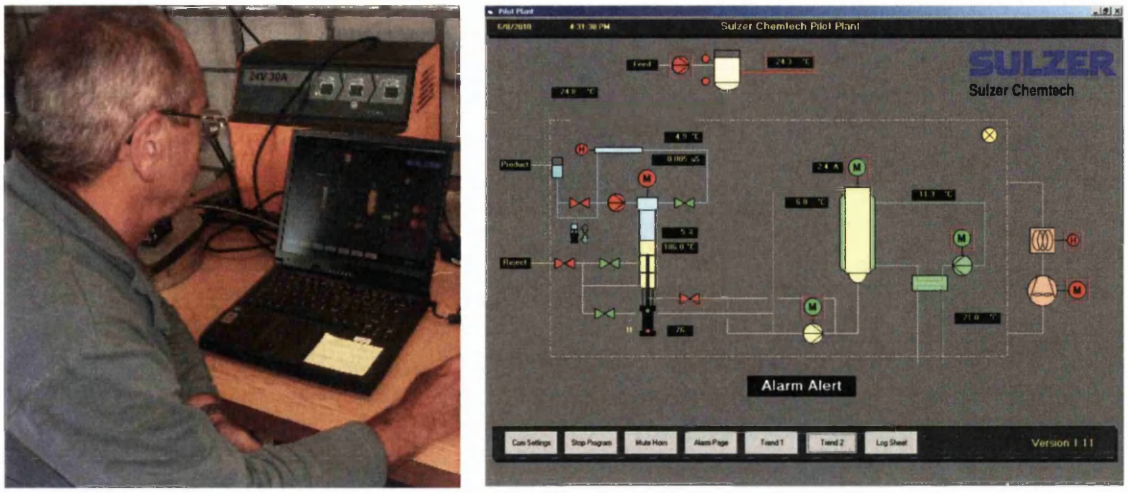

(a) Notebook computer with a package (b) Screen shot of the pilot plant software

Fig. 6.9: *Apparatus for controlling and maintaining the pilot plant.*

Fig (6.10) (a) shows the wash column unit with melt after the filling process, while Fig (6.10) (b) shows the wash column unit with crystals whilst optimizing the washing operation.

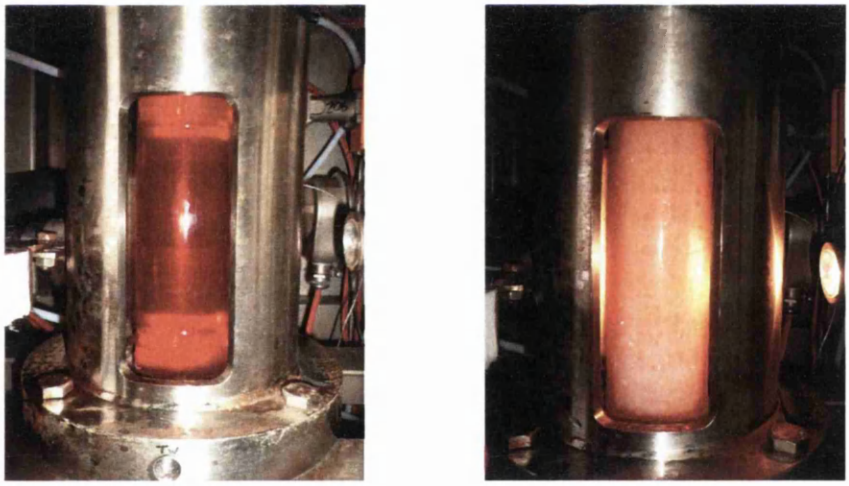

(a) Wash column with melt (b) Wash column with crystals

Fig. 6.10: *Cylindrical glass of wash column.*

The body of the pilot plant contains two sight glasses, which are installed in the front of the wash column unit as shown in Fig (6.6). The sight glasses enable the user to visually observe the behaviour of the separation process and monitor performance of the piston drive.

As illustrated in Fig (6.6), the pilot plant has an insulated feed tank installed above the crystalliser. The feed tank is covered with a lid, which is used to avoid thermal energy losses and protect the feedstock from the entry of dust, suspended matter, particles, etc. The feed tank has a resistance wire (i.e. heating element), wrapped around it, to control the feed temperature inside the tank during pilot plant operation. The resistance wire heating is controlled and driven by a computer.

6.6 Experimental Procedure

The operating procedure for the experiments is summarised in Fig (6.11). These experiments were carried out in batch mode, with assistance of Sulzer's technicians, namely, F. Lippuner and H. Engstler. The initial operating parameters were set by the inventor of the treatment unit, i.e. H. Jansen.

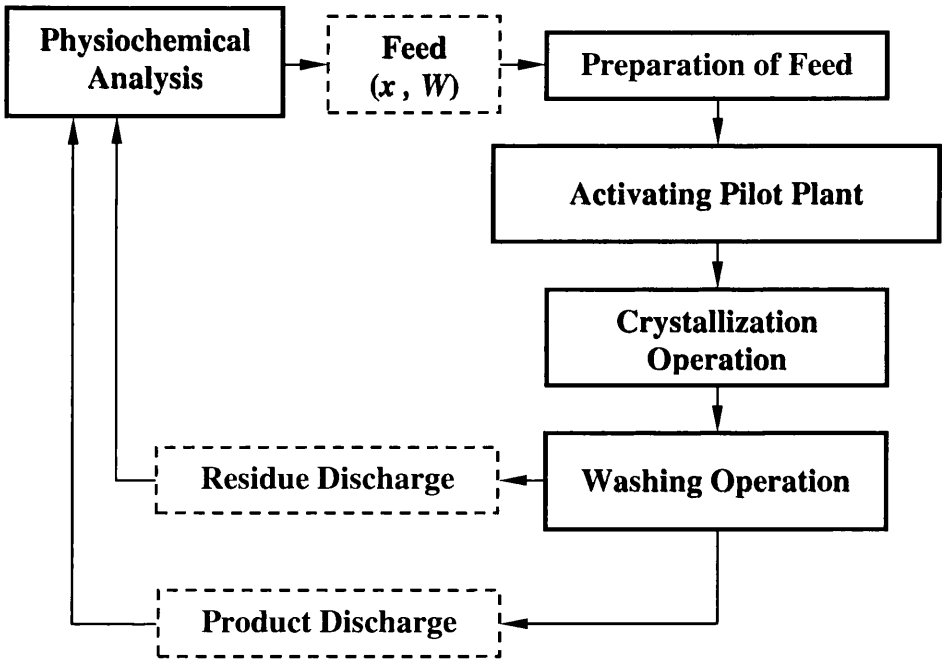

Fig. 6.11: *Simplified block diagram of the operational procedure for the suspension crystallisation experiments, where x and W are feed concentration (ppm) and sample weight, respectively.*

The preparation phases of the feed sample before starting the experiment are filling, adding colour indicator, blending, loading the crystallisation and separation loops, air bleeding, and sampling as shown in Fig (6.12).

(a) Filling (b) Feed before adding colour indicator

(c) Adding colour indicator (d) Blending the mixture

(e) Final feed before loading the system (f) Bleeding air and sampling

Fig. 6.12: *Preparation phases before operating the pilot plant.*

Initially, the feed valve was set to a fully closed position, and the feed tank was loaded with a predetermined amount of feed as shown in Fig (6.12) (a). Unfortunately, the separation process of the wash column was controlled by means of light cells (this is due to the pilot plant being designed for food applications), and since the RO retentate is colour-less, a colour indicator (Chromotrope FB, MKBD4111, Sigma-Aldrich) needed to be added before the experiments were carried out. Before starting the experiment, the final feed sample was

made by dissolving a weighed amount of a colour indicator in a known weight of RO retentate. Upon completion of the feed preparation, the feed tank was then covered with a lid.

The crystallisation and separation loops were then filled with a feed sample by opening the feed valve. The air bleeding procedure was performed to remove air from the crystallisation and separation loops through the ventilation valves, as shown in Fig (6.12) (f). Alongside air bleeding, a sample of the final feed was taken for the physiochemical analysis.

Before activating the operation of the pilot plant through the notebook computer, the heat transfer unit (HTU) was operated, and simultaneously, the internal circulation of the HTM takes place inside the refrigerant heat exchanger of the pilot plant. The HTU temperature controller was manually set to -6°C to refrigerate the crystalliser by means of the refrigerant heat exchanger. However, the HTM temperature of the refrigerant heat exchanger was not reduced below the freezing temperature of the feed before starting the ice scraper motor of the crystalliser and melt circulation pump; otherwise the scraper blades of the crystalliser would be damaged or stick due to the formation of crystals.

Following activation of the heat transfer unit, the feed valve was manually closed. Therefore, the remaining feed inside the feed tank will be automatically fed to the crystalliser by means of the melt circulation pump, when the pilot plant begins to output product water.

Upon completion of the filling procedures and activation of the HTU, the computer control system was prepared to operate the pilot plant. As illustrated schematically in Fig (6.13), the package offers seven operational buttons (i.e. icons), which are; "Com Settings", "Stop Program", "Mute Horn", "Alarm Page", "Trend 1", and "Trend 2", and "Log Sheet", presented at the bottom of the display screen. These operational buttons have functions depending on the particular operation being carried out. For example, Fig (6.13) shows a schematic process flow diagram on the display screen for executing the operating control strategy, which is available under a "Com Settings" option. The operating settings of the pilot plant are fully managed within this option. The operation of the pilot plant is terminated through a "Stop Program" option. When an operational problem is detected, the warning horn sounds (this can be terminated on the display screen via a "Mute Horn" option). The causes of the operational problems can be determined on the display screen via an "Alarm Page"

option. The operational buttons, such as "Trend 1", "Trend 2", and "Log Sheet", are available for monitoring and recording the operational status of the pilot plant during the experiment. In this experimental study, the operational data, including feed tracing, discharge and close time, crystallisation temperature, residue temperature, wash temperature, wash front percentage, wash front temperature, time cycle action, stroke, tracing lines, and cabinet temperature were continuously monitored and recorded along the actual running hours. In addition, the HTM temperature generated from heat transfer unit, bed height, and product concentration (e.g. electrical conductivity, freezing point, and TDS) were measured and recorded over a specific time period. A complete record of the operational data is shown in Appendix A6-1 – A6-2. Throughout the experimental investigation, the trends in the temperature profiles of the HTM and residue were monitored and recorded on the display screen via a "Log Sheet" option.

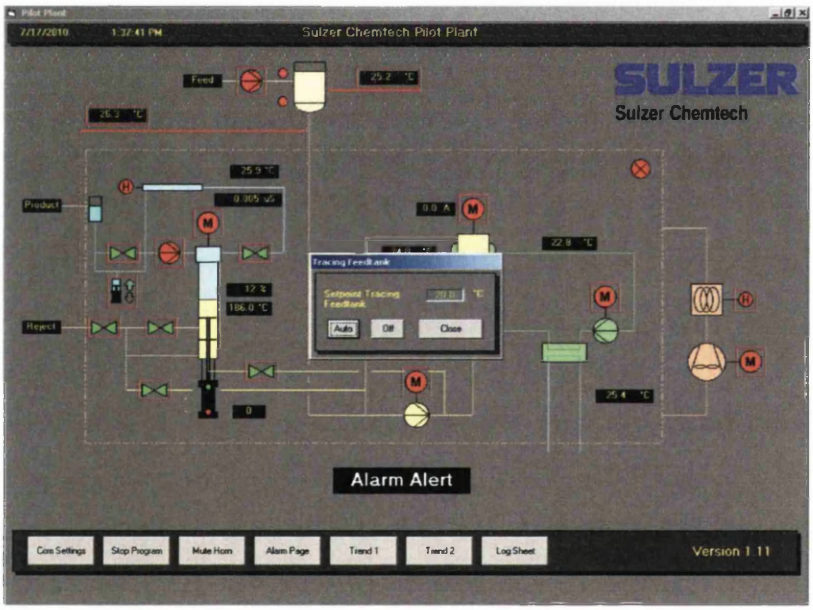

Fig. 6.13: *Screen shot of the pilot plant software with a dialog window of feed tank setting.*

Upon selection of the feed tank symbol, within the "Com Settings" option, a dialog window will be displayed (see in Fig (6.13)), giving the user an option to determine the operating mode, which is either automatic or turning off. The user can also insert the set-point temperature for the feed tank. This procedure is then followed by closing the dialog window via a "Close" option.

In order to specify the desired operating settings of the wash column, the wash column logo (symbol) must to be selected, leading to a dialog window as illustrated in Fig (6.14). This dialog window enables the user to specify the desired operating settings for the wash column system. For all experiments, the wash column settings were set to constant values. Details of the wash column settings are given in Appendix 6, found in a CD attached to the thesis (see file name: Appendix, Microsoft Excel spreadsheet, Sheet: Appendix 6, Tables A6-1 – A6-2). However, the time cycle adjustment was initially set to 120 seconds at the beginning of the experiment. For clarification, the time cycle adjustment is the total time for completing the four stroke cycle for the piston drive in the wash column.

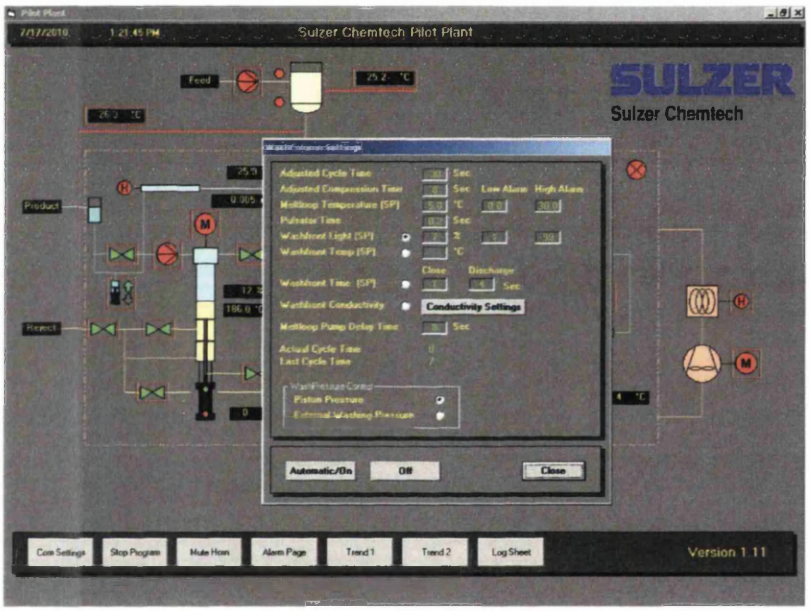

Fig. 6.14: *Screen shot of the pilot plant software with a dialog window of wash column settings.*

The operating mode of some equipment in the pilot plant must be set to automatic. This was achieved by selecting the desired equipment symbol button (which is available in the "Com Settings" option), giving the user an option to select the operating mode, either automatic or manual. An example for determining the operating mode of the ice scraper motor is illustrated in Fig (6.15). This procedure was applied individually for the majority of equipment in the pilot plant, including the product circulation pump (i.e. Meltloop pump) (M-220), slurry supply valve (YV-201), product output valve (YV-204), feed pump (YSV-400), filtrate discharge valve (YV-202), filtrate recycle valve (YSV-205), filtrate reject valve (YV-203), heating system (i.e. Melter) (H-200), and meltloop pressure valve (YSV-206).

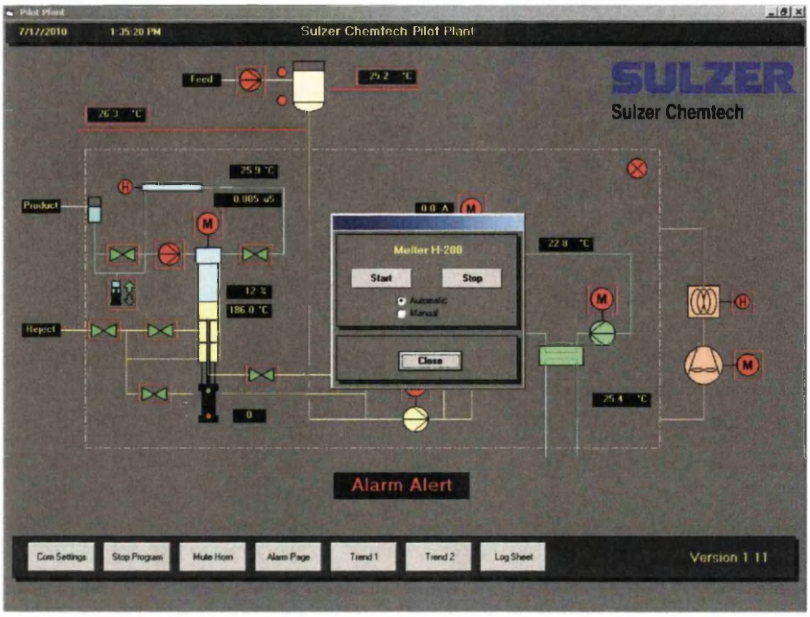

Fig. 6.15: *Screen shot of the pilot plant software with a dialog window for setting the heating system of melting loop (i.e. melter).*

Upon selection of other equipment, such as the ice scraper motor (M-101), the melt circulation pump (M-102), the refrigerant circulation pump (M-104), and the ice scraper motor (M-200), a dialog window will be displayed, giving the user the option to either activate or deactivate the operation of the selected system. An example of this is illustrated in Fig (6.16). For all the ice scraper motors, the motor rotational speed was kept at a constant value of 1500 rpm.

After the above tasks have been completed, the pilot plant is operated in automatic mode. Apart from the heat transfer unit, the operation of the pilot plant is managed completely by the computer's software. The user can check the operational status of the equipment through the colour of the symbol of the equipment. For instance, green means that the system is in operation, while red indicates that the system is not yet operational.

For all tests, the wash column logo was selected once more, to insert new values for the time cycle adjustment throughout the experiment. The time cycle adjustment was gradually decreased, at intervals, from 120 seconds to 60 seconds.

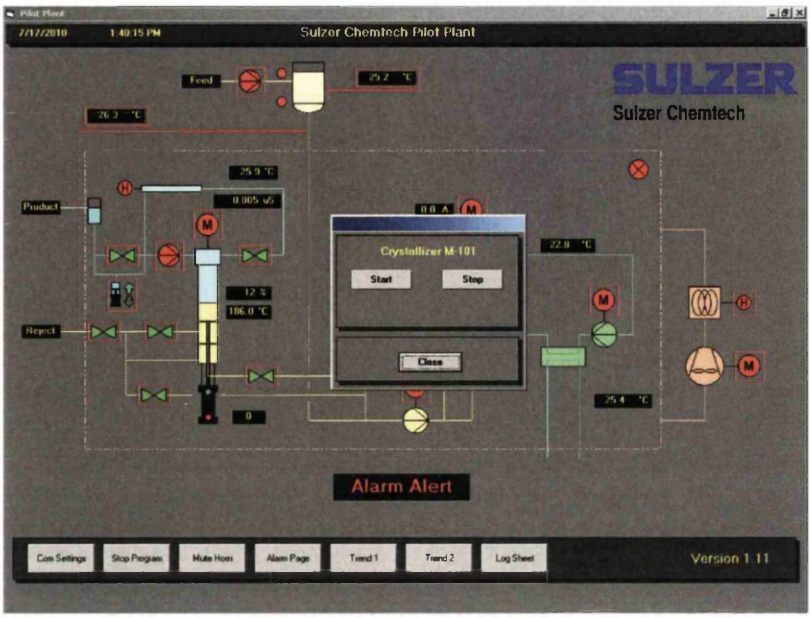

Fig. 6.16: *Screen shot of the pilot plant software with a dialog window for setting the scraper motor in the crystalliser.*

When the pilot plant is operated, the crystallisation temperature was reduced to a desired value (which mainly depends on feed concentration); for instance, -10°C was applied for RO retentate. For clarification, the crystallization temperature means the temperature of the HTM used for refrigerating the crystallizer. A reduction in a crystallisation temperature leads to a decrease in the temperature of the bulk liquid (which will be known as operating residue temperature) to a slightly lower value than the freezing point of the feed. The ice crystals are easily nucleated and formed inside the crystalliser because the cooled melt inside the crystalliser is agitated by two methods, which are stirring and melt circulation. The ice scraper assembly is also used as an agitator inside the crystalliser, while the melt is continuously re-circulated inside the crystalliser by means of a melt circulation pump. When the ice crystals are initiated on a cooled surface, these crystals are periodically scraped off (via the scraper's blades) and removed to the bulk liquid. The crystal growth occurs on the crystals suspended in the bulk liquid [Ulrich and Glade, 2003]. The nucleation behaviour and growth process for the tested solution were monitored though the trend of residue temperature profile, which is available on the display screen via a "Log Sheet" option.

As suspension ice forms, the solute concentration increases, leading to a decrease in the freezing point of the remaining residual liquid. Therefore, the crystallization temperature was further reduced. The aim of this step is to produce an estimated 30 wt% crystal slurry in the

crystallizer. For clarification, the weight ratio of crystal slurry inside the crystallisation loop will be identified and referred to, in the course of this chapter, as crystal slurry ratio. The crystal slurry ratio must be balanced in the crystalliser throughout the pilot plant operation. The crystal suspension is then transported to the wash column. The washing steps for the wash column unit then take place to purify the crystals and output product water.

When the crystals can be visually observed through the glass window of the wash column, the wash column symbol was selected in order to reduce the time cycle adjustment from 60 to 35 seconds. Throughout the experiment, the key-parameter (i.e. time cycle adjustment) was changed according to the separation performance of wash column unit, dictated by the quality of product water.

In the wash column, the crystals are compressed to a firm crystal bed by means of a piston drive. Above the piston head, the compressed crystal bed is surrounded by mother liquor, including impurities. On the opposite side of the compressed crystal bed, the crystal bed is scraped off (via a scraper) and becomes slurry (once more) in a melting loop. The crystals are melted via a heating system (i.e. Melter) installed in a simple heat exchanger.

This pilot plant has never before been examined for treating RO retentate; so, there is no reference data available for such an application. Although there are a number of operating parameters that can be used to optimise and improve the performance of the pilot unit, only two key-parameters, namely the time cycle adjustment and the crystallization temperature, were periodically adjusted based on trial and error. When the desired quality of product water was obtained, then the settings of these two parameters were kept constant until the quality of product water started to decline slightly.

Therefore, product water samples were periodically (i.e. at specific time intervals throughout the experiment) collected from the melting loop for physiochemical analysis of TDS, electrical conductivity, and freezing point. The electrical conductivity gives an instant reading to evaluate the quality of product water before collection of the final product water. When the product water reaches a desired quality, the product valve was set to the fully open position to collect the final product water from the melting loop as shown in Fig (6.17). If the

product water is of poor quality, the product valve was set to the fully closed position to carry out further purification of the final product water through the separation loop.

Fig. 6.17: *Collection of final product water samples for run 1.*

When the product water is collected, the solute concentrations will increase. Consequently the freezing point of the remaining residual liquid is reduced. As mentioned previously, the crystallisation temperature was reduced gradually over time, in order to maintain the crystal slurry ratio at 30 wt%; otherwise, the performance of the pilot plant will deteriorate.

This experimental investigation dealt with two different types of residual liquids, which have different physiochemical properties. The first will be known as the "operating residue", and is re-circulated with ice slurry inside the crystallisation loop. When the experiment is completed, the pilot plant must be shut down to collect the residual liquid for physiochemical analysis. When the pilot plant is turned off, separation of the remaining ice slurry from the operating residue inside the crystallisation and separation loops was impossible, and even so, the remaining ice slurry would not be purified. Therefore, the remaining ice slurry inside these loops was melted and mixed with the remaining residual liquid i.e. operating residue. Therefore, the final residual liquid (which will be known as the "final residue") has completely different physiochemical properties than that in the operating residue. For instance, the salt concentration of the operating residue must be higher than that of the final residue. However, the final residual liquid was separated from the crystallisation and melting

loops by gravity. This residual liquid was then collected and taken for physiochemical analysis.

7.7 Results and discussion

The trial tests were limited in run number and time to only achieve the objectives of this chapter. A summary of the experimental data is presented in Table (6.1). A complete record of the experimental data and performance parameters versus actual running time is also given in Tables A6-1 – A6-4 in Appendix 6. For clarification, performance optimisation of the pilot plant was performed based on the maximum salt rejection ratio. Sub-runs a-1, b-1, and c-1 represent trial tests to optimise performance of the pilot plant, and to determine the operating limits and the optimal process conditions. These tests correspond to a multistage operation, in order to increase the water recovery ratio of the suspension pilot plant whilst carrying out the experiments. For commercial applications, the actual operation of the suspension crystallisation process will be carried out in a single-stage process. For the optimised pilot plant operation, sub-runs a-2 and b-2 examined the performance of pilot plant to minimise the RO retentate as much as possible and to determine the quality of product water. T1 represents the overall experimental data of sub-runs a-1, b-1, and c-1, whereas T2 represents the overall experimental data of sub-runs a-2 and b-2. This means that T1 and T2 represent a continuous operation test corresponding to single-stage operation.

Table (6.1) shows that the pilot plant was tested with different salt concentrations of RO retentate ranging from 61,139 up to 99,886 ppm. Table (6.1) also shows that sub-runs a-1 and a-2 utilised the RO retentate from the Kadhmah (RO) desalination plant as a feed material. The TDS value of the feed water used in sub-run a-1 is slightly higher than that in sub-run a-2. This is due to the different mass ratio between the colour indicator and RO retentate for sub-run a-1 compared to sub-run a-2. Before starting sub-run a-1, the feed sample was prepared by dissolving a mass of 10.53 g of colour indicator into a mass of 116.959 kg of RO retentate. For sub-run a-2, the feed sample was prepared by dissolving a mass of 3.09 g of colour indicator into a mass of 86.829 kg of RO retentate. Details of the samples preparation are given in Tables A6-1 and A6-3 in Appendix 6. The concentration of colour indicator was slightly reduced in order to reduce the colour concentration of feed, and improve the separation performance and wash column performance, which is controlled by light cells

Run	Sub - Run	Feed			Product			Residue			WR*	SR**	RT	APFR
		Mass	TDS	Freezing Point	Mass	TDS	Freezing Point	Mass	TDS	Freezing Point				
		(kg)	(ppm)	(°C)	(kg)	(ppm)	(°C)	(kg)	(ppm)	(°C)	(%)	(%)	(h)	(kg/h)
1	a-1	116.97	61,200	-3.10	23.51	1,200	-0.07	93.46	76,292	-4.23	20.10	98.04	3.13	7.50
	b-1	93.46	76,292	-4.23	22.12	200	-0.03	71.34	99,886	-5.80	23.67	99.74	2.93	7.54
	c-1	71.34	99,886	-6.07	4.65	15,000	-0.52	66.69	105,805	-6.20	6.52	84.98	0.63	7.34
T1		116.97	61,200	-3.10	50.28	2,036	-0.11	66.69	105,805	-6.20	42.99	96.67	6.7	7.50
2	a-2	86.832	61,139	-3.10	21.713	80	-0.03	65.119	81,498	-4.50	25.01	99.87	2.93	7.40
	b-2	65.119	81,498	-4.50	13.599	160	-0.04	51.52	103,004	-5.90	20.88	99.80	1.83	7.42
T2		86.832	61,139	-3.10	35.312	111	-0.03	51.52	103,004	-5.90	40.67	99.82	4.77	7.41

Table 6.1: *Summary of performance data for the pilot plant used for treating different salt concentrations of RO brine, where; WR is the permeate water recovery ratio, SR is the salt rejection ratio, RT is the running time, and APFR is the average product flow-rate.*

** Water recovery ratio is computed as mass ratio of product water to the treated feed. Water recovery ratio = (product / feed) x 100.*

*** Salt rejection ratio describes the quantity of salt which is removed by the suspension pilot-plant computed as a percentage. Salt rejection ratio = ((feed concentration - product concentration) / feed concentration) x 100.*

activated by the colour of the ice crystal bed. Upon completion of each sub-run, the final product was collected for chemical analysis, whereas the final residual liquids were collected at the end of the final sub-runs c-1 and b-2 for chemical analysis. The results for this remaining residual liquid from sub-runs a-1, b-1, and a-2 were analytically determined using mass and salt balance formula, and the phase diagram. Fig (6.18) shows the water samples of product and residue that have been collected and taken for physiochemical analysis. Full chemical analyses were carried out on water samples from run 2.

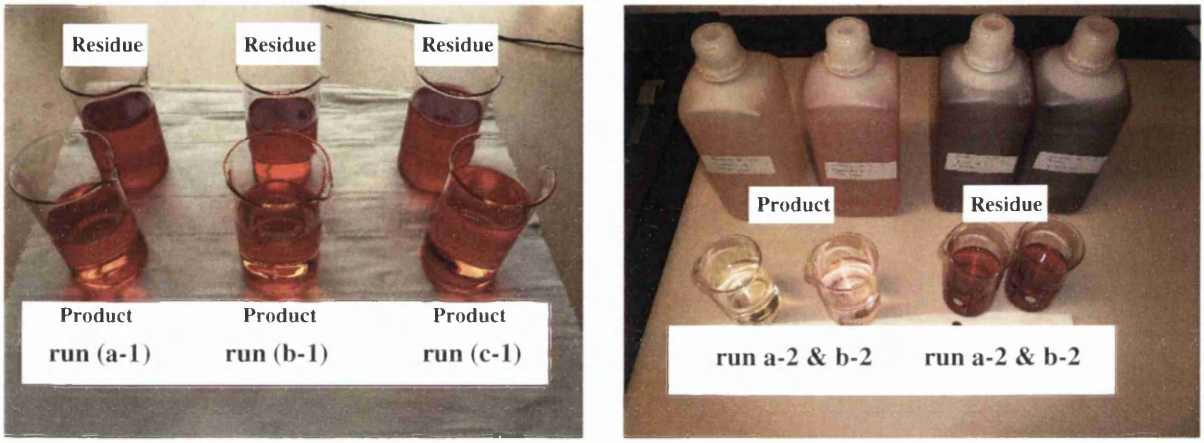

(a) Water samples from run 1 (b) Water samples from run 2

Fig. 6.18: *Final product water and residue samples for runs 1 and 2.*

Although sub-runs a-1, b-1, and c-1 represent initial trial parametric tests used for optimising the operating key-parameters, nevertheless, preliminary experimental results show that the suspension pilot plant was potentially capable of recovering high purity product from RO retentate. Table (6.1) shows that the overall salt rejection and permeate water recovery ratios were 96.67% and 42.67%, respectively, for run 1. The pilot plant tested was able to reduce the TDS value from 61,200 ppm down to 2,036 ppm, taking into account that, the TDS value of feed and permeate product were 61,200 and 1,200 ppm respectively, for sub-run a-1, and were 76,292 and 200 ppm respectively, for sub-run b-1, as shown in Table (6.1). In sub-run a-1, the pilot plant produced a final product at a TDS value, which is slightly higher than that in drinking water standards, which should be not be exceeding 1,000 and 500 ppm according to the World Health Organization (WHO) and Food and Drug Administration (FDA) standards, respectively [Sumerjian, 2011]. When the process key-parameters of the pilot plant were set to within the optimum operating limits in the subsequent freezing stage (i.e. sub-run b-1), the pilot plant was potentially capable of producing a final product ready for immediate use, taking into consideration that the salt concentration of feed (used in sub-run

b-1) was higher than that in sub-run a-1. This was mainly due to the optimum operating conditions not being known, and applied in the initial test i.e. run a-1. When the operating temperature of the residual liquid reached -8.2°C, deterioration in the separation performance of the pilot plant was observed, resulting in product water quality becoming relatively poor, for sub-run c-1. However, the pilot plant produced saline water of near brackish water quality. With regard to deterioration in the performance of the pilot plant, further investigation was carried out in sub-run b-2 to check whether this limitation occurred due to process optimisation or other factors, which will be discussed later herein this section.

In general, the total results from run 1 (see Table (6.1)) for the final product were quite encouraging. Nonetheless, the pilot plant did produce a final product of near drinking water standards in terms of TDS. As mentioned previously, this was mainly due to the optimal operating conditions not being determined and applied in the initial test (i.e. run a-1). Moreover, the quality of product water declined further, because of deterioration of pilot plant performance, when the operating temperature of the residual liquid reached -8.2°C.

As for run 2, the performance of the pilot plant was monitored over an actual operational period of 4.77 hours. The actual testing period was longer than the stated running time, due mainly to minor optimisations performed for the pilot plant to improve the quality of product water before collection. Fig (6.19) shows the operating and performance parameters for the pilot plant versus actual running time. Fig (6.19) (a) shows that the start-point temperature of crystallisation and operating residue were -11.3 and -4.6°C, respectively, while the end-point temperature of crystallisation and operating residue were -19.4 and -8.2°C, respectively. Fig (6.19) (b) shows that the time cycle adjustment was kept at a constant value (which is 35 seconds) during the course of operation, while the time cycle action averaged about 29 seconds up to 2.77 h of actual operation, and then rapidly declined to an average time of 21.5 seconds. Therefore, the reduction in the time cycle action indicated a decrease in the operational period of the separation process, leading to an increase in the total product water output. The maximum and minimum values of time cycle action were 31 and 20 seconds, respectively. Fig (6.19) (c) shows that the bed-height averaged about 31 mm, and more specifically, the bed-height was maintained at constant value (which is 30 mm) from the operational period of 2.93 h until the end of the test. The average product flow-rate was 7.41 kg/h as shown in Table (6.1). During the course of operation, final product water samples

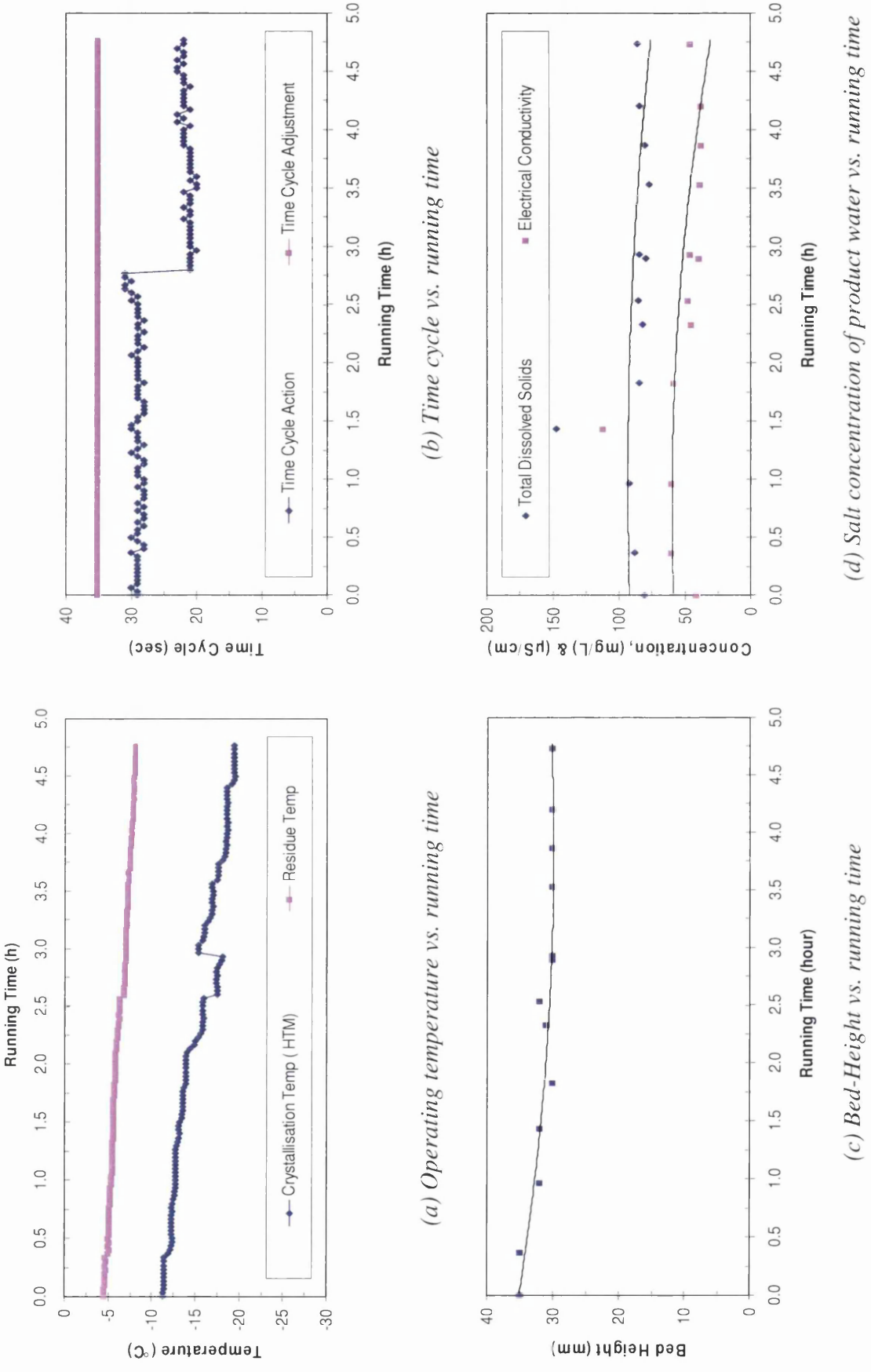

(a) Operating temperature vs. running time *(b) Time cycle vs. running time*

(c) Bed-Height vs. running time *(d) Salt concentration of product water vs. running time*

Fig. 6.19: *Experimental data of run 2.*

were periodically collected from the melting loop for chemical analysis. Fig (6.19) (d) shows that the maximum and minimum TDS value of product water sample was 174 and 77 mg/L, respectively. This means that the TDS values of product water measured below 175 ppm at all times, which gives a clear indication that the pilot plant was potentially capable of producing a final product water of near drinking water quality. During the collection of product water samples, the pilot plant was occasionally able to produce product water of near transparent solution, similar to drinking water as shown in Fig (6.20). Visual observations confirmed the physiochemical analyses. The colour indicator in these product water samples disappeared entirely in comparison with feed sample, which indicates that the dissolved salts have been significantly reduced. However, a slight amount of colour indicator was visually observed in the other samples of product water, and therefore the final product water samples from runs a-2 and b-2 contain a slight amount of colour indicator as shown in Fig (6.18). Nonetheless, these were much lighter than the feed sample. For commercial applications, the appearance of colour indicator will not represent an obstacle that could negatively affect the commercial application. The underlying reason is that the separation process of wash-column will be controlled via electrical conductivity instead of light cells. Hence, the colour indicator will not be used and so will not be observed in the final product water.

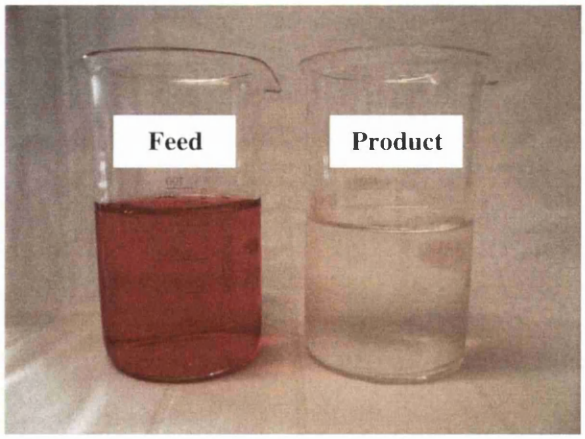

Fig. 6.20: *Product water sample from sub-run (a- 2) in comparison with feed sample.*

In general, the overall results from run 2 proved that suspension crystallisation was able to lower the salt concentration from 61,139 ppm to 111 ppm at considerable yield. Table (6.1) shows that the overall product water recovery and salt rejection ratios were 40.67 and 99.82%, respectively. The concentration of RO retentate achieved was over 59% at a TDS value of 103,004 ppm.

A summary of physiochemical analysis of the water samples for run 2 in comparison with Kadhmah (RO) desalination plant is presented in Table (6.2). The Kadhmah (RO) desalination plant consists of two RO units using a series product staging method. Table (6.2) shows that the average TDS value of seawater fed to the RO plant was 49,074 ppm, while the TDS value of RO retentate fed to the suspension pilot plant was 61,139 ppm. Nevertheless, the TDS value of product water of the suspension plant is slightly lower than that in the RO plant, taking into account that the feed concentration of the suspension pilot plant is much higher than that in the RO plant. Furthermore, the RO plant consists of two stages of RO units, while the suspension unit is a single stage. The salt rejection ratio of the suspension pilot plant is slightly higher that that of the RO plant, where the salt rejection ratios were 99.82 and 99.67%, respectively. In addition, the water recovery ratio of suspension pilot plant is much higher than that of the RO plant, where the water recovery ratios were 40.67 and 14.28%, respectively. Table (6.2) shows that the average hardness ion values of Ca^{2+}, Mg^{2+}, and $(SO_4)^{2-}$ for RO retentate fed to the suspension crystallisation were 1,476, 1,463, and 4,800 mg/L, respectively. The suspension crystallisation pilot plant was capable of reducing the hardness ions down to approximately 6, 10, and 4 mg/L, respectively. Also, Table (6.2) shows that the RO retentate fed to the suspension pilot plant was enriched with Na^+ and Cl^- ions at concentrations of 20,881 and 32,200 mg/L, respectively, whereas the suspension pilot plant was able to reduce these concentrations down to about 141 and 100 mg/L, for the same ions, respectively.

Table (6.3) compares the major ionic composition of product water from the suspension pilot plant to famous bottled water brands that are commercially sold in the markets of many countries around the world. This gives a clear indication that the product water of the suspension pilot plant emulates international and regional premier bottled waters. Although the product water from the suspension pilot plant was enriched with Na^+ and Cl^- ions in comparison with RO product (see Table (6.2)), these concentrations are still within the accepted limits, and are comparable to, and comply with international standards for drinking and bottled waters as shown in Table (6.4). Table (6.4) provides clear evidence that the product water from the suspension pilot plant was produced within the allowable international limits, in terms of TDS, pH, and major ionic composition. Table (6.4) shows that the product water from suspension pilot plant contains acceptable levels of Na^+ and Cl^-

Parameter	Unit	Kadhmah (RO) Desalination Plant			Sulzer Suspension Pilot Plant (run 2)		
		Feed	Product	Brine	Feed	Product	Residue
Mass	kg	-	-	-	86.832	35.312	51.52
Flow Rate	(m^3/h)	27.30	3.9*	21.9	-	0.007	-
pH	-	7.13	7.6	7.42	7.42	7.20	7.40
TDS	(mg/L)	49,074	160	61,139	61,130	111	103,004
Conductivity	(mS/cm)	63.6	0.43	76	76	0.35	124
Freezing Point	(°C)	-2.76	-0.13	-3.1	-3.1	-0.11	-5.88
Ca^{2+}	(mg/L)	1,080	50	1,476	1,476	5.7	1,454 (> 1,476)
Mg^{2+}	(mg/L)	1,387	2	1,463	1,463	10.24	1,902
Na^{+}	(mg/L)	16,523	12	20,881	20,881	141	23,475
Cl^{-}	(mg/L)	25,480	18	32,200	32,200	100.27	79,101
$(HCO_3)^{-}$	(mg/L) as Ca CO_3	175.6	135	241.2	241.2	1.8	364
$(SO_4)^{2-}$	(mg/L)	3,900	3	4,800	4,800	3.69	7,352
NO_3^{-}	(mg/L)	2.7	1.7	2	2	< 0.05	3.5

Table 6.2: *Major physiochemical analysis of water samples of suspension pilot plant in comparison with Kadhmah (RO) desalination plant.*

** First stage of RO membrane assembly produces product water of 8 m^3/h and 6.5 m^3/h is fed to second stage of RO membrane assembly, while the remaining product water of first stage (i.e. 1.5 m^3/h) is not used and drained (see Fig (6.21)).*

Parameter	Unit	Pilot Plant	Abraj	Al-Rawdatain	Gulfa	Buxton	Highland Spring	Volvic	Evian
		Under Research	Kuwait	Kuwait	U.A.E.	UK	UK	France	France
pH	-	7.2	7.8	7.8	8.1	7.4	7.8	7.0	7.18
TDS	(mg/L)	111	112	168	120	280	170	109	309
Ca^{2+}	(mg/L)	6	25	45	19	55	40.5	11.5	80
Mg^{2+}	(mg/L)	10	5	7	29	19	10.1	8	26
Na^{+}	(mg/L)	141	7	9	21	24	5.6	11.6	6.5
Cl^{-}	(mg/L)	100	55	9	56	37	6.1	13.5	6.8
$(HCO_3)^{-}$	(mg/L) as Ca CO_3	1.8	50	155	155	248	150	71	357
$(SO_4)^{2-}$	(mg/L)	4	20	22	44	13	5.3	6.9	12.6
NO_3^{-}	(mg/L)	< 0.05	1	8	5.9	< 0.1	3.1	6.3	3.7

Table 6.3: *Chemical composition of product water of suspension pilot plant in comparison with national and international premier bottled water brands.*

Parameter	Unit	Pilot Plant	WHO	IBWA	CAC	LIBNOR	FDA	EU
		Under Research	Drinking Water	Bottled Water	Bottled Water	Bottled Water	Bottled Water	Bottled Water
pH	-	7.2	6.5-9.5	6.5-8.5	-	6.5-8.5	-	6.5-9.5
Conductivity	(μS/cm)	347	-	-	-	-	-	2500
TDS	(mg/L)	111	1,000	500	-	500	500	-
Ca^{2+}	(mg/L)	6	-	-	-	81	-	-
Mg^{2+}	(mg/L)	10	-	-	-	50	-	-
Na^{+}	(mg/L)	141	-	-	-	150	-	200
Cl^{-}	(mg/L)	100	250	250	-	200	250	250
$(SO_4)^{2-}$	(mg/L)	4	-	250	-	250	250	240
NO_3^{-}	(mg/L)	< 0.05	50	44	50	45	44	50

Table 6.4: *Chemical composition of product water of suspension pilot plant in comparison with international standards related to the quality of drinking water and bottled water adopted from Sumerjian (2011), where; WHO: The World Health Organization (WHO), IBWA: International Bottled Water Association, CAC: Codex Alimentarius Commission, LIBNOR: Lebanese Standards Institution, FDA: Food and Drug Administration, and EU: European Union standards.*

ions, while maintaining low concentrations in hardness ions (such as; Ca^{2+}, Mg^{2+}, and $(SO_4)^{2-}$) and NO_3^-.

In general, experimental data has proven the suspension pilot plant is potentially capable of providing a product ready for immediate use, i.e. for human consumption, and simultaneously able to concentrate the waste stream of RO plant to a considerable degree. The performance results obtained provided clear evidence that the proposed treatment system would be ideal for concentrating the RO retentate, and more specifically, the RO retentate with a TDS value of less than 80,000 ppm.

In order to increase the permeate water recovery ratio, the operating temperature of the residue can be reduced down to -15°C, as long as the eutectic point is still far away from the residue temperature. When the operating residue temperature was reduced below -8.2°C in sub-run b-2, a gradual deterioration in the separation performance of the pilot plant was observed. The TDS value of the product water increased rapidly up to 1,500 ppm, and then fluctuations in the TDS value of product water occurred, with a gradual increase until this value reached 15,000 ppm. At this stage, a number of attempts were made to improve the quality of product water by optimising the key operating parameters. Unfortunately, all these attempts failed to improve the product quality. In fact, this phenomenon was previously detected in run 1, more specifically in sub-run c-1, and similar behaviour was also noticed during operation, at an operating residue temperature of -8.2°C. This confirms that the allowable operating temperature of the residue should not be less than -8.2°C. The reason for this performance deterioration may be explained by one of the following; (i) the optimal operating conditions were not reached at low operating temperature, and this was due to the experimental investigation being carried out over a limited number of tests, and key operating parameters; (ii) the solubility limit of one or some salts in the residual liquid might have been reached. Table (5.7) shows the solubility limits of major salts available in seawater. Although precipitation of solid salts was not visually observed from the experiments, Table (6.2) demonstrates signs of precipitation of salts composed of the following ions; Ca^{2+}, Mg^{2+}, and Na^+, because there are significant percentage losses in their ionic concentration, which are 41.47, 22.66, and 33.11%, respectively; (iii) precipitation of solid colour indicator. However, based on the visual observation, there was no clear sign of salts precipitation composed of colour indicator in the remaining residual liquid, and in the

pilot plant equipment throughout the experiments; and (iv) precipitation of solid sodium sulphate (i.e. $Na_2SO_4.10H_2O$) in the residual liquid. According to [Pounder, 1965], when the temperature of seawater is reduced below -8.2°C, some of the sodium sulphate might be precipitated. This means that the seawater will exist in three different phases, solid H_2O, solid sodium sulphate ($Na_2SO_4.10H_2O$), and remaining residual liquid. This critical temperature (i.e. -8.2°C) does not represent the eutectic temperature for seawater. However, at this temperature, some solid salt phase begins to appear in the remaining residual liquid [Pounder, 1965]. Precipitation of solid salts was not visually observed from the experiments. However, there is a sign of precipitation of salts composed of $(SO_4)^{2-}$ and Na^+ since the percentage losses in their ionic concentration are 9.09 and 33.11%, respectively (Table (6.2)).

Table (6.1), specifically sub-run c-1, shows that the pilot plant was able to reduce the TDS value of the feed from 99,886 ppm down to 15,000 ppm. The experimental results were not encouraging when the operating temperature of the residue reached -8.2°C or less, where the pilot plant did not produce a final, near potable quality, product. However, the pilot plant produced final water of near brackish water quality that can be easily treated by brackish water RO membranes to reach a final product water of near drinking water quality. This gives a clear indication that the suspension crystallisation system can be used for desalting RO retentate, in a rectification stage, and also for concentrating the residue of a previous stage, at a stripping stage.

This experimental investigation dealt with two different types of residual liquids, namely a final residue and the operating residue. The water sample of the operating residue was not considered for chemical analysis in this study, as the remaining ice crystals could not be separated from the operating residue. However, the operating residue will be considered as the final residue for commercial applications, because commercial plant will be equipped with a filtration system, which enables recovery of the remaining ice crystals from the crystalliser. According to Sulzer, two possible scenarios for recovering the remaining ice crystal from the crystalliser can be applied. The first scenario is to remove the ice crystals and operating residue from the crystalliser, and these are separated by a filtration system, and then the ice crystals can be purified and recovered via a wash column unit. The second scenario is to remove the operating residue from the crystalliser leaving the ice crystals behind through a filtration system. This means that the remaining ice crystals will be mixed

with the incoming feed water in the crystalliser before starting the subsequent freezing stage. The step helps either; (i) to dilute the incoming feed water and simultaneously decrease the incoming feed temperature (when the incoming feed temperature is higher than its freezing point), which will result in an increase in the permeate water recovery ratio compared to the previous stage as the feed concentration will be significantly reduced, or (ii) to maintain the crystal slurry ratio at 30 wt% ready inside the crystallization loop when the temperature of the incoming feed reaches its freezing point.

The first scenario might be more feasible for desalting and concentrating RO retentate, and this is due to the increased total permeate water recovery ratio and simultaneously reduced waste stream (as far as possible). However, the economic aspects (i.e. capital cost and energy consumption), and process simplicity and reliability must be taken into consideration to determine which scenario is the most suitable for desalination applications.

The product water recovery ratios for the pilot plant were theoretically computed at different temperatures of operating residue. These analytical calculations were performed on different saline waters, such as ocean seawater, Arabian Gulf seawater, and Reverse Osmosis (RO) brine. Details of the analytical calculations and results are given Tables A6-5 – A6-10 in Appendix 6. For simplification, several assumptions were considered in these analytical calculations, namely; (i) the TDS value of product water was assumed to be 111 ppm as found in the experimental run 2 (see Table (6.1)); (ii) The mass of feed was assumed to be 86.832 kg, i.e. the same as that in experimental run 2 (see Table (6.1)); (iii) The TDS value of feed is constant, which is dependant on the type of saline water being treated (i.e. ocean seawater (35,000 ppm), Arabian Gulf seawater (49,000 ppm), and RO brine (61,000 ppm)); (iv) The TDS values of the residue were obtained from a phase diagram. By rearranging salt and mass balance formulas, the remaining unknowns, which are the masses of product and residue, can be theoretically obtained, leading to the permeate water recovery ratio being determined; (v) The pilot plant can produce a final product water of near drinking water standards, until the residue temperature reached -15°C; (vi) The operating residue was assumed to be the final residue (i.e. all ice crystals in the pilot plant were recovered and purified).

Fig (6.21) shows the influence of feed concentration and residue temperature upon the water recovery ratio. As expected, the water recovery ratio is not proportional to both the feed salt concentration, and the residue temperature. Fig (6.21) shows that the lower residue temperature leads to an increase in the water recovery ratio. This is in agreement with the experimental data presented in Fig (6.21). Moreover, the lower initial salt concentration of feed leads to an increase in the water recovery ratio. When the pilot plant is individually fed with ocean seawater, Arabian Gulf seawater, and RO brine, then at residue temperature of -6°C, the estimated permeate water recovery ratios are 66.09%, 52.48%, and 40.72%, respectively. When the residue temperature is further decreased to -8.2°C, then the permeate water recovery ratios will be increased to 72.83%, 61.92%, and 52.49%, for the same saline waters, respectively. By reducing the residue temperature down to -15°C, then the estimated permeate water recovery ratios reached 82.28%, 75.17%, and 69.02%, for the same saline waters, respectively.

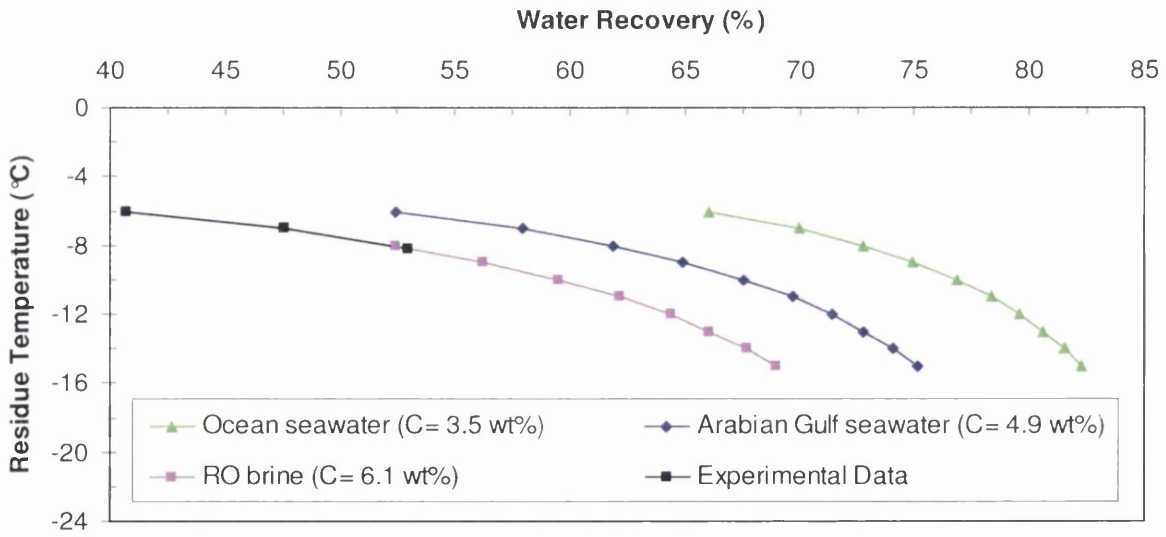

Fig. 6.21: *Predicted and experimental data of water recovery ratio measured at different residue temperature for different types of saline water.*

The scale-up for such an application is straightforward, because commercial plant can be established by adding the appropriate number of crystallisation and separation loops to achieve the required capacity [Ulrich and Glade, 2003]. This experimental investigation was carried out with the RO retentate of Kadhmah (RO) desalination plant, and so Kadhmah (RO) desalination plant was used as an example for scaling-up the suspension plant. This example will give an estimated figure of the mass and salt concentration of the three liquid

streams for large-scale application using continuous mode. These figures were also used for estimating the water treatment costs. The proposed treatment system was scaled-up according to the experimental results obtained from run 2, taking into consideration that the temperature of the operating residue was -8.2°C. Hence, a water recovery ratio of 53% was obtained from the experimental graph as shown in Fig (6.21). The TDS value of product was 111 ppm (i.e. mass percent of 0.01%) according to run 2 results (see Table (6.1)), whereas the volume flow-rate of product was determined by the water recovery ratio. The salt concentration of the residue was determined from the phase diagram corresponding to -8.2°C, whereas the volume flow-rate of the residue was determined by mass balance. A novel treatment option configuration, which represents an integration of RO plant and suspension crystallisation plant is shown in Fig (6.22). Fig (6.22) also shows that the estimated figures for the salt concentration of the feed, product, and residue are 6.1%, 0.01%, and 13% by weight of salt, respectively, whereas estimated figures for the volume flow-rates are 21.9 m^3/h, 11.61 m^3/h, and 10.29 m^3/h, for the same water streams, respectively. According to Sulzer, this commercial plant can be established without any limitation; however, such an application might be hindered by the economic aspect, e.g. capital and operational costs.

Table (6.5) shows the estimated annual rates of drinking water production, RO retentate, and residual liquid of Kadhmah RO plant, suspension commercial plant, and combined desalination plant. Table (6.5) shows that the estimated annual rate of RO retentate was significantly reduced from 191.84 to 90.14 ton/year by treating the RO retentate of Kadhmah RO plant through a large-scale application of the suspension crystallisation process. Furthermore, the production of drinking water can be substantially increased from 34.17 to 135.87 ton/year by incorporating the commercial scale suspension crystallisation process into Kadhmah RO plant.

The crystal slurry ratio was recommended to be maintained at 30 wt% before starting to collect the product water. However, the product water collection depends mainly on the desired quality. Therefore, simple calculations were performed to determine the theoretical value of the crystal slurry ratio, and the corresponding residue temperature used for run 2 (i.e. sub-run a-2). These calculations were also used to obtain the temperature of operating residue corresponding to the crystal slurry ratio of 30 wt%. Details of the analytical calculations and the results are given in Tables A6-11 – A6-12 in Appendix 6. The theoretical

results showed that the crystal slurry ratio and the operating residue temperature are 26.37% and -4.6°C, respectively, for run 2 (i.e. sub-run a-2). In order to maintain the crystal slurry ratio at 30%, then the temperature of operating residue must be reduced down to -4.9°C, according to the analytical calculations.

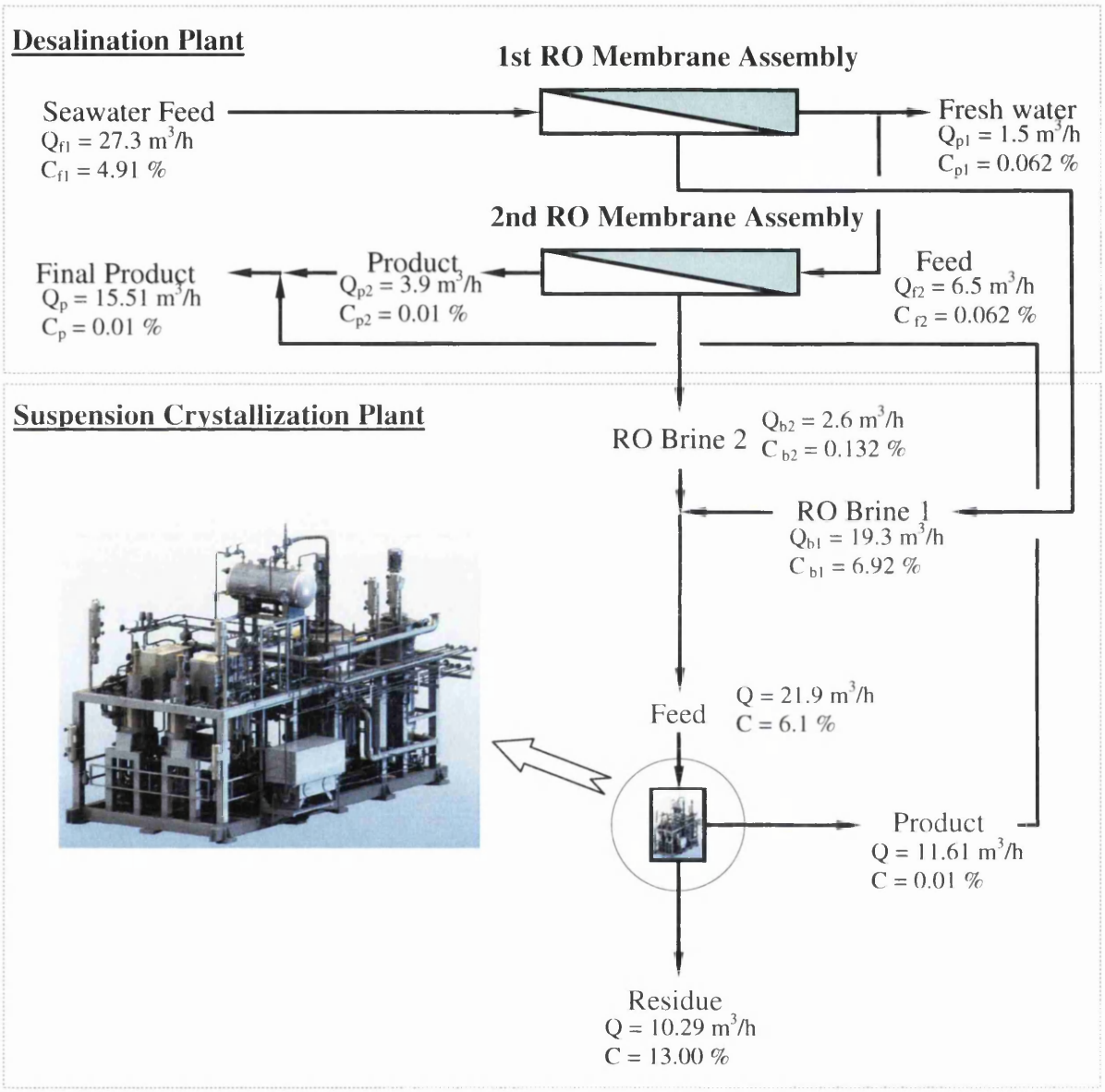

Fig. 6.22: *Combination of commercial plant of seawater Reverse Osmosis (RO) membrane desalination plant coupled with suspension crystallization plant, where; Q is the volume flow-rate (m^3/h), and C is the salt concentration, where subscript f= feed-water, p= product water, b= brine, and 1 and 2 refer to the stage number.*

Kadhmah RO Plant			Suspension Plant			Combined Plant		
Feed	Product*	Brine	Feed	Product	Residue	Feed	Product*	Residue
(t/y)	(t/y)	(t/y)	(t/y)	(t/y)	(t/y)	(t/y)	(t/y)	(t/y)
239.15	34.17	191.84	191.84	101.70	90.14	239.15	135.87	90.14

Table 6.5: *Estimation of the annual rates of all water streams of Kadhmah RO desalination, suspension crystallisation, and combined plants, where (t/y) represents ton per year.*

** The first stage of the RO membrane assembly produces product water at 8 m^3/h and 6.5 m^3/h of this is fed to the second stage RO membrane assembly, while the remaining product water from the first stage (i.e. 1.5 m^3/h which is equivalent to 13.14 t/y) is not used and drained (see Fig (6.22)).*

6.8 Power Requirement Analysis

The accurate specification of a complete commercial plant used for desalting RO retentate depends mainly on the specification conditions, for which the commercial plant is designed. Therefore, different plant capacities including the proposed scaled-up plant (see Fig (6.21)) were considered in the present analysis. Furthermore, different quality levels of feed and product water were covered in this analysis. The power requirement analysis for the proposed commercial plant involves three main steps; namely, mass-balance, stage calculation, and refrigeration. Details of the analytical calculations and results are given in Tables A6-13 – A6-16 in Appendix 6, found in a CD attached to the thesis (see file name: Appendix_1, Microsoft Excel spreadsheet, Sheet 1, Tables: A7.1-4).

In order to determine the equipment required, and the power consumption of a commercial plant, a typical example of a commercial plant was used. In this context, the following assumptions were made: (i) the mass flow rate and salt concentration of the feed water are 17,800 kg/h and 6 wt%, respectively, (ii) the water recovery and salt rejection ratios of the commercial plant are 50% and 100%, respectively, (iii) the power consumption of the pre-cooling unit, feed intake facilities, pre-treatment system, post-treatment unit, and auxiliary equipment and pumps were not considered in the power requirement analysis.

First Step: Mass Balance

The first step in developing a design model for the commercial plant is to establish a scheme for determining the mass flow-rate and salt concentrations for all streams of the commercial

plant. For any desalination system, the mass flow-rate of feed water (m_f) must equal the sum of the mass flow-rates of product water (m_p) and brine (m_b), as given by:

$$m_f = m_p + m_b \tag{6.1}$$

Also, the overall salt and mass balance can be analytically determined by:

$$m_f x_f = m_p x_p + m_b x_b \tag{6.2}$$

where x represents the salinity, while the subscripts f, p, and b refer to the feed-water, product, and brine (i.e. residual liquid), respectively.

By substituting equation (6.1) into (6.2), the mass flow rate of the product water can be theoretically calculated as follows:

$$m_p = m_f \left[\frac{x_b - x_f}{x_b - x_p} \right] \tag{6.3}$$

When the mass flow rate of the product water is determined, then the mass flow rate of the brine can also be determined by re-arranging equation (6.1), which gives:

$$m_b = m_f - m_p \tag{6.4}$$

Alternatively, the values of mass flow rate of the product water and salt concentration of residual liquid can be theoretically determined in terms of the water recovery ratio (WR) and salt rejection ratio (SR); since these ratios were previously assumed. The WR and SR ratios are given by:

$$WR = \left(\frac{m_p}{m_f} \right) \times 100 \tag{6.5}$$

$$SR = \left(1 - \frac{x_p}{x_f}\right) \times 100 \tag{6.6}$$

The mass flow rate of the product water can be calculated from equation (6.5), whereas the salt concentration of residual liquid can be theoretically determined by substituting equations (6.5) and (6.6) into equation (6.2), which gives;

$$x_b = \frac{m_f x_f}{m_b} \tag{6.7}$$

Table (6.6) shows the overall results of salt and mass balance for the proposed commercial plant. These results will be considered in the second and third steps of the power requirement analysis.

Feed		**Product**		**Residue**	
Mass Flow-Rate	**Salt Concentration**	**Mass Flow-Rate**	**Salt Concentration**	**Mass Flow-Rate**	**Salt Concentration**
(kg/h)	(wt%)	(kg/h)	(wt%)	(kg/h)	(wt%)
17,800	6	8,900	≈ 0	8,900	12

Table 6.6: *Results of overall mass balance (adapted from Sulzer).*

Second Step: Stage Calculation

This stage is mainly devoted to estimating the capacity and quantity of the equipment items, which are required for the proposed commercial plant. Stage calculations involved the following equations:

The mass flow rate of ice production (m_i) equals the mass flow rate of product water.

$$m_i = m_p \tag{6.8}$$

The mass flow rate of liquid out (m_{LO}) also equals the mass flow rate of ice production.

$$m_{LO} = m_i \tag{6.9}$$

The weight ratio of the residue (R_r) can be described by the following expression:

$$R_r = 1 - R_i \tag{6.10}$$

where (R_i) is the weight ratio of crystal slurry. For the case of a single freezing-stage process, the weight ratio of crystal slurry of 100% was considered.

The mass flow rate of Liquid In (m_{LI}) is given by:

$$m_{LI} = m_p + \frac{m_i}{R_r} \tag{6.11}$$

The m_{LI} must equal the sum of the mass flow rates of the ice slurry out (m_{SO}) and liquid out (m_{LO}), which can be theoretically calculated by the following:

$$m_{LI} = m_{SO} + m_{LO} \tag{6.12}$$

Rearranging equation (6.12), m_{SO} can be calculated as follows:

$$m_{SO} = m_{LI} - m_{LO} \tag{6.13}$$

Table (6.7) shows the stage calculation results. Table (6.8) shows a list of installation items of equipment at different sizes used for building commercial plants (adapted from Sulzer).

Stage	Ice Production (m_i)	Ice Ratio (R_i)	Liquid In (m_{LI})	Liquid Out (m_{LO})	Ice Slurry Out (m_{SO})
	(kg/h)	(%)	(kg/h)	(kg/h)	(kg/h)
1	8,900	100	17,800	8,900	0

Table 6.7: *Results of stage calculation (adapted from Sulzer).*

According to the analytical calculations, the items of equipment to be supplied for the proposed commercial plant were selected from Table (6.8). Table (6.9) shows each item of equipment listed separately with its installed and anticipated operating power. The total energy consumed by the sum of the items in the equipment list is 113 kW as shown in Table (6.9).

Third Step: Refrigeration

The heat transfer rate (i.e. heat energy (Q_f)) for cooling the feed water is given by:

$$Q_f = m_f C_p (T_2 - T_1) \tag{6.14}$$

where m_f, C_p, T_1, and T_2 represent the mass flow-rate of feed, specific heat capacity of RO retentate, and start-point and residue temperatures of the feed, respectively.

Table (6.10) illustrates the results of the energy consumption due to refrigerating the feed. The start-point temperature of feed was assumed to be 0°C, in order to minimise the energy consumption. This can be achieved by cooling the incoming feed through the heat exchanger, which is used as a pre-cooling system. The power consumption of the pre-cooling unit was not studied in this analysis. Table (6.10) shows that a total energy of 170.3 kW will be required to reduce the temperature of the feed water with a mass flow-rate of 17,800 kg/h from 0°C to -8.2°C.

Equipment	Growth Vessel					Crystalliser					Wash-Column			
	Size (m^3)					Size (m^2)					Size (mm)			
	0.6	3.0	5.0	7.5	10.0	0.5	2.0	4.0	6.0	12.0	220	350	600	1,000
	Anticipated Operating Power (kW/piece)													
Vessels	7.5	15.0	22.0	22.0	30.0									
Crystalliser						3.0	5.5	7.5	15.0	22.0				
Melt Circulation Pump						1.5	3.0	4.0	5.5	7.5				
HTM Circulation Pump						-	2.2	3.0	5.5	7.5				
Wash-Column Scrapper											2.0	5.5	7.5	11.0
Melt Loop Pump											0.5	0.75	1.5	2.5
Piston Drive											Pneumatic		7.5	15.0

Table 6.8: *Recapitulation of electrical drives for standard process components in kilowatt (kW) (adapted from Sulzer).*

Equipment	Quantity	Installed Energy Capacity	Total Energy Consumption	Unit Energy Consumption Percentage	Total Energy Consumption	Factor	Heat to product		
Unit	-	kW/Piece	kW	(%)	kW		kW	S1	S2
30 m^3 Growth Vessel	1	55	55	60	33	0.9	29.7	29.7	0
12 m^2 Crystalliser	6	22	132	30	39.6	0.9	35.64	35.64	0
Melt Circulation Pump	6	7.5	45	80	36	0.9	32.4	32.4	0
W100 Scrapper	2	11	22	25	5.5	0.9	4.95	4.95	0
W100 Melt Loop Pump	2	2.5	5	80	4	0.9	3.6	3.6	0
W100 Hydraulic Unit	2	15	30	25	7.5	0.9	6.75	6.75	0
HTM Circulation Pump	6	7.5	45	80	36				
HTM Circulation Pump (1)	0	3	0	80	0				
HTM Charger Pump	1	3	3	80	2.4				
Compressor	1	859	859	70	601				
Condenser	0	0	0	80	0				
Total	27	-	1195.73		765.113	-	113.04	113	0

Table 6.9: *Capital equipment of the proposed plant design (adapted from Sulzer).*

Feed	Feed Temperature	Residue Temperature	Specific Heat Capacity	Total	
(m_f)	(T_1)	(T_2)	(C_p)	(Q_f)	
(kg/h)	(°C)	(°C)	(kJ/kg.°C)	(kJ/h)	(kW)
17,800	0	-8.2	4.2	613,032	170.3

Table 6.10: *Results of energy consumed for refrigerating the feed (adapted from Sulzer).*

The heat energy required for changing the phase of the liquid at a mass flow-rate of 8,900 kg/h to solid (i.e. ice crystals) is calculated from:

$$Q_p = m_p \Delta H_f \tag{6.15}$$

Table (6.11) shows that a total energy of 823.25 kW will be required to change the phase of product water with a mass flow-rate of 8,900 kg/h from liquid to solid, i.e. producing ice crystals.

Mass ice crystal (m_p)	Latent Heat of Fusion of water (ΔH_f)	Total (Q_p)	
(kg/h)	(kJ/kg)	(kJ/h)	(kW)
8,900	333	2963,700	823.25

Table 6.11: *Results of energy consumed for changing the phase of product mass flow-rate.*

A summary of the specific power consumption of the proposed plant design is given in Table (6.12). The total power requirements for such a typical plant design, having a capacity of 8,900 kg/h, is 124 kWh/m^3. The total power consumption however is high. The energy consumed for changing the phase of product mass (see Table (6.11)) represents the highest portion of the total power consumption, which is approximately 74%.

Specific Power Consumption	Unit	Total
Refrigerating Feed	kW	170
Ice production	kW	823
Heat to product	kW	113
Total Process Refrigeration Load	kW	1107
Power Consumption by Ice Production	kWh/m^3	92
Total Energy Consumption	kWh/m^3	124

Table 6.12: *Summary of the energy consumption of the proposed plant design.*

The plant specific power consumption was determined for different plant capacities. Fig (6.23) shows plots of predicted specific power consumption versus the mass flow-rate of product water. Fig (6.23) illustrates that the specific power consumption fell sharply from 143.3 to 102.5 kWh/m^3 as the production rate increased from 300 to 2,000 kg/h, and is then followed by a slight decrease in specific power consumption until its value reached 89.7 kWh/m^3 when the production rate of the plant reached 10,000 kg/h. This clearly indicates that designing plants for higher production rates would result in a significant reduction of power consumption.

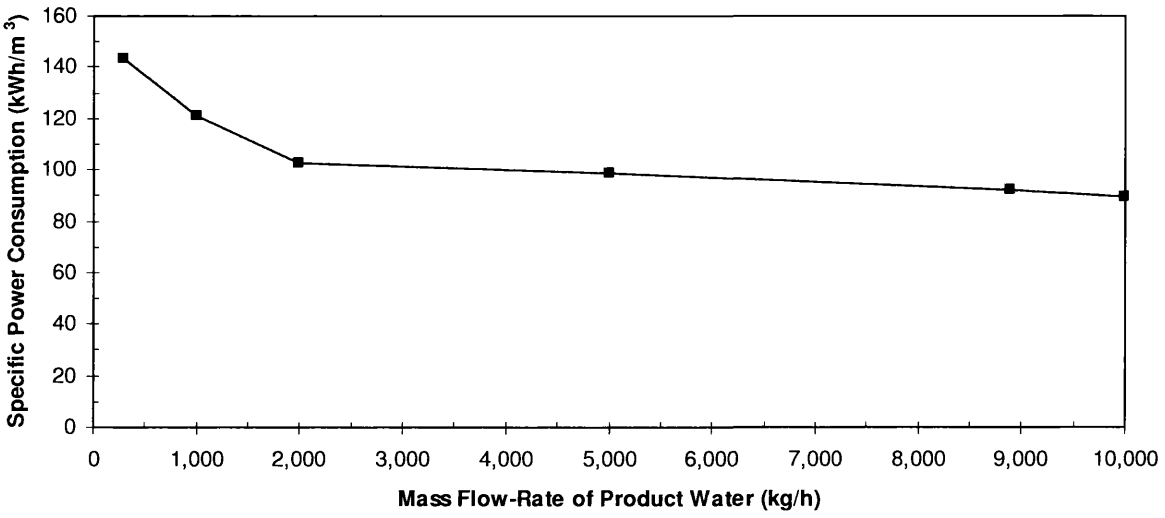

Fig. 6.23: *Plant specific power consumption versus the product mass flow-rate adapted from Sulzer.*

In addition, Table (6.13) shows 5 case studies determined via the present analysis. Cases 1, 2, and 3 were applied to desalting, using RO retentate, Arabian Gulf seawater, and ocean seawater, respectively, as feed water. As for case 4, the power consumption of the commercial plant was estimated for treating RO retentate in order to produce a final product water of near seawater salinity level, instead of deionised water. In case 5, the power consumption of the adopted commercial plant was determined according to the results of scaling-up data presented in Fig (6.22). By comparing cases 1 and 3 (see Table (6.13)), the estimated power consumption was seen to decrease as the TDS value of feed water is decreased. This indicates that the power consumption is proportional to the salt concentration of feed water.

The commercial plant can be optimised to produce final product water of near seawater level, in terms of TDS value, resulting in higher production rates. By comparing cases 1 and 4 (see Table (6.13)), the power consumption was significantly decreased from 124 to 72 kWh/m^3 by increasing the salt concentration of product water from 0 to 49,000 ppm. This clearly indicates that the power consumption can be significantly reduced by increasing the salt concentration of product water. For such an application, the treated water can be easily desalted by seawater RO membranes to reach a final product water of drinking water quality at a much lower treatment cost compared to that in a separate suspension crystallisation plant. As for the empirical and scaling-up data (i.e. case 5), the estimated power consumption is equivalent to 120 kWh/m^3 as shown in Table (6.13).

Case No.	Type of saline water	Feed TDS (mg/L)	Product TDS (mg/L)	Water Recovery (%)	Power Consumption (kWh/m^3)
1	RO retentate	60,000	0	50	124
2	Arabian Gulf seawater	49,000	0	62	118
3	Ocean seawater	35,000	0	73	114
4	RO retentate	60,000	49,000	86	72
5	RO retentate	62,000	111	53	120

Table 6.13: *Summary of the energy consumption of the proposed plant design for treating different types of saline water.*

6.9 Conclusions

This study assessed and validated the viability of using a suspension crystallisation process as a water desalination system for producing drinking water, while concentrating the RO retentate. The tests were limited in their number, and were just enough to draw clear and reasonable conclusions on the separation performance of the proposed desalination system in such an application. The experiments were performed on a suspension pilot plant operating in batch mode.

Although the pilot plant was not equipped for desalination applications, the results were highly encouraging, because it was capable of providing a substantial amount of near potable product water, and simultaneously concentrating the RO brine. The water analysis results showed that the product water quality was comparable to international drinking and bottled water standards. The experimental results showed that the water recovery was around 41%, while the salt rejection ratio reached over 99%. Therefore, the suspension crystallisation process might be competitive with other desalination processes in RO brine applications. Based on the experimental results, the Sulzer suspension crystallisation process was scaled-up and combined with a commercial plant using RO membrane technology. The production rate for the combined plant was estimated and compared to the RO plant only. The theoretical results proved that the combined plant is able to produce a substantial amount of drinking water much more than in the separate RO plant. This was achieved by concentrating the waste steam to a considerable extent.

On the other hand, simple economic analysis was carried out to estimate the power consumption for different applications and also to determine the factors influencing the energy consumption. In general, production rate, and feed and product water concentrations are the main influences on the power consumption of the suspension crystallisation process. The power consumption was estimated and can be varied from 72 to 124 kWh/m^3 for RO brine applications. However, the estimated power consumption is considered to be high when compared to any conventional desalination technology used for seawater applications.

CHAPTER VII:

INVESTIGATING THE FEASIBILITY OF THE STATIC CRYSTALLISATION PROCESS FOR TREATING DIFFERENT CONCENTRATIONS OF REVERSE OSMOSIS BRINES

7.1 Introduction

In the previous Chapters (i.e. 5 and 6), falling film and suspension crystallisation processes were used and examined individually for concentrating/desalting RO brine. According to the experimental results, the suspension crystallisation process was capable of producing high purity product water, reaching drinking water quality standards, at a reasonable product water recovery ratio. On the other hand, the falling film crystallisation process was capable of producing a substantial amount of product water at reasonable quality, reaching Arabian Gulf seawater standards, i.e. feed water of the RO seawater membrane plant. Although the volume of RO brine was significantly reduced and concentrated through the mentioned technologies, the salt concentration of the residual liquids, which were left behind, reached such a high level that these streams cannot be treated further, either by falling film or suspension crystallisation technologies. These waste streams must then be treated in an environmentally friendly way, or they will have severe negative impact on the surrounding environment.

According to the phase diagram of RO brine—given previously in Fig (5.12) (a), the solid layer crystallisation technologies, and more specifically the static crystallisation process, is potentially capable of further concentrating the residue. This is because there is a reasonable temperature difference between the freezing points of the residues, which were discharged from the suspension and falling film crystallisation technologies, and the eutectic temperature of NaCl salt—by far the most dominant dissolved salt compared to other dissolved salts. Therefore, this chapter deals with an experimental investigation into the performance of a static crystallisation process used to treat such waste streams.

A Sulzer static crystalliser was used, with different salt concentrations of RO brines, to assess and validate the technical feasibility of the adopted treatment system. According to Sulzer's experts, this technology has not previously been examined or applied to treating concentrated solutions of RO brine. Thus, there was a lack of experimental data on the performance of this technology in such applications. This investigation represents the first laboratory examination to successfully gather valuable, quantitative information concerning the separation performance of the proposed technology in such applications. This investigation also provided useful and important information on combining two different commercial plants, including the integration of falling film–static crystallisation plants, and integration of suspension–static crystallisation plants. These integrated plants can be used individually as a pre-concentrator system for future commercial applications in RO seawater or brackish-water desalination plants.

The main objective of this study is to determine the viability and assess the technical feasibility of using static crystallisation and sweating processes to produce final product water (either close to the quality of seawater or RO retentate) by concentrating the residues discharged from prior processes, such as the falling film and the suspension crystallisation processes. The specific aims related to this chapter are:

i) To prepare, operate, and test the static crystalliser, with/without use of the sweating process, at different operating conditions while collecting performance data. Along with concentrated solutions of RO brine, Arabian Gulf seawater, and NaCl solutions were individually used and tested as feed water in this study.

ii) To verify the influence of several key parameters, namely feed salt concentration, crystallisation time and temperature, sweating time and temperature, cooling rate, and growth rate, on the performance of the static crystallization and sweating processes, in terms of salt rejection and water recovery.

iii) To validate and evaluate the process' technical merits for future application on a large commercial scale.

iv) To shed light on the effectiveness of the static crystallisation process, combined with a sweating process, in the rejection of the major components

of ionic concentration, such as Ca^{2+}, Mg^{2+}, $(SO_4)^{2-}$, $(HCO_3)^-$, Cl^-, Na^+, etc. in samples from feed, product, and residue water.

7.1.1 Description of the Static Crystallisation Process and Basic Operation

The static crystallisation process is one of the melt crystallisation technologies that was previously introduced in Chapter 5. According to Ulrich and Glade (2003), the important advantages of solid layer crystallisation technologies are (i) incrustation problems are avoided, as these incrustations represent the solid layer, which will eventually be separated, melted, and recovered as final product water; (ii) easily controllable crystal growth rates, due to the driving force being dependant on the temperature difference at the refrigerated surface area of the plate; (iii) a simplified separation process due to absence of an ice slurry. Thus, complicated ice separation and washing equipment, usually used in conventional desalination through freezing processes and melt suspension crystallisation technologies, is avoided. Furthermore, no moving parts are involved in the process equipment (apart from circulation pump); (iv) the operation of the post-crystallisation treatments, such as washing and sweating, are simple; and (v) multistage process design can easily be applied. On the other hand, the limitations of these technologies are summarised in four main points. According to Ulrich and Glade (2003), (a) the surface area of the refrigerated plate is limited; (b) the crystal layer adhered on the heat transfer surface requires an increase in temperature driving force to maintain the constant growth rate; otherwise a reduction in production rate will occur with increasing thickness; (c) the crystallisation and post-crystallisation operations are limited in batch operating mode. This is because the desired crystal layer has to be completely melted and separated from the crystalliser, before starting the subsequent crystallisation operations. This method requires additional energy for the melting process and partial heating up of the whole apparatus. (d) In the case of a multistage process, the operational cost is dramatically increased due to the repetition of the crystallisation process, while the production rate of the overall multistage process is decreased. The last two points may be avoided at some point, when the solid layer crystallisation technology is operated in continuous mode.

The static crystallisation process, which was investigated in this study, is characterised as a stagnant melt with the use of forced convection principles, in batch operating mode. The Sulzer static crystalliser differs from conventional static crystallisers in that it utilises a vertical plate heat exchanger type rather than a tube type heat exchanger, as shown in Fig (7.1). The vertical plate is immersed inside a tank filled with a stagnant melt, enabling the crystal layer to nucleate and grow on a cooled exterior surface of the heat exchanger. The latter is cooled and heated by means of internal circulation of a Heat Transfer Medium (HTM). The operating conditions of the HTM are managed and controlled via a PID temperature controller of the refrigeration system.

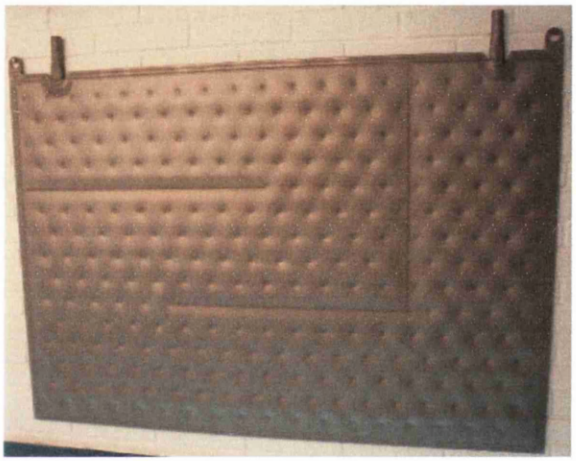

Fig. 7.1: *Plate type heat exchanger used in the commercial Sulzer static crystalliser.*

A typical example of the commercial crystalliser, using Sulzer's static crystallisation process, is illustrated in Fig (7.2), and consists of a sealed tank, number of vertical plate heat exchangers, melt inlet and outlet, and HTM inlet and outlet. As shown schematically in Fig (7.2), the vertical plate heat exchanger is placed inside a tank, where both represent a crystalliser. The latter is provided with a HTM refrigeration unit along with a PID temperature controller. The principles of the Sulzer static crystallisation process are described in more detail in the references [Ulrich and Glade, 2003; Sulzer, 2004]. Sulzer have developed over 200 applications since starting efforts in this field [Ulrich and Glade, 2003], where some typical applications are given in Chapter 5. A wide range of plant capacities for the static crystallisation process is available at Sulzer Chemtech Ltd.

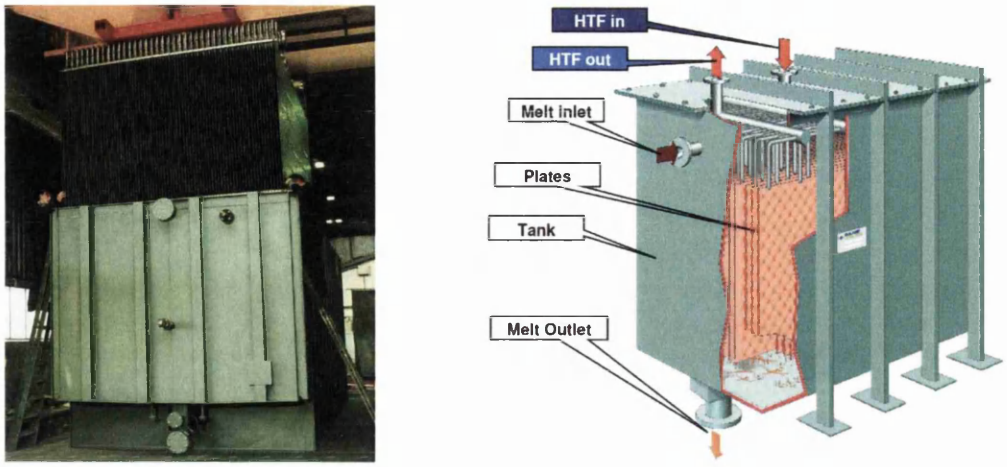

(a) Sulzer static crystallizer (b) Schematic diagram of static crystalliser

Fig. 7.2: *Sulzer commercial static crystalliser [Ulrich and Glade, 2003; Sulzer, 2004].*

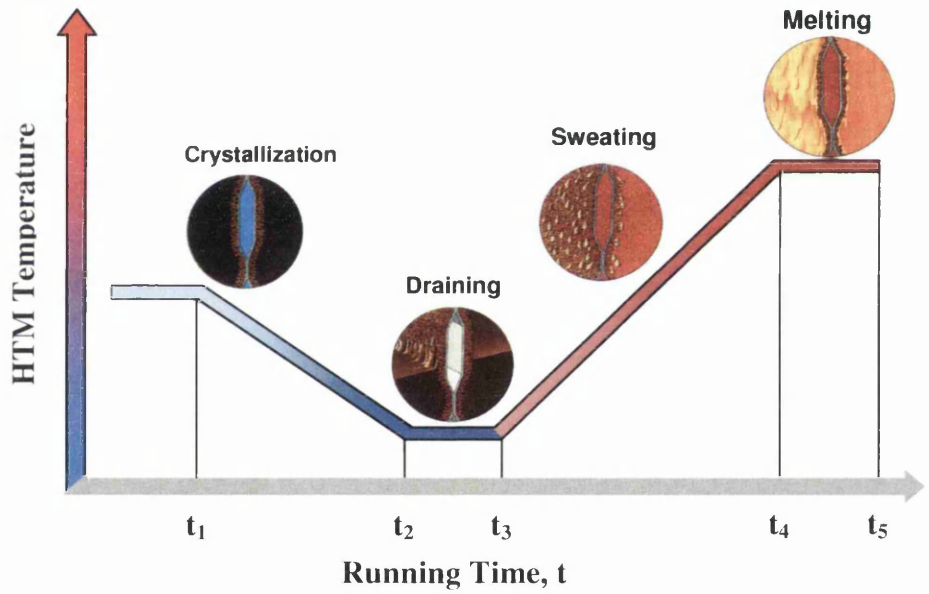

Fig. 7.3: *Process set-point temperature-time profile [Ulrich and Glade, 2003; Sulzer, 2004].*

Similar to the principles of operation of the Sulzer falling film crystallisation plant (given in Chapter 5), the main phases of the Sulzer static crystallisation process are six successive processes, namely (i) filling, (ii) pre-cooling, (iii) nucleation, (iv) crystallisation, (v) partial melting (sweating), and (vi) melting. Fig (7.3) shows the process set-point HTM temperature versus the running time of a complete freezing stage. The major phases of the Sulzer static crystallisation technology, such as crystallisation, draining, sweating, and melting, are also illustrated in Fig (7.3). The set-points temperature and time of these phases is controlled through a PID temperature controller driving the refrigeration system.

(i) Filling process

The crystalliser is filled with the desired mass of feed by opening the melt inlet valve, enabling the melt to flow into the crystalliser through a melt inlet line as shown in Fig (7.2) (b). When the crystalliser is completely loaded with the predetermined amount of feed, then the melt inlet valve is closed.

(ii) Pre-cooling

By passing cold HTM into each vertical plate heat exchanger, the HTM absorbs heat from the melt through the refrigerated surfaces of the plate heat exchanger, and consequently, the temperature of the melt is slowly reduced. By continuously circulating the cold HTM around a plate heat exchanger, the temperature of the melt is lowered until it reaches the predetermined temperature of the melt, which is slightly lower than the freezing point of the feed.

(iii) Nucleation

Once the temperature of the melt reaches the predetermined temperature, a seed ice crystal is usually added to achieve nucleation of ice crystals, which then grow gradually on the heat transfer surface during the crystallisation process.

(iv) Crystallization

When the cold HTM is continuously circulated in a plate heat exchanger, a uniform crystal layer is allowed to grow and build up as an ice slab on the heat exchanger refrigerated surface. By operating the crystallisation step with a linear cooling ramp, the temperature of the flowing HTM is linearly reduced over the running time of the crystallisation process. The variation of the temperature of the HTM, as a function of the crystallisation time, is shown in Fig (7.3). As the thickness of the ice slab increases, the impurities are rejected from the growing crystal layer, and are gradually concentrated in the remaining melt [Ulrich and Glade, 2003]. When the predetermined crystallisation time is reached, then the crystallisation process is deactivated and the residue is collected from the crystalliser through the melt outlet line (see (Fig 7.2) (b)). The residue is then either taken to the drain discharge or to an intermediate storage vessel for performing a multistage operation as previously explained in Chapter 5.

(v) Partial melting (Sweating)

This process is similar to that in the Sulzer falling film crystallisation plant, which was previously described in Chapter 5. Fig (7.3) shows the temperature profile for the partial melting process.

(vi) Melting

This process is also identical to that of the Sulzer falling film crystallisation plant, which was explained previously in Chapter 5. Fig (7.3) shows the behaviour of the temperature profile during the melting process.

7.1.2 Multi-Stage Design and Basic Operation

Similar to the principles of operation of the Sulzer falling film crystallisation plant, the multistage design and basic operation is usually carried out as described in Chapter 5.

7.2 Preparation of Feed Samples

The residues discharged from the falling film and suspension crystallisation processes (see Chapters 5 and 6) were individually collected, and tested as feed water in this laboratory investigation. Alongside these residues, aqueous solutions of sodium chloride and process brines were also used and tested individually as feed samples in this experimental study. The initial salt concentration of the feed stream, using synthetic water, was 3.5 wt%. The sodium chloride salts (CH-4133 Pratteln 1, Nr.: 8431, BAGT 64656, Schweizer rheinsalinen) and high purity water, produced via an ultra-pure water purification system (Destillo, Einweg-Patrone D2), were used for preparing the aqueous solutions of sodium chloride. The preparation of NaCl solutions was performed as described in Chapter 4. As for the process brines, Reverse Osmosis (RO) brine and Arabian Gulf seawater, were also used and examined individually as feed samples in this study. The preparation of process brines was carried out as described in Chapter 5.

7.3 Physicochemical Analysis and Measuring Instruments

The physicochemical analysis of the water samples and the measuring instruments are described in Chapter 5.

7.4 Experimental Setup

Figs (7.4) and (7.5) show the laboratory scale setup and Sulzer static crystallisation pilot unit, which were used in this investigation. Sulzer have previously designed and constructed this equipment for investigating new fields of application. In this study, the majority of the experiments were conducted in a laboratory setup with the feed materials as mentioned. The pilot plant, on the other hand, was investigated for concentrating RO brine only.

As shown in Fig (7.4) (a), the laboratory pilot scale setup consisted of two crystallisers with capacities of 1.5 L and 6 L. These crystallisers were separated from each other, and individually connected to the same refrigeration unit, as shown in Fig (7.4) (b). The internal diameters of these two crystallisers are 50 and 70 mm, respectively, while their lengths are 0.8 m and 1.6 m, respectively. The two crystallisers each contain a single insulated thermo-stated double wall reaction vessel (see Fig (7.4) (a)). This contains a vertical tube, in which the crystal layer grows as a cylindrical shell during the crystallisation operation as shown in Fig (7.4) (c). The crystallisers are made of stainless steel, and each was provided with a stainless steel mesh as shown in Fig (7.4) (d). The mesh was placed underneath the crystalliser (above the sampling valve) in order to avoid the escape of ice crystals during the separation of residual liquid (during draining phase) and sweating fractions (during sweating phase). The feed process is achieved as shown in Fig (7.4) (e).

Fig (7.6) shows a schematic diagram of the laboratory and pilot scale setup along with the main equipment. A mixture of ethylene glycol and deionised water was used as a HTM in the refrigeration system. The operating temperature of the HTM was measured via a built-in instant read digital thermometer on the HTM bath circulator. The drain valve (11) which will be known as the sampling point is a hand-operated stainless steel ball valve installed beneath the crystalliser (see Figs (7.4) (f) and (7.6)). The underlying purpose is to use this valve to remove (or collect) the water samples (such as residue, sweat fractions, and product) from the crystalliser. As shown in Figs (7.4) (f) and (7.6), the experimental setup was provided with a heat gun pointed towards the sampling valve in order to avoid ice encasing.

(a) Experimental setup

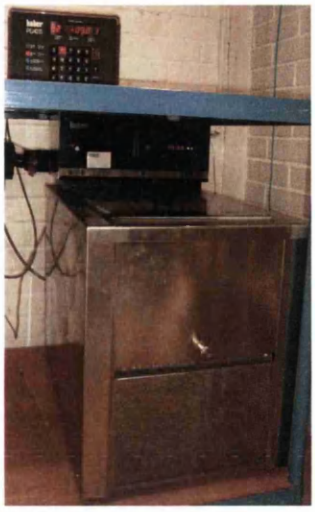

(b) Refrigeration system

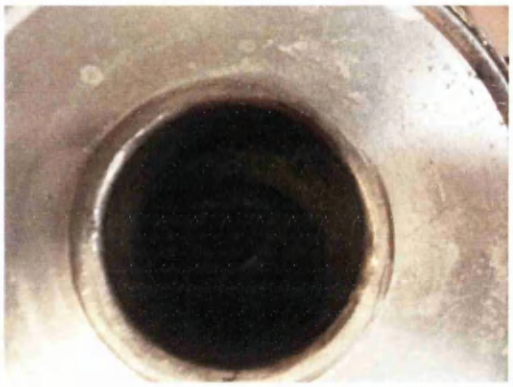

(c) Top view of a crystalliser with ice layer

(d) Stainless steel mesh

(e) Feeding process

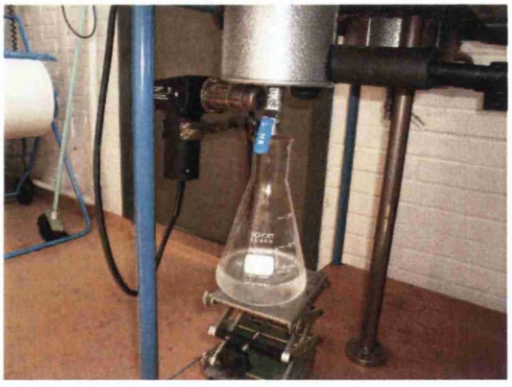

(f) Sampling process

Fig. 7.4: *Laboratory pilot scale setup, and main equipment and processes.*

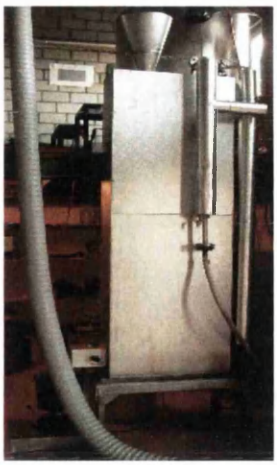

(a) Pilot plant crystallizer

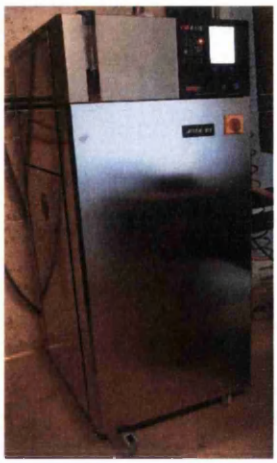

(b) Refrigeration unit

(c) Internal view of an empty crystallizer

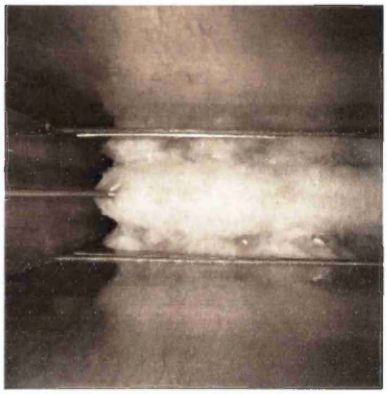

(d) A crystalliser with crystal layer

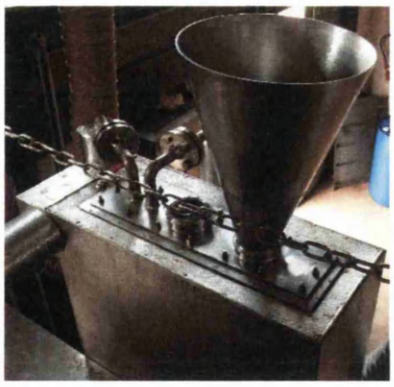

(e) Funnel and top-view of crystallizer

(f) Drain valve (sampling point)

Fig. 7.5: *Pilot plant apparatus and main equipment.*

Alongside the laboratory pilot scale setup, a preliminary experimental investigation was carried out on the pilot plant having a crystalliser capacity of 70 L. Fig (7.5) shows the skid mounted pilot plant unit and main equipment used in this investigation. The pilot plant represents a straightforward scale-up pilot unit since the commercial scale crystallizer is designed directly by increasing the surface area and number of the plates in the heat

exchanger. The crystalliser of the pilot plant was provided with three vertical heat exchanger plates, in which four crystal layers grow as ice slabs during the crystallisation operation as shown in Figs (7.5) (c) and (d). The height and width of this crystalliser tank is 2 × 0.5 m, whereas each vertical heat exchanger plate is 1.95 × 0.45 m. The pilot plant was provided with a laboratory balance (Mettler-Toledo GmbH, ID1 Plus) attached to the crystalliser's tank in order to measure the loaded mass of feed material inside the crystalliser. In addition, the pilot plant was provided with a heat transfer unit (Huber, Unistat 615) via tubes for low temperature applications, as shown in Fig (7.5) (b). The heat transfer unit contains a refrigerated thermostatic bath, bath circulator, HTM (Huber, Thermal Fliud: DW-Therm M90.200.02), and PID temperature controller are constructed in one compartment. Also, the pilot plant was provided with a removable stainless steel funnel for the purpose of facilitating the filling process (see Fig (7.5) (e)).

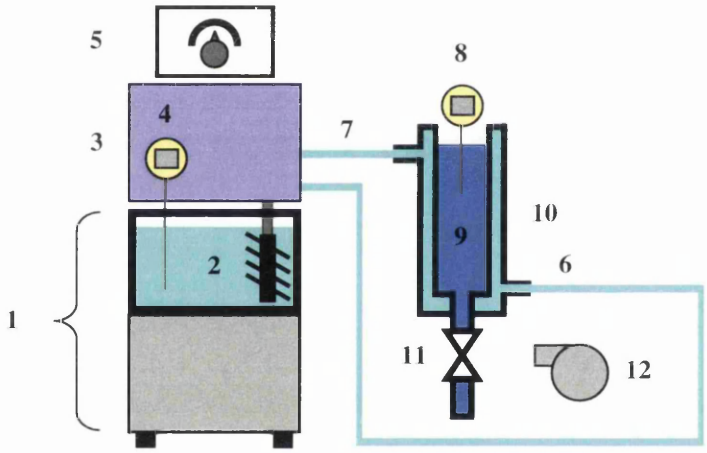

Fig. 7.6: *Schematic of laboratory pilot scale setup with (1) Refrigeration unit and thermostatic bath (Huber, HS 40, Renggli Laboratory systems), (2) heat transfer medium (HTM), (3) HTM bath circulator (Huber HS40), (4) built-in digital thermometer, (5) PID temperature controller (Huber PD 420), (6) and (7) inlet and outlet HTM pipelines, respectively, (8) instant digital thermometer (Taylor, Model: 9847N), (9) feed sample, (10) double wall reaction vessel, (11) sampling valve (HK, stainless steel ball valve, O.D 1/4"), and (12) heat gun (Weller 1095).*

In general, the concept of the refrigeration systems used for the two laboratory setups is the same. The refrigeration system involves the use of a PID temperature controller and

refrigeration unit, attached to the thermostatic bath (see Fig (7.6)). The thermostatic bath stores a HTM. The refrigeration system has a HTM pump, which is connected to the crystalliser by means of inlet and outlet insulated metal hoses. The HTM pump circulates the HTM from the thermostatic bath into the crystalliser. The process set-point temperature and time are controlled by means of the PID temperature controller.

7.5 Experimental Procedure

The principal unit operations considered in the crystallisation experiments were pre-cooling, seeding, crystallization, residue separation, total melting, and product separation. For the sweating experiments, a partial melting process was considered with the mentioned principal unit operations.

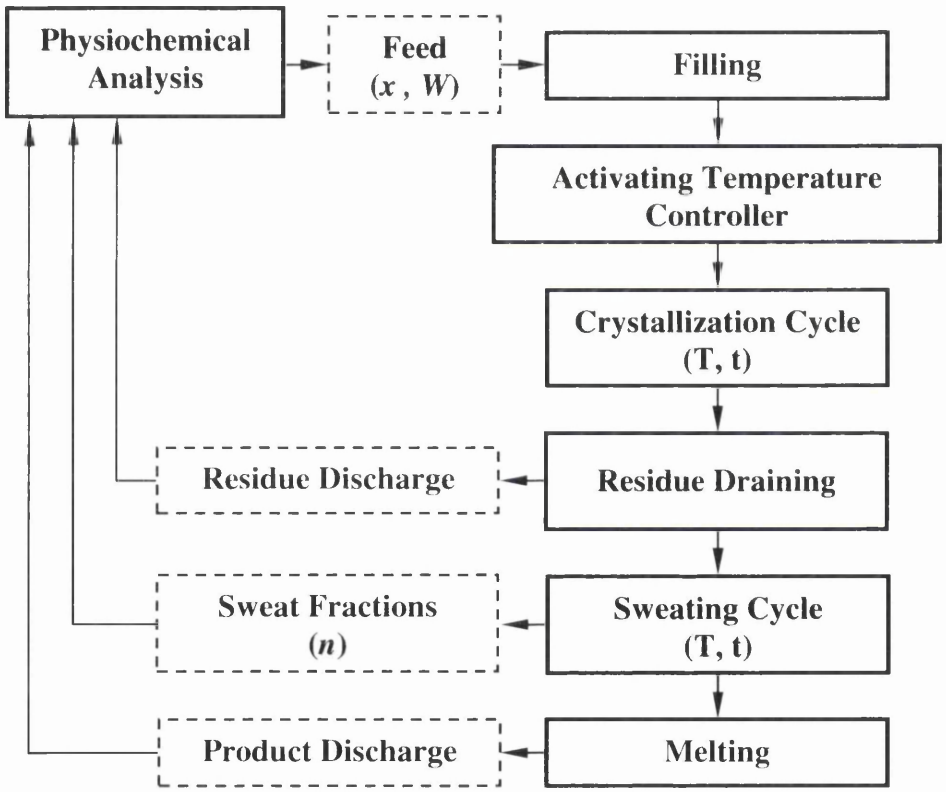

Fig. 7.7: *Simplified block diagram of the operational process for the experiments, where; x_f is the feed concentration (ppm), W is the sample weight (kg), t is the running time (minute), T is the temperature (°C), and n is the number of sweat fractions.*

The operating procedures for crystallisation and sweating operations using all experimental setups are shown schematically in Fig (7.7). The experiments were investigated in batch

mode. Prior to conducting any test, the feed sample was prepared and then the physiochemical analyses were performed. During this process, the refrigeration system was operated, and simultaneously the internal circulation of the HTM took place inside the crystalliser. As illustrated in Fig (7.3), the investigated set-point temperatures and running times were set at desired values on the PID temperature controller without activation of the refrigeration operational cycle. The reason behind this is to give enough time for the refrigeration system to cool down, and be prepared for the test, before starting the experiment. Then the sampling valve was fully closed and the crystalliser filled with the desired mass of feed sample (see Fig (7.4) (e), for an example). The crystalliser was then covered with a lid (see Fig (7.4) (a)). The purpose of using a rubber lid is to protect the feed material from the entry of undesirable materials, such as dust, suspended matter, particles, etc.

The operational cycle of the refrigeration system was turned on, leading to the predetermined set-point temperatures and times that were inserted into the PID temperature controller to be followed (see Fig (7.3)). At the initial stage, the crystalliser was refrigerated by internal circulation of the HTM. Therefore, when the feed temperature reaches a value slightly lower than the freezing point, which represents the start-point temperature for crystallisation (see t_1 in Fig (7.3)), because of the heat transfer resistance, a seed ice crystal was added to the crystalliser to achieve formation of ice crystals, which were then gradually grown as a cylindrical shell (for the case of the laboratory pilot scale setup) or an ice slab (for the case of the pilot plant) on a cooled surface immersed in the feed over the duration of the experiment. This crystal layer was progressively and slowly grown on a refrigerated surface perpendicularly outward to the surface leading to the formation of an evenly thin crystal coat on the refrigerated surface.

When the HTM temperature reached the end-point temperature of crystallisation (see t_2 in Fig (7.3)), the sampling valve at the bottom of the crystalliser was opened manually to collect the remaining liquid phase (i.e. residue) in a laboratory beaker (for the case of the laboratory pilot scale setup) or a stainless steel barrel (for the case of the pilot plant). The ice layer remained adhered to the refrigerated surface until the end of the draining stage (see t_3 in Fig (7.3)).

When the temperature of the HTM reached the start-point temperature for partial melting (i.e. sweating), the collection vessel was replaced with another vessel to collect the sweated melt, while the vessel which contained the residue sample was taken for physiochemical analysis. For the sweating experiments, the crystal layer was further purified by conducting a partial melting process (see t_3 and t_4 in Fig (7.3)). This was achieved practically by gently increasing the temperature of HTM to a desired temperature, leading to gradual heating of the crystal layer inside the crystalliser. Hence the ice crystal layer partially melted inside the crystalliser as the temperature of the HTM increased. According to the predetermined mass of sweated melt and time, this sweated melt including trapped and adherent material, was collected throughout the sweating operation. This means that the sampling valve was set to fully open until the end of the sweating process. According to Ulrich and Glade (2003), the partial melting process is similar to a washing process used in a suspension crystallisation technology, and serves as further purification of the adherent crystal layer. All beakers including the sweated melts were then taken for further analyses. For crystallisation experiments, the process set-point temperature and time for partial melting operation were set at specific values minimising the running time of the partial melting process, leading to a reduction in the total running time of one crystallisation stage. The sampling valve was set to fully closed, since the sweated melt samples were not collected in the case of the crystallisation experiments.

When the endpoint temperature of the sweating process was reached, for the case of sweating experiments, the vessel which contains the sweated melt was replaced with another vessel for collecting the final water sample i.e. product water. For the crystallisation experiments, the sampling valve at the bottom of the crystalliser was manually opened to collect the melted crystal layer, i.e. product water. The melting operation was applied by further increasing the temperature of HTM to the desired temperature at which the remaining/purified crystal layer was totally melted to provide the product water (see t_5 in Fig (7.3)). The product water was drained off from the crystalliser through the sampling point and taken for further analysis.

7.6 Results and Discussion

The phase diagram and relationships between the key parameters, including salt concentration, freezing point, and electrical conductivity, were given previously in Chapter 5. A complete record of process data, operating temperature profiles, full physiochemical

analysis, and crystalline impurity content versus sweating times are given in Tables A7-1 – A7-18 in Appendix 7, found on the CD attached to the thesis (see file name: Appendix_1, Microsoft Excel spreadsheet, Sheet 1, Tables: A7.1-4). For all tests, the results of the average growth rate were analytically computed by assuming that the dimensions and shape of the solid ice layer are for cylindrical geometry, in the cases using a crystalliser tube, and rectangular, for the cases using a plate heat exchanger. The cooling rates were analytically calculated by dividing the temperature difference, between the end-point and start-point temperatures of the crystallisation operation, by the crystallisation time (Ulrich and Glade, 2003). The theoretical power consumption for the static crystallisation experiments was analytically determined by the heat transfer rates for cooling the feed water and changing the phase of the liquid, as described previously in Chapter 4.

In general, the experimental conditions that have been used in this study are shown in Table (7.1).

Run No.	Exp. Setup	Feed Source	Feed Conc. (%)	Crystallisation		Sweating	
				Time (*hr*)	End-Point HTM Temp. (°*C*)	Time (*hr*)	End-Point HTM Temp. (°*C*)
1 – 7	LPS	NaCl Solution	3.5	2 – 24	-2.3 – 8	2	-2.9 – 0.8
1 – 14	LPS	Process Brines	5.1 – 15	3.5 – 12.5	-10 – -23	1 – 4	-23 – 0
1 – 8	PP	RO Brine	6.1	4 – 24	-4	-	-

Table 7.1: *Operating parameters and conditions for crystallisation and sweating experiments, where; PP is the pilot plant and LPS is the laboratory pilot scale setup.*

7.6.1 Parametric study of crystallisation and sweating processes

The first group of experiments was carried out with feed samples using aqueous solutions of sodium chloride. These experiments were performed on the laboratory pilot scale setup using

a 1.5 L capacity crystalliser. The investigated salt concentration of feed samples was 3.5 wt%. These experiments were performed in a feed stage process, i.e. single freezing stage. The operating conditions tested are illustrated in Table (7.2).

A summary of the experimental data for runs 1 – 3 (i.e. crystallisation experiments) is given in Table (7.3). The salt rejection ratio was found to be inversely proportional to the average growth rate. However, the water recovery ratio was found to be proportional to the average growth rate (see Table (7.3)). For instance, by comparing the results of run 1 and 3 (see Tables (7.2) and (7.3)), the salt rejection (SR) increased from 24.2% to 59% when the average growth rate was reduced from 5.63 mm/h to 0.04 mm/h. Consequently, the water recovery (WR) was significantly reduced from about 70% to 8.3%. The salt concentration of product water, on the other hand, decreased (i.e. improved) as the end-point temperature of the crystallisation operation reduced, as illustrated in Tables (7.2) and (7.3). This indicates that the product quality is sensitive to the variations of the end-point temperature of crystallisation operation.

Run	Feed			Crystallization			Sweating		
	M	C	FP	T_1	T_2	t_C	T_1	T_2	t_S
	(g)	(wt%)	(°C)	(°C)	(°C)	(h)	(°C)	(°C)	(h)
1	1,500	3.5	-2.2	-2.30	-8.00	2	Not applied		
2					-6.00				
3					-2.90	24			
4	1,500	3.5	-2.2	-2.30	-2.90	12	-2.90	0.80	2
5						24			
6						36			
7						72			

Table 7.2: *Operating conditions of crystallisation and sweating tests using 1.5L static crystalliser for treating NaCl solutions. The notations such as M, C, and FP represent mass, salt concentration, and freezing point, respectively, whereas T_1 and T_2 represent the start-point and end-point temperatures, respectively, while t_C, and t_S represent running times of crystallisation and sweating processes, respectively.*

Run	Feed			AGR	Product			WR	SR	Residue		
	M	C	FP		M	C	FP			M	C	FP
	(g)	(%)	(°C)	(mm/h)	(g)	(%)	(°C)	(%)	(%)	(g)	(%)	(°C)
1	1,500	3.5	-2.2	5.63	1,048	2.7	-1.7	69.9	24.2	452	5.5	-3.5
2	1,500	3.5	-2.2	3.96	801	2.4	-1.5	53.4	31.3	699	4.8	-3.0
3	1,500	3.5	-2.2	0.04	124	1.4	-0.9	8.3	59.0	1,376	3.7	-2.3

Table 7.3: *Experimental data of crystallisation tests using runs 1-3. The notations are as follows: M, C, and FP represent mass, salt concentration, and freezing point, respectively; AGR, WR, and SR represent the average growth rate, permeate water recovery, and salt rejection, respectively.*

As illustrated in Table (7.2), the apparatus was also examined for different time retention of the crystallisation operation, ranging from 12 to 72 h (see runs 4 – 7). These experiments were carried out at constant operating conditions for the sweating process (see Table (7.2)). The salt concentrations of crystal layers, before and after the sweating process, were investigated. A summary of the experimental results is given in Fig (7.8). The results compare the performance of the static crystallisation, before and after the sweating process. Furthermore, the power consumption was determined for these experiments. Fig (7.8) (a) shows that the salt rejection ratio was dramatically reduced after increasing the average growth rate. This confirms the previous findings regarding the influence of the average growth rate on salt rejection ratios, as well as the effect of sweating. Fig (7.8) (b) shows the salt rejection ratio as a function of the cooling rate of the crystallisation process, as well as the effect of sweating. The results proved that the lower growth rates, dictated by slow crystallisation rate (i.e. higher cooling rates), are of great importance in improving the separation performance of the static crystallisation process. These findings are compatible with previous work by Richa *et al.* (2011) on the effect of cooling rate and average growth rate on the salt concentration of the product water. The effect of crystallisation time on the salt concentration of product can be observed in Fig (7.8) (c), when the end-point temperature was maintained at a constant value. The results indicate that the process is very sensitive to changes in crystallisation time. By comparing the purity of crystal layers, before and after the sweating process, the salt rejection ratio was improved by using the sweating

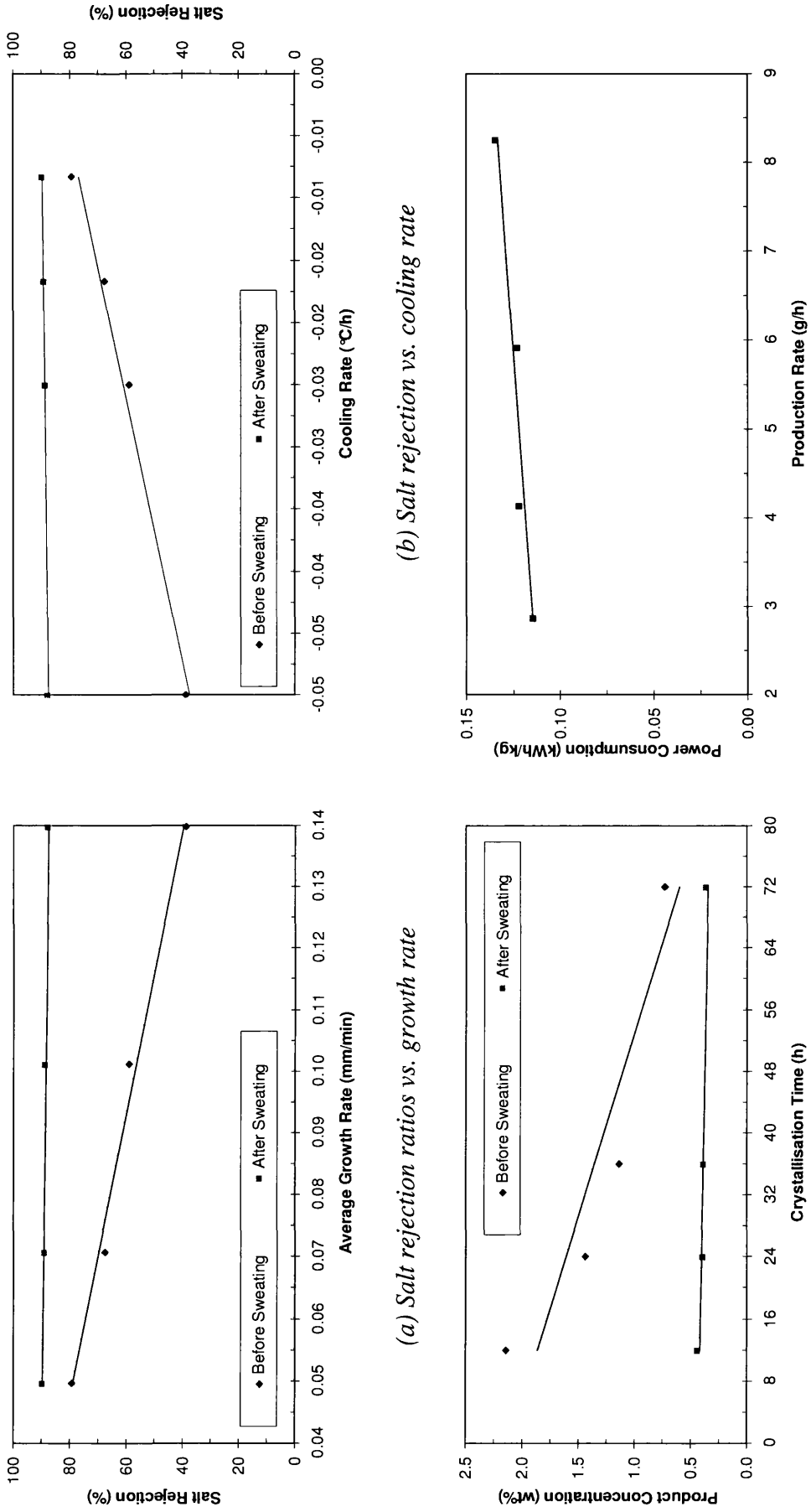

(a) Salt rejection ratios vs. growth rate

(b) Salt rejection vs. cooling rate

(c) Product concentration vs. crystallisation time

(d) Power consumption vs. production rate

Fig. 7.8: *Preliminary experimental results for the static crystallisation and sweating experiments using the operating conditions of runs 4-7.*

process, as shown in Fig (7.8) (c). A strong decrease in salinity of the crystal layer was observed when the sweating process was applied. Furthermore, the total freezing stage time was dramatically reduced, when compared to that in the crystallisation operation without sweating. For instance, a crystal layer was obtained at a salt concentration of 0.73 wt% by using the crystallisation process separately (i.e. without sweating process) with a crystallisation time of 72 h; in contrast, another crystal layer was produced at a lower salt concentration (i.e. 0.44 wt%) and at lower crystallisation time (i.e. 12 h), when a sweating operation was incorporated into the static crystallisation process, and applied for 2 h. Therefore, the experimental results suggested that it would be an ideal treatment system to optimise the operating conditions of crystallisation and sweating operations to achieve the desired quality rather than optimising and applying the crystallisation operation separately. The calculations of theoretical power consumption for the experiments, on the other hand, give an averaged value of 0.123 kWh/kg as shown in Fig (7.8) (d).

7.6.2 RO brine treatment – using a pilot plant with a crystalliser capacity of 70L

In the second series of experiments, the potential capability of the Sulzer static crystallisation process (without use of a sweating process) for concentrating and treating RO brine was investigated. These experiments were carried out on a pilot plant (see Fig (7.5)) using a feed stage process.

The investigated volume of feed water was 70 L. The actual operating period of the crystallisation experiments was varied from 4 to 24 h. The investigated start-point and end-point temperatures of crystallisation operation were -4°C and -8°C respectively. The results of the separation performance and the computed power consumption of the investigated pilot plant are shown in Fig (7.9). Results of salt concentration of product, as a function of the growth and cooling rates are shown in Figs (7.9) (a) and (b), respectively. The trends of these results are clearly observed to be in agreement with the previous investigation, as given in the first series of the experiments. As shown in Fig (7.9) (c), the minimum and maximum salt concentrations of product water were 3.46 and 4.49 wt%, respectively, whereas the water recovery was stabilised at an averaged value of 73%. This indicates that the investigated pilot plant, within study domain, was capable of providing a substantial amount of product water of near ocean seawater standards. As a result, the treated water can be further easily desalted

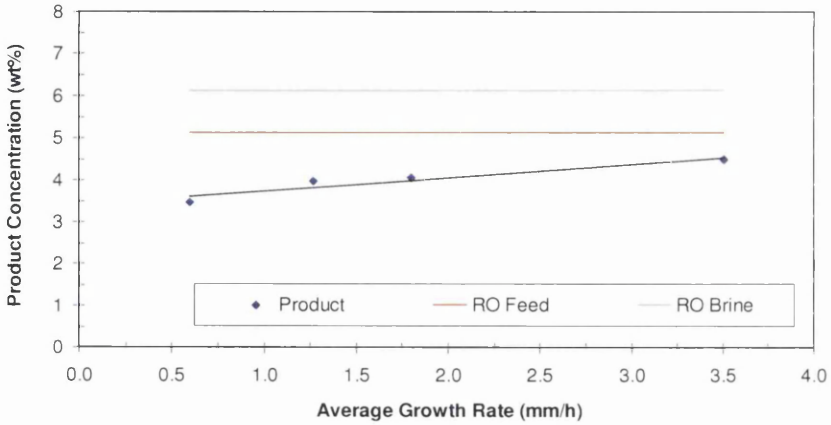

(a) Production concentration vs. growth rate

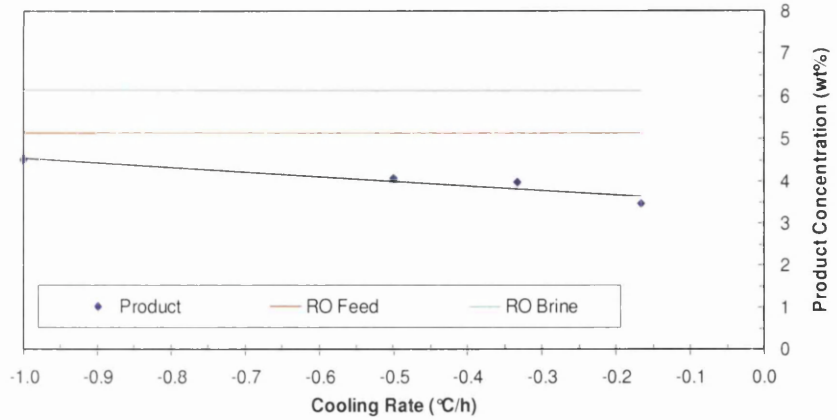

(b) Production concentration vs. cooling rate

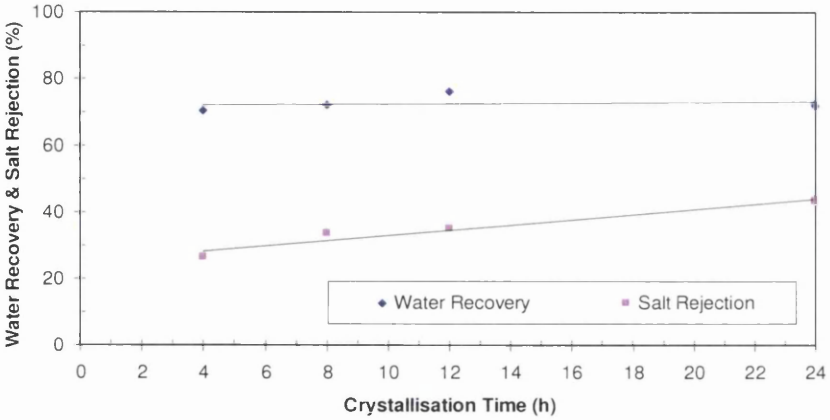

(c) Water recovery & salt rejection vs. crystallisation time

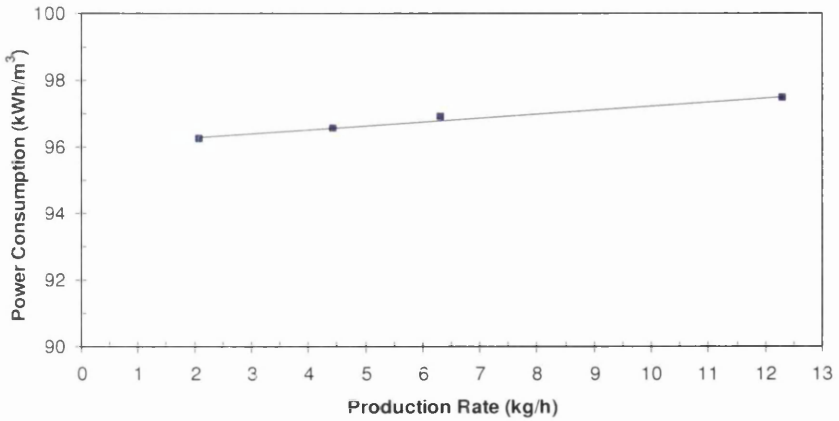

(d) Power consumption vs. production rate

Fig. 7.9: *Summary of experimental results for the static crystallisation pilot plant used for treating RO brine.*

either by a sweating process, increasing the number of rectification stages, or simply by recycling the treated water into the main feed stream of the seawater RO membrane plant to obtain a final product of drinking water. When the desired salt concentration of product water is required to be similar to that of Arabian Gulf seawater, then the experimental results suggested reducing the retention time of the crystallisation process (i.e. less than 4 h) in future studies. This is because crystal layers were experimentally produced at a lower salt concentration, when compared to Arabian Gulf seawater. By reducing the overall running time of the freezing stage, a significant increase in the production rate would be expected, which will lead to a dramatic fall in the operational cost. As for the energy consumption, Fig (7.9) (d) shows a plot of the theoretical results of the power consumption versus the production rate. The theoretical power consumption for the investigated pilot plant gave an averaged value of 97 kWh/m^3.

7.6.3 Process brine treatment – using the laboratory pilot scale setup with a crystalliser capacity of 6L

The third group of experiments were carried out on feed samples using process brines to determine the number of influences on the performance of the static crystallisation process. These experiments were carried out on the laboratory pilot scale setup using a crystalliser capacity of 6 L. The experiments were performed in a feed stage process, using crystallisation and sweating process. The salinities of crystal layers, before and after the sweating process, were studied.

The first investigation was carried out on feed samples using concentrated RO brine with a salt concentration of 12 wt%; this was previously taken from the residue sample of suspension crystallisation experiments (see Chapter 6). This investigation was carried out to determine the influence of cooling rate of crystallisation operation on the salt separation of the static crystallisation process as well as the effect of the sweating process. The investigated cooling rates of the crystallisation were -0.48 and -0.80 °C/min, whereas the sweating process was maintained at constant operating conditions.

Figs (7.10) (a) and (b) show the influences of several factors, such as: cooling rate of crystallisation operation, crystal mass ratio, and sweating time, on the salt concentration of

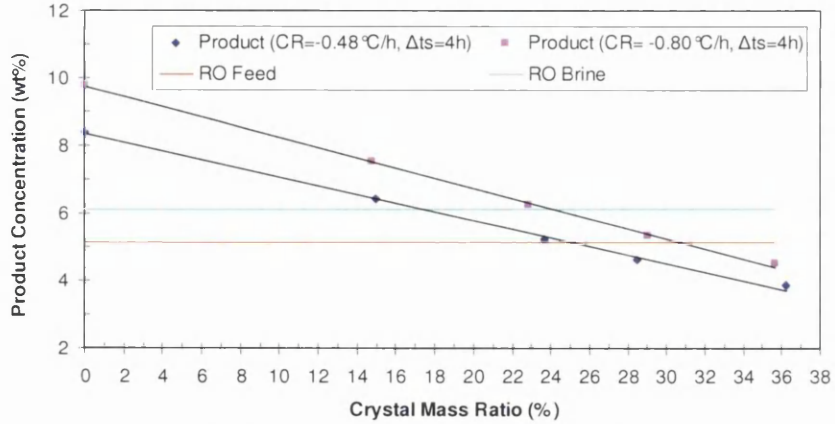

(a) Product concentration vs. crystal mass ratio

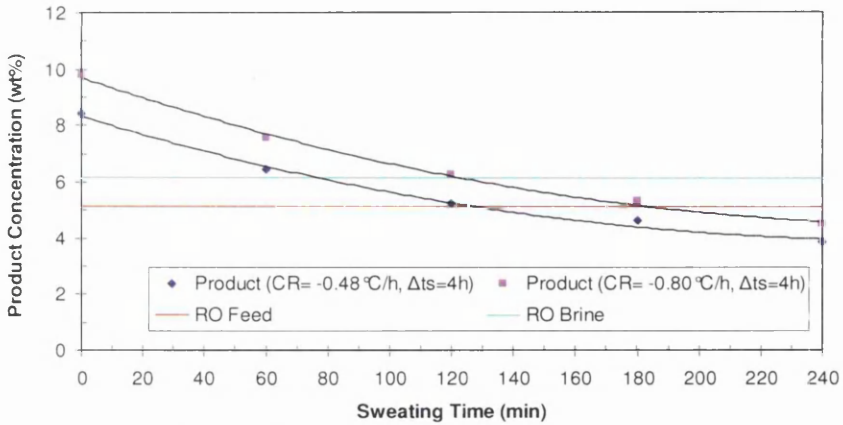

(b) Product concentration vs. sweating time

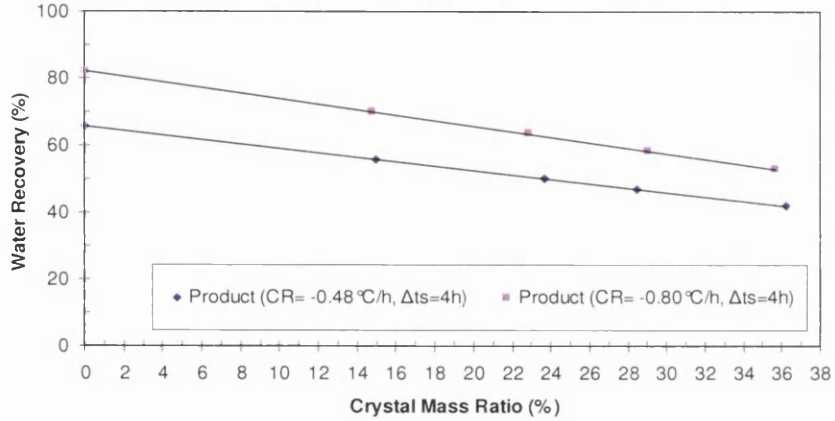

(c) Water recovery vs. crystal mass ratio

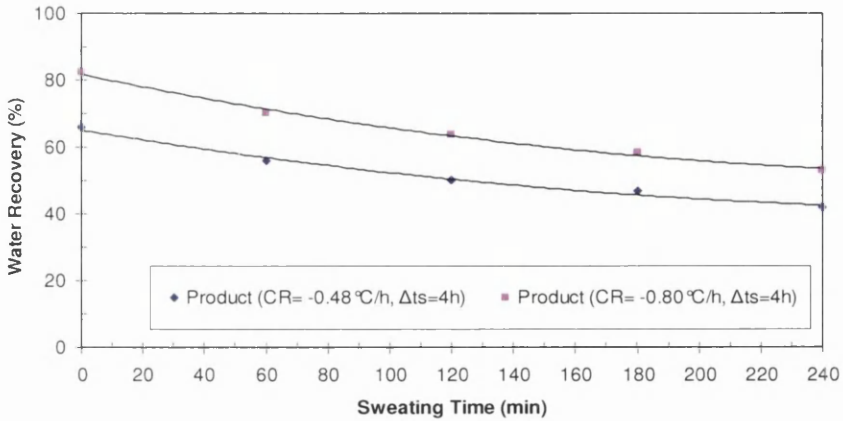

(d) Water recovery vs. sweating time

Fig. 7.10: *Influence of cooling rate of the crystallisation process and effect of the sweating process on the salt concentration of the crystal layer and permeate water recovery ratio, where CR is the cooling rate, and Δts is the sweating time. The investigated feed water concentration was 12 wt%, using the concentrated RO brine disposed from the suspension crystallisation experiments (see Chapter 6).*

the crystal layer. The salt concentration of the crystal layer decreased (i.e. improved) as the cooling rate of the crystallisation process increased, as observed previously in different experiments. For instance, before performing the sweating process, the salt concentration of the crystal layer was reduced from 9.78 wt% to 8.40 wt% by decreasing the cooling rate of the crystallisation process from -0.80 to -0.48 °C/min (Fig (7.10) (a)). Figs (7.10) (a) and (b) show that the sweating process was found effective in improving the salinity of the crystal layer, where a notable reduction in the salt concentration of product was observed through increasing the crystal mass ratio and sweating time. For instance, for the case of the crystallisation rate of -0.80 °C/min, the salt concentration of the crystal layer was reduced from 9.78 wt% to 4.50 wt% when the crystal mass ratio reached 35.64%. For the case of the crystallisation rate of -0.48 °C/min, the salinity of the crystal layer was further reduced by the sweating process, where the salt concentration of crystal layer was lowered from 8.40 wt% to 3.68 wt% when the crystal mass ratio reached 36.25%. In general, the salt rejection ratio was increased, via a sweating operation, as the crystal mass ratio and sweating time increased. For instance, in the case of a crystallisation rate of -0.48 °C/min, the salt rejection ratio before the sweating process was 29.96 %. In contrast, the final salt rejection ratio increased to 67.84 % after performing the sweating operation under the investigated operating conditions. The trend of this finding was also in agreement with the case of the crystallisation rate of -0.80 °C/min, where the salt rejection ratio, before a sweating operation, was 18.50 %. The final salt rejection ratio, in contrast, was increased to 62.46 % after carrying out the sweating process.

When the desired salinity of the crystal layer is required to be near that of Arabian Gulf seawater, then the experimental results suggested reducing the time retention in the crystallisation process to 3 h and 2 h for the cases of the crystallisation rate of -0.80 and -0.48 °C/min, respectively. In contrast, when the desired salinity of the crystal layer is required to be near the RO brine, then the experimental results suggested further reduction in the time retention of the crystallisation process to 2 h and 1 h for the crystallisation rates of -0.80 and -0.48 °C/min, respectively. As mentioned previously, the production rate can be substantially increased by reducing the overall running time of the freezing stage, and thus the operational cost will be dramatically decreased. The results of water recovery ratio and cooling rate of the crystallisation process as a function of the mass crystal ratio and sweating time are shown in Figs (7.10) (c) and (d). The water recovery was found to decrease with increasing crystal

mass ratio and sweating time, and to increase with decreasing crystallisation rate. The trends of these findings are in agreement with all the experimental results given in Chapter 7.

The second study was performed using the previous experimental conditions, except for changing the investigated crystallisation rate and sweating time. The examined crystallisation rate was set at constant value, i.e. - 2 °C/min, while the sweating process was carried out at sweating rates of 5.5 and 22 °C/min. This study was performed to evaluate the change of sweating time on the salinity of the crystal layer. A summary of the experimental results is shown in Fig (7.11). Figs (7.11) (a) and (b) show that the salt concentration of the product water was improved as the sweating time was increased. Fig (7.11) (b) shows that the salt concentration of the crystal layer was lowered from 11.28 to 8.10 wt%, when the sweating rate was set to 22 °C/min, which corresponds to a poor sweating efficiency. This was because the salt concentration of the final product water was relatively poor when compared to the RO brine. When the sweating rate was set to 5.5 °C/min, the salt concentration of crystal layer decreased to 4.74 wt%, which corresponds to a reasonable separation performance since the final product water is close to Arabian Gulf seawater standards. In other words, the salt rejection ratio was significantly increased, via a sweating operation, as the sweating rate increased. For instance, the calculations of the salt rejection ratio, before the sweating operation, give 4.38 %, while the final salt rejection ratio, in contrast, was increased to 32.47 % after carrying out the sweating process at a sweating rate of 22 °C/min. In contrast, the salt rejection ratio was significantly increased to 60.47 % after performing the sweating operation at a sweating rate of 5.5 °C/min. This clearly indicates that the salt rejection ratio is inversely proportional to the sweating rate.

When the desired salt concentration of the crystal layer was required to be close to that of the RO brine, then the experimental results suggested lowering the sweating time down to 3 h for the cases of the sweating time 5.5 °C/min; in contrast, the sweating time must be further extended for the sweating rate of 22 °C/min to reduce the salt concentration of crystal layer down to that of the RO brine. However, this action may be accompanied by a dramatic fall in the water recovery ratio, when compared to that in the sweating process with lower rates. As previously mentioned, the reduction in the sweating time has a positive impact on the production rate and operational cost. The crystal mass ratio was found to be proportional to

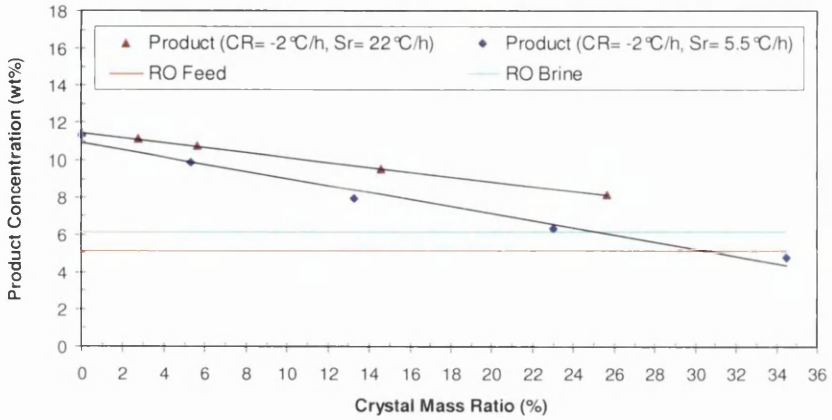

(a) Product concentration vs. crystal mass ratio

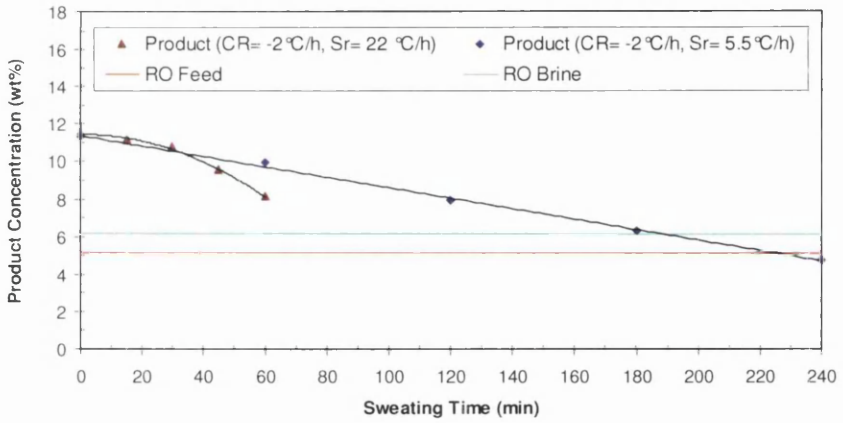

(b) Product concentration vs. sweating time

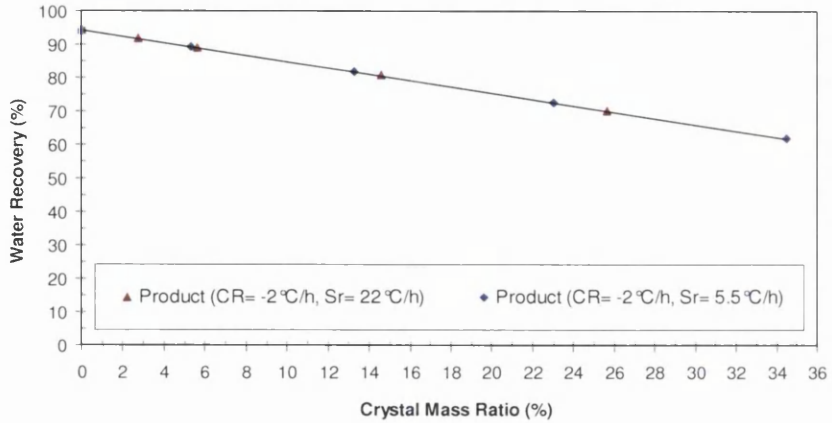

(c) Water recovery vs. crystal mass ratio

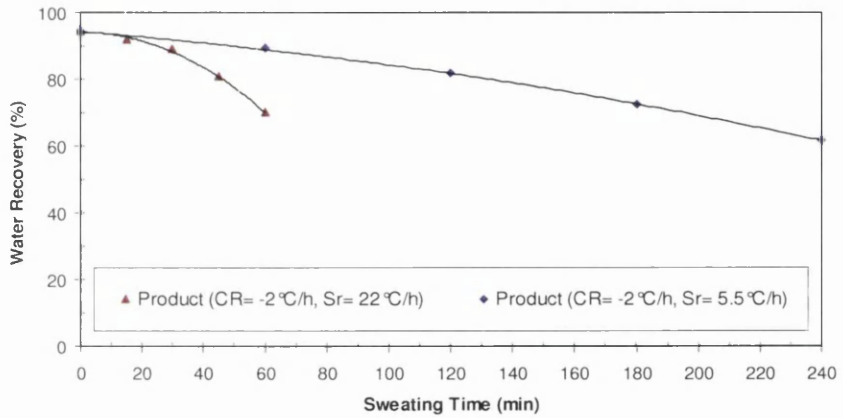

(d) Water recovery vs. sweating time

Fig. 7.11: *Influence of sweating time on the salt concentration of the crystal layer and permeate water recovery ratio, where CR is the cooling rate, and Sr is the sweating rate. The investigated feed water concentration was 12 wt%, using the concentrated RO brine disposed from the suspension crystallisation experiments (see Chapter 6).*

the sweating time, as shown in Fig (7.11) (c). The water recovery ratio was dramatically decreased as the sweating time is increased (see Figs (7.11) (c) and (d)).

The third investigation was performed with two different types of feed samples using Arabian Gulf seawater and RO brine. This investigation was performed to find out the effect of feed salt concentration on the quality of the crystal layer at low crystallisation temperature. The investigated endpoint temperature of crystallisation was set at -23°C, which was slightly lower than the eutectic temperature of NaCl salt. The crystallisation and sweating times were set at 5.5 and 4 h, respectively. The experimental results of the investigated treatment system are shown in Fig (7.12).

The experimental results clearly indicate that the separation performance of the crystallisation and sweating processes were negatively affected by a slight increase of the salt concentration of the feed water, as shown in Figs (7.12) (a) and (b). The product concentration was found to be proportional to the feed concentration, in agreement with all previous experiments. However, the water recovery ratio did not change with a slight increase in the salinity of feed water. As shown in Figs (7.12) (c) and (d), the amount of residue samples was nil, which was due to the amount of feed samples that were completely frozen after carrying out the crystallisation process. Figs (7.12) (a) and (b) show that the sweating process was capable of reducing the salinity of the crystal layer down to 2.49 and 3.64 wt% for the cases of treating Arabian Gulf seawater and RO brine, respectively.

For the experiment with RO brine, clear signs of solid salts precipitation in the sweat fraction were visually observed. The harvested salts were collected and experimentally measured, giving about 12 g. Table (7.4) demonstrates the water chemistry results for the water samples. The mass and salt balance calculations showed that the percentage loss in the residual liquid is about 9%. Table (7.4) also confirms the signs of precipitation of salts composed of Na^+, Cl^-, Ca^{2+}, Mg^{2+}, and $(SO_4)^{2-}$ ions, since the calculations of the percentage losses in their ionic concentration give about 14, 14, 26, 37, and 20 % respectively. The main reason for the solid salts precipitation may be explained by operating the crystallisation process under a critical temperature, which is lower than eutectic temperature of NaCl.

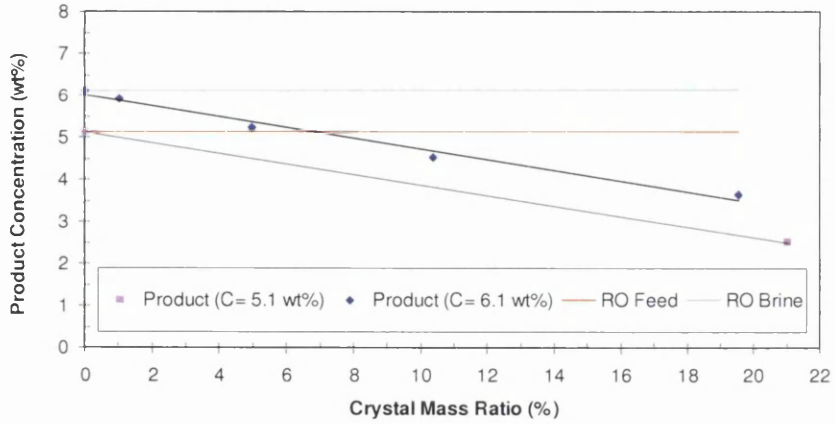

(a) Product concentration vs. crystal mass ratio

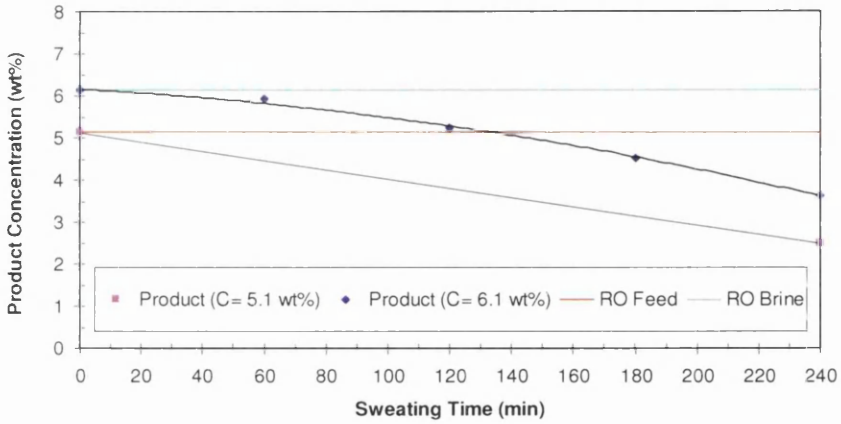

(b) Product concentration vs. sweating time

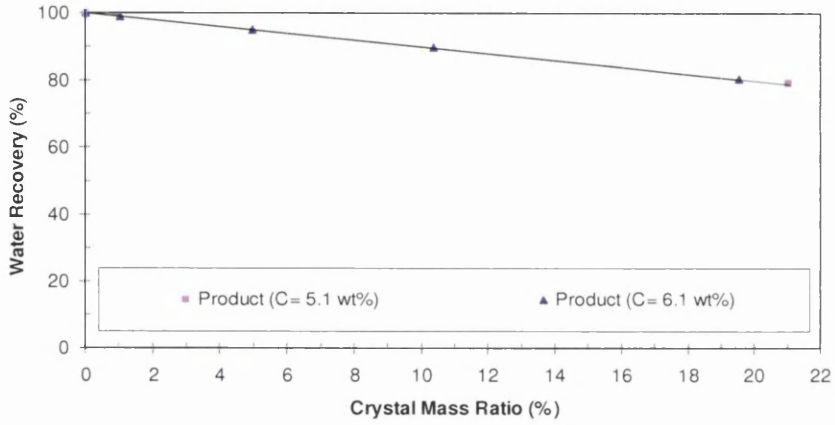

(c) Water recovery vs. crystal mass ratio

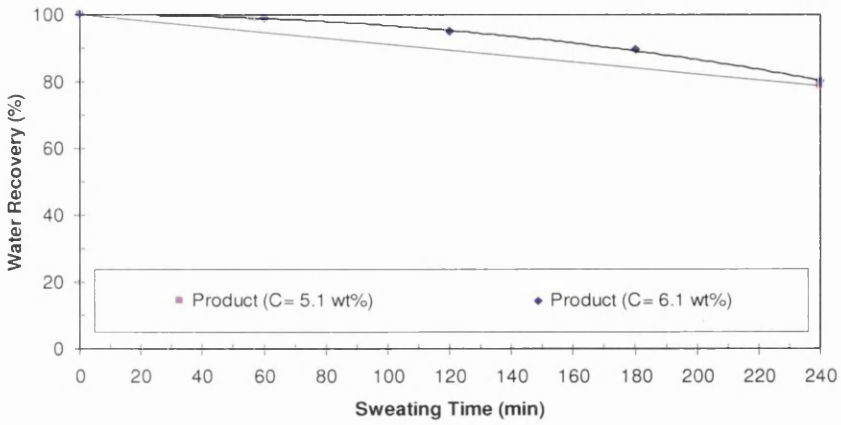

(d) Water recovery vs. sweating time

Fig. 7.12: *Influence of salt concentration of feed water on the performance of the static crystallisation and sweating processes, where C is the salt concentration of the feed water. The experimental conditions are: start-point and end-point temperatures of -5 and -23 °C, respectively, and the sweating time is 4 hours.*

Parameter	Units	Feed	Product	Residue*
Mass	(kg)	6.047	4.865	1.182
Conductivity	mS/cm	76.60	44.60	164.80
Salt Concentration	(wt%)	6.11	3.64	14.75
Melting Point	(°C)	-3.24	-2.07	-9.62
Ca^{2+}	mg/L	1,476	840	3,040
Mg^{2+}	mg/L	1,463	778	2,717
Na^{+}	mg/L	20,881	15,174	38,324
$(SO_4)^{2-}$	mg/L	4,800	3,280	10,790
$(HCO_3)^{-}$	mg/l as CaCO3	241.2	161.3	380.7
Cl^{-}	mg/L	32,200	23,400	59,100

Table 7.4: *Water chemistry analysis for concentrating RO brine, where the collected sweating fraction samples were mixed together and identified as "residue*" for the full chemical analysis.*

The experimental results suggested, for the case of RO brine concentration, to reduce the crystallisation time from 4 to 1 h to provide a final product water of near the quality of Arabian Gulf seawater, in terms of salinity (see Figs (7.12) (a) and (b)). Thus, this action will substantially increase the water recovery ratio from 80.45 to about 99% (see Fig (7.12) (d)), taking into account that there will be precipitation of solid salts, discharged with sweating fractions for such an application.

The fourth investigation was carried out on RO brine. The investigated end-point temperatures were -10 and -23°C, where the crystallisation and sweating times were set at 5.5 and 4 h, respectively. This investigation was carried out to determine the influence of end-point crystallisation temperature on the salinity of crystal layer and water recovery ratio.

Fig (7.13) shows the variation of the salt concentration of crystal layer and water recovery ratio, as a function of the crystal mass ratio and sweating time. A clear tendency of decreasing salt concentration in the crystal layer with increasing end-point crystallisation temperature can be observed as shown in Fig (7.13) (a) and (b). For example, for the case

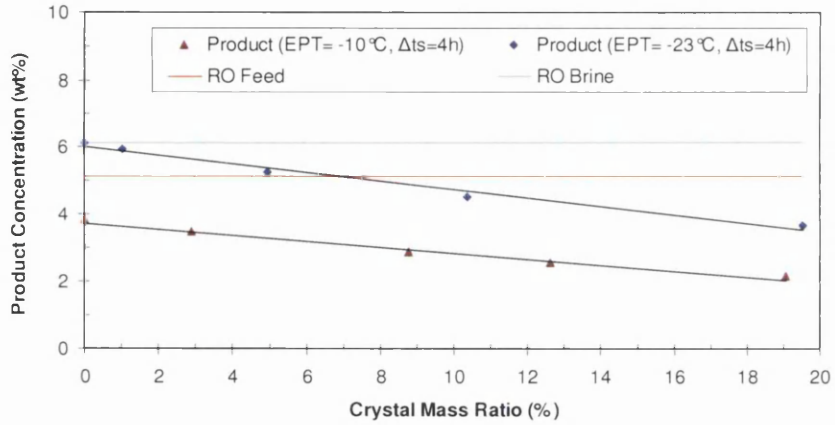

(a) Product concentration vs. crystal mass ratio

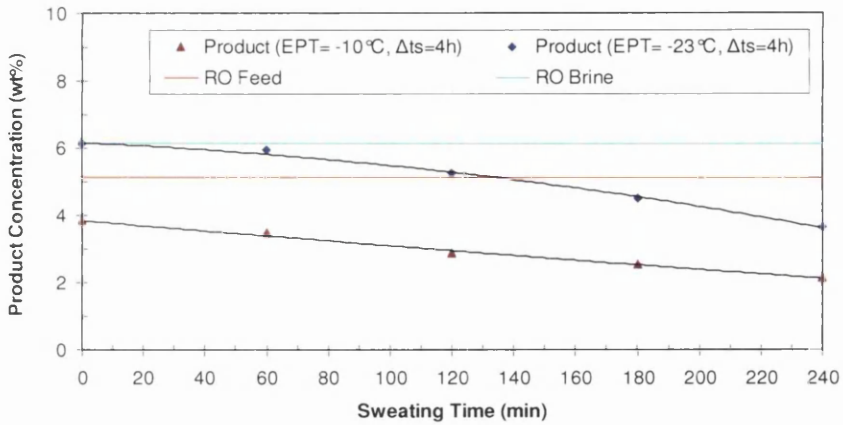

(b) Product concentration vs. sweating time

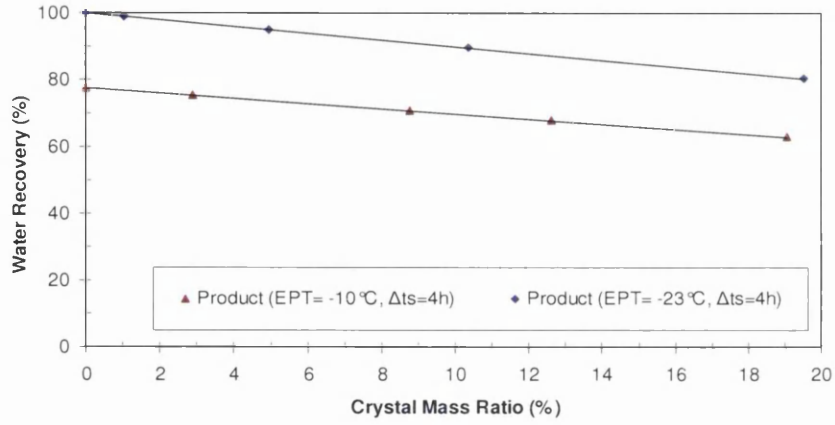

(c) Water recovery vs. crystal mass ratio

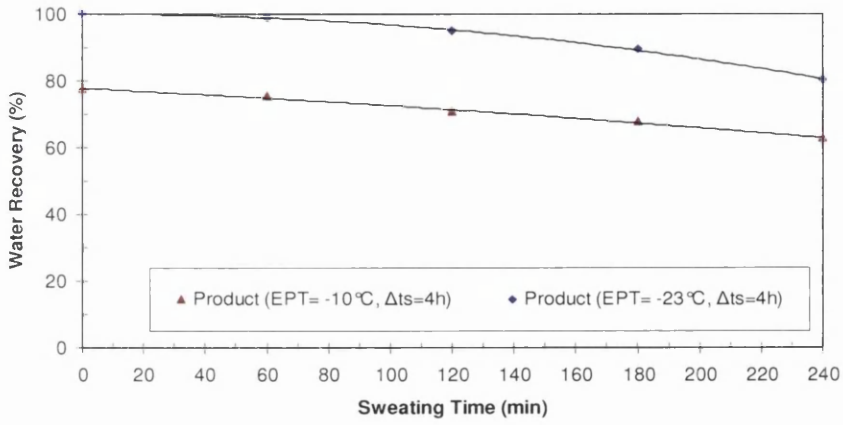

(d) Water recovery vs. sweating time

Fig. 7.13: *Influence of endpoint temperature of the crystallisation stage on the product water concentration and sweating performance, where EPT is the end-point temperature, and Δts is the sweating time. The investigated operating conditions are; materials: start and end-point of crystallisation temperature are -5 to -23°C, respectively, for a crystallisation time of 5.5 hours, and sweating time of 4 hours.*

with an end-point temperature of -23°C, the calculations of the salt rejection ratio, before the sweating operation, give 0 %, because the feed sample was completely frozen. In contrast, the final salt rejection ratio increased dramatically to 40.39 % after carrying out the sweating process. The salt rejection ratio, before the sweating operation, was 37.73 %, for the case where the end-point temperature was -10°C. The salt rejection ratio increased to 65.17 % after sweating. This indicates that the end-point crystallisation temperature is proportional to the salt rejection ratio.

A dramatic increase in the water recovery ratio was observed as the end-point crystallisation temperature was reduced as shown in Figs (7.13) (c) and (d). This gives a clear indication that the water recovery ratio is inversely proportional to the end-point crystallisation temperature. For the test with an end-point temperature of -23°C, the water recovery ratio was 100% (see Figs (7.13) (c) and (d)), as the residual liquid was nil during the draining phase, because the mass of feed was completely frozen. As for the performance of the sweating process, the salinity of the final product water reached 2.13 wt% and 3.64 wt% at end-point crystallisation temperatures of -10 and -23°C, respectively, whereas the water recovery ratios reached 62.75% and 80.45%, respectively.

In the fifth investigation, the residues discharged from the falling film and suspension crystallisation processes (see Chapters 5 and 6) were individually collected, prepared and tested as feed water. This means that the investigation was carried out on two highly concentrated RO brines with salinities of 14.78 and 13.00 wt%. The investigated start-point and end-point temperatures were -10 and -19°C, respectively. The crystallisation and sweating times were set at 5.5 and 4 h, respectively. This investigation was carried out to determine the potential capability of using the static crystallisation technology as a pre-concentration system for concentrating the mentioned residues. The salt concentrations of crystal layers, before and after the sweating process, were measured in order to determine the optimal operating conditions. In this investigation, the overall experimental results, including salt and mass balances, will be considered for scaling up the proposed treatment system to commercial applications.

Results of salt concentration of product and water recovery, as a function of the crystal mass ratio and sweating time are shown in Fig (7.14). Figs (7.14) (a) and (b) show the variation of

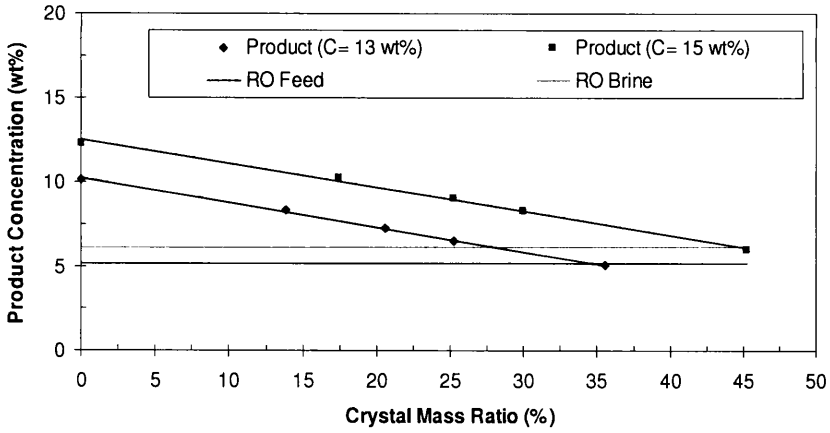

(a) Product concentration vs. crystal mass ratio

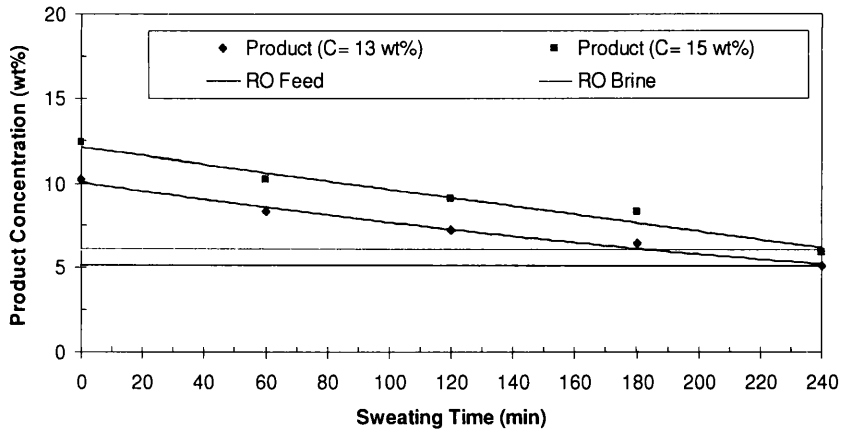

(b) Product concentration vs. sweating time

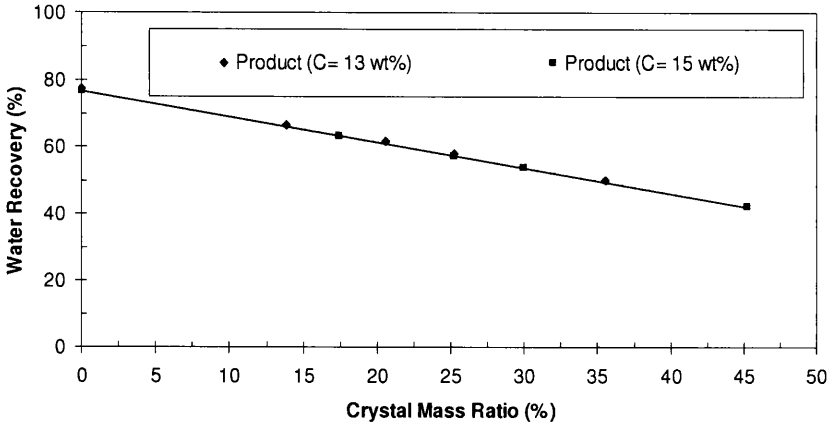

(c) Water recovery vs. crystal mass ratio

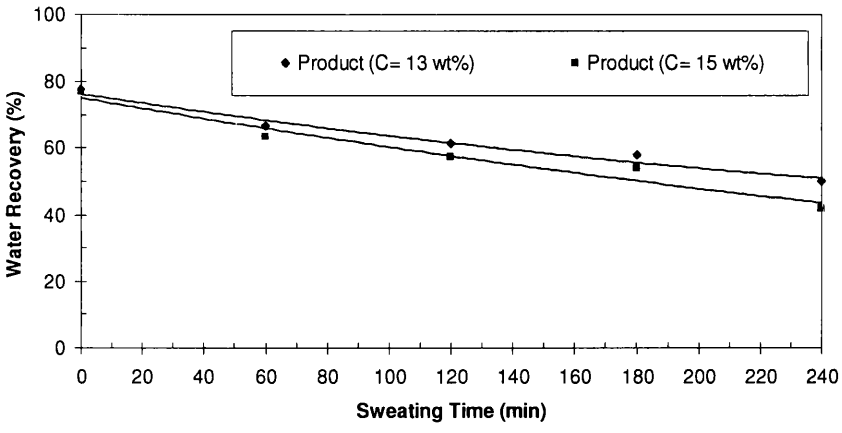

(d) Water recovery vs. sweating time

Fig. 7.14: *Operating conditions and experimental results for static crystallisation using laboratory apparatus with a 6L crystalliser. Operating conditions are: feed solutions of RO brine (with concentrations of 13 wt% and 15 wt%, respectively), start and end-point of crystallisation temperature are -9 to -19°C, respectively, at a crystallisation time of 12.5 hours, and sweating time of 4 hours.*

the salt concentration of the crystal layer (investigated at different feed concentrations) as a function of the mass crystal ratio and sweating time. Agreement with the findings of the previous investigation, concerning the influence of feed concentration, mass ratio, and sweating time, on the product quality is clearly observed. Figs (7.14) (c) and (d) show the effect of several influences, such as feed concentration, crystal mass ratio, and sweating time, on the water recovery ratio. In general, the salinity of the feed waters with salt concentrations of 13.00 and 14.78 wt% were lowered to 6.11 wt% and 5.06 wt% respectively, whereas the final water recovery ratios reached 41.90% and 49.84%, respectively. For the case of a treating feed with a salinity of 13.00 wt%, the salt rejection ratio, before the sweating operation, was 21.63 %, whereas the sweating process was capable of increasing the salt rejection up to 61.10%. In contrast, for the case of treating a feed with a salinity of 14.78 wt%, the salt rejection ratio, before the sweating operation, was 17.87 %, which was then significantly increased to 60.46 % after performing the sweating process. The results showed that, for the feed concentration of 14.78 wt%, the minimum sweating time that should be considered is 4 h. This is because when the sweating time was less than 4 h relatively poor quality product water was produced. As for the feed concentration of 13.00 wt%, the minimum sweating time that can be considered was either 3 or 4 h. This is because the sweating process at a running time of 3 h was capable of providing a crystal layer of near RO brine standards (see Fig (7.14) (a)), whereas a sweating time of 4 h can further reduce the salinity of crystal layer, leading to a final product water of near Arabian Gulf seawater, in terms of salt concentration. Thus, production rate will be increased for such an application, leading to a reduction in the operational cost.

7.6.4 Scaling-up of the Sulzer static crystallisation technology

The performance data obtained from the fifth investigation provided clear evidence that the static crystallisation process, using a single freezing stage with use of a sweating process, was capable of producing a significant amount of seawater or RO brine from highly concentrated RO brine, whilst simultaneously minimising the volume of the waste stream as far as possible. The scale-up for the Sulzer static crystallisation process is straightforward, since the commercial static crystallizer is usually built by increasing the surface area and number of the plates. Although the fifth investigation was carried out on the laboratory pilot scale setup using the crystalliser with a capacity of 6 L, the examined apparatus, according to

Sulzer, gives almost the same separation performance as the pilot plant. Hence, the proposed commercial plants were scaled up based on the experimental results.

The combination of commercial plants, which were previously proposed in Chapters 5 (see Fig (5.18)) and 6 (see Fig (6.23)), were used as examples for scaling-up the integration of the RO desalination plant with the existing portfolio of Sulzer melt crystallisation technologies, namely suspension, falling film, and static crystallisation processes, under continuous operation. These examples will give an estimation of the separate plant's capacity including the salinities of all liquid streams, which represent crucial factors for evaluating the actual water treatment investments.

Based on the findings of the experimental investigation, three novel treatment option configurations are possible to deal with RO brine concentration. As shown schematically in Figs (7.15) and (7.16), treatment options 1 and 2 involve integration of a RO plant, and Sulzer suspension and static crystallisation plant. The difference between these two treatment options (i.e. treatment option 1 and 2) is that the product water provided from the static crystallisation plant, in the treatment option 1 (see Fig (7.15)), is recycled into the main stream of feed water of the RO plant. In contrast, the static crystallisation plant, in treatment option 2 (see Fig (7.16)), produces saline water which is recycled back to join the main feed stream of the suspension crystallisation plant. On the other hand, treatment option 3 involves the integration of a RO plant, and Sulzer falling film and static crystallisation plant, as shown schematically in Fig (7.17). The estimated figures for the volume flow-rates and salt concentrations of all liquid streams of each commercial plant are illustrated in Figs (7.15) – (7.17). According to Sulzer, the proposed commercial plants can be designed and built without any constraint; however, such an application might be hindered by the economic barriers associated with the investment costs.

Table (7.5) shows the estimated annual rates of all liquid streams and salt concentration of the combined commercial plants. The conventional RO plant cannot compete with any treatment option given in Table (7.5), in terms of the production rate and reduction in the volume of the waste stream (see Table (7.5)). In terms of the production rate, treatment option 2 is the most preferable treatment option, since these combined plants produce the

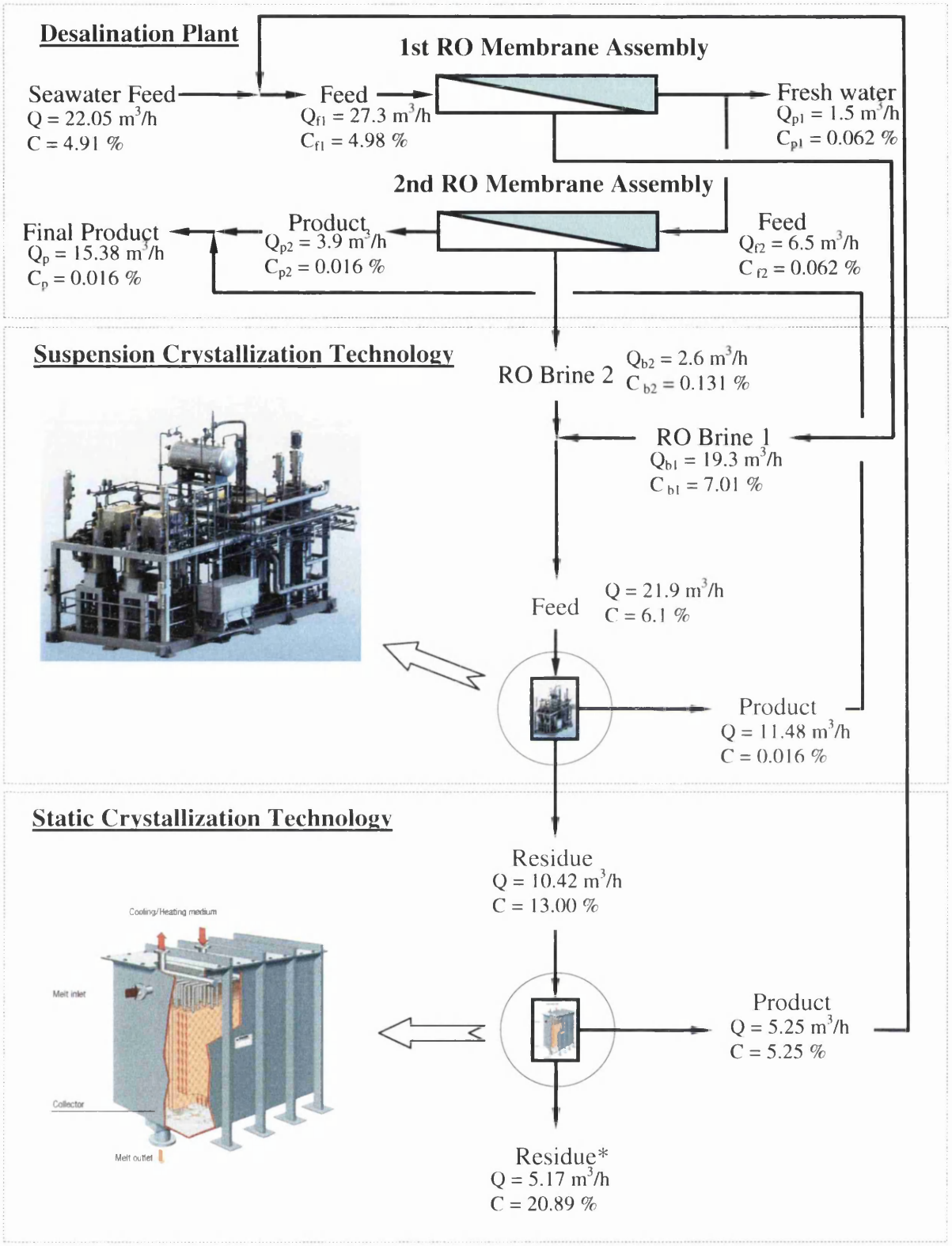

Fig. 7.15: *Treatment option 1, a combination of commercial plant comprising a seawater Reverse Osmosis (RO) membrane desalination plant coupled with suspension and static crystallization plants, where Q is the volume flow-rate (m^3/h), and C is the salt concentration, and subscripts f= feed-water, p= product water, b= brine, and 1 and 2 refer to the stage number.*

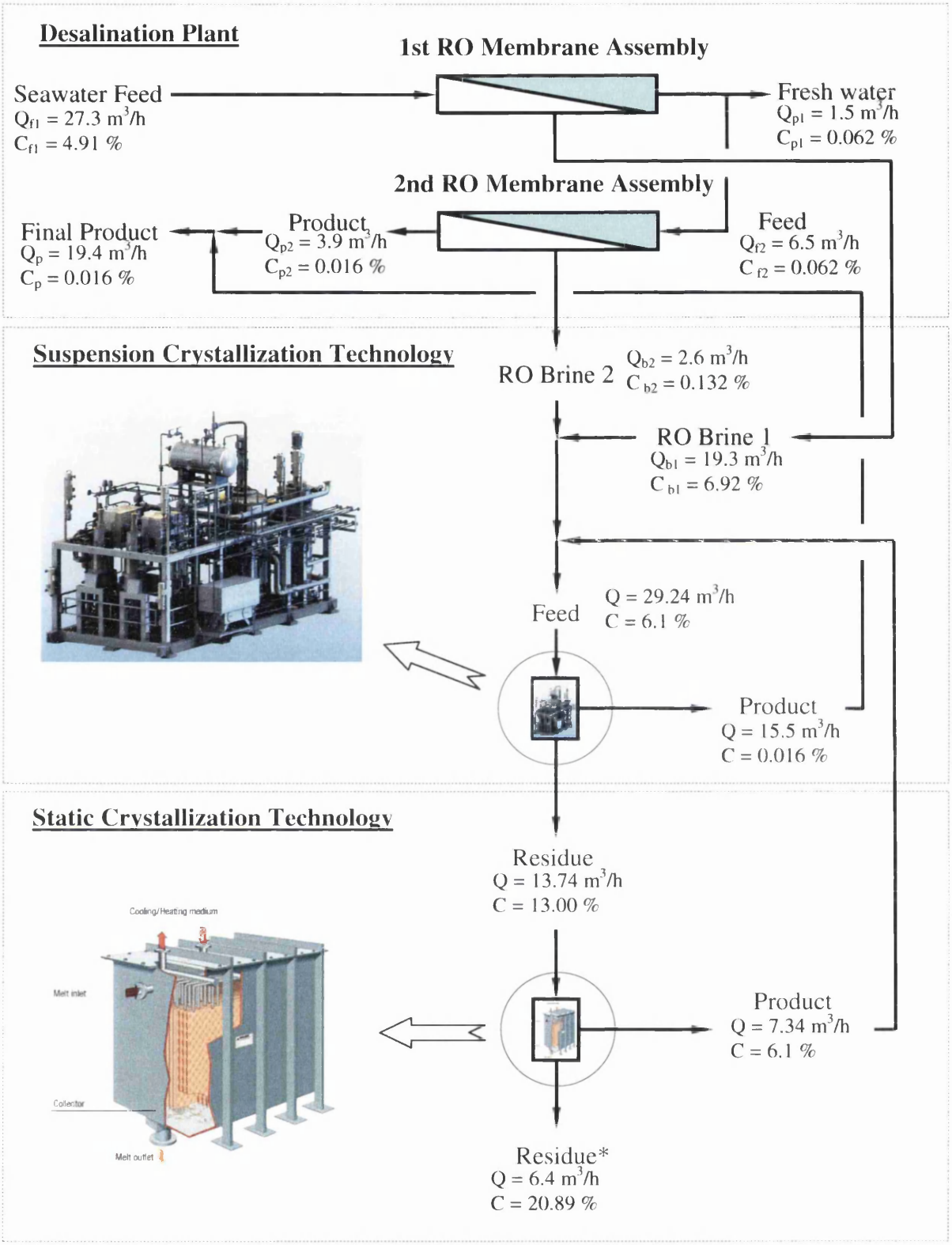

Fig. 7.16: *Treatment option 2, a combination of commercial plant comprising a seawater Reverse Osmosis (RO) membrane desalination plant coupled with suspension and static crystallization plants, where Q is the volume flow-rate (m^3/h), and C is the salt concentration, and subscripts f= feed-water, p= product water, b= brine, and 1 and 2 refer to the stage number.*

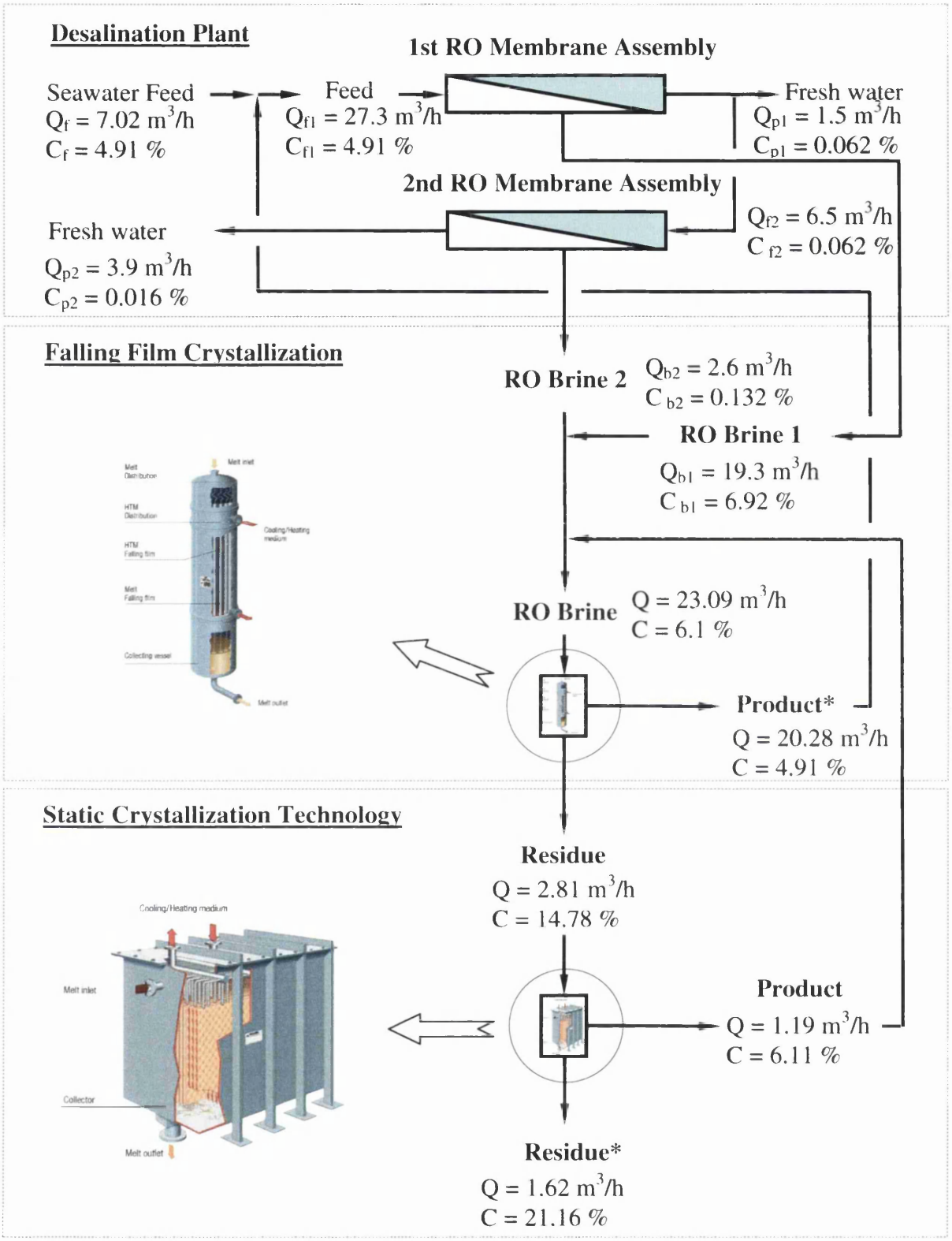

Fig. 7.17: *Treatment option 3, a combination of commercial plant comprising a seawater Reverse Osmosis (RO) membrane desalination plant coupled with Sulzer falling film and static crystallization plants, where Q is the volume flow-rate (m^3/h), and C is the salt concentration, and subscripts f= feed-water, p= product water, b= brine, and 1 and 2 refer to the stage number.*

highest annual rate of product water (see Table (7.5)). Furthermore, this treatment option offers a substantial reduction in the volume of the waste stream in comparison with the conventional RO plant (see Table (7.5)). However, the disadvantage of treatment option 2 is that the exploitation of natural water resource will remain the same as the conventional RO plant (see Fig (7.16)). In contrast, treatment option 3 is the most preferable option, in terms of RO brine concentration and preservation of the natural water resource. This is because the proposed treatment option can significantly reduce the volume of the waste stream to the lowest level, when compared to the other treatment systems (see Table (7.5)). Alongside the RO brine concentration, such a treatment option can preserve a significant amount of natural water resource from exploitation. This is achieved by recycling the product water of the Sulzer falling film crystallisation plant to join the main feed stream of the RO membrane plant (see Fig (7.17)). The calculations showed that the estimated annual rate of the feed intake of the RO membrane plant can be dramatically reduced from 239.154 down to 61.5 ton/year. However, the disadvantage is that the production rate of this treatment option is equivalent to that in the conventional RO plant (see Table (7.5)). Treatment option 1, on the other hand, is capable of increasing the production rate, while simultaneously reducing a substantial amount of the waste stream, as illustrated in Table (7.5). Such a combination can also preserve a reasonable amount of natural water resource from exploitation (see Fig (7.15)). The calculations showed that the estimated annual rate of the feed intake of the RO membrane plant can be lowered from 239.154 to 193.05 ton/year.

Treatment Option	Feed		Product*		Brine	
	(t/y)	(wt%)	(t/y)	(wt%)	(t/y)	(wt%)
Conventional RO Plant	239.15	4.91	34.17	0.01	191.84	6.11
Treatment Option 1	239.15	4.91	134.73	0.01	45.29	20.89
Treatment Option 2	239.15	4.91	169.94	0.01	56.06	20.89
Treatment Option 3	239.15	4.91	34.17	0.01	14.19	21.16

Table 7.5: *Estimation of the annual rates and salt concentration of all water streams of Kadhmah RO desalination, and treatment option 1, 2, and 3, where (t/y) represents ton per year.* * *The first stage of the RO membrane assembly produces product water at 8 m^3/h, where 6.5 m^3/h of this is fed to the second stage RO membrane assembly, while the remaining product water from the first stage (i.e. 1.5 m^3/h which is equivalent to 13.14 t/y) is not used and drained (see Fig (7.15)).*

In general, the overall salt rejection ratio is same, which is 99.8%, whereas the overall water recovery ratios for the conventional RO plant, and treatment option 1, 2, and 3 are 14.29, 56.34, 71.06, and 14.29%, respectively.

The estimated power consumption was theoretically computed for each crystallisation process in the proposed treatment options, and is presented in Table (7.6). In general, the values of the theoretical power consumption were varied. This was because the theoretical power consumption is affected by several factors, such as plant capacity (i.e. volume of feed water), the production rate, and the salt concentration of the residue (more specifically the freezing point of the residue).

Treatment Option	Process	Estimated Power Consumption (kWh/m^3)
Treatment Option 1	Suspension crystallisation	110.79
	Static crystallisation	136.53
Treatment Option 2	Suspension crystallisation	110.59
	Static crystallisation	134.03
Treatment Option 3	Falling film crystallisation	96.13
	Static crystallisation	144.88

Table 7.6: *Summary of the energy consumption of the crystallisation process involved in the proposed treatment option.*

7.7 Conclusions

This chapter was devoted to the experimental evaluation and validation of the separation performance of the static crystallisation process for concentration of different salinity RO brines. The experiments were carried out on laboratory bench scale, and a pilot plant in batch operating mode. The majority of tests were devoted to highly saline RO brines produced from falling film and suspension crystallisation processes. Alongside the process brine, aqueous solutions of sodium chloride were also tested. Several influences upon the separation performance of crystallisation and sweating processes were investigated and determined.

In general, the results proved that the static crystallisation process, within a single stage without a sweating process, was able to concentrate a significant amount of RO brine while producing saline water of near Arabian Gulf seawater quality. As for the experiments with highly concentrated RO brines, the results proved that the treatment system, for a single stage, was not able to lower the tested feed down to RO brine without using a sweating process. By optimising the crystallisation and sweating operations, the product water salinity was improved and lowered to RO brine and seawater levels. Therefore, the results were highly encouraging, and suggested the application of the static crystallisation process for concentrating highly saline RO brine. Thus, the static crystallisation process was scaled up and combined with a commercial RO plant and falling film crystallisation plants for minimising the waste stream and maximising the production rate and/or preserving natural water resource. Simple calculations were made to estimate the power consumption for different treatment systems. The power consumption of the static crystallisation was varied from 134 to around 145 kWh/m^3 in such an application.

CHAPTER VIII:

CONCLUSIONS AND RECOMMENDATIONS

The primary concern of this study was to seek the most feasible and applicable freezing desalination technologies that are potentially capable of desalting and/or concentrating the dissolved ionic content of liquid streams, especially those brines causing severe pollution. Therefore, various forms of melt crystallisation processes, namely solid layer and suspension crystallisation, were considered and experimentally investigated for such an application. These experimental studies were intended to evaluate and validate the separation performance of each treatment process. In general, the experimental investigation was carried out at both laboratory bench scale and using pilot plant with aqueous solutions of sodium chloride and process brines as feed samples. The experimental work also focused on a number of important parameters influencing the separation performance of the investigated treatment systems.

At the moment there is no best freezing desalination technology which can be considered among the investigated processes because each examined treatment system has its own advantages and disadvantages. For example, Table (8.1) shows the general comparison of the characteristics of the solid crystal layer and suspension crystallisation processes including the pros and cons of each process. In addition to this, determining the best desalination by freezing process will vary from one application to another depending on a number of important factors, such as physiochemical characteristics of feed water (including salinity and hardness level), desired product concentration, volume of water to be treated, residue volume and concentration, the solubility limit of some salts, eutectic temperature of salts, final brine disposal method, site-specific conditions, the federal effluent limitation guidelines, and capital and operational costs. However, when the selection of the treatment option that will be considered is based on the quality of product water, such as obtaining drinking water, then the best selection of desalination by freezing process would be the suspension crystallisation. On the other hand, the solid layer crystallisation processes (e.g. falling film and static crystallisation processes) were found as the best treatment options when the selection that will be considered is based on preserving a large volume of natural water resource from exploitation and minimising the waste stream to the minimum level. In general, Table (8.2) summarises the performance of the examined melt crystallisation

Feature	Crystallisation Process	
	Solid Crystal Layer	**Suspension**
Process Concept	Based on the formation of a crystal layer on a cooled heat exchanger	Based on the formation of crystals which are freely suspended in the mother liquor
Process Equipment	No moving parts except HTM circulation pump for the static crystallisation process (and melt circulation pump, stirrer, air-pump, ultrasonic device for the dynamic crystallisation processes)	Moving parts (e.g. circulation pumps, scrapers, piston drive)
Operation	Discontinuous (predominantly)	Continuous (predominantly)
Washing Equipment	Partial melting (sweating) or rinsing	Piston type wash-column
Temperature of Melt	Close to above solidification temperature	Below solidification temperature
Melt Flow-Rate	• No for static crystallisation • High for falling film crystallisation	Low
Heat Withdraw	Through crystal layer	Through the melt
Crystal Growth Rate	High	Low
Relative Interface Crystal-Melt	Low	High
Product Transportation	Simple	Difficult
Solid-Liquid Separation	Simple	Difficult
Encrustation Problems	No	Accessible (removed continuously by scraper)
Scale-up	Simple	Difficult
Energy Consumption	High	Low

Table 8.1: *General comparison of the characteristics of the solid crystal layer and suspension crystallisation processes [Ulrich and Glade, 2003].*

Crystallisation Process	**Feed Concentration (wt%)**	**Product Quality** (wt%)	**Water Recovery** (%)	**Pros**	**Cons**
Static	6 13 15	4.5 6 4.9	90 42 50	1. No Encrustation problems 2. Good controllable crystal growth 3. Scale-up is simple 4. Simple solid-liquid separation 5. Control and operation is simple (no slurry handling) 6. Simple in post-treatment crystallisation 7. Ease staging opportunities 8. No moving parts except circulation pump or stirrer for dynamic concept	1. Limited area of heat transfer surface 2. Requires high temperature driving force 3. Requires additional energy heat and time for separating and melting the crystal layer 4. Batch operating mode
Mechanically Stirred	0.5	1.5	55	See static pros except point 3	1. See static cons 2. Difficult to scale-up
with Ultrasonic Device	0.5	0.08	15	See static pros	See static cons
with Air-Pump	0.5	0.25	58		
Falling Film	6	4.9	88		
Suspension	6	≈ 0.01 (Drinking water)	53	1. Less energy consumption 2. Continuous operating mode 3. Superior purification can be produced from a single stage 4. Producing high purity products (i.e. drinking water or distilled water) 5. higher crystal production rate per unit volume of equipment	1. Crystallisation and washing processes are difficult 2. Contains complicated moving parts 3. Solid-liquid transportation and separation are difficult 4. Scale-up is difficult 5. Encrustation problems 6. Control and operation is difficult (requires ice slurry handling)

Table 8.2: *Summary of performance of the examined technologies.*

technologies at various feed water concentration ranging from 0.5 to 15 wt%. Pros and cons for each given treatment system are also covered in Table (8.2). Table (8.3) summarises the performance of a number of the proposed treatment options by combining the melt crystallisation technologies with RO plant. These treatment options were introduced for costal and inland desalination plants aimed at increasing the water recovery and/or minimising the waste stream to the minimum level. In general, treatment options 3, 5, and 6 are the best selection for increasing the drinking water production and simultaneously decreasing the waste stream to certain limits, whereas treatment options 2, 4, and 7 are the best selection for only decreasing the waste stream to minimum levels at constant production rate. However, treatment option 4 has a significant disadvantage which is that the production rate of the static crystallisation process is low when compared to falling film crystallisation.

8.1 Static and Agitated Crystallisation Processes

This study evaluated the validity of static crystallisation processes, with and without agitation systems for saline water applications. The objective of this study was to verify several influences, namely feed concentration, crystallisation temperature, crystallisation time, and agitation rate, upon the salt rejection and water recovery ratios. This investigation was carried out on a single freezing stage, without use of a sweating process. The tested agitation systems were a bubbling process, a mechanically stirred system, and an ultrasonic process. Aqueous feed solutions of 0.5, 3.5, and 7.0 wt% sodium chloride were used and a phase diagram was established for the freezing points of the investigated feed samples.

The results of the static crystallisation experiments showed that the salinity of product water is very sensitive to changes in crystallisation temperature. This was because the salt concentration of the product was relatively poor for all feed samples, including low feed concentrations when the crystallisation temperature was -11.5°C. When the crystallisation temperature was increased to -4.8°C, a dramatic decrease in product salinity was observed. In fact, the salt rejection ratio was slightly improved with increasing crystallisation time (in the cases where crystallisation temperature was -11.5°C). This was because the heat transfer rate was reduced as the thickness of the crystal layer increased. Thus, this action leads to lower crystal growth rate as the crystallisation time is increased. The product concentration was found to be proportional to the feed concentration, whereas the water recovery ratio was

No.	Treatment Option	Feed Concentration (wt%)	Product Concentration (wt%)	Water Recovery (%)	Brine Concentration (wt%)	Concentration (%)
1	RO Plant (see Fig (5.18))	4.9	≈ 0.01 (Drinking water)	14.3	6.1	85.7
2	RO plant combined with falling film crystallisation (see Fig (5.18))	4.9	≈ 0.01 (Drinking water)	14.3	14.8	33.1
3	RO plant combined with suspension crystallisation (see Fig (6.22))	4.9	≈ 0.01 (Drinking water)	57	13	37.7
4	RO plant combined with static crystallisation (see Table (A7-13))	4.9	≈ 0.01 (Drinking water)	14.3	20.5	6.2
5	RO plant combined with suspension and static crystallisation – Option 1 (see Fig (7.15)	4.9	≈ 0.01 (Drinking water)	56.3	20.9	18.9
6	RO plant combined with suspension and static crystallisation – Option 2 (see Fig (7.16))	4.9	≈ 0.01 (Drinking water)	71.1	20.9	23.4
7	RO plant combined with falling film and static crystallisation (see Fig. (7.17))	4.9	≈ 0.01 (Drinking water)	14.3	21.1	5.9

Table 8.3: *Summary of performance of the proposed treatment options.*

found proportional to the crystallisation time and inversely proportional to the crystallisation temperature and feed concentration.

In general, the experimental results indicate that the agitation systems can improve the salt concentration of product water for feed salinities of 3.5wt% and below. For the purpose of scaling up, the bubbling process seems to be the most feasible technique, since this method can be easily installed in a commercial static crystalliser.

Although this study was carried out within a limited operating condition (and without a sweating process), the results were highly encouraging. Hence, the assessment of agitated crystallisation process should be further investigated with a wider range of operating parameters and limits, as well as applying the sweating process aimed at improving the separation performance. The recommendation is for the crystalliser capacity to be increased to a suggested range of 1.5 to 6.0 L, taking into account that the investigated agitation system might be changed to higher agitation rates corresponding to the crystalliser's capacity. Detailed technical-economic analysis and studies are recommended to be taken into consideration in future research to estimate the actual power consumption of the investigated agitated crystallisation process and compare the figures obtained to those for the static crystalliser.

8.2 Ice Maker Technology

An ice maker machine, which utilises the falling film crystallisation principle, was evaluated as a water treatment system for saline water applications. The experiments were limited in their number, but were enough to draw clear and reasonable conclusions that achieved the objectives of this study. Different parameters influencing the separation performance were investigated using the ice maker.

Within the domain studied, the experimental investigation gave a clear indication that the feed concentration has a significant influence on the salt rejection and water recovery ratios. For the feed samples with low salt concentrations, the salt rejection and water recovery ratios were strongly dependant on the ice thickness and flow-rate. For the feed samples with high salt concentration, only the water recovery ratio was influenced by ice thickness and flow-

rate. The salt rejection ratio did not significantly changed within the predetermined values of the influential operating parameters.

The power consumption, on the other hand, was found to be strongly dependant on three important factors, namely the water recovery ratio, and the salt concentrations of the feed and product water. The production rate dramatically increased when producing a final product water that is comparable to seawater quality. This leads to a significant reduction in the power consumption when compared to the seawater desalination application. In order to estimate the actual power consumption of the treatment/desalination system using the adopted ice maker technology, detailed technical-economic analysis and studies on industrial pilot scale must be taken into consideration in future research. The water recovery, salt rejection, and concentrations ratios should also be considered as influential parameters in future power requirement analysis. Furthermore, other associated factors, including capital equipment and costs, power requirements, and operating labour, are highly recommended for future consideration, in terms of technical-economic studies.

Multistage processing using the icemaker was also investigated. The results showed that the ice maker was not able to reduce the salinity of seawater down to potable water (at 500 ppm) or even down to irrigation water (at 1,500 ppm) levels within three stages. Within the studied domain, the tested ice maker technology cannot compete with conventional seawater desalination technologies for producing potable or irrigation water, however, the separation performance of the ice maker, in terms of water recovery and salt rejection ratios, might be improved by investigating the studied and other influential parameters within a wider range of operating limits. Also, according to Ulrich and Glade (2003), the impurity within ice crystals can be significantly reduced by conducting post-crystallisation treatment, such as rinsing, diffusion washing or sweating processes. Therefore, these post-treatment processes are highly recommended as the subject of further research. The application of the ice maker, and more specifically the falling film crystallisation process (involving both crystallisation and sweating operations) has to be well optimised, in order to find out the actual technical and economical feasibility in the field of seawater desalination.

RO brine concentration experiments were also tested, and the ice maker was found to be effective in removing significant amounts of dissolved salt from various concentrated

solutions of RO brine over four successive freezing stages. The initial experimental results suggested that four-stages at least were necessary to lower the concentration ratio to less than 16%, for a water recovery ratio above 84%. The quality of the overall product water was comparable to the RO feed (i.e. Arabian Gulf seawater), with respect to the salt concentration, without having the need to use post-treatment crystallisation processes, such as sweating, rinsing, and washing. This means that the treated waters can easily be further desalted by recycling the treated water back to join the main feed stream of a RO plant. In general, this investigation proved that the adopted treatment system and technology is encouraging and highly attractive for concentrating RO brines.

The simultaneous production of treated water and concentration of RO brine represents a major advantage of this novel technology. Moreover, the tested ice maker technology is by far a less complicated process, when compared to the conventional freezing desalination technologies, since mechanical moving parts (apart from the circulation pump) and the complications of separation and post-treatment crystallisation processes are eliminated. Furthermore, the adopted technology can be easily scaled-up for commercial applications. Although commercially-available ice making technologies are not designed for saline water applications, minor modifications made to existing designs will enable a change in application. By combining the facilities of RO membrane technology with those of the ice maker, or similar technology, great benefits would be rendered for inland RO desalination plants. For instance, preserving the limited amount of natural water resources, reduction in chemical additives and cost of pre-treatment, reduction in the capacity and cost of intake facilities, a significant reduction in the appearance of viruses, bacteria, and colloids, significant reduction in the volume of waste streams causing the most severe pollution problems, enhancing the safe disposal methods, reduction in the capacity and water treatment costs of the subsequent concentration processes and/or disposal system. Hence, the examined treatment system may compete with other conventional treatment/concentration technologies.

The majority of previously published articles have focused on seawater desalination by freezing to produce a product of near drinking water quality, whereas concentrating RO brines by freezing to produce a final product water of near brackish water or seawater standards has, to the best knowledge of the researcher, never been investigated and was

overlooked. Therefore, special attention should be given to such an application. Furthermore, this study must be taken into consideration for future research with use of an industrial scale plant to evaluate and validate the actual performance and efficiency of salt separation and water recovery ratio. Therefore, attention must be given to ice-making machines and similar technologies in future research.

8.3 Sulzer Falling Film Crystallisation Process

This study assessed and validated the performance of solid layer crystallisation and sweating processes, using Sulzer's falling film crystallisation pilot plant, for desalting and concentrating different concentrations of process brines, including Arabian Gulf seawater and RO retentate. Unlike the conventional 'desalination by freezing' technologies, the examined treatment process does not include the complicated solid-liquid separation and washing equipment, as it relies on the freeze-melt principle.

Due to the absence of appropriate data on seawater and brine applications, different parameters influencing the crystallisation and sweating separation efficiencies were investigated using the pilot plant operating in batch mode. The experimental investigation provided a clear indication that a number of parameters, namely feed concentration, crystallisation temperature, cooling rate, and average growth rate, had a strong influence on the separation performance of the crystallisation process, in terms of salt rejection ratios. The purity of the product water was found to be proportional to the crystallisation temperature and cooling rate, and inversely proportional to the feed concentration and average growth rate. The purification efficiency of the sweating process, on the other hand, was found to be strongly dependant on four important factors, namely the salt concentration of the crystal layer, sweating rate, sweating time, and the crystal mass ratio. The purity of the crystal layer was found to be proportional to the sweating time and crystal mass ratio, and inversely proportional to the crystal layer salinity and sweating rate.

The separation performance of a multistage process, using two successive freezing stages, was investigated with the sweating process for the seawater desalination application. The results of the experimental investigation were somewhat encouraging. Although the water recovery ratio was reasonable, the salt concentration of the final product of the rectification stage was relatively poor when compared to drinking water. Therefore, the quality of the final

product water may be improved by further optimising the temperature and rates of crystallisation and sweating processes. This is because the mentioned parameters greatly influence the purification efficiency of crystallisation and sweating processes; otherwise, a second rectification stage must be taken into consideration to achieve further purification. The overall production rate of the multistage process, on the other hand, is a critical and crucial factor for the assessment of the economical feasibility of the proposed treatment system. Therefore, the overall running time and water recovery ratio of the multistage process must be maintained at reasonable levels; otherwise a significant increase in the water treatment costs will be expected. Therefore, these key parameters must be considered and applied under strict control in future research in the field of seawater desalination. The preliminary results concluded that the Sulzer falling film crystallisation technology will be hindered by process reliability and economic aspects in seawater desalination applications. As a result, the proposed treatment option cannot compete with the available conventional water desalination technologies, e.g. RO membrane seawater and thermal desalination technologies.

As for the RO concentration experiments, the experimental data proved that a single freezing stage, without use of sweating process, was capable of producing a significant amount of product water, and simultaneously reducing the volume of RO retentate to a minimum as far as possible. The quality of the final product water (in terms of salinity and ionic composition) was found to be comparable with Arabian Gulf seawater, and was ready for immediate re-use as feed water for a RO membrane desalination plant. Based on the experimental results, a maximum water recovery ratio of 86% was achieved, whereas the theoretical calculations, using mass and salt balance formulas, determined that the maximum water recovery ratio can be increased to 92%. In order to increase the experimental water recovery ratio, the commercial Sulzer plant should be modified and equipped with one of the following suggested equipments; (i) Replacing the existing pump with another type of pump that can be run dry without exposing the pump to the risk of damage, taking into account that the selected pump must be suitable for the chemical characteristics of the RO brine, and can be used under the operating conditions of Sulzer's plant. Thus, the pump can be operated at the minimum level of water in the collecting tank during the crystallisation process; (ii) changing the design of the existing collecting tank by modifying the shape of the lower surface of the tank into a conical shape that fits the size and shape of the existing melt circulation pump.

The conical shape will help to receive and gather a greater amount of melt, leading eventually to extending the operation of the pump during the crystallisation process to recovering more crystal mass, i.e. maximising the water recovery ratio and minimising the water level in the collecting tank.

By concentrating RO brine in a single freezing stage without use of the sweating process, a number of important advantages can be rendered to the Sulzer plant; these are (a) the sweating process will be completely eliminated from the freezing stage, so there is no product mass loss i.e. crystal mass ratio will be neglected. As a result, the crystal layer will be maintained at maximum mass; (b) the time retention of the freezing stage will be substantially reduced, since the partial melting process will be carried out in the fastest possible way, and the production rate will be dramatically increased; and (c) additional power consumption of the sweating process will be avoided.

The experimental results gave a clear indication that the Sulzer technology can be operated under any operating conditions, within the domain studied, as long as the desired quality of product water is equivalent to Arabian Gulf seawater, i.e. feed water of a RO plant. As a result, influencing factors, such as crystallisation temperature, crystallisation time, cooling rate, and average growth rate, are no longer sensitive to the product quality in such an application. This allows the treatment system to be run at a wider range of operating limits for the RO brine concentrations. However, low operating crystallisation temperatures and rates may be limited by operational water treatment costs.

In general, the performance data of the proposed Sulzer plant was highly encouraging in reducing the volume of the RO retentate to a minimum, and substantially increasing the volume of treated water. Therefore, the Sulzer plant might be competitive with other treatment systems used for RO brine concentration. The advantages of the Sulzer plant are absence of pre-treatment and post-treatment systems, absence of chemical additives, absence of moving parts (apart from melt and HTM pumps), absence of complicated separation equipment, process simplicity, ease of operation and maintenance, and less susceptibility to the major technical limitations in seawater desalination plants, such as scaling, fouling and corrosion. As for the economical aspect, lower operational costs can be achieved, since the latent heat of fusion of ice is one seventh for boiling or distillation processes, whereas the

capital cost can be substantially lowered by using low-cost materials, such as plastic. Furthermore, ease of operation and process simplicity reduce the labour costs substantially, while ease of maintenance and lower maintenance costs due to absence of complicated separation equipment and moving parts dramatically reduces the maintenance costs.

The examined pilot plant was scaled-up according to the performance data obtained from experiments, in order to integrate the commercial falling film crystallisation plant with the Kadhmah RO membrane desalination plant. Sulzer confirmed that the proposed commercial falling film crystallisation plant can be built without any technical problem. Such a combination offers great advantages, including: preserving natural water resource from exploitation and minimising the volume of waste stream. In addition to this, the combined plant offers number of great benefits to the desalination plant, which will be given in section (8.5)

As treatment of RO retentate is a new application for the Sulzer falling film crystallisation process, the assessment and verification of the performance of the examined pilot plant combined with actual RO plant should be considered and studied in continuous operating mode in future research. This research area should be given special attention due to the extensive use of natural water resources in water desalination plants, and more specifically in inland RO desalination plants.

The separation efficiency of feed and rectification stages was assessed with the use of a sweating process for desalting RO brine. The results of the product water obtained from the feed and rectification stages were found to be relatively poor, when compared to drinking water standards. Since the crystallisation and sweating experiments were carry out with a limited number of key operating parameters, further experimental investigation is recommended for a wider range of parameters in future research. The suggested key parameters for the crystallisation experiments are feed concentration, crystallisation temperature, cooling rate, and average growth rate. The suggested key parameters for the sweating experiments are the salt concentration of the crystal layer, sweating rate, sweating time, and the crystal mass ratio. On the other hand, the separation performance of the stripping stages was investigated with use of the sweating process for concentrating and treating the highly concentrated solution of RO brine. The results of the experimental

investigation for the stripping stage were not encouraging. This was because the stripping stage was not able to reduce the concentration of product water down to RO feed or RO brine salinities. In fact, the quality of the product water of the stripping stage was significantly poor, as the product quality was comparable to the feed water of the stripping stage. Therefore, the performance results obtained provided clear evidence that the Sulzer falling film crystallisation would not be an ideal process for a stripping stage, because the technology cannot deal with a highly concentrated solution of RO brine.

Throughout the experimental investigation with feed and rectification stages, scaling and fouling problems were not visually observed, which was confirmed through the results of chemical analysis for all liquid streams. However, precipitation of solid salts was visually observed in the stripping stage and the results of water chemistry analysis had confirmed that there was loss in some ions. This was due to several factors, such as low crystallisation temperature (which was lower than the eutectic temperature of NaCl salt), feed water with a high TDS value, and high levels of minerals including hardness ions. Therefore, these factors must be taken into consideration in future research, in order to avoid the precipitation of solid salts in the stripping stage. Suggested solutions are reducing crystallisation temperature, higher cooling rate, increasing sweating rate and time, and increasing mass crystal ratio. In addition, in order to collect the precipitated solid salts in a collecting tank, a mesh filter strainer screen is recommended to be installed in the collecting tank. The precipitated solid salts can be easily drained with the residual liquid under the influence of gravity by means of a drain valve.

In general, the laboratory investigation confirmed that this Sulzer falling crystallisation technology would again be an ideal treatment system for concentrating RO brines rather than producing drinking water.

8.4 Sulzer Suspension Crystallisation Process

The primary concern of this study was to evaluate the technical feasibility of using suspension crystallisation technology as a treatment system for desalting and concentrating RO retentate.

Initial trial tests were conducted on a suspension pilot plant operating in batch mode. For the optimised pilot plant operation, the overall product water recovery and concentration ratios were around 41% and 59% respectively, for the actual test, and were in the range of 53% and 47%, in the case of the commercial plant, respectively. The overall salt rejection ratio was more than 99%, whereas the ionic rejections for Ca^{2+}, Mg^{2+}, Na^{+}, $(SO_4)^{2-}$, $(HCO_3)^{-}$, and Na^{-} were as high as 99%. The product water quality achieved was within the allowable limits for international drinking and bottled water standards (as illustrated in Table 6.4), with respect to the salt concentration and major ionic composition. Furthermore, the quality of product water was found to be comparable with different types of international and regional premier bottled water, in terms of major ionic composition. The experimental data proved that at least, a single stage of the suspension crystallisation process was potentially capable of producing a significant amount of product water that is ready for immediate use in human consumption, and simultaneously concentrating the RO retentate to a considerable ratio.

The results of the experimental investigation were highly encouraging for increasing the overall water recovery ratio of the water desalination plant and concentrating the waste stream i.e. RO retentate. Therefore, the proposed process should be competitive with other brine disposal methods for desalination processes, taking into account that the proposed technology has benefits which include better energy consumption, absence of a pre-treatment system, and less susceptible to the major technical problems in desalination plants, such as scaling, fouling and corrosion. Furthermore, the capital cost can be dramatically reduced by using inexpensive materials, e.g. plastic.

The current product water ratio for the pilot plant was limited to a maximum of 53% for a maximum salt rejection ratio. This was due to the reduced performance of the pilot plant when the salt concentration of the residual liquid reached 103,000 ppm, which resulted in the quality of the product water being relatively poor and unacceptable. This performance deterioration was observed in two different experimental runs. There were many possible reasons behind this performance deterioration, however, the main reason was not confirmed, and is still not understood. Therefore, further experimental investigation is needed to increase the water recovery ratio at maximum salt rejection ratio, in order to decrease the volume of RO retentate as far as possible. For future investigation, a pilot plant equipped with electrical conductivity sensors rather than light cells to control the separation process of

the wash column is highly recommended, in order to avoid adding a colour indicator. Also, prior to conducting the experimental investigation on RO retentate with a TDS of 103,000 ppm, it is highly recommended to use an aqueous solution of sodium chloride (NaCl) initially, with the specified salt concentration to verify the performance of the pilot plant.

The residual liquid stream produced from the pilot plant can cause severe pollution problems when this waste stream is not disposed of in an environmentally-friendly way. Solutions for concentrating/disposing of the residue of the suspension pilot plant should be considered in future research. Integrated multistage suspension (i.e. suspension-suspension) or suspension-static systems is recommended to be the subject of further research.

As treatment of RO retentate is a new application for the suspension crystallisation process, the evaluation of suspension pilot plant should continue. The aim is to improve the separation performance by increasing the total product water recovery. This particular application should be given special attention due to the extensive use of inland and coastal RO desalination plants, and the potential for use in other industrial sectors, such as petroleum industries.

Since the experimental investigation was conducted with a limited number of key operating parameters, a wider range needs to be taken into consideration in any future study. The suggested key-parameters for the crystallisation loop are crystallisation temperature (cooling rate), rotation frequency of scraper motor (i.e. scraper speed), number of scrapers, crystallisation residence time, ice slurry ratio (i.e. suspension density), and flow-rate of melt circulation pump. The suggested key-parameters for the separation loop are piston stroke, crystal bed-height, porosity of piston head of wash-column, and ice size, shape, and habit (which can be determined via a microscopic device).

In the economic analysis carried out, the power consumption and associated cost was strongly dependant on three important factors, namely the production rate, and the salt concentration of feed and product water. Indeed, designing plants for higher production rates would result in a significant reduction of waste streams, as well as the power consumption. Higher levels of salt concentration in the product water are also able to significantly reduce the power consumption cost. Detailed technical-economic analysis studies on integrated RO-

suspension plant and separate RO and suspension crystallisation plants are recommended for future research. The production rate, and the salt concentration of feed and product water should be considered as influential parameters for future power requirement analysis. Also, the associated factors, including capital equipment and costs, power requirements, and operating labour, are recommended to be taken into consideration in future technical-economic studies.

8.5 Sulzer Static Crystallisation Process

The performance of the static crystallisation process was experimentally evaluated and validated for RO brine concentration applications. The experimental study presents a new application for the Sulzer static crystallisation process. Aqueous solutions of sodium chloride and different salinities of process brines were investigated individually as feed samples. The laboratory investigation focused on the feed samples of highly concentrated RO brines, which were discharged from prior processes, namely the falling film and the suspension crystallisation.

A number of important parameters influencing the separation performance of crystallisation and sweating processes were investigated, not only on the laboratory bench scale, but also in a pilot plant (for some experiments). The key findings of the crystallisation experiments provided a clear indication that the investigated parameters, including feed concentration, crystallisation temperature, crystallisation rate, and average growth rate, had a strong influence on the separation performance of the crystallisation step. For example, the salt rejection ratio was found to be proportional to the crystallisation temperature and cooling rate, and inversely proportional to the feed concentration and average growth rate. The water recovery ratio, on the other hand, was found to be inversely proportional to the crystallisation temperature, cooling rate, and feed concentration, but proportional to the average growth rate. As for the sweating process, the separation performance of this technique was found to be strongly dependant on the salinity of the crystal layer, sweating rate, sweating time, and crystal mass ratio. The salt concentration of the crystal layer was found to be inversely proportional to the sweating time and crystal mass ratio, and proportional to the crystal layer salinity and sweating rate. The sweating operation was found to be effective in improving the purity of the crystal layer, and enhanced the separation efficiency of the static crystallisation process. However, the disadvantage of using the sweating method is associated with two

crucial factors, namely mass loss and freezing-stage time. Therefore, the sweating rate must be optimised at a reasonable limit to minimise the mass loss, and reduce the time of the freezing-stage; otherwise a substantial increase in the investment costs of water treatment will be encountered. In order to provide final product water at reasonable cost and reasonable reliability, the investigated influences of the crystallisation and sweating operations, more specifically the cooling and sweating rates, must be appropriately co-optimised.

The experimental results for concentrating RO brine, using a pilot plant, proved that a single freezing stage, without use of the sweating process, was capable of producing a significant amount of treated water, while the RO retentate was concentrated to a reasonable level. The salinity of the treated water was found to be comparable with Arabian Gulf seawater, and was ready for immediate re-use as feed water for a RO membrane desalination plant. By eliminating the sweating process, several advantages can be rendered to the Sulzer static crystallisation plant, for instance, mass loss will be avoided, a dramatic fall in the overall time for the freezing stage, significant increase in production rate, and a noticeable reduction in power consumption. On the other hand, the RO brine was tested at various crystallisation temperatures, which were higher and lower than the eutectic temperature of sodium chloride salt. These experiments were performed on the laboratory pilot scale setup with use of the sweating process. Similar findings to the previous investigation were observed in this study, and apart from that, the water recovery ratio was substantially increased for the case of crystallisation temperature lower than the eutectic temperature of sodium chloride salt.

As for the experiments on minimising the volume of the highly concentrated RO brines, the separation performance of a single stage process was investigated with the sweating process. The results of the experimental investigation were highly encouraging, since the volume of the waste stream was reduced to a minimum level. Although the final product water of the static crystallisation technology was not comparable to either drinking water or seawater standards (for some cases), the proposed process was able to further concentrate the highly concentrated RO brines as far as possible, while providing a significant amount of treated water, close to the quality of RO brine or seawater (for some cases). Based on the quality of the product water, the recommendation is for the treated water to be reused and recycled, either to join the main feed stream of the prior crystallisation process (i.e. falling film crystallisation and/or suspension crystallisation) or RO membrane plant. In order to achieve

the optimum water utilisation and exploitation, as well as environmental protection, three treatment options were individually proposed. These comprised an RO plant coupled with a combination of Sulzer crystallisation plants scaled up based on the experimental results for concentrating RO brine. The power consumption, on the other hand, was theoretically determined for each treatment option.

Alongside RO brine concentration, the proposed three treatment options offer a significant increase in the production rate of drinking water and/or preserving a substantial amount of natural water resource from the RO plant's exploitation. Also, the treatment options, which were proposed in this study, are highly recommended to be considered for future research using combined pilot plants tested in continuous operating mode. This applied research is of great importance, because it offers a number of important solutions for significant problems facing inland RO membrane desalination plants. These solutions are associated with several aspects, such as water supply, safe disposal, the environment, and preservation of natural water resources. Furthermore, the proposed treatment options offer important additional benefits that can be rendered to the RO membrane plant. These benefits are as follows: (i) reduced feed intake capacity; (ii) less floor space requirements for the feed intake and pre-treatment facilities; (iii) reduced capital and operational costs of the feed intake and pre-treatment units; (iv) minimised operational and capital costs of advanced treatment systems, such as Ultra-Filtration (UF), and Micro-Filtration (MF), when these systems are used; (v) reduced suspended solids and microbiological activity; (vi) reduced plugging and fouling problems; (vii) reduced colloidal fouling load on the RO membrane, leading to lower and stabilised the Silt Density Index (SDI) and turbidity; (viii) increased lifespan of RO membranes; (ix) minimising the operational challenges of the pre-treatment system; (x) reduced RO membrane cleaning frequency; (xi) reduced overall operational costs of the RO plant; (xii) minimising the chemical additives consumed by the pre-treatment unit and RO membrane cleaning frequency; (xiii) minimising the environmental problems by reducing the chemical additives; (xiii) avoiding the effects of seasonal climatic changes, i.e. fluctuation of feed temperature, on the performance of the RO membrane unit; and (xiv) hot feed water, which is usually encountered in hot climate countries, can be avoided.

In general, the experimental investigation showed that the Sulzer static crystallisation process was feasible for concentrating RO retentate of different salinities. The experimental

data can be used as a reference for crystallisation and sweating optimisation in commercial applications. The experimental results were highly encouraging, and proved that the treatment system is a powerful pre-concentration unit for minimising different concentrations of RO brine. The important advantages of the proposed technology are similar to that in the Sulzer falling film crystallisation process, which are given previously in section (8.3). As a result, the Sulzer static crystallisation process might be competitive with other pre-concentration systems, which are currently available on the commercial market.

Due to absence of appropriate experimental data in the literature, and the limited number of experimental runs (as presented in this study), the separation performance of the static crystallisation process technology for water desalination applications, and more specifically RO brine concentration, should be further investigated. Since the parameters affecting the crystallisation and sweating processes were investigated within a limited range and number of experimental runs, carrying out further investigation with a wider range of parameters is highly recommended in future research. The suggested key parameters for the crystallisation tests are feed concentration, start and end-point crystallisation temperatures, crystallisation time, cooling rate, and average growth rate. The suggested key parameters for the sweating tests are the salt concentration of the crystal layer, sweating rate, sweating time, and the crystal mass ratio. Visual observation using microscopy is highly recommended in future studies by conducting microscopic examinations to determine the crystal morphology. On the other hand, mathematical modelling to simulate the behaviour of a static crystallisation process, including sweating process, for concentrating RO brine is recommended. Models can be used to predict the mass and salt concentration of the crystal layer at various operating conditions.

APPENDICES:

The following appendices are found in a CD attached to the thesis

Appendix A3: A complete record of experimental data on static and agitated crystallisation processes

- File name: Appendix, Microsoft Excel spreadsheet, Sheet: Appendix A3

Appendix A4: A complete record of experimental data on ice maker machine

- File name: Appendix, Microsoft Excel spreadsheet, Sheet: Appendix A4

Appendix A5: A complete record of experimental data on Sulzer falling film crystallisation pilot plant

- File name: Appendix, Microsoft Excel spreadsheet, Sheet: Appendix A5

Appendix A6: A complete record of experimental data on Sulzer suspension crystallisation pilot plant

- File name: Appendix, Microsoft Excel spreadsheet, Sheet: Appendix A6
- File name: Appendix_5_A5-1, PDF, Operational temperature profiles

Appendix A7: A complete record of process data, operating temperature profiles, full physiochemical analysis, and crystalline impurity content versus sweating times

- File name: Appendix, Microsoft Excel spreadsheet, Sheet: Appendix A7

REFERENCES:

Ahmad M., and Williams, P., 2009. Application of salinity gradient power for brines disposal and energy utilisation. *Desalination* 10 (2009), pp. 220 - 228.

Ahmad, M., and Williams, P., 2011. Assessment of desalination technologies for high saline brine applications – Discussion Paper. *Desalination* 30 (2011), pp. 22-36.

Ahmed, M., Arakel, A., and Hoey, D., 2003. Feasibility of salt production from inland RO desalination plant reject brine: a case study. *Desalination*, 158 (2003), pp. 109-117.

Ahmed, M., Shayya, W. H., Hoey, D., Mahendran, A., and Morris, R., 2000. Use of evaporation ponds for brine disposal in desalination plants. *Desalination*, 130(2), pp. 155-168.

Alhazmy, M. M., 2009. Feed water cooler to increase evaporation range in MSF plants. *Energy*, 34 (1), January 2009, pp. 7-13.

Alklaibi, A.M., and Loar, N., 2004. Membrane-distillation desalination: status and potential. *Desalination* 171 (2), pp. 111-131.

Al-Obaidani, S., Curcio, E., Macedonio, F., Di Profio, G., Al-Hinaid H., and Drioli, E., (2008). Potential of membrane distillation in seawater desalination: Thermal efficiency, sensitivity study and cost estimation, 2008. *Journal of Membrane Science*, 323 (1), pp. 85-98.

Auleda, J., Raventós, M., Sánchez, J., Hernández, E., 2011. Estimation of the freezing point of concentrated fruit juices for application in freeze concentration, *Journal of Food Engineering* 105 (2) 289-294.

Ayres, R. W., and Swanson, D. F., Seeger Refrigerator Company, 1954. *Ice cube making apparatus*, St. Paul, Minn., U.S. Pat.: 2,682,155.

Ayres, R. W., and Swanson, D. F., Whirlpool Cooperation, 1961. *Ice cube forming machine*, St. Paul, Minn., U.S. Pat.: 2,995,905.

Barduhn, A. J., *Freezing processes for water conversion in the United States*, First International symposium on water desalination, 3-9 October 1965, Washington D. C., USA.

Barnard, W. C., and Hodapp, D. C., Whirlpool Cooperation, 1971. *Icemaker with water distributor*, White Bear Lake, Minn., U.S. Pat.: 3,580,008.

Bochenek, R., Sitarz, R., Antos D., 2011. Design of continuous ion exchange process for the wastewater treatment. *Chemical engineering science*, 66 (2011), pp. 6209-6219.

Bond, R., and Veerapaneni, V., Awwa Research Foundation, 2007. *Zero liquid discharge for inland desalination.* [Online] Available at: <http://www.waterrf.org/ProjectsReports/PublicReportLibrary/91190.pdf> [Accessed 14 October 2011].

Boonnasa, S., Namprakai, P., and Muangnapoh, T., 2006. Performance improvement of the combined cycle power plant by intake air cooling using an absorption chiller. *Energy*, 31 (12), pp. 2036-2046.

Bostjancic, J., and Ludlum, R., 1994. *Reducing wastewater to dryness: Zero liquid discharge case studies at new power plants*, Resources Conservation Company (RCC).

Brandt, H., Macero, El., and Tait, J., Aquatech Services Inc., 1997. *Process for brine disposal*, United States, US Patent 5,695,643, Application Number: 129692.

Brown, C., Sheedy, M, 2002. *A new ion exchange process for softening high TDS produced water*, SPE/Petroleum Society of CIM/CHOA, held in Calgary, Alberta - November, paper No. 78941

BUCO Heat Transfer Technology, 2011. *Chip Ice Maker.* [Online] Available at: < http://www.htt-ag.com/en/products/industrial-ice-maker-machine> [Accessed 20 January 2012].

Buros, O.K., 2000. *ABCs of desalting*, 2nd ed. S.I., International Desalination Association (IDA), Topsfield, Massachusetts, United States of America.

Cath, T. Y., and Childress, A. E., Elimelech, M., 2006. Forward osmosis: Principles, applications, and recent developments. *Journal of Membrane Science*, 281(1-2), pp. 70-87.

Chen, J.C.T., 1984. Methods for rapid prediction of walt quality and influent-water quality effects on hardness leakage in steam-flood water. *Journal of Petroleum Technology*.

Clayton, A.R., Foundation for Water Research, 2006. *Desalination for water supply.* [Online] Available at: <http://www.fwr.org/desal.pdf> [Accessed 14 October 2011].

Cohen, B., 1983. A renewable energy source. *American Journal of Physics*, 51 (1), pp. 75-76.

Cole-Parmer, 2010. *Operating manual and part list for Cimarec™ stirring hot plates.* [Online] Available at: <http://www.coleparmer.com/catalog/manual_pdfs/LT1072X1%20Cimarec.pdf> [Accessed 2nd December 2010].

Curcio, E., Ji, X., Profio, G., Sulaiman, A.O., Fontananova, E., and Drioli, E., 2010. Membrane distillation operated at high seawater concentration factors: Role of the membrane on $CaCO_3$ scaling in presence of humic acid. *Journal of Membrane Science*, 346 (2), pp. 263-269.

Da˛browski, A., Hubick, Z., Podkos´cielny, P. and Rubens, E., 2004. Selective removal of the heavy metal ions from water sand industrial wastewaters by ion-exchange method. *Chemosphere*, 56, pp. 91-106.

Delft, D.v., *Freezing physics : Heike Kamerlingh Onnes and the quest for cold.* History of science and scholarship in the Netherlands. 2007, Amsterdam: Koninklijke Nederlandse Akademie van Wetenschappen. vi, ISBN 978-90-6984-519-7.

Dirach, J., Nisan, S. and Poletiko, C., 2005. Extraction of strategic materials from the concentrated brine rejected by integrated nuclear desalination systems. *Desalination*, 182, pp. 449-460.

Dreizin, Y., 2006. Ashkelon seawater desalination project — off-taker's self costs. *Desalination*, 190 (1-2), pp. 104-116.

El-Bourawi, M.S., Ding, Z., Ma, R. and Khayet, M., 2006. *A* framework for better understanding membrane distillation separation process. *Journal of Membrane Science*, 285 (1-2), pp. 4-29.

El-Dessouky, H.T., and Ettouney, H. M., *Fundamentals of salt water desalination.* 2002. Elsevier Science, Amsterdam, ISBN: 9780444508102.

El-Sayed, E., and El-Sayed, Y., 2007. *The advantages and the challenges of zero liquid discharge desalination*, In: 3rd International Conference on Desalination Technologies, Sharm El -Sheikh, Egypt, May 7 – 8, 2007, Conference Proceedings.

Encyclopedia of Desalination and Water Resources (DESWARE), 2011. *Energy Requirements of Desalination Processes.* [Online] Available at: <http://www.desware.net/desa4.aspx> [Accessed 13 October 2011].

Flores, V. and Cabassud, C., 1999. A hybrid membrane process for Cu(II) removal from industrial wastewater, comparison with a conventional process system. *Desalination*, 126, pp. 101-108.

Fritzmann, C., Löwenberg, J., Wintgens, T. and Melin, T., 2007.State-of-the-art of reverse osmosis desalination. *Desalination* 216 (2007), pp. 1-76.

GAE NIRO, MESSO technologies group, 2003. *Evaporation technologies.* [Online] Available at: <http://www.niro.com/mde/cmsresources.nsf/filenames/Evaporation.pdf/$file/Evaporation.pdf> [Accessed 13 October 2011].

GAE NIRO, Process engineering division, 2011. *Crystallization in theory and practice.* [Online] Available at: <http://www.niroinc.com/evaporators_crystallizers/crystallization.asp> [Accessed 13 October 2011].

Gálvez, J.B., García-Rodríguez, L., and Martín-Mateos, I., 2009. Seawater desalination by an innovative solar-powered membrane distillation system: the MEDESOL project. *Desalination* 246 (1-3), pp. 567-576.

GEA, 2011. *Suspension crystallization.* [Online] Available at: < http://www.gea-messo-pt.com/geacrystal/cmsdoc.nsf/WebDoc/webb7pzduj > [Accessed 22nd November 2011].

GEV, 2007. *Spare parts suitable for*: *Whirlpool.* [Online] Available at: <http://www.gev-online.co.uk/fileadmin/templates_gev_co_uk/pdf/refrigeration/gev_uk_refrigeration_whirlpool.pdf> [Accessed 11 November 2010].

Gorin, C., 2010. *Extraction of uranium from seawater.* [Online] Available at: <http://large.stanford.edu/courses/2010/ph240/gorin2> [Accessed 15 October 2011].

Ohya, H., Suzuki, T., and Nakao, S., 2001. Integrated system for complete usage of components in seawater: a proposal of inorganic chemical combined in seawater. *Desalination*, 134 (1–3), pp. 29-36.

Hanbury, W., Hodgkiess, T., and Morris, R., 1993. *Desalination Technology 93*, United Kingdom (Glasgow): Porthan Ltd.

Heide, E., Wagener, K., Paschke, M., and Wald, M., 1973. *Extraction* of uranium from sea water by cultured algae. *Natur Wissenschaften*, 60 (9), pp. 431-431.

Hernández, E., Raventós, M., Auleda, J., Ibarz, A., 2009. Concentration of apple and pear juices in a multi-plate freeze concentrator, *Innovative Food Science & Emerging Technologies* 10(3) 348-355.

Hernández, E., Raventós, M., Auleda, J., Ibarz, A., 2010. Freeze concentration of must in a pilot plant falling film cryoconcentrator, *Innovative Food Science & Emerging Technologies* 11(1) 130-136.

Howe, K. J., Corridor, Department of civil engineering, University of New Mexico, 2009. *Technical challenges to concentrate disposal from inland desalination.* [Online] Available at: <http://www.unm.edu/~cstp/Reports/H2O_Session_4/4-7_Howe.pdf> [Accessed 14 October 2011].

Hoyle, B., and Dasch, E., Water encyclopedia, 2011. *Natural Brines.* [Online] Available at: <http://www.waterencyclopedia.com/Bi-Ca/Brines-Natural.html> [Accessed 13 October 2011].

Index Mundi, 2011. *Uranium Monthly Price - US Dollars per Pound.* [Online] Available at: <http://www.indexmundi.com/commodities/?commodity=uranium&months=60> [Accessed 15 October 2011].

Jeppesen, T., Shu, L., Keir, G. and Jegatheesan V., 2009. Metal recovery from reverse osmosis concentrate. *Journal of Cleaner Production*, 17 (2009), pp. 703-707.

Johnson, W., 1976. State-of-the-art of freezing processes, their potential and future, *Desalination*, 19, pp. 349-358.

Jones, A.T., and Finley, W., 2003. *Recent development in salinity gradient power*, Proceedings Oceans 2003, Vol. 4, pp. 2284 - 2287, Print ISBN: 0-933957-30-0.

Kanno, M., 1984. Present status of study on extraction of uranium from sea water. *Journal of nuclear scientific and technology*, 21(1), pp. 1-9.

Karnofsky, G., and Steinhoff, P., 1960. Saline Water Conversion by Direct Freezing with Butane, Rep. 40, 67 pp. *Washington DC: National Technical Information Service.*

Kim, K.J. and Ulrich, J., 2002. A quantitative estimation of purity and yield of crystalline layers concerning sweating operations. *Journal of Crystal Growth* 234, (2-3) pp. 551-560.

Kumar, S. A., Pandey, S. P., Shenoy, N. S. and Kumar, S. D., 2011. Matrix separation and preconcentration of rare earth elements from seawater by poly hydroxamic acid cartridge followed by determination using ICP-MS. *Desalination*, 281, pp. 49-54.

Lattemann, S., and Höpner, T, 2003. *Seawater desalination: impacts of brine and chemical discharge on the marine environment*, Balaban Desalination Publications, Italy, ISBN: 0866890629.

Lawson, K.W., and Lloyd, D.R., 1997. Membrane distillation. *Journal of Membrane Science* 124 (1), pp. 1-25.

LeeWebWorks LLC, 2007. *Water Softeners*. [Online] Available at: <http://www.homecents.com/h2o/h2o_soft/index.html> [Accessed 28 October 2011].

Lemmer, S., Klomp, R., Ruemekorf, R., Scholz, R., 2001. Preconcentration of Wastewater through the Niro Freeze Concentration Process, *Chemical Engineering Technology*, 24(5) (2001) 485-488.

Lorain, O., Thiebaud, P., Badorc, E., Aurelle, Y., 2001. Potential of Freezing in Wastewater Treatment: Soluble Pollutant Applications, *Water Researc*h, 35(2) 541-547.

Martinetti, C.R., Childress A.E., and Cath, T.Y., 2009. High recovery of concentrated RO brines using forward osmosis and membrane distillation. *Journal of Membrane Science*, 331 (1-2), pp. 31-39.

McKetta, J., and Anthony, R, 2002. *Encyclopedia of chemical processing and design*, Marcel Dekker Inc., USA, Vol. 69, pp. 313, ISBN: 9780824726218.

Miller, J.E., Sandia National Laboratories, 2003. *Review of water resources and desalination technologies*. [Online] Available at: <http://www.sandia.gov/water/docs/MillerSAND2003_0800.pdf> [Accessed 14 October 2011].

Mitchell, A. J., Sabelhaus, H. P., and Tinney, J. P., Whirlpool Corporation, 2003. *Ice maker with magnetic water conditioner*, Benton Harbor, USA, Pub. No.: US 2003/0024263 A1

Miyawaki, O., Liu, L., Shirai, Y., Sakashita, S., Kagitani, K., 2005. Tubular Ice System for Scale-up of Progressive Freeze-Concentration, *Journal of Food Engineering*, 69 (2005) 107-113.

Mommaerts, G.J., 1999. *Softening of produced water: which system is best for your application*, Proc. SPE International Thermal Operations and Heavy Oil Symposium, 17-19 March 1999, Bakersfield CA.

Mulder, M., 1996. *Basic principles of membrane technology*, 2nd ed., Kluwer Academic Publishers, Netherlands. ISBN: 9780792342472.

Myerson, A, 2002. *Handbook of industrial crystallisation*, 2002, 2nd edition, Butterworth-Heinemann, ISBN: 0750670126.

NALCO, 1998. *Ion exchange processes.* [Online] Available at: <http://www.onlinewatertreatment.com/literature/Nalco/docs/Tf-024.pdf> [Accessed 24 October 2011].

National Research Council (U.S.), 2009. *Desalination: a national perspective*, National Academy Press Washington, D.C, United States of America, ISBN: 9780309119238.

Nebbia, G. and Menozzi, G., 1968. Early experiments on water desalination by freezing. *Desalination* 5 (1968), pp. 49-54.

OECD, 2004. Water Consumption. OECD Environmental Data Compendium. *OECD* (2004) 136-137.

Pankratz, T., 2008. *Zero liquid discharge systems are operating challenge*, Water Desalination Report: 44(7):1.

Pintar, A., Batista, J., Levec, J., 2001. Integrated ion exchange/catalytic process for efficient removal of nitrates from drinking water. *Chemical Engineering Science.* 56, pp. 1551-1559.

Pols, H.B., and Harmsen, G.H., 1994. Industrial wastewater treatment today and tomorrow. *Water Science & Technology*, 30 (3), pp. 109-117.

Post, J.W., Veerman, J., Hamelers, H.V.M., Euverink, G.J.W., Metz, S.J., Nymeijer, K., and Buisman, C.J.N., 2007. Salinity gradient power: Evaluation of pressure-retarded osmosis and reverse electrodialysis. *Journal of Membrane Science*, 288 (1-2), pp. 218-230.

Pounder, E. R., 1965. *Physics of ice*, Great British: Pergamon Press Ltd., Library of Congress Catalogue Card No. 65-21141.

Rahman, M., and Ahmed, M., 2006. *Freezing melting process and desalination: review of the state of the art*, Sultanate of Oman, Separation & purification reviews, Copyright: Taylor & Francis Group. 35(2), pp. 59-96.

Rahman, M., Ahmed, M., and Chen, X., 2007. Freezing–melting process and desalination: review of present status and future prospects. *International Journal of Nuclear Desalination*, 2(3), pp. 253-264.

Rich, A., Youssef, M., Nourimane, B., Denis, M., Souad, A., Christine, B., Naoual, S., Jean-Paul, K., Tijani, B., Ahmed, B. and Stephane, V., 2011. Freezing desalination of seawater in a static layer crystallizer. *Desalination* 269, pp. 142-147.

Rodrígues, M., Luque, S., Alvarez, J.R., Coca, J. 2000. A Comparative Study of Reverse Osmosis and Freeze Concentration for Removal of Valeric Acid from Wastewaters, *Desalination*, 127 (2000), pp. 1-11.

Sánchez, J., Hernández, E., Auleda, J., Raventós, M., 2011. Freeze concentration of whey in a falling-film based pilot plant: Process and characterization, *Journal of Food Engineering* 103(2) 147-155.

Sather, A., Berryman, O., and Rebek, J., 2010. Selective recognition and extraction of the uranyl ion. *Journal of the American chemical Society*, 132(39), pp. 13572-13574.

Schwochau, K., 1984. *Extraction of metals from seawater*, Topics in Current Chemistry 124 (91), pp. 91-133.

Seko, N., Katakai, A., Hasegawa, S., Tamada, M., Kasai, N., Takeda, H., Sugo, T. and Saito, K., 2003. Aquaculture of uranium in seawater by a fabric-adsorpent submerged system, *Nuclear Technology*, 144 (2), pp. 274-278.

Semerjian, L., 2011. Quality assessment of various bottled waters marketed in Lebanon, Earth and environmental science. *Environmental Monitoring and Assessment*, 172 (1-4), pp. 275-285.

Sethi, S., Walker, S., Drewes, J., and Xu, P., 2006. Existing & emerging concentrate minimization & disposal practices for membrane systems. *Florida Water Resources Journal*, pp. 38-48.

Shone, R.D.C., 1987. The freeze desalination of mines waters. *Journal of the South African Institute of Mining and Metallurgy*, 87(4), pp. 107-112.

Skilhagen, S.E., Dugstad J.E., and Aaberg, R.J., 2008. Osmotic power – power production based on the osmotic pressure difference between waters with varying salt gradients. *Desalination*, 220(1-3), pp. 476-482.

Spiegler, K. S., and El-Sayed, Y. M., 1994. *A desalination primer*, Italy: Balaban Desalination Publications, ISBN: 0866890343.

Spiegler, K. S., and Laird, A. D. K., 1980. *Principles of desalination "Part A"*. 2nd ed., London: Academic Press INC., Vol. 1, ISBN: 0126567018.

Spiegler, K. S., and Laird, A. D. K., 1980. *Principles of desalination "Part B"*. 2nd ed., London: Academic Press INC., Vol. 1, ISBN: 0126567018.

Spiegler, K. S., 1966. *Principles of desalination*. London: Academic Press INC., ISBN: 0126567018.

Spiro, D.A., 2009. Ion exchange resins: a retrospective from industrial and engineering chemistry research. *Industrial & Engineering Chemistry Research*, 48, pp. 388-398.

Sugo, T., 1999. *Uranium recovery from seawater*. [Online] Available at: <http://www.jaea.go.jp/jaeri/english/ff/ff43/topics.html> [Accessed 15 October 2011].

Sulzer Chemtech Ltd, 2011. *Suspension crystallization*. [Online] Available at: < http://www.sulzerchemtech.com/desktopdefault.aspx/tabid-2245> [Accessed 22nd November 2011].

Sulzer, 2004. *Suspension crystallisation technology*, Sulzer Chemtech Ltd., Switzerland. [Online] Available at: <http://www.sulzerchemtech.com/portaldata/11/Resources//Brochures/PT/Suspension_Crystallization_Technology.pdf> [Accessed 5 July 2009].

Sulzer, 2005. *Sulzer Chemtech, Fractional crystallisation*, Sulzer Chemtech Ltd., Switzerland. [Online] Available at: <http://www.sulzerchemtech.com/portaldata/11/Resources//Brochures/PT/Fractional_Crystallization-e.pdf> [Accessed 5 July 2009].

Szacsvay, T., Noser, P., and Posnansky, M., 1999. Technical and economic aspects of small-scale solar-pondpowered seawater desalination systems. *Desalination*, 122 (2-3), pp. 185 - 193.

T., Tähti, 2004. *Suspension melt crystallization in tubular and scraped surface heat exchangers*. [Online] Available at: <http://sundoc.bibliothek.uni-halle.de/diss-online/04/04H181/t1.pdf> [Accessed 22nd November 2011].

Tamada, M., 2009. *Current status of technology for collection of uranium from seawater*. [Online] Available at: <http://www.physics.harvard.edu/~wilson/energypmp/2009_Tamada.pdf> [Accessed 15 October 2011].

Tillberg, F., Royal Institute of Technology, KTH, Stockholm, 2004. *ZLD systems – an overview*. [Online] Available at: <http://www.xzero.se/docs/zldanover.pdf> [Accessed 14 October 2011].

Turnbull, D., 1965. The undercooling of liquids. *Scientific American*, 212, pp. 38-46.

U.S. Congress, Office of Technology Assessment, 1988. *Using Desalination Technologies for Water Treatment*. [Online] Available at: <http://www.princeton.edu/~ota/disk2/1988/8842/8842.PDF> [Accessed 14 October 2011].

Ulrich, J., and Glade, H., 2003. *Melt crystallisation*, Germany: Shaker Verlag, ISBN: 3-8322-1533-6.

United Nations, 2001. *Water desalination technologies in the ESCWA member countries*, New York: United Nations, Report No.: E/ESCWA/TECH/2001/3.

Valverde, J.L., DeLucas, A., Carmona, M., Pe´ rez, J.P., Gonza´ lez, M. and Rodrı´guez, J.F., 2006. Minimizing the environmental impact of the regeneration process of an ion exchange bed charged with transition metals. *Separation and purification technology*, 49, pp. 167-173.

Van der Ham, F., Witkamp, G.J., de Graauw, J., and van Rosmalen, G.M., 1998. Eutectic freeze crystallization: Application to process streams and waste water purification, Chemical *Engineering and Processing*, 37 (2), pp. 207-213.

Walton, J., Lu, H., Turner, C., Solis, S., and Hein, H., 2004. *Solar and Waste Heat Desalination by Membrane Distillation*, College of Engineering, United of Texas, El Paso, Texas, United States of America, Agreement No.: 98-FC-81-0048, Program Report No.: 81.

Weiss P., 1973. Desalination by freezing, Practice of Desalination (ed. R Bakish), pp. 260-270, *New Jersey: Noyes Data Corporation*, New Jersey.

Whirlpool, 2009. *Theory of operation.* [Online] Available at: < http://www.truetex.com/ice_machine_gi1500.pdf> [Accessed 10 March 2009].

Whirlpool, 2010. *User manual: Manual service.* [Online] Available at: <http://www.whirlpoolparts.co.uk/downloads/ServiceManual.pdf> [Accessed 10 March 2009].

Whirlpool, 2011. *Whirlpool K20 and Whirlpool K40 machines.* [Online] Available at: < http://www.whirlpoolk40.co.uk/#/spare-parts/4531731979> [Accessed 10 March 2009].

Whitman, W. C., Johnson, W. M., and Tomczyk, J. A., 2004. *Refrigeration and Air Conditioning Technology*, 5th ed. USA: Delmar Cengage Learning, ISBN: 1401837654.

Wiegandt, H., 1960. Saline Water Conversion by Freezing: an Integral Processing Unit Using a Secondary Refrigerant, Rep. 41, 51 pp. *Washington DC: National Technical Information Service.*

Younos, T., and Tulou, K. E., 2005. Overview of desalination techniques. *Journal of Contemporary Water Research & Education*, 132 (1), pp. 3-10.

Ziegra Ice Machines, 2011. *Flake Ice Comparison.* [Online] Available at: < http://www.ziegra.co.uk/Ice%20machines%20and%20ice%20makers.html?gclid=CMb57ey 9i68CFQnP3wodP1sv-g > [Accessed 20 January 2012].